

MOLECULAR NERVE REPAIR



VRIJE UNIVERSITEIT

# Molecular Nerve Repair

**The molecular properties of the injured peripheral nerve  
and the application of viral vectors to enhance regeneration**

ACADEMISCH PROEFSCHRIFT  
ter verkrijging van de graad Doctor aan  
de Vrije Universiteit Amsterdam  
op gezag van de rector magnificus  
prof. dr. L.M. Bouter,  
in het openbaar te verdedigen  
ten overstaan van de promotiecommissie  
van de faculteit der Aard- en Levenswetenschappen  
woensdag 3 december 2008 om 10:45 uur  
in de aula van de universiteit,  
de Boelelaan 1105  
door

*Martijn Rudolf Tannemaat*

geboren te Madrid, Spanje

Promotor: prof. dr. J. Verhaagen

Copromotores: dr. G.J. Boer

dr. M.J.A. Malessy

The research described in this thesis was conducted at the Netherlands Institute for Neuroscience. This research was financially supported by the department of Neurosurgery, Leiden University Medical Center, grants from the Netherlands Brain Foundation (project numbers 12Fo4.02 and 15Fo7), a grant from the Prinses Beatrix Fonds, a grant from the International Spinal Cord Research Trust (STR090) and a gift from S. Matser-van Nulck.

*The publication of this thesis was financially supported by*

Nederlands Instituut voor Neurowetenschappen

Remmert Adriaan Laan Fonds

J.E. Jurriaanse stichting

van Leersum Fonds KNAW

Sanofi Aventis

Bayer Schering Pharma

GlaxoSmithKline

Boehringer Ingelheim

#### *About the cover*

The image on the cover is a long-exposure photograph of cars driving on a highway. The trails left by their head- and taillights bear a striking visual resemblance to axons in the peripheral nerve. Like these cars, regenerating axons need both the energy to continue to move forward (“the engine”) and a sense of direction (“the steering wheel”), but ultimately, it is the road along which they travel that determines their destination. Following this analogy, our current understanding of peripheral nerve regeneration could be summarized by a quote from Gautama Siddharta, the founder of Buddhism: “You cannot travel the path until you have become the path itself”. To improve the outcome of reconstructive surgery for patients who are affected by peripheral nerve injury, we will have to deepen our understanding of the interaction between regenerating axons and the nerve tissue that surrounds them. Perhaps in the future we will then be able to cite another great philosophical mind, “Doc” Emmett Brown from the movie *Back to the Future*, and proclaim: ‘Roads? Where we’re going we don’t need roads!’

*Book design:* Henk Stoffels, Amsterdam

*Print:* Gildeprint bv, Enschede

*Voor mijn ouders*



# Contents

|           |   |     |
|-----------|---|-----|
|           | Scope and outline of this thesis  | 9   |
| CHAPTER 1 | Introduction: the application of viral vectors to enhance regeneration after peripheral nerve repair<br><i>Neurological Research (in press)</i>   | 11  |
| CHAPTER 2 | Human neuroma contains increased levels of semaphorin 3A, which surrounds nerve fibres and reduces neurite extension in vitro<br><i>Journal of Neuroscience. 2007 Dec 26;27(52):14260-4</i>   | 25  |
| CHAPTER 3 | Gene expression profiling provides novel insights in the molecular basis of misrouting of axons through the neuroma in continuity in obstetrical brachial plexus injuries: a preliminary report<br><i>Manuscript in preparation</i> | 39  |
| CHAPTER 4 | Genetic modification of human sural nerve segments by a lentiviral vector encoding nerve growth factor<br><i>Neurosurgery. 2007 Dec;61(6):1286-94; discussion 1294-6.</i>   | 77  |
| CHAPTER 5 | Neuroregenerative effects of lentiviral vector-mediated GDNF expression in reimplanted ventral roots<br><i>Molecular and Cellular Neuroscience. 2008 Sep;39(1):105-17</i>   | 93  |
| CHAPTER 6 | Differential effects of lentiviral vector-mediated overexpression of NGF and GDNF on regenerating sensory and motor axons in the transected peripheral nerve<br><i>European Journal of Neuroscience (in press)</i>                  | 121 |
| CHAPTER 7 | Summary and general discussion  | 143 |
|           | Nederlandse samenvatting  | 155 |
|           | References  | 163 |
|           | List of publications  | 175 |
|           | Co-author affiliations  | 177 |
|           | Dankwoord   | 179 |
|           | Curriculum vitae  | 183 |





## Scope and outline of this thesis

Injury to the peripheral nerve is a serious condition that causes sensory and motor impairments of the affected limb. At present, the only treatment strategy for severe nerve lesions is microsurgical repair. Surgical techniques have evolved significantly over the past decades, but nonetheless, a considerable degree of functional impairment remains in the majority of patients after nerve reconstruction. It is generally accepted that surgery has reached an optimal technical refinement. New concepts are therefore needed to improve the functional recovery of patients with severe peripheral nerve injury. As described in introductory **Chapter 1**, it is likely that in the future such concepts will arise from insights obtained by molecular neurobiological research. Viral vector-mediated gene transfer in the nervous system has matured significantly over the last decades and is now a clinically viable tool for the long-term, local delivery of proteins that may enhance peripheral nerve regeneration at a molecular level.

The overall objective of this thesis can be divided in two distinct, but related aims: 1) to investigate the molecular properties of the human peripheral nerve lesion and 2) to explore the possibilities to manipulate regeneration of the peripheral nerve at a molecular level with the aid of lentiviral (LV) vectors.

Scar formation in the injured peripheral nerve (e.g. after a stretch injury) is considered to be detrimental for the regeneration of axons and subsequent functional recovery, although the molecular basis for this phenomenon is not fully understood. In **Chapter 2**, we show that the chemorepulsive axon guidance protein semaphorin 3A is present in the human peripheral nerve scar and may contribute to its outgrowth-inhibitory properties. Building on this result, we performed a genome-wide analysis of gene expression in the human peripheral nerve scar, the results of which are described in **Chapter 3**. We discovered that the expression of many proteins was differentially regulated in the nerve scar, and a significant proportion of these are involved in either scar formation or guidance of regenerating axons.

The newly discovered proteins that influence regeneration described in Chapters 2 and 3 may in the future become targets for therapies to enhance the functional outcome of peripheral nerve surgery, but this approach depends on the ability to locally increase (or decrease) their expression. In the following chapters, we explored the use of viral vectors as a means to enhance the expression of so-called neurotrophic factors in the peripheral nervous system.

In **Chapter 4**, we develop a method to insert a gene into cells of the cultured human nerve by means of LV vectors. Furthermore, we show that the application of an LV vector carrying a gene encoding nerve growth factor (NGF) leads to long-term production of biologically active NGF. With the method described in this chapter, the LV

vector could theoretically be applied without changing the routine practice of nerve grafting, so this approach could be a powerful novel adjuvant therapy for peripheral nerve surgery. However, a key question is whether the application of viral vectors can actually improve the outcome of nerve repair surgery.

Therefore, in **Chapter 5**, we studied the effect of LV vector-mediated overexpression of brain-derived neurotrophic factor (BDNF) and glial cell line-derived neurotrophic factor (GDNF) on regeneration of motoneurons after nerve root avulsion and reimplantation in the rat. LV vector-mediated overexpression of GDNF does indeed reduce atrophy of avulsed motoneurons and increase the sprouting of regenerating axons into reimplanted roots, but unfortunately, these axons fail to exit the area of high GDNF expression, resulting in impaired long distance regeneration.

In **Chapter 6**, we studied the effect of LV vector-mediated overexpression of NGF and GDNF on regeneration of the rat peripheral nerve. Similar to the results described in the previous chapter, high levels of GDNF trap regenerating motor axons, whereas the regeneration of sensory neurons is unaffected. The effects of NGF on the regeneration of either motor or sensory neurons appeared to be very limited. Lentiviral vector-mediated overexpression of both NGF and GDNF causes profound but different changes in regenerating sensory neurons, specifically those sensory neurons that play a role in the perception of pain. These findings have important implications for future research into difference between the regenerative response of motor and sensory neurons and for a better understanding of the pathogenesis of pain.

The final chapter, **Chapter 7**, is a summary of the preceding chapters, followed by a discussion on how the obtained results will influence future research. Specifically, I will speculate in this Chapter on how the clinical practice of peripheral nerve surgery will be influenced by a better understanding of the molecular basis of regeneration and on ways to fully realise the potential of emerging therapeutics from the field of molecular neurobiology.

# Chapter 1

## Introduction: the application of viral vectors to enhance regeneration after peripheral nerve repair

Martijn R Tannemaat, Joost Verhaagen, Martijn J Malessy

*Neurological Research (in press)*

### **Abstract**

Despite great advances in surgical repair techniques, a considerable degree of functional impairment remains in the majority of patients after peripheral nerve reconstruction. New concepts to promote regeneration of the peripheral nerve are needed since it is generally held that surgery has reached an optimal technical refinement. These future concepts will likely be aimed at influencing peripheral nerve regeneration at a molecular level using viral vectors. Several neurotrophic factors stimulate regeneration of the peripheral nerve, but the effects of the exogenous application of these factors have so far been limited, possibly as the result of their fast degradation and unwanted side-effects after systemic application. These problems can be resolved with the recent development of non-toxic, non-immunogenic viral vectors that drive local, long-term transgene expression. Retroviral vectors have been used successfully for the *ex vivo* transduction of Schwann cells, prior to seeding in artificial nerve guides. Lentiviral (LV) vectors direct long term transgene expression in Schwann cells in rat peripheral nerves. LV vectors are also capable of transducing cultured segments of human sural nerve thereby providing “proof of concept” for the feasibility of genetic modification of sural nerve transplants in a clinical setting. In the near future, viral vectors will increasingly be used to study a wide range of neurotrophic factors and other potentially therapeutic proteins for their effect on peripheral nerve regeneration in animal models. If this approach leads to beneficial effects on regeneration and functional recovery, the safety and clinical applicability of these viral vectors will allow the rapid translation of basic research to clinical trials. This makes the use of viral vectors a highly attractive concept that holds great promise as a novel adjuvant therapy to peripheral nerve reconstruction.

### **Introduction: peripheral nerve repair**

The first series of successful surgical reconstructions of the peripheral nerve were described shortly after the Second World War<sup>1</sup>. Since then, a better understanding of peripheral nerve anatomy, the evolution of surgical techniques, including epineurial suturing and the introduction of the operation microscope, have led to a significant

improvement in the clinical outcome of surgery. Surgery is currently the preferred treatment for the transected nerve and consists of direct, tension-free, suture coaptation of nerve stumps. A detrimental factor to nerve regeneration is the occurrence of fibrosis in the gap, which may lead to neuroma formation thereby greatly reducing the chance of successful axonal regeneration. In such instances, the neuroma is resected and autologous nerve grafts are used as scaffolds to bridge the gap between the proximal and distal nerve stumps.

Functional recovery after peripheral nerve reconstruction is almost never complete, and a considerable degree of functional impairment usually remains. The clinical outcome of repair is especially limited in adults, in proximal nerve lesions such as brachial plexus lesions and when long nerve transplants have to be used<sup>1</sup>. It is generally held that microsurgery has now reached an optimal technical refinement and new concepts have to be developed to further promote recovery of function after peripheral nerve repair<sup>2</sup>. A new conceptual framework is currently emerging from a better understanding of the molecular basis of nerve regeneration and the application of novel intervention strategies, including viral vector mediated gene transfer. In this review, we first describe the pathophysiology of nerve injury. Then we discuss the molecular mechanisms involved in regeneration of the peripheral nerve, with a special emphasis on the role of neurotrophic factors and how they have been applied exogenously to enhance the results of nerve repair. Subsequently, we discuss the currently available non-viral and viral vectors for gene transfer and summarize their use in models for peripheral nerve repair so far. Finally we analyse both the strong points of the concept of gene therapy and the current limitations that have to be resolved before it can be applied in the clinic for peripheral nerve repair.

### **The pathophysiology of nerve injury**

Sunderland's classification of nerve injuries in five degrees (based on the relative integrity of axons, endoneurial tubes and epineurium and the formation of scar tissue) is the most commonly used today<sup>1</sup>. MacKinnon added the term "sixth-degree injury, neuroma-in-continuity"<sup>3</sup>, which is essentially a mixture of different degrees of injury within the same nerve. The neuroma-in-continuity is a surgically challenging problem, as it is difficult to clinically estimate the degree of injury and the corresponding potential for functional recovery<sup>4</sup>. Mild lesions are characterized by spontaneous recovery, but this may take several months to become evident, especially in proximal nerve injuries such as the brachial plexus injury. Severe lesions require surgical reconstruction, but the outcome of surgery for these lesions is negatively affected by a prolonged waiting period<sup>1</sup>. The current consensus is that surgical exploration is indicated when clinical examination does not show functional recovery of the associated muscles after an empirically defined waiting period<sup>5</sup>.

It is generally accepted that fibrosis, the formation of a collagenous scar at the site of injury, is detrimental to functional recovery, although the molecular basis of this phenomenon is not fully understood <sup>1,3,4</sup>. Myofibroblasts appear to proliferate at the site of nerve injury, producing collagen and thus contributing to scar formation <sup>5</sup>. Fibroblasts also express the inhibitory proteoglycan NG2, which may play a part in blocking axon regeneration through scar tissue <sup>6</sup>.

### **Molecular mechanisms involved in peripheral nerve regeneration**

Nerve regeneration starts within hours of axonal injury. Proximally, each axon sends out several sprouts. A growth cone at the tip of each sprout contains receptors for basal lamina components and neurotrophic factors <sup>4</sup>. The regenerating axons are both physically guided to the appropriate targets by the basal lamina tubes and attracted by neurotrophic factors. If basal lamina tubes have ruptured, the chance for outgrowing axons to successfully re-establish contact with the appropriate end organs is greatly reduced <sup>7</sup>. Successful regeneration requires more than just the outgrowth of axons into the distal stump. In any case, a number of elongating axons are inevitably lost due to malcoaptation, to suture line scarring and to discrepancies in the cross-sectional dimensions of the proximal and distal stump, respectively. In addition, misrouting of axons into functionally inappropriate endoneurial tubes results in either regenerated, but useless axons or dysfunctional phenomena such as synkinesia or dysesthesia <sup>8</sup>.

Distal from the injured axon, Schwann cells distal from the site of transection change from their myelinating state into an activated nerve outgrowth-promoting state. These Schwann cells express a wide range of neurotrophic proteins including nerve growth factor (NGF), neurotrophin-3 (NT-3), neurotrophin-4/5 (NT-4/5) and brain-derived neurotrophic factor (BDNF), glial cell-line derived neurotrophic factor (GDNF, a member of the transforming growth factor superfamily) and ciliary neurotrophic factor (CNTF, a neuroactive cytokine) <sup>9</sup>. Spinal motoneurons and different subtypes of sensory neurons in the dorsal root ganglion differ in their sensitivity for these neurotrophic factors. Motoneurons express the neurotrophin receptor p75, the receptor for BDNF, tropomyosin receptor kinase (trk)B, and the multi-component receptor for GDNF composed of a common signal transduction subunit, ret and the GDNF family receptor (GFR) $\alpha$  <sup>9</sup>. The dorsal root ganglion contains at least three subpopulations of sensory neurons, nociceptive, peptidergic neurons that express the receptor for NGF, trkA, proprioceptive neurons that express the receptor for NT3, trkC, and a population of neurons that are defined by their ability to bind to the Griffonia simplicifolia isolectin B<sub>4</sub>, which express the receptors for GDNF, GFR $\alpha$  and ret <sup>10</sup>. The function of the latter population of neurons is not entirely clear, but they appear to play a role in nociception <sup>10</sup>.

The initially elevated expression of neurotrophic factors by Schwann cells, and their corresponding capability to support regeneration decreases after a period of several

weeks to months<sup>9</sup>. This contributes significantly to the lack of long distance regeneration and poor functional recovery after proximal peripheral nerve lesions<sup>11</sup>. Interestingly, the expression of several of these factors is different in Schwann cells from sensory nerves and motor nerves and this differential expression improves regeneration of motoneurons through motor nerve grafts compared to sensory grafts and vice versa<sup>12</sup>. This demonstrates the profound and differential influence of neurotrophic factors on the regeneration of subpopulations of neurons (figure 1).

Given their physiological role in regeneration and the apparent decrease of these factors over time, it is not surprising that neurotrophic factors have been applied experimentally in attempts to enhance functional recovery of the peripheral nerve. Unfortunately, their application has been hampered for a number of reasons. First, systemic or intraventricular administration of a neurotrophic factor can cause side

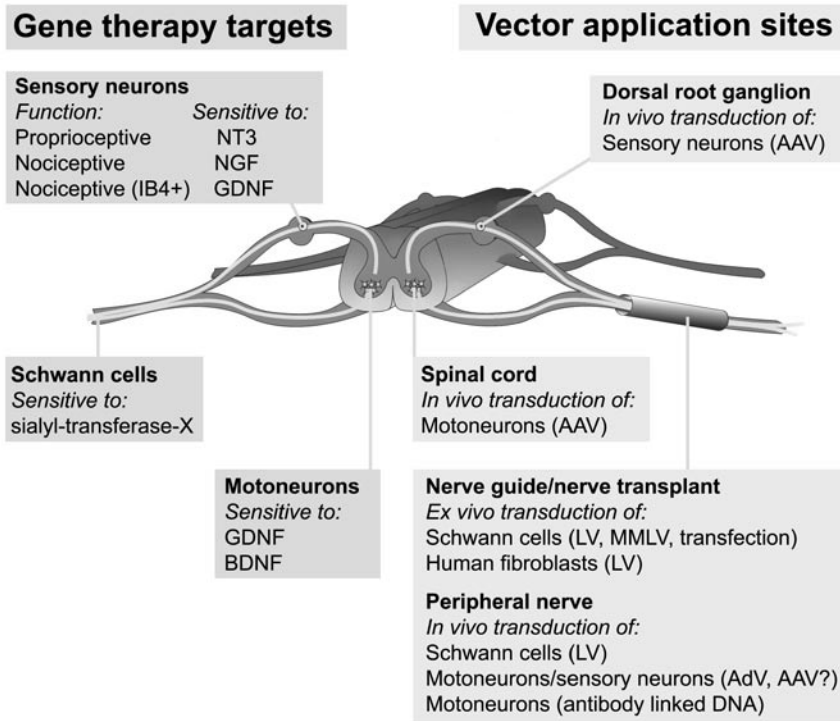


**Figure 1** Schematic representation of the spinal cord and the peripheral nerve, with motoneurons in the spinal cord and sensory neurons in the dorsal root ganglion projecting into the peripheral nerve. On the left, potential cellular targets for the application of gene therapy and their known sensitivity to various neurotrophic factors are shown. On the right, an overview is shown of the sites where nonviral and viral vectors have been applied and which cell types have been transduced.

effects<sup>14</sup>. A clinical trial with repeated local cutaneous injections of NGF to treat diabetic neuropathy was unsuccessful because pain at the site of injection made it impossible to reach the level of NGF required for neuroprotection<sup>13</sup>. Second, neurotrophic factors penetrate poorly into nervous tissue. In brain parenchyma, for instance, they diffuse only 1 to 2 mm<sup>14</sup>. Finally, neurotrophic factors have a short half-life and a tendency to degrade fast<sup>15,16</sup>, necessitating repeated applications if the goal is to achieve a sustained effect on a time consuming process like regeneration<sup>17</sup>.

Perhaps due to these problems, the results of the experimental application of neurotrophic factors to enhance regeneration in nerve repair models have not been overwhelmingly positive. The addition of recombinant NGF or GDNF to fibrin sealant applied at the site of nerve repair leads to minor improvements in functional recovery tests, and only NGF increases the number of regenerated motoneurons<sup>18</sup>. The application of NT4 in a similar model led to modest, but significant improvements in functional recovery, axon numbers and myelination of axons<sup>19</sup>. The application of NGF or NT3 through osmotic mini-pumps did not lead to long-lasting improvements of anatomical or functional recovery at 12 weeks post-lesion in a rat model for sciatic nerve transection<sup>20</sup>. A combination of GDNF and BDNF applied at the site of repair through osmotic mini-pumps increased the number of regenerated motoneurons in a model of chronic axotomy<sup>21</sup>, while the effect of BDNF alone appears to be either inhibitory or stimulatory, depending on the dose applied<sup>22</sup>.

In conclusion, the small and inconsistent effects previously found with exogenous neurotrophic factors may in part be related to the difficulties in the delivery of these factors. Here we will argue that a gene-therapy-based delivery strategy may resolve these problems.

### **Viral vectors: tools for local, sustained expression of therapeutic proteins**

Gene therapy can be defined as the introduction of genetic material into living cells with the aim of treating a disease, and the inserted gene is referred to as a transgene. Cells can be genetically modified outside the body and then reimplanted (usually referred to as *ex vivo* gene therapy) or the genetic material can be applied directly to cells in the living organism (usually referred to as direct *in vivo* gene therapy).

Compared to the local or systemic application of a protein, gene therapy has three main advantages: 1) Genes encoding any desired protein with therapeutic potential can in principle be introduced in the target cell; 2) Transduced cells will continuously express the therapeutic protein, effectively turning them into “biological mini-pumps”. This is especially useful for proteins that degrade quickly, such as neurotrophic factors; 3) Local expression of a transgene by transduced cells mimics the physiological situation as it results in locally elevated protein levels thereby in principle preventing unwanted effects on more distant cell populations.



There are several methods to insert genetic material into living cells, which can broadly be divided in non-viral and viral approaches. Transfection, which creates transient pores in the cell membrane to allow the uptake of DNA, is a common non-viral method to insert genetic material to cultured cells *ex vivo*. For non-viral *in vivo* gene transfer to cells, DNA molecules can be linked to targeting antibodies <sup>23</sup>.

Viral vectors are modified viruses that have retained the ability to insert foreign genetic material into cells, but are unable to replicate within the cell. Viral vector-mediated delivery of genetic material into cells is referred to as “transduction”. They contain an expression cassette containing a promoter, a gene of choice and other elements regulating expression. In the peripheral nerve, viral vectors can be used to either transduce Schwann cells distally from the transected nerve fibers (to induce expression of neurotrophic factors or extracellular matrix proteins) or to transduce neurons (to mediate expression of outgrowth-stimulatory proteins, survival factors or receptors for neurotrophic factors). Although viral vectors can be injected into the spinal cord to transduce neurons <sup>24</sup>, for purposes of clinical applicability, vectors that are capable of retrograde transduction, i.e. after injection in the nerve, are more desirable. In the next section we will provide an overview of the experimental application of viral vectors in various models for peripheral nerve injury. Figure 1 provides a schematic representation of the peripheral nerve, highlighting the possible application sites and targets of viral vectors.

### **Different types of vector and their application in the peripheral nerve**

Over the last 25 years, a range of viral vectors have been developed based on retrovirus, herpes simplex virus (HSV), adenovirus (AdV), adeno-associated virus (AAV) and lentivirus (LV). The characteristics of both non-viral vectors and most viral vectors have been studied in models for peripheral nerve regeneration.

#### *Non-viral gene transfer*

Experiments with Schwann cells that were genetically modified by *ex vivo* transfection showed that the overexpression of different isoforms of fibroblast growth factor-2 (FGF-2) has differential effects on regeneration through synthetic nerve guides. 18-kDa-FGF-2 appears to inhibit the myelination of regenerating axons, whereas 21-/23-kDa-FGF-2 mediates the recovery of sensory function and long-distance myelination of regenerating axons <sup>25,26</sup>. The effect of the overexpression of the different isoforms of FGF-2 was not compared to the autologous nerve graft.

Although these studies show significant effects of overexpression of FGF-2 on regeneration, the transfection protocol used requires the removal, culture and reimplantation of autologous Schwann cells in nerve guides and only leads to short term expression of the transgene.



Non-viral vectors have also been applied *in vivo* to the transected peripheral nerve. The injection of DNA encoding GDNF linked to an antibody that binds to the p75 receptor led to the retrograde transduction of motoneurons, expression of the transgene for at least 10 weeks and increased survival of axotomized motoneurons<sup>23</sup>. An exciting possibility of this approach is that in principle, specific neurons can be targeted with antibodies directed against specific neurotrophin receptors, but the number of transduced cells and the level of transgene expression with this method are relatively low compared to what is normally seen with the use of viral vectors.

#### *Early retroviral vectors*

A retroviral vector based on the moloney murine leukaemia virus (MMLV) was the first viral vector for gene transfer<sup>27</sup>. Retroviral vectors insert the gene of interest into the host genome and direct long term transgene expression. As it only infects dividing cells, this vector is less suitable for direct *in vivo* gene transfer to the nervous system, which mostly contains post-mitotic cells, but it is a reliable method to transduce cells *ex vivo* prior to implantation. This approach has been used to induce overexpression of NGF in fibroblasts prior to implantation in the brain of human Alzheimer's disease patients<sup>28</sup>. In the peripheral nerve, retroviral vectors have been applied in 2 studies to transduce Schwann cells *ex vivo* prior to being seeded in artificial nerve guides. Regeneration was significantly enhanced through nerve guides containing GDNF-expressing Schwann cells compared to empty nerve guides, but similar to guides filled with naïve Schwann cells<sup>28</sup>. Hence, the overexpression of GDNF had an added, albeit small, benefit in this specific model. In an approach aimed at stimulating nerve regeneration indirectly by influencing the migration of Schwann cells, a retroviral vector was used to transduce Schwann cells to express sialyl-transferase-X, a protein that enhances Schwann cell motility, prior to being seeded in silicone tubes. This led to significantly increased fiber diameter, myelin thickness and functional recovery compared to non-transduced SCs<sup>29</sup>.

Both experiments described above show that *ex vivo* transduced Schwann cells enhance regeneration when compared to naïve Schwann cells in artificial nerve guides. Unfortunately, in both experiments regeneration through tubes with transduced Schwann cells was not compared to the surgical strategies currently in clinical use, e.g. direct coaptation of nerve ends or autologous nerve grafting. It will be essential to show a significantly improved regeneration compared to autologous nerve grafting in the future if artificial nerve guides containing modified Schwann cells are to become a clinically viable strategy.

#### *Herpes Simplex viral vectors*

Among the first to be applied directly *in vivo* to the nervous system were viral vectors

based on the Herpes Simplex Virus (HSV), which was chosen for its innate neurotropism, maintenance of life-long latency in neurons and its large cloning capacity<sup>30,31</sup>. An interesting property of HSV-based vectors in the light of peripheral nerve regeneration is that they are capable of retrogradely transducing spinal motor and sensory neurons after injection in the rat or mouse sciatic nerve, leading to the expression of a reporter gene for up to 1 month<sup>32</sup>. However, HSV vectors also have a number of limitations, including virus-associated toxicity<sup>32</sup>. Furthermore, it has been notoriously difficult to produce HSV stocks that are of sufficient titer for in vivo use and are completely free of replication-competent helper virus<sup>33</sup>.

### *Adenoviral vectors*

AdV vectors are derived from adenovirus. They are relatively easy to produce and can transduce both dividing and non-dividing cells. Their most important limitation is that an immune response to transduced cell causes inflammation and tissue damage and limits the duration of transgene expression<sup>32</sup>. The in vivo application of AdV vector to the peripheral nerve after a crush injury leads to high levels of transgene expression in a large number of Schwann cells<sup>34</sup>, but disappears after approximately 2 weeks. Such a short period of expression, however, may be enough in proof-of concept studies. An additional benefit of AdV is that it can be applied to transduce neurons either directly or retrogradely. The injection of AdV into the intact rat sciatic nerve led to the expression of the reporter gene in small-diameter neurons of the dorsal root ganglion<sup>35</sup>. The local application of AdV leads to transduction of motoneurons in the nucleus ambiguus<sup>36,37</sup>. AdV-mediated expression of GDNF in the laryngeal nerve after a crush injury led to improved functional recovery, an increase in the diameter of regenerated axons and promoted myelination<sup>37</sup>. AdV-mediated overexpression of BDNF and GDNF had a neuroprotective effect in a model of vagal nerve avulsion<sup>36</sup>. Treatment with adenovirus encoding GDNF, BDNF, or transforming growth factor beta2 significantly prevents the loss of facial motoneurons after avulsion, enhances choline acetyltransferase immunoreactivity and prevents the induction of nitric oxide synthase activity in these neurons<sup>38</sup>.

### *Adeno-associated viral vectors*

Adeno-associated virus is a small virus that occurs naturally in humans and some primates. Vectors based on AAV have rapidly gained popularity, as they are non-toxic, do not elicit an immune response against transduced cells and direct long term transgene expression<sup>39</sup>. In the AAV vector systems currently in use, all viral protein-encoding genes have been deleted and substituted with a transgene expression cassette. The AAV prototype, AAV2, preferentially infects neurons and is capable of transducing sensory neurons in the dorsal root ganglion<sup>40</sup> and motoneurons in the spinal cord

after direct injection<sup>24</sup>. The AAV-mediated overexpression of BDNF and GDNF led to enhanced survival of motoneurons in a rat model for nerve root avulsion<sup>24</sup>. Although there has been one report of the retrograde transduction of spinal motoneurons in mice with AAV2<sup>42</sup>, it has been difficult to obtain similar results in larger mammals. Unfortunately, AAV2 does not transduce Schwann cells, but new AAV serotypes that are currently emerging have tropism for different cell types<sup>39</sup>. AAV is the subject of several clinical trials for nervous system diseases including Alzheimer's disease ([www.ceregene.com](http://www.ceregene.com)) and Parkinson's disease<sup>41</sup>. To our knowledge, no adverse effects of the in vivo application of AAV have been reported so far in these trials.

### *Lentiviral vectors*

The first lentiviral vector reported to stably transduce non-dividing cells in vivo was based on the human immunodeficiency virus<sup>42</sup>. Recently, additional lentiviral vectors have been developed, including a vector based on equine infectious anemia virus (EIAV). In general, lentiviral vectors have a favourable toxicity profile, infect dividing and non-dividing cells and direct long term transgene expression in the nervous system<sup>43</sup>. Lentiviral vectors insert the transgene into the host genome. Tropism for specific cell types depends on which vector capsid is used. Currently, the vesicular stomatitis virus G glycoprotein (VSV-G) is the envelope that is most commonly used to pseudotype LV as it infects a wide range of cells. Pseudotyping a lentiviral vector with Rabies G protein (RabG) makes it capable of transducing motoneurons retrogradely<sup>44</sup>. Overexpression of GDNF in motoneurons by a RabG coated EIAV vector enhances cell survival in a mouse model for amyotrophic lateral sclerosis<sup>45</sup>.

In our laboratory, the direct in vivo injection of a VSV-G coated lentiviral vector in a peripheral nerve led to transgene expression by Schwann cells up to 16 weeks in a model for ventral root avulsion and reimplantation (~~Hendriks et al, in press~~). This is therefore an attractive vector for the long term delivery of neurotrophic factors in a model for peripheral nerve regeneration. Furthermore, the injection of a lentiviral vector into cultured segments of human sural nerve led to the transduction of large numbers of cells and the continuous production of biologically active NGF (~~Tannemaat et al, in press~~). In contrast to the transduction of Schwann cells in the rat peripheral nerve, we found that in the human nerve, predominantly fibroblasts outside nerve fascicles were transduced (figure 2). This was likely the result of physical properties of the fascicles in the human nerve, which contains dense, highly myelinated fascicles. The flow of viral vector particles naturally follows a path of least resistance after injection, resulting in a buildup of vector particles in the loose tissue surrounding the fascicles. These differences between the transducibility of rat and human nerve tissue show the importance of performing experiments on human material as well as animal models. An appealing aspect of the LV-mediated transduction of nerve grafts is that it can be

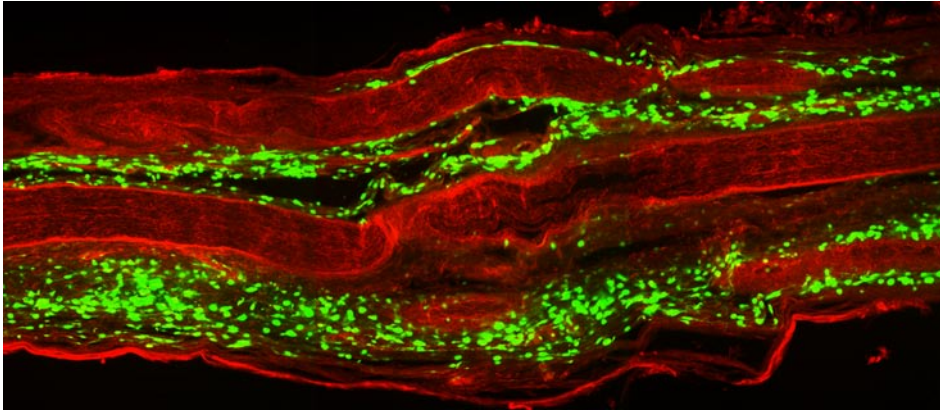


**Figure 2** Image of a cultured human sural nerve after injection of a lentiviral vector encoding green fluorescent protein, showing numerous bright green cells expressing the transgene. Transduced cells are located within the epineurium, surrounding nerve fascicles (red), but no green cells are found within densely myelinated fascicles themselves. More details on this study can be found in Chapter 4.

performed without changing the routine practice of nerve grafting. Table 1 provides an overview of all methods of gene transfer described above, with the emphasis on those properties that are relevant for application in the peripheral nerve.

### **Future perspectives and conditions to be met for clinical application**

Although viral vector mediated overexpression of neurotrophic factors has great benefits as a novel method to investigate and perhaps improve the results of peripheral nerve repair, there are a number of technical and biological issues that have to be addressed before any clinical application can be considered. The sensitivity of the different neuronal subpopulations of the peripheral nerve to different neurotrophic factors<sup>9</sup> and recent research on the differential expression of several neurotrophic factors by Schwann cells of sensory and motor nerves<sup>12</sup> clearly show that there is an exciting possibility to specifically modify the regenerative response of different populations of neurons in the lesioned peripheral nerve with viral vectors. However, it must be shown unequivocally that the overexpression of neurotrophic factors has a beneficial effect on functional recovery in clinically relevant models for peripheral nerve lesions before clinical application can be considered. Other issues that need to be resolved can broadly be divided in three categories: potential problems with the viral vectors themselves, potential problems inherent to the overexpression of neurotrophic factors and issues related to the long term local production of these substances. These concerns will be discussed in more detail below.

|                      |   | Non-viral methods                    |                                 | Viral vectors    |                            |                 |  |                 |
|----------------------|---|--------------------------------------|---------------------------------|------------------|----------------------------|-----------------|--|-----------------|
|                      |   | Trans-<br>fection<br>of a<br>plasmid | Anti-<br>body-<br>linked<br>DNA | Retro-<br>viral  | Herpes<br>Simplex<br>Viral | Adeno-<br>viral | Adeno-<br>associ-<br>ated viral<br>(sero-<br>type 2) | Lenti-<br>viral |
| Gene transfer        | <i>ex vivo</i>                          | +                                    | -                               | +                | +                          | +               | +  | +               |
|                      | <i>in vivo</i>                          | -                                    | +                               | -                | +                          | +               | +  | +               |
| Cell type            | neurons (direct)                        | -                                    | +                               | -                | +                          | +               | +  | +               |
|                      | neurons (retrograde)                    | -                                    | +                               | -                | +                          | -               | -/+*   | -/+**           |
|                      | Schwann cells                           | <i>(ex vivo)</i>                     | ?                               | <i>(ex vivo)</i> | -                          | +               | -  | +               |
| Transgene expression | short-term                              | +                                    | +                               | +                | +                          | +               | +  | +               |
|                      | long-term                               | -                                    | +                               | +                | -                          | -               | +  | +               |
| Safety               | Immune response to transduced cells     | -                                    | -                               | -                | +                          | +               | -  | -               |
|                      | non-toxic vector                        | +                                    | +                               | +                | -                          | -               | +  | +               |
|                      | clinical grade vector batches available | +                                    | ?                               | +                | -                          | -               | +  | -               |

**Table 1** Various properties of methods currently in use to genetically modify cells in the peripheral nervous system. \*AAV2 has been reported to retrogradely transduce motoneurons in mice, but these results have so far not been replicated in larger mammals. \*\* Retrograde transduction of motoneurons has been reported with Rabies G protein coated lentiviral vector, but not with *vesicular stomatitis virus glycoprotein* coated lentiviral vector.

### *Potential issues related to viral vectors*

The two most promising vectors currently available are AAV and LV, which have highly favourable toxicity profiles. However, the applicability of AAV in peripheral nerve regeneration studies will be greatly improved with the development of serotypes that are capable of either retrogradely transducing neurons consistently in a rat model<sup>46</sup> or effectively transducing Schwann cells. Although LV has the capacity to transduce Schwann cells, it has been argued that stable producer cell lines must be developed before lentiviral vectors can be used in a clinical setting<sup>43</sup>.

### *Potential issues related to neurotrophic factors*

The second potential drawback of neurotrophic factors as therapeutic agents is that some of them, specifically NGF and BDNF, are important modulators of pain<sup>10</sup>. NGF is upregulated in inflammatory conditions, and NGF-neutralizing molecules are effective analgesic agents in many models of persistent pain. It should be noted, however, that the autonomously elevated levels of NGF distal to the lesion site after a peripheral nerve lesion<sup>9</sup> do not lead to pain in patients suffering from peripheral nerve injuries<sup>1</sup>.

An advantage of viral vector-mediated overexpression of NGF in this respect may be that the location, production and release of NGF closely mimic the physiological situation. After the clinical trial to treat diabetic neuropathy with recombinant NGF failed because of the local pain caused by injection of NGF in the skin, the principal investigator of that trial stated that these adverse side-effects could possibly have been prevented through the use of viral vector-mediated delivery of NGF <sup>47</sup>.

### *Potential issues related to long term local production*

A third possible problem with transduction of cells in the peripheral nerve, is the fact that neurite outgrowth appears to be the result of a gradient of neurotrophic factors, both *in vitro* <sup>48</sup> and *in vivo* <sup>17,49</sup>. Regenerating neurites grow towards an increasing concentration of neurotrophic factor. Viral vector-mediated expression, however, results in elevated levels of neurotrophic factor confined to the area of transgene expression. Regenerating fibers will therefore grow towards, but not past an area of viral vector-mediated overexpression, as this requires them to continue to regenerate against a negative gradient of neurotrophic factor. This phenomenon has been observed after viral-vector mediated overexpression of BDNF and GDNF in a model for root avulsion and has been described as the “candy store effect” <sup>24</sup>. However, it may be possible to avoid this pitfall with the use of viral vectors in which transgene expression can be switched off after regenerating axons have entered the nerve repair site. Viral vectors in which transgene expression is regulated by a tetracycline have been developed <sup>50</sup>. In cells transduced by these vectors, the production of the therapeutic protein can be switched on (or off) *in vivo* through the oral intake of doxycycline. In an animal model for Alzheimer’s disease this vector has been shown to effectively regulate local transgene expression and neuronal rescue in the brain <sup>51</sup>, and it has been shown recently that in a spinal cord lesion model, trapping of regenerating fibers could be avoided by transient local expression of neurotrophic factors with regulatable gene expression <sup>52</sup>. However, issues regarding the potential immunogenicity of the tetracycline-controlled transactivator, which is of bacterial origin <sup>50</sup>, will have to be resolved before clinical application can be considered.

### **Concluding Remarks**

In recent years, the understanding of the important role that neurotrophic factors play in regeneration of the peripheral nerve has expanded significantly. Furthermore, proteomics <sup>53</sup> and micro-array based gene expression profiling techniques <sup>54,55</sup> now make it possible to investigate the molecular basis of both peripheral nerve injury and regeneration in even more detail. The discovery of novel factors, in particular axon guidance molecules, will be instrumental to investigate the role of these proteins in directing regenerating nerve fibers to the correct target cells. This is central to the

success of novel treatment strategies since misrouting of nerve fibers is a frequent problem in peripheral nerve repair<sup>8</sup>. Combining the newly gained insights in the role of neurotrophic factors (and perhaps the discovery of novel axon guidance molecules) with viral vector-mediated gene delivery will allow future research to effectively study their role on peripheral nerve regeneration *in vivo*.

The safety and favourable toxicity profile of current viral vectors, specifically LV and AAV, makes them suitable for application in humans. For peripheral nerve research, this will make it easier to translate positive results obtained in the laboratory to clinical trials with human subjects. For these reasons, the use of viral vectors is a highly attractive concept that holds great promise as a novel adjuvant therapy to microsurgical peripheral nerve reconstruction.





# Chapter 2

Human neuroma contains increased levels of semaphorin 3A, which surrounds nerve fibres and reduces neurite extension in vitro

Martijn R Tannemaat, Joanna A Korecka, Erich ME Ehlert, Matthew RJ Mason, Sjoerd G van Duinen, Gerard J Boer, Martijn J Malessy, Joost Verhaagen

*Journal of Neuroscience*. 2007 Dec 26;27(52):14260-4

## Abstract

Neuroma formation after peripheral nerve injury is detrimental to functional recovery and is therefore a significant clinical problem. The molecular basis for this phenomenon is not fully understood. Here we show that the expression of the chemorepulsive protein semaphorin 3A (sema3A), but not semaphorin 3F, is increased in human neuroma tissue that has formed in severe obstetric brachial plexus lesions. sema3A is produced by fibroblasts in the epineurial space and appears to be secreted into the extracellular matrix. It surrounds fascicles, mini-fascicles or single axons, suggesting a role in fasciculation and inhibition of neurite outgrowth. Lentiviral vector-mediated knockdown of Neuropilin 1, the receptor for sema3A, leads to increased neurite outgrowth of F11 cells cultured on neuroma tissue, but not of F11 cells cultured on normal nerve tissue. These findings demonstrate the putative inhibitory role of sema3A in human neuroma tissue. Our observations are the first demonstration of the expression of sema3A in human neural scar tissue and support a role for this protein in the inhibition of axonal regeneration in injured human peripheral nerves. These findings contribute to the understanding of the outgrowth inhibitory properties of neuroma tissue.

## Introduction

Severe peripheral nerve lesions can cause life-long functional impairments. A typical example is the obstetric brachial plexus injury that occurs in 2-3 per 1000 births <sup>5,6</sup>. Severe traction to the brachial plexus during birth induces the formation of intraneural scar tissue. This is known as neuroma-in-continuity <sup>3</sup>, and constitutes an environment that inhibits nerve regeneration <sup>1</sup>. Resection of the neuroma and bridging of the gap with autologous nerve grafts in order to connect proximal and distal nerve stumps usually results in some axonal regeneration, but functional recovery is never complete. Therefore, neuroma formation is a significant clinical problem.

The molecular basis for the outgrowth-inhibitory properties of neuromas is not fully understood <sup>1</sup>, but may be partly due to the excessive proliferation of fibroblasts which in turn produce inhibitory molecules <sup>5,6</sup>. A number of molecules have now

been identified which are growth-inhibitory in the nervous system, e.g. Nogo, chondroitin sulphate proteoglycans and chemorepulsive axon guidance proteins<sup>57</sup>. In the peripheral nerve neuroma, the secreted chemorepulsive axon guidance proteins semaphorins 3A (sema3A) and 3F (sema3F) may be of particular importance, for several reasons. First, their expression is upregulated in the rat sciatic nerve distal to a lesion<sup>58,59</sup>. Second, the receptor for sema3A, neuropilin 1 (npn1), is constitutively expressed in motoneurons and sensory neurons of the peripheral nerve<sup>60,61</sup> and adult sensory neurons remain sensitive to sema3A<sup>62,63</sup>. Finally, in the developing brachial plexus, sema3A and sema3F coordinate the timing and fasciculation of motor axon growth and determine the dorso-ventral organisation of motor axon projections<sup>64</sup>.

We studied the expression of sema3A and sema3F in neuroma tissue from 9 obstetric brachial plexus injury patients that was removed during reconstructive surgery. Tissue from the same nerve trunk proximal to the neuroma served as a control. A small segment of this proximal nerve stump is routinely harvested for intra-operative neuropathological assessment, as its quality influences surgical decision-making<sup>65</sup>. The availability of this material provided us with the unique opportunity to compare, within a single nerve, two types of tissue with contrasting properties: the outgrowth-inhibitory environment of the neuroma and the outgrowth-supporting environment in the stump proximal to the neuroma.

Here we show that the expression of sema3A, but not sema3F, is induced in fibroblasts present in neuroma tissue of obstetric injuries to the upper brachial plexus. Sema3A is localized around fascicles or around individual axons and inhibits the outgrowth of neurites from a neuronal cell line cultured on slices of human neuroma tissue. This is the first demonstration of the expression of this chemorepulsive protein in human neural scar tissue and the results point to a role for sema3A in the inhibition of axonal regeneration in injured human peripheral nerves.

## Materials and Methods

### *Material*

The average age of patients was 5 months (range 4 to 6 months). Nerve and neuroma material was harvested during reconstructive brachial plexus surgery, snap-frozen within 15 min after surgical removal and stored at -80°C. All material used in this study was anonymised according to the proper use code of the Pathology Department of the Leiden University Medical Center (LUMC). Neuroma material consisted of the upper branches of the brachial plexus: spinal nerve C6 (n=2) or the superior trunk of the brachial plexus (n=7). The proximal nerve stump consisted of a segment of the spinal nerve C5 (n=7) or C6 (n=2). All material was diagnosed intraoperatively as neuroma or proximal nerve stump suitable for grafting according to previously described criteria<sup>65</sup>.

*RNA isolation and qPCR*

Tissue samples were homogenized in 3 ml Trizol (Life Technologies) per 100 mg using an ultra-turrax device. After phase separation by addition of chloroform, the aqueous phase was mixed with an equal volume of 70% ethanol, further purified with an RNeasy Mini column (Qiagen) and stored at -80°C. The quality of the RNA was determined using a 2100 Bioanalyzer (Agilent). The average RNA integrity number was 8.2 (range 6.4-9.3). cDNA was synthesized from 150 ng RNA using Superscript II (Invitrogen). Real-time qPCR on sema3A and sema3F expression was performed with SYBR-green master mix (Applied Biosystems) on an ABI5700 (Applied Biosystems) <sup>66</sup>. Expression levels were normalised using the geometric mean of the 3 reference genes B2M, YWHAZ and HMBS <sup>67</sup>, which were selected from a total of 6 potential reference genes as being the most stably expressed genes in our samples. See supplemental table 1 for a list of all primer sequences.

*In situ hybridization*

A 590 basepair (bp) fragment ranging from bp 1726 to 2316 was cut from a plasmid containing the full-length human sema3A cDNA <sup>68</sup> with the restriction enzymes NcoI and HindIII and subcloned into pBluescript (Stratagene). This region was selected for the construction of riboprobe because of its limited homology to other secreted semaphorins. Digoxigenin-labeled sense and antisense cRNA probes were made as

**Supplemental table 1** List of reference genes and their primer sequences used for quantitative PCR.

| <i>neuroma and nerve</i> |                                   |                              |
|--------------------------|-----------------------------------|------------------------------|
| Gene                     | Forward primer                    | Reverse primer               |
| sema3A                   | 5'-AGTCTGGTGAATAAATGGACAACATTC-3' | 5'-GACCTGGCACTGAGCAAATCA-3'  |
| sema3F                   | 5'-TTAAGTGGCTGTTCCAGCGA-3'        | 5'-AAGCGGTCCTCTGCACGA-3'     |
| B2M                      | 5'-TGCTGTCTCCATGTTTGTATGTATCT-3'  | 5'-TCTCTGCTCCCCACCTCTAAGT-3' |
| HMBS                     | 5'-GGCAATGCGGCTGCAA-3'            | 5'-GGGTACCCACGCGAATCAC-3'    |
| YWHAZ                    | 5'-ACTTTTGGTACATTGTGGCTTCAA-3'    | 5'-CCGCCAGGACAAACCAGTAT-3'   |
| <i>F11 cells</i>         |                                   |                              |
| Gene                     | Forward primer                    | Reverse primer               |
| nfn1                     | 5'-CTGTGCAAAACCAACAGACCTAGAT-3'   | 5'-GTTCTTGTCGCCTTCCCTTCT-3'  |
| β-Actin                  | 5'-GCTCCTCCTGAGCGCAAG-3'          | 5'-CATCTGCTGGAAGGTGGACA-3'   |
| GADPH                    | 5'-TGCACCACCAACTGCTTAGC-3'        | 5'-GGCATGGACTGTGGTCATGA-3'   |
| Ef1α                     | 5'-ACCCTCCACTTGGTCGTTTTG-3'       | 5'-AGCTCCTGCAGCCTTCTTGTC-3'  |

described previously<sup>68</sup>, but to increase binding specificity, alkaline hydrolysis of the probe was not performed, resulting in a probe length of 590 bp. *In situ* hybridisation was performed on 10 µm thick transverse cryostat sections as described previously<sup>69</sup> with a probe concentration of 600 ng/ml and a hybridisation temperature of 67°C. The specificity of the hybridisation signal was verified by comparison with the sections processed with sense probe under identical conditions.

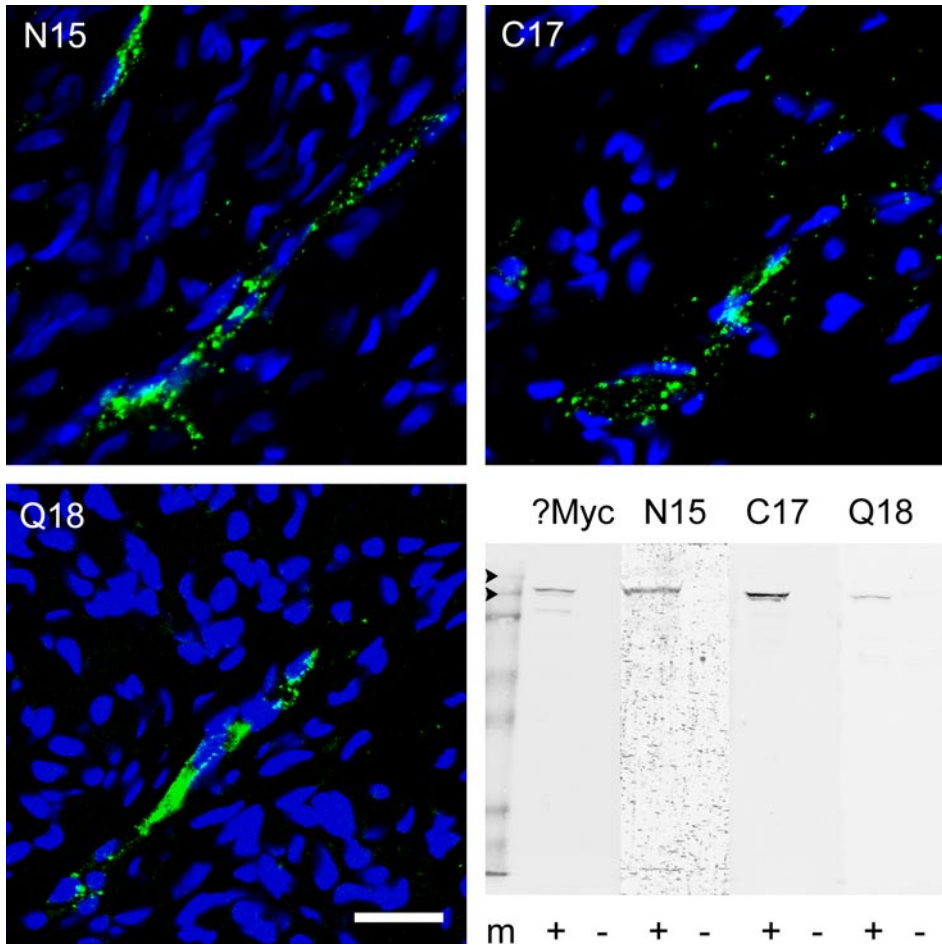
### *Immunohistochemistry*

Neuroma and proximal nerve stump samples were cut into transverse, 20 µm thick cryostat sections and fixed in 4% paraformaldehyde in 0.1 M sodium phosphate buffer pH 7.4 for 20 min. Immunohistochemistry was performed<sup>70</sup> with the primary antibodies mouse anti-Neurofilament (1:1000, 2H3 ascites; Dev. Stud. Hybridoma Bank, Univ. of Iowa) to visualise neurites, rabbit anti-S100 to visualise Schwann cells (1:200, Dako) and rabbit anti-Fibronectin (1:100, Chemicon) to visualise fibroblasts. To visualise sema3A, N15 goat anti-sema3A (1:25, Santa Cruz), C17 goat anti-sema3A (1:25, Santa Cruz) and Q18 goat anti-sema3A (1:25, Santa Cruz) were used. These three sema3A antibodies bind to distinct epitopes in sema3A. N15 binds to an epitope that lies within a region corresponding to amino acids 25-75 of the human sema3A protein, C17 to a region corresponding to amino acids 721-771 and Q18 to an epitope corresponding to a region between amino acids 675-725 (supplemental figure 1, information on epitopes from manufacturer).

For neurofilament and S100/fibronectin, Donkey anti-Mouse-Cy3 and Donkey anti-Rabbit-Cy3 were used as secondary antibodies respectively (1:400, Jackson ImmunoReagents, Westgrove, USA). For N15, C17 and Q18, biotinylated anti-Goat antibody (1:800, Vector laboratories) was used followed by Streptavidin-Cy2 (1:800, Jackson ImmunoReagents).

### *Short-hairpin-mediated knockdown of npn1 in a neuronal cell line*

F11 cells are derived from a fusion of mouse embryonic neuroblastoma cells and rat dorsal root ganglion neurons<sup>71</sup>. Neurite outgrowth in these cells can be induced by withdrawal of serum and the addition of forskolin to the culture medium. To knock down the expression of npn1 in F11 cells, they were transduced at a multiplicity of infection of 50 with a lentiviral (LV) vector expressing a short-hairpin (sh) RNA targeting the npn1 sequence CTTCAACCCACATTTTCGAT under an H1 promoter<sup>72</sup> next to a CMV promoter driving the expression of Green Fluorescent Protein (GFP). As a control, F11 cells were transduced with an LV vector encoding an shRNA targeting the Arabidopsis sequence AGATCCTCTGTTCTCTCTC (which has no homology to mammalian genes). Knockdown of npn1 was determined with qPCR as described above using primers and reference genes listed in supplemental table 1.



**Supplemental Figure 1** Antibody specificity. The anti-sema3A antibodies N15, C17 and Q18 give a similar, punctate pattern of staining on adjacent sections. Western Blot on the lysate of cells transfected with a plasmid expressing myc-tagged sema3A (+), shows a single band at approximately 105kD with all 3 sema3A antibodies. The same band is also stained with the myc-antibody. No bands are visible in the lysate of untransfected cells (-). Arrowheads in the marker lane (m) indicate the 115 and 82 kD marker bands

#### *Culture of F11 cells on neuroma sections and quantification of neurite outgrowth*

2.5 x 10<sup>4</sup> F11 cells, transduced with either npn1 knockdown or control vector, were plated onto thawed 20 µm thick cryostat sections of freshly frozen nerve or neuroma from 5 patients in 500 µl Dulbecco's modification of Eagle's medium containing 0.5% fetal bovine serum, 100 IU/ml penicillin, 100 µg/ml streptomycin, 2 mM Glutamax (Sigma) and 20 µg/ml forskolin. After 48 h, cells were fixed in 4% paraformaldehyde in

0.1 M sodium phosphate buffer and coverslipped. For each condition, three standardized images of GFP positive F11 cells were randomly made using a Zeiss Axioplan 2 microscope and an Evolution QEi digital camera (MediaCybernetics). A total number of 1599 cells and their neurites were manually outlined by an observer blinded to the treatment using Image-Pro Plus software (version 5.1, MediaCybernetics) and the total neurite outgrowth per cell was calculated. The values for npn1 knockdown or control cells were averaged for each nerve and neuroma (n=5 in four groups) before statistical analysis.

### *Statistical Analysis*

All samples were tested for normality with a Shapiro-Wilk test. In cases where  $W > 0.05$ , a paired two-tailed Student's T-test was performed, in all other cases a Wilcoxon signed-rank test was performed. A p-value  $< 0.05$  was considered significant.

## **Results**

### *Neural architecture*

Neurofilament staining showed a difference in the cellular architecture of the proximal nerve stump and the neuroma (figure 1a). In the proximal nerve stump, axons aligned tightly within fascicles and were oriented perpendicular to the transverse section. The neuroma usually had a much larger cross-sectional area (figure 1a, insets), in which axons could be identified in fascicles, mini-fascicles or as single axons. Fascicles were oriented in different directions in a chaotic pattern within the epineurium.

### *qPCR*

The expression levels of sema3A and sema3F as determined by qPCR and compared directly to the proximal nerve stump from the same patient showed a 1.8 fold higher level of sema3A in the neuroma tissue ( $p=0.008$ ), whereas no difference was observed for sema3F (figure 1b).

### *In situ hybridisation*

In situ hybridisation was performed to determine the cell type that expresses sema3A in the neuroma. Hybridisation with the antisense sema3A probe resulted in strong staining of large epineurial and perineurial cells with a typical fibroblast-like morphology surrounding fascicles (figures 2b and 2c) or mini-fascicles (figure 2e). Both the antisense and the sense probe revealed some staining of other structures, particularly of myelinated axons (figures 2a and 2b). This was considered to be background staining and not the result of specific binding to sema3A mRNA.

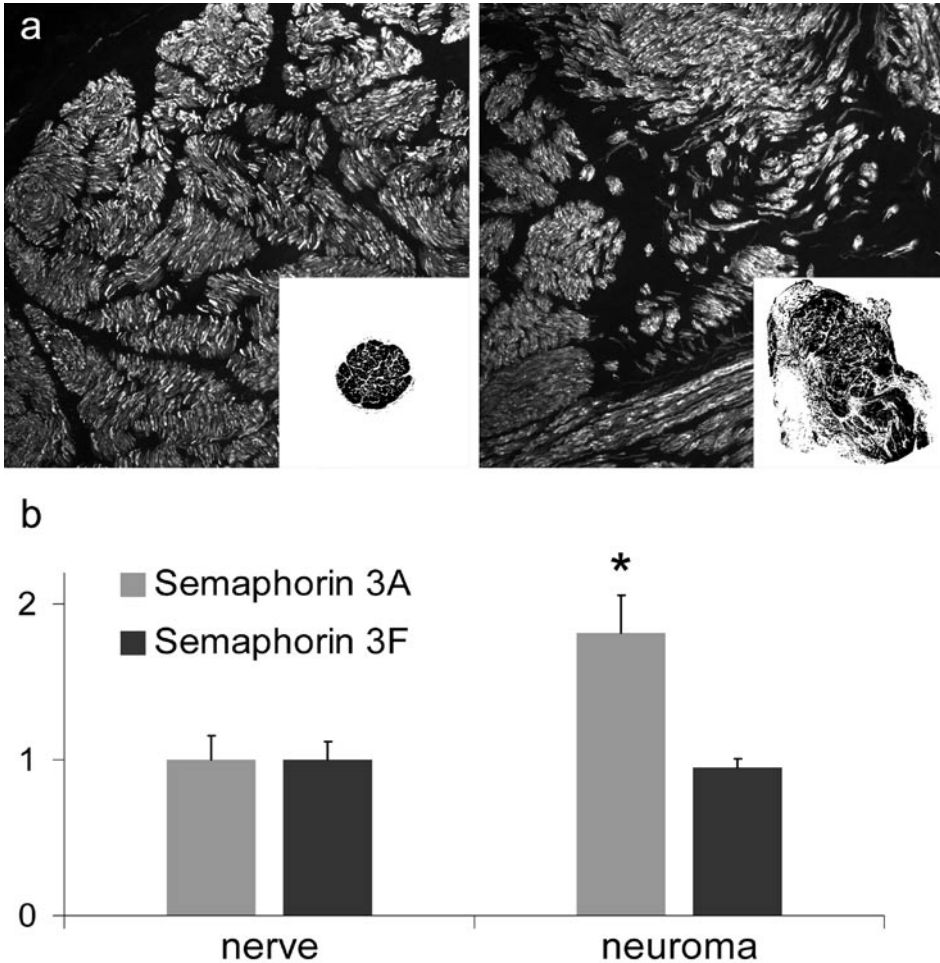


**Figure 1** Structure of the proximal nerve stump and neuroma from the human brachial plexus and the expression of semaphorin 3A and 3F.

a) Neurofilament staining of cross-sections of the proximal nerve stump and the neuroma. In the nerve (left panel), compact fascicles contain high numbers of closely aligned nerve fibres. In the neuroma (right panel), nerve fibres are randomly oriented, grouped in either fascicles, mini-fascicles or as single fibres. *Insets*: Representative images of cross-sections of nerve and neuroma, showing that the neuroma is larger and more irregularly shaped than the nerve. Scale bar = 250  $\mu$ m.

b) The average expression of *sema3A* as determined by qPCR is 1.8-fold higher in the neuroma than in the proximal nerve stump ( $p=0.008$ , Wilcoxon signed-rank test), whereas the expression of *sema3F* does not differ significantly. Bars indicate average  $\pm$  SEM for  $n=9$ .



### Immunohistochemistry

Sema3A could be visualized with the N15 antibody in some proximal nerve stumps (n=4), in which case it was almost always located in the epineurial space on the outer boundaries of the nerve (figure 3a) or in between fascicles. Very rarely, an area within a fascicle was weakly positive for sema3A (figure 3b). In contrast, sema3A staining could be seen in neuroma tissue from all 9 patients and the intensity of sema3A staining was much higher than in proximal nerve stumps. It was present in a typical punctate pattern in small, defined areas within the section, apparently secreted into the extracellular matrix. In some neuromas sema3A was also present more diffusely between nerve fascicles (figure 3c). Sema3A was observed in close proximity to mini-fascicles (figures 3c, 3e and 3f) or single nerve fibres (figure 3d). Sema3A staining was not observed around all fascicles but appeared to be present around a subset of nerve bundles. When a mini-fascicle was cut transversely, sema3A staining often appeared to surround the axon bundles (figure 3f). 3-Dimensional reconstructions of z-stacked confocal images revealed an intimate relation between secreted sema3A and axons (supplemental movie 1). Highly similar and overlapping staining patterns in adjacent sections were obtained with all three antibodies. See the supplemental data for further details on sema3A antibody specificity.

Immunohistochemistry for S100, neurofilament and sema3A (figure 2e) revealed S100 positive Schwann cells enveloping axons. No colocalisation of S100 and sema3A was observed (figure 2f). Immunohistochemistry for fibronectin and sema3A showed that sema3A was primarily present in fibronectin-rich areas associated with perineurial fibroblasts (figure 2d), consistent with the expression of sema3A mRNA by fibroblast-like cells surrounding nerve fascicles (cf. figure 2). These observations demonstrate that fibroblasts are the primary source of sema3A in the neuroma.

**Figure 2** Extrafascicular fibroblasts are the primary source of sema3A.

- a) *In situ* hybridisation with the sense probe shows some staining of myelin that is also seen with the antisense probe, but the intense staining of extrafascicular cells is not present.
- b), c) and e) Hybridisation with the antisense probe shows cells with a strong fibroblast-like morphology expressing sema3A. The highest expression levels are seen (b) surrounding fascicles, (c) between fascicles and (e) surrounding mini-fascicles.
- d) Immune histology for fibronectin (red), sema3A (N15 antibody, green) and cell nuclei (blue): sema3A is present in fibronectin-rich areas between fascicles.
- f) Immune histology for S100 (red), neurofilament (blue) and sema3A (green): S100-positive Schwann cells surround axons and do not colocalise with sema3A. The localisation of the sema3A protein closely resembles the staining of sema3A mRNA obtained with *in situ* hybridisation.

Arrows point at areas of sema3A expression, scale bar = 50  $\mu$ m in all images.



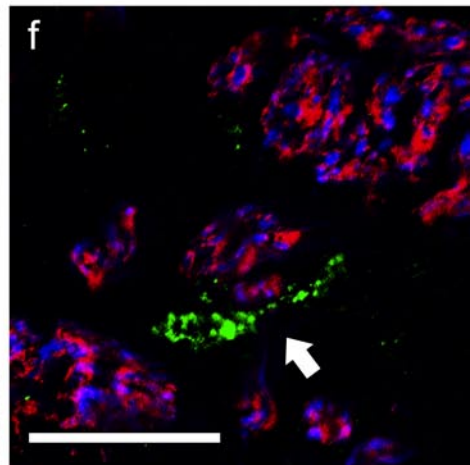
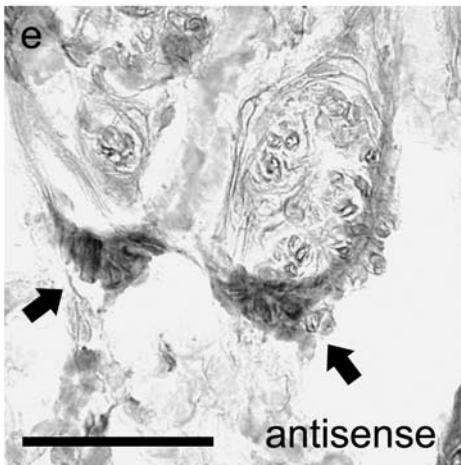
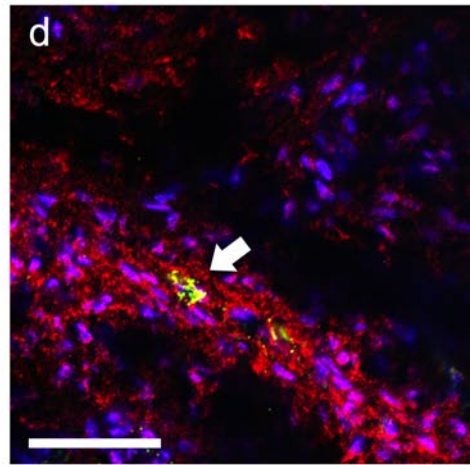
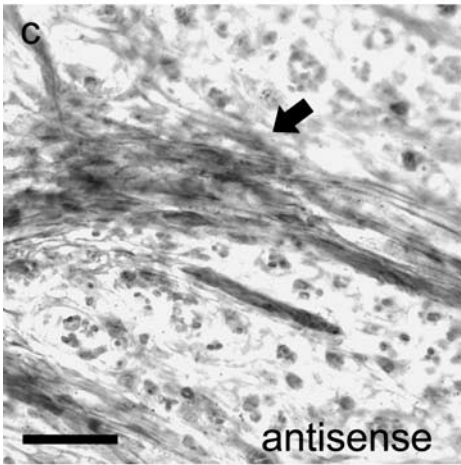
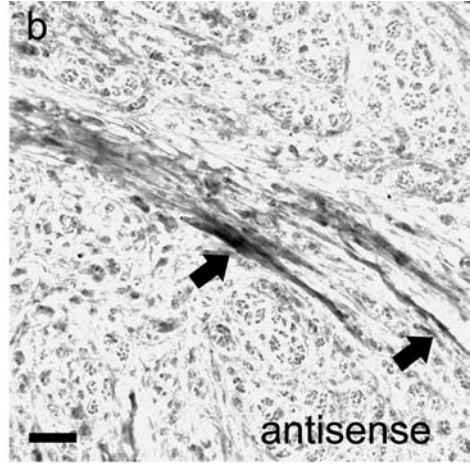
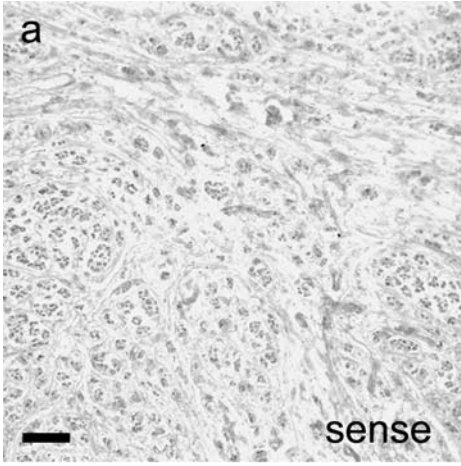


**Figure 3** Immune histology for sema3A and neurofilament in the human proximal nerve stump and neuroma. sema3A (N15 antibody, green), neurofilament (2H3 antibody, red) and cell nuclei (Topro, blue) are visualized.

a) *Proximal nerve stump*: sema3A expression was usually low and limited to the epineurium surrounding a fascicle.

b) *Proximal nerve stump*: Rarely, a weak sema3A signal was observed within a fascicle.

c) *Neuroma*: sema3A is present in a diffuse pattern in the epineurial space in the neuroma, with the highest intensity of staining in the proximity of a mini-fascicle (arrowhead).

d) *Neuroma*: sema3A surrounding a single axon.

e) and f) *Neuroma*: sema3A surrounding a minifascicle. A 3-dimensional projection of a z-stack of Figure 2e is available online.

Arrows point at areas of sema3A expression, arrowhead points at mini-fascicle, scale bar = 20  $\mu\text{m}$  in all images.

### *Neurite outgrowth assay*

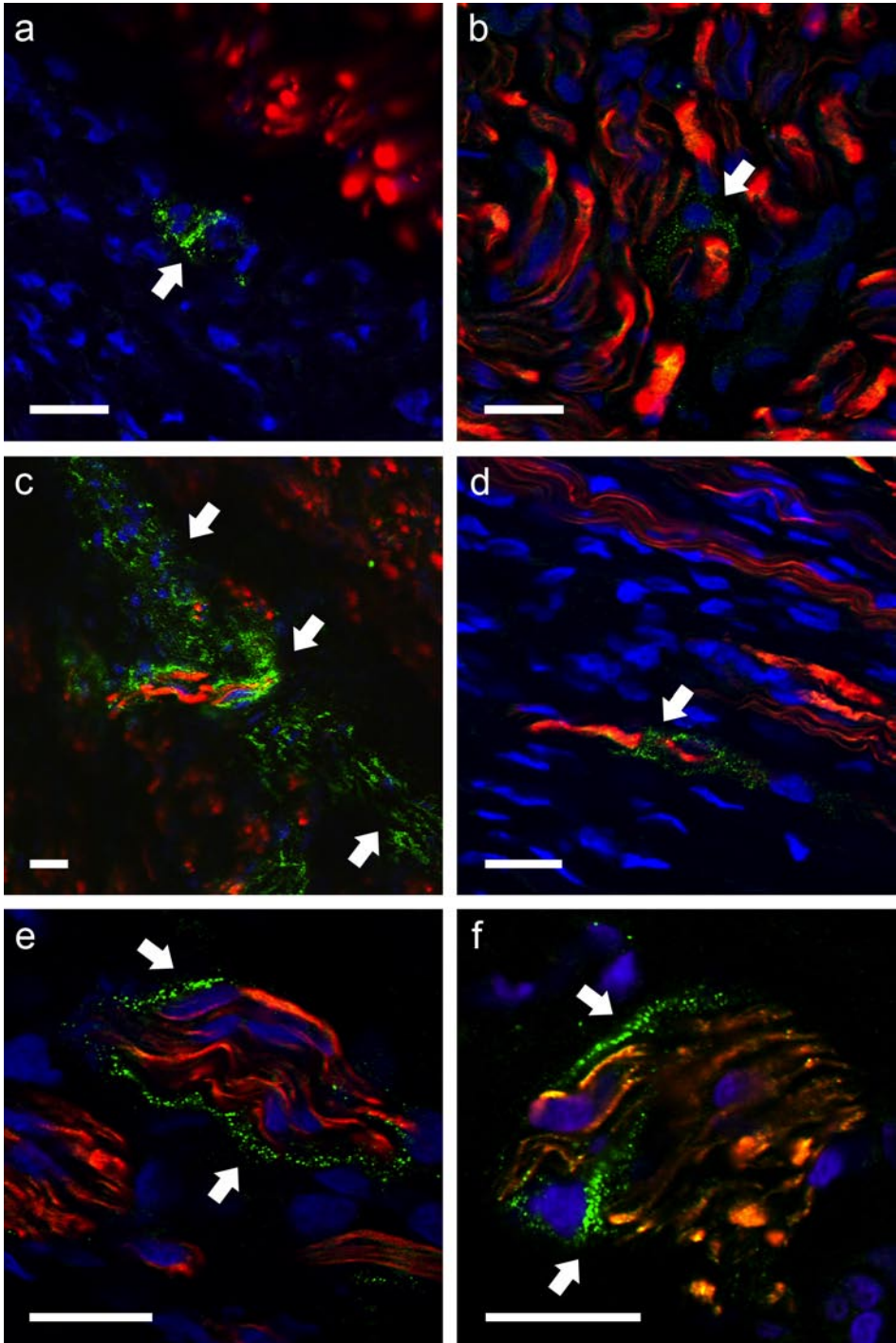
F11 cells plated on neuroma sections displayed significantly less outgrowth as compared to F11 cells plated on nerve sections (60 vs 83  $\mu\text{m}$ ,  $p < 0.05$ ; figure 4b). LV mediated expression of an shRNA targeting npn1 resulted in a knockdown of 77% of npn1 expression. Knockdown of npn1 did not affect neurite length of F11 cells grown on nerve sections ( $p = 0.69$ ). In contrast, on neuroma sections the total neurite outgrowth per cell was increased for cells with a knockdown of npn1 expression (101 vs 60  $\mu\text{m}$ ,  $p < 0.01$ , figure 4b). LV vector mediated knockdown of npn1 thus leads to increased neurite outgrowth of F11 cells when plated on neuroma tissue but not when plated on nerve tissue. This indicates that in the neuroma, sema3A has a chemorepulsive effect on growing neurites.

### **Discussion**

It is widely accepted that neuroma formation at the site of a human peripheral nerve lesion is deleterious to functional recovery. Little is known, however, about the molecular basis for this phenomenon<sup>1</sup>. In this study, we show for the first time that several months after the initial trauma the secreted chemorepulsive protein sema3A is present in human neuroma tissue.

Sema3A is expressed by epineurial and perineurial fibroblasts but not by Schwann cells. Lesion-induced upregulation of class 3 semaphorins was first noted in meningeal fibroblasts that form the core of the neural scar after penetrating CNS injuries in a rat model<sup>73,74</sup>. Sema3A is also induced in epineurial and perineurial fibroblasts distal to a rat peripheral nerve lesion<sup>58</sup>. These observations suggest that the activation of fibroblasts at lesion sites in both the CNS and PNS results in enhanced expression of inhibitory proteins like sema3A.

Sema3A protein appears to be secreted by fibroblasts and surrounds neurites and fascicles in a punctate pattern typical for extracellular matrix proteins<sup>70,75</sup>. The close



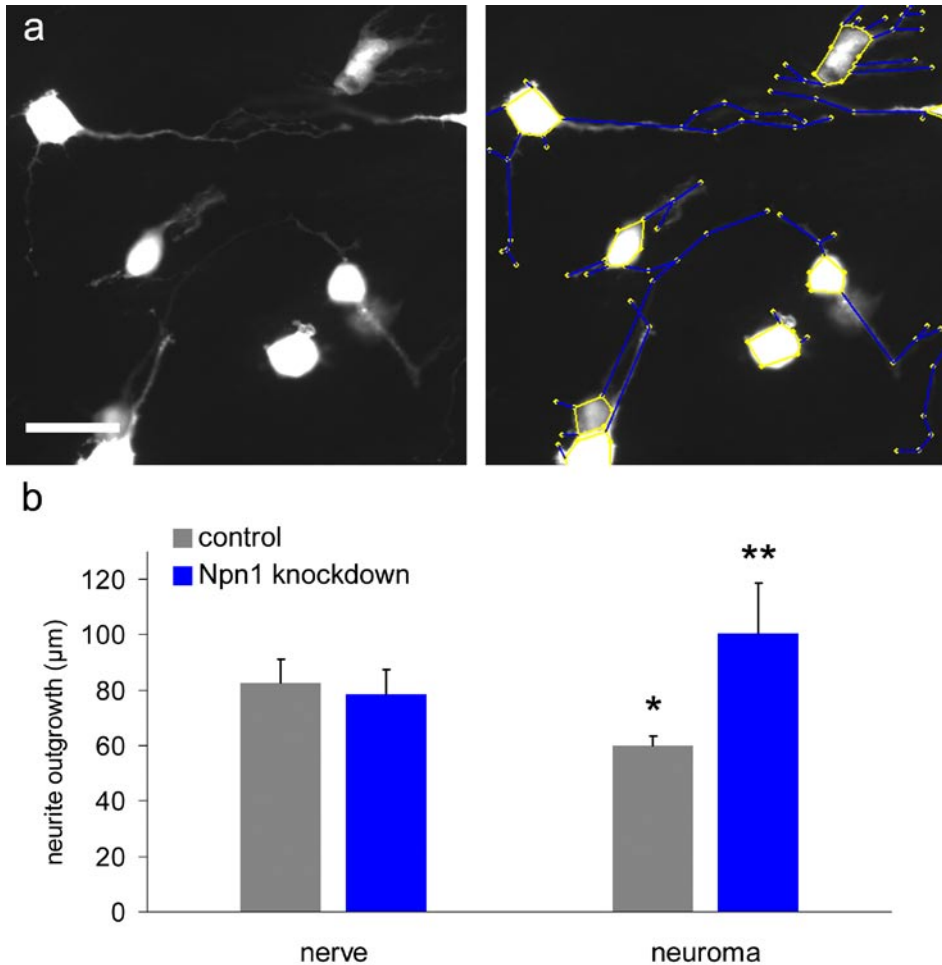


**Figure 4** Neurite outgrowth of F11 cells is inhibited on neuroma sections in vitro. Knockdown of Npn1 increases neurite outgrowth on neuroma, but not on normal nerve tissue.

a) Left panel: F11 cells cultured on neuroma tissue for 48 hours. Most F11 cells extend at least one neurite. Right panel: cells (yellow lines) and neurites (blue lines) were manually outlined by an observer blinded to the treatment. Scale bar = 50 µm.

b) Quantification of outgrowth: Neurite outgrowth of wild type F11 cells is inhibited on neuroma tissue compared to control F11 cells on nerve tissue (\* $p < 0.05$ , paired two-tailed Student's t-test). Knockdown of npn1 leads to an increase in neurite outgrowth per cell on neuroma tissue (\*\* $p < 0.01$ , paired two-tailed Student's t-test), but has no effect on the neurite outgrowth of F11 cells grown on normal nerve tissue.



proximity of sema3A to axons and its neurite outgrowth-inhibitory effect on F11 cells suggest that sema3A contributes to the fasciculation of regenerating neurites through a mechanism of “surround repulsion”, similar to what has been observed during development <sup>64</sup>. Secreted sema3A binds to extracellular chondroitin sulphate proteoglycans (CSPGs) in vitro <sup>70</sup>. CSPGs <sup>76</sup> and peripheral nerve-derived fibroblasts <sup>6</sup> induce fasciculation in vitro. A possible interaction between secreted semaphorins and CSPGs may therefore stimulate fasciculation in the neuroma.

We propose that a severe traction injury to the brachial plexus causes a disruption of the normal architecture of the nerve and leads to proliferation and redistribution of fibroblasts from the epineurial and perineurial sheets within the nerve. During the process of neuroma formation sema3A is expressed by fibroblasts. In less severe nerve injuries, this may prevent regenerating axons from growing into epineurial tissue and thus help guide them towards the distal endoneurial tubes. There, Schwann cells produce a wide range of neurotrophic factors <sup>77</sup>, eventually leading to successful regeneration. The neuroma material used in this study, however, was obtained from patients without clinical signs of spontaneous functional recovery. This suggests that in these severe lesions, the proliferation of sema3A secreting fibroblasts contributes to an environment that is hostile to regenerating fibres and counteracts the outgrowth-enhancing effects of the more distally located Schwann cells, leading to trapping of neurites within the fibrous scar. Recently a naturally occurring small molecule was discovered that antagonizes sema3A and promotes recovery of function in a rat model of spinal cord injury <sup>78</sup>. Progress in creating an animal model for the peripheral nerve neuroma <sup>79</sup> will allow future studies on the effect of this compound on axonal regeneration through neuroma tissue. Such studies could lead to novel strategies that may be applied as an adjuvant therapy to peripheral nerve surgery.

## Supplemental data Chapter 2

### *Supplemental methods: Western blot*

Western blots were performed as described previously <sup>80</sup> of neuroma tissue extract and of cells transfected 48 h previously with a plasmid expressing myc-tagged sema3A <sup>70</sup>, with control lysate of untransfected cells. The three anti-sema3A antibodies N15, C17 and Q18 (1:25, Santa Cruz) and mouse anti-Myc (1:1000, Santa Cruz) served as primary antibodies. anti-Goat IrDye 800 (1:5000, Rockland) and Donkey anti-Mouse-Cy5 (1:1000) were used as secondary antibodies. Blots were scanned and analysed using an Odyssey scanner and software (Li-COR Biosciences).

### *Supplemental results: Western blot*

Western blotting showed that all three sema3A antibodies stained a single 105kD band in the lysate of cells transfected with myc-tagged sema3A, which colocalised

with a myc-stained band. No bands were visible in medium from untransfected cells (supplemental figure 1). No bands could be detected on Western blots from neuroma tissue homogenate (data not shown). This may have been caused by the relatively low abundance of sema3A in this tissue, as it is expressed in specific areas within the neuroma in only a subpopulation of cells.

# Chapter 3

## Gene expression profiling provides novel insights in the molecular basis of misrouting of axons through the neuroma in continuity in obstetrical brachial plexus injuries: a preliminary report

Martijn R Tannemaat, Koen Bossers, Sjoerd G van Duinen, Martijn J Malessy, Joost Verhaagen  
*Manuscript in preparation*

### Abstract

Obstetrical Brachial Plexus Injuries (OBPI) are caused by traction which only rarely results in a true rupture of nerve elements. The nerve lesion typically found during exploration is a neuroma in continuity. We performed an in-depth analysis of the molecular properties of the neuroma in continuity of 8 OBPI patients with no clinical signs of functional recovery, by combining genome-wide gene expression profiling with immunohistochemical staining.

Immunohistochemical staining for neurofilament showed a reduced density and highly disorganised growth pattern of axons. Furthermore, axons were oriented in patterns that are highly suggestive for the presence of axonal guidance cues in the neuroma in continuity. Micro-array based gene expression analysis identified 722 genes that are differentially regulated in the neuroma compared to the proximal stumps. The Gene Ontology classes “extracellular matrix”, “cell adhesion” and “axon guidance” are significantly overrepresented in the list of regulated genes. A total of 18 genes with a previously documented role in axonal guidance were differentially regulated. Immunohistochemical staining for versican, one of the differentially regulated genes, showed that this proteoglycan is selectively expressed in the vicinity of regenerating axons. The results described in this paper lead to the conclusion that the human neuroma in continuity contains a considerable number of highly disorganised axons, that misrouting is a major contributing factor to the lack of functional recovery and that the regenerative paths of these axons appear to be influenced by a unique combination of axon guidance cues that are differentially expressed by the glial cells of the peripheral nerve neuroma. These differentially expressed genes may govern the disturbed axonal regeneration process in neuroma tissue and can therefore form the starting point for the development of novel therapeutic intervention strategies aimed at promoting functional recovery following OBPI.

### Introduction

In contrast to neurons of the central nervous system, axotomised neurons of the peripheral nerve are capable of regeneration<sup>81</sup>. However, the degree of functional

recovery depends on the severity of the lesion <sup>1</sup>. When axons are severed, but the nerve fascicles remain intact (axonotmesis), the prognosis is generally good, whereas a disruption of the integrity of the entire nerve (neurotmesis) usually results in only limited functional recovery <sup>4</sup>.

Obstetrical Brachial Plexus Injuries (OBPI) are among the clinically most challenging nerve injuries. They occur in 2 to 3 per 1000 births and an estimated 10% of these do not recover spontaneously and completely <sup>56</sup>. In these injuries, severe traction to the brachial plexus during birth rarely results in a true rupture of nerve elements. Instead, a neural scar (neuroma in continuity) is formed, which can be a mixture of both axonotmetic and neurotmetic injury types <sup>3</sup>. As it is usually not possible to clinically determine the degree of injury of such lesions, the current approach is to await spontaneous recovery. At present, the consensus is that surgical exploration is indicated when clinical examination does not show functional recovery after a waiting period of 3-9 months <sup>82-84</sup>. However, the outcome of nerve surgery is negatively affected by a prolonged waiting period <sup>1</sup>.

Resection of the neuroma and bridging of the gap with autologous nerve grafts in order to connect proximal and distal nerve stumps usually results in axonal regeneration. Nonetheless, even after reconstructive surgery, functional recovery of more distal targets such as the hand is never complete <sup>85</sup>. Therefore, the neuroma in continuity is a significant clinical problem with serious consequences.

Many outgrowth-inhibitory molecules have been discovered in the scar that forms after spinal cord injury (reviewed in <sup>57</sup>). Much less is known about the biological mechanisms that lead to scar formation in the peripheral nerve and cause its inhibitory effect on functional recovery. Fibrosis caused by activated fibroblasts has been described to be detrimental to functional recovery <sup>1,5</sup>. Furthermore, the proteoglycan NG2 is present in human peripheral nerve scars and appears to block axon regeneration through scar tissue <sup>6</sup>. The expression of nerve growth factor (NGF) is upregulated in painful end-neuromas and may contribute to the pathogenesis of pain <sup>86</sup>. Finally, we have recently shown that the chemorepulsive axon guidance molecule semaphorin 3A is expressed in the human neuroma in continuity and contributes to the outgrowth-inhibitory microenvironment <sup>87</sup>.

To investigate the molecular properties of the human neuroma in continuity, we performed a genome-wide gene expression analysis of neuroma tissue that was removed during reconstructive surgery from 8 severe OBPI patients with no signs of spontaneous recovery of function. Proximal to the neuroma, the nerve has a morphology that closely resembles a normal unlesioned nerve. This proximal nerve stump is the source of nerve fibers growing into nerve transplants <sup>65</sup>. A small segment of this proximal nerve stump is routinely harvested for intra-operative neuropathological assessment, as its quality influences surgical decision-making <sup>65</sup>. By performing comparative gene



expression profiling on neuroma and proximal nerve tissue from the same patient, in combination with a gene ontology analysis, we identified a unique set of differentially expressed genes that was enriched in genes involved in the modification of the extracellular matrix, cell adhesion and axonal guidance.

## Materials and Methods

### *Patient Material*

The average age of OBPI patients was 5 months (n=8; range 4 to 6 months; see table 1 for additional patient details). Nerve and neuroma material was harvested during reconstructive brachial plexus surgery, snap-frozen within 15 min after surgical removal and stored at -80°C. All material used in this study was anonymised according to the proper use code of the Pathology Department of the Leiden University Medical Center (LUMC). Neuroma material was derived from the superior trunk of the brachial plexus. The proximal nerve stump consisted of a segment of the spinal nerve C5 (n=4) or C6 (n=4) (figure 1; table 1). All material was diagnosed intraoperatively as neuroma or high quality proximal nerve stump suitable for the application of a nerve graft according to previously described criteria <sup>65</sup>.

### *Micro-array based gene expression analysis*

#### RNA ISOLATION AND QUALITY

Tissue dissection was performed by using a cryostat to cut 50 µm sections. A total of 20-30 serial, transverse sections from neuroma and proximal nerve stump were collected in pre-chilled 2 ml tubes and immediately put on dry ice. Tissue yields were typically around 50 mg. Total RNA was isolated using a combination of Trizol-based

**Table 1** Material used for micro-array based gene expression profiling. Table lists patient age in days (equals time post-injury), anatomical location of nerve and neuroma tissue, RNA quality and fluorescent dye used to label cRNA. \*RIN: RNA Integrity Number.

| # | Age (days) | Nerve | RIN* | dye | Neuroma                        | RIN* | dye |
|---|------------|-------|------|-----|--------------------------------|------|-----|
| 1 | 127        | C5    | 8.9  | Cy5 | Superior trunk brachial plexus | 8.0  | Cy3 |
| 2 | 130        | C5    | 7.9  | Cy3 | Superior trunk brachial plexus | 7.8  | Cy5 |
| 3 | 169        | C6    | 7.5  | Cy5 | Superior trunk brachial plexus | 8.6  | Cy3 |
| 4 | 148        | C5    | 9.3  | Cy3 | Superior trunk brachial plexus | 9.1  | Cy5 |
| 5 | 108        | C6    | 8.7  | Cy5 | Superior trunk brachial plexus | 8.6  | Cy3 |
| 6 | 138        | C6    | 7.4  | Cy3 | Superior trunk brachial plexus | 8.3  | Cy5 |
| 7 | 116        | C5    | 7.2  | Cy5 | Superior trunk brachial plexus | 7.8  | Cy3 |
| 8 | 146        | C6    | 7.2  | Cy3 | Superior trunk brachial plexus | 7.5  | Cy5 |

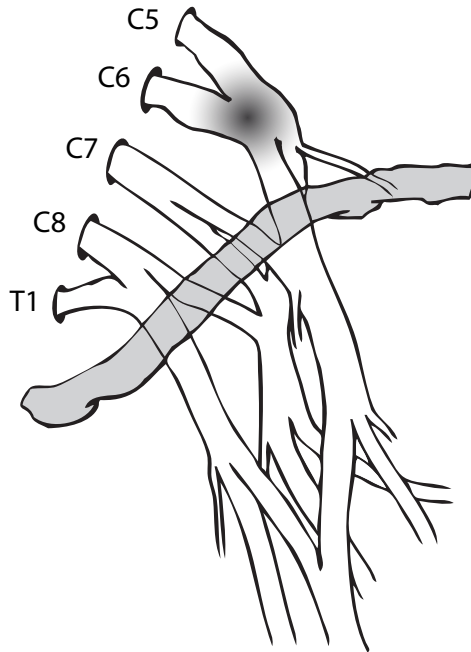


**Figure 1** Schematic overview of the brachial plexus, location of the neuroma

and RNeasy Mini Kit RNA isolation methods. Briefly, samples were homogenized in ice-cold Trizol (Life Technologies, Grand Island, New York, 3 ml Trizol per 100 mg tissue) with an ultra-turrax (IKA-Labortechnik, Staufen, Germany). After phase separation by addition of chloroform, the aqueous phase was transferred to a new RNase-free 1.5ml tube, and mixed with an equal volume of 70% RNase-free ethanol. Samples were then applied to an RNeasy Mini column (Qiagen, Valencia, California), and processed according to the RNeasy Mini Protocol for RNA Cleanup (version june 2001, from Step 3). RNA yields and purity were determined using a NanoDrop ND-1000 spectrophotometer (Nanodrop Technologies, Wilmington, Delaware). RNA integrity was determined by the RNA Integrity Number (RIN) as measured by the Agilent 2100 bioanalyzer (Agilent Technologies, Palo Alto, California). Overall, the isolated RNA was of high integrity, with an average RNA integrity number of 8.1 (range 7.2-9.3).

#### SAMPLE LABELING AND MICROARRAY HYBRIDIZATION

For microarray analysis, Agilent 44K Whole Human Genome arrays (Agilent Technologies) were used. Sample labeling and microarray hybridization and processing were performed according to manufacturer's instructions. Briefly, per patient, 200 ng of RNA from both nerve and neuroma tissue were linearly amplified and alternately labeled with either Cy3-CTP or Cy5-CTP (Perkin Elmer) with the Agilent Low RNA

Input Fluorescent Linear Amplification Kit (Agilent Technologies, protocol version 2.0, August 2003). Prior to hybridization, equal amounts (1  $\mu$ g) of Cy3 and Cy5 labeled RNA were hydrolyzed for 30 min at 60°C in 1x fragmentation buffer (Agilent Technologies). The fragmented targets were hybridized to a microarray by incubating for 17 hours at 60°C in 1x target solution (Agilent Technologies) in a rotating hybridization chamber. After hybridization, the arrays were washed at RT for 5 min in 6xSSPE/0.005% N-Lauroylsarcosine (Sigma-Aldrich, St Louis, Missouri) and 1 min in 0.06xSSPE/0.005% N-Lauroylsarcosine. Finally, microarray slides were washed for 30 seconds in acetonitrile (Sigma-Aldrich) and dried in a nitrogen flow. Microarrays were scanned using an Agilent DNA Microarray Scanner at 5  $\mu$ m resolution and 100% PMT setting. Microarray scans were quantified using Agilent feature extraction software (version 8.5.1).

#### GENE EXPRESSION ANALYSIS

Raw gene expression data generated by the feature extraction software were imported into the R statistical processing environment (<http://www.r-project.org>), and analyzed using the LIMMA package in Bioconductor (<http://www.bioconductor.org>). Intra-array normalization was performed using the loess algorithm. For some genes or expressed sequence tags (EST), multiple probes were present on the array. In these cases, the relative expressions of all probes for this gene or EST were averaged to produce a single value resulting in a relative expression value of a total of 30,983 unique genes and ESTs. P-values for differential expression between nerve and neuroma were corrected for multiple testing using the Bonferroni correction algorithm. Genes or ESTs with a corrected p-value < 0.05 were considered significantly regulated.

#### GENE ONTOLOGY OVERREPRESENTATION ANALYSIS

Gene ontology classes (GO)<sup>88</sup> that were overrepresented in the final list of significantly regulated unique genes were identified with the TopGO analysis software package for R using the *elim* algorithm<sup>89</sup>. This method improves the detection of biologically relevant classes by taking into account the underlying GO-graph topology. Approximately 56% of the unique genes and ESTs were GO-annotated. TopGO analysis was performed for the three top-level branches “biological process”, “cellular component” and “molecular function”, using all unique genes and ESTs as a background dataset. GO classes with a p-value < 0.01 were considered significant. For the three analyses described above, diagrams were plotted based on the 5 most significantly overrepresented GO-classes and their position in the gene ontology database.

#### ANALYSIS OF DIFFERENTIALLY EXPRESSED GENES

Following the calculation of expression levels and p-values for all genes on the array, and the unbiased GO analysis to identify significantly overrepresented GO-classes, the list of differentially expressed genes was further analysed in the following ways: (1) gene families of which multiple members were significantly regulated were identi-

fied (2) a literature search was performed for individual genes of interest. In this last search, emphasis was placed on genes that are a member of significantly overrepresented GO-classes, genes that are a member of a gene family with multiple regulated members and genes with a previously described or putative role in scar formation or modulation, peripheral nerve regeneration or axon guidance.

### *Immunohistochemistry*

From 3 patients, all material was used for RNA isolation for microarray analysis. From the remaining patients, material, 20 µm thick transverse cryostat sections were collected from both nerve and neuroma tissue for immunohistochemistry. The following primary antibodies were used: mouse anti-neurofilament (1:1000, 2H3 ascites; Dev. Stud. Hybridoma Bank, Univ. of Iowa) and chicken anti neurofilament (1:100, Millipore, Billerica, USA ) to stain axons and mouse anti-versican (1:1, a gift from dr R. Asher) to stain versican. *Wisteria floribunda* agglutinin (WFA) histochemistry was performed by incubating sections in biotinylated WFA (20 µg/ml; Sigma, Zwijndrecht, The Netherlands). Immunostaining was performed as described previously<sup>90</sup>. Briefly, sections were fixed in 4% paraformaldehyde in 0.1 M sodium phosphate buffer pH 7.4 for 20 min, washed three times in 0.1 M Tris/HCl-buffered saline pH 7.4 (TBS), incubated in TBS containing 0.3% Triton X-100 and 5% fetal bovine serum (blocking buffer) for 1 h and in blocking buffer containing the primary antibody (and/or biotinylated WFA) overnight at 4°C. The next day, sections were washed three times in TBS and incubated with blocking buffer containing Alexa594- or Alexa488-labelled secondary antibodies or streptavidin (Invitrogen, Carlsbad, USA) for 2 h. Finally, the sections were washed in TBS, mounted in Aquatex (Merck, Darmstadt, Germany) and coverslipped.

## **Results**

### *Aberrant patterns of axonal growth in the peripheral nerve scar*

A neurofilament staining of transverse sections revealed significant differences between the organisation of axons in the proximal nerve stump and in the neuroma (figure 1A). In the proximal nerve stump, the large majority of axons (>95%) are oriented perpendicular to the transverse section and axons are neatly aligned in well-defined nerve fascicles (figure 2A). In contrast, most axons in the neuroma have lost their longitudinal orientation and several aberrant patterns of axon alignment can be distinguished. In general, the density of axons appears to be significantly lower than in sections of the proximal nerve stump. Most axons in the neuroma are oriented in different directions in a chaotic pattern (figure 2B). Single axons that appear to be isolated within the neuroma tissue are observed regularly, but the majority of axons are aligned in small “mini-fascicles” that contain several axons that appear to have

regenerated in the same direction. Commonly, the separation of a mini-fascicle into two smaller mini-fascicles, as well as the merging of two mini-fascicles into one larger fascicle was observed (figure 2CEF). These findings indicate that fasciculation (the tendency of regenerating axons to closely align in fascicles) and defasciculation occurs frequently in the neuroma. Occasionally, two axons enter a mini-fascicle and then continue their growth in opposite directions (figure 2D), while some axons appear to leave one mini-fascicle and join another mini-fascicle nearby (figure 2F). Finally, the regenerative trajectory of axons in the neuroma is not always straight and some axons appear to make 180 degree turns in their direction of outgrowth (figure 2G). In some sections of neuroma tissue, small areas were found in which axons had an orientation similar to the axons in nerve sections, e.g., perpendicular to the transverse section in an apparently normal fascicle (results not shown). These areas appeared to represent nerve fascicles that were relatively spared by the initial trauma.

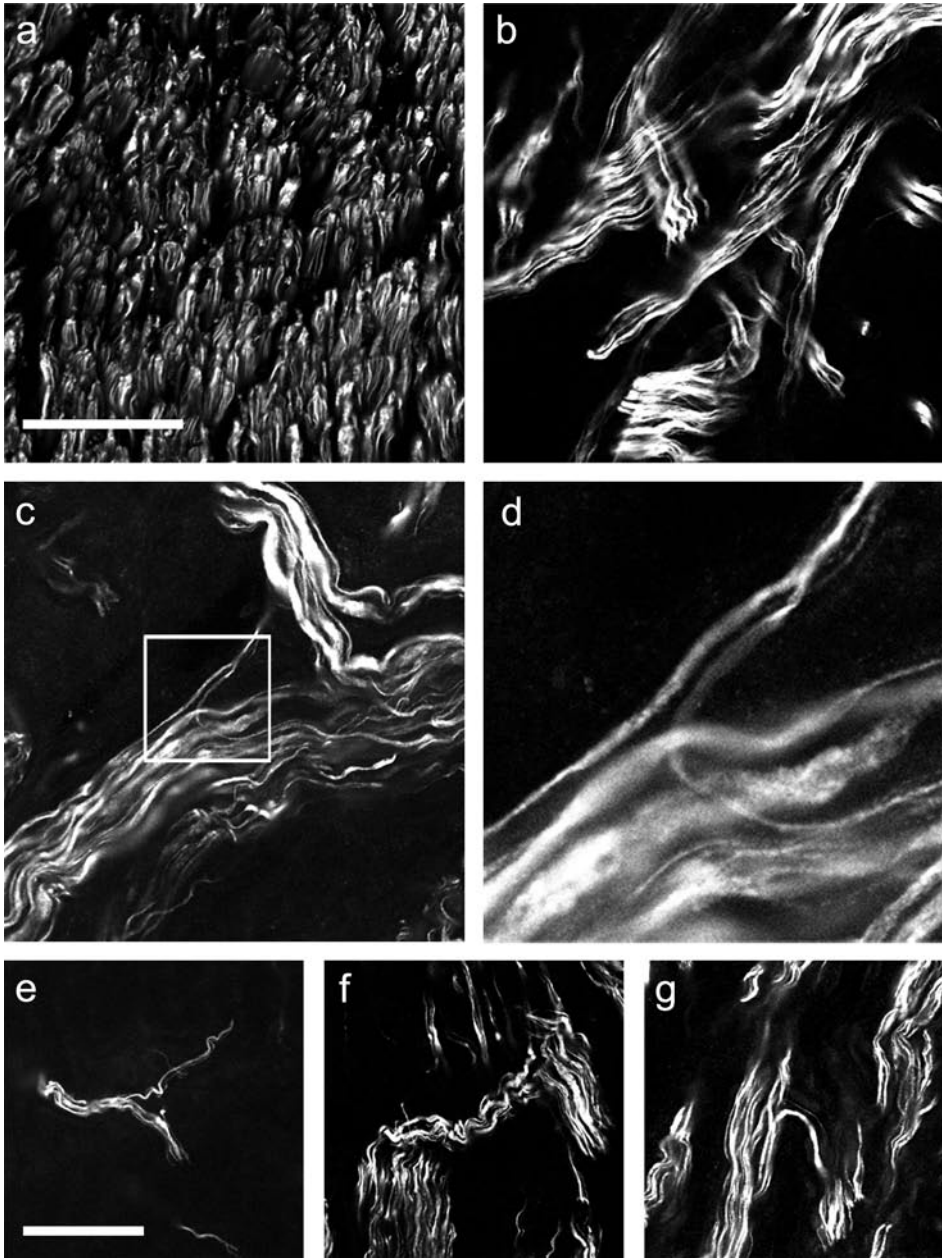
In conclusion, the anatomical observations described above indicate that the regenerative path of axons in a neuroma is disorganized as a result of an aberrant pattern of growth involving frequent fasciculation, defasciculation and turning events.

#### *Gene expression analysis*

To identify differences in gene expression between neuroma and the proximal nerve stump, we performed a genome-wide micro array analysis to compare the transcriptome of these 2 types of tissue in 8 individual patients. The expression of 722 unique genes differed significantly in neuroma tissue compared to nerve tissue (346 genes up- and 376 genes downregulated). Supplemental table 1 provides a complete list of all significantly regulated genes. This list of significantly regulated genes was then analysed in 3 ways: 1) a GO overrepresentation analysis was performed, 2) the list was analysed for gene families of which multiple members were significantly regulated and 3) the list was searched for individual genes with a known or putative effect on scar formation/modulation, axon guidance, fasciculation and/or peripheral nerve regeneration.

#### *Gene ontology analysis*

For functional data mining, the list of significantly regulated genes was subjected to GO analysis using the TopGO *elim* method. A GO-class is overrepresented if more genes in this class are differentially expressed in neuroma tissue than can be expected by chance. With a cut-off of  $p < 0.01$ , a total of 36 GO-classes were significantly overrepresented in the top-level branch “biological process”, 9 in the branch “cellular component” and 20 in the branch “biological process”. A list of all significantly overrepresented GO-classes is presented in table 2. The five most significantly overrepresented classes in each top-level branch are listed below.



For the top-level branch “biological process” the most significantly overrepresented classes were: “cell adhesion” (GO:0007155, 51 genes), “axon guidance” (GO:0007411, 13 genes), “phosphate transport” (GO:0006817, 12 genes), “detection of calcium ion” (GO:0005513, 4 genes) and “cholesterol biosynthetic process” (GO:0006695, 6 genes).



**Figure 2** Axons in the peripheral nerve scar are disorganized, but appear to be subject to specific guidance cues in the extracellular matrix surrounding them.

a) Transverse section of proximal nerve stump that were stained with anti-Neurofilament to identify axons and imaged with a confocal laser scanning microscope. All axons are aligned perpendicular to the section within well organized fascicles.

b) Axons in a neuroma are disorganized and are oriented in different directions. They often appear to grow in “mini-fascicles” containing several axons.

c) Two mini-fascicles merging (or diverging, as the direction of outgrowth could not be determined on transverse sections), suggesting that they are sensitive to fasciculation/defasciculation cues.

d) Higher magnification of the boxed area in (c) shows two axons entering a mini-fascicle and continuing to grow in opposite directions, indicating that they are sensitive to attractive cues present in the mini-fascicle. Two mini-fascicles diverge (e) and axons cross from one mini-fascicle to another (f)

g) An axon exits a mini-fascicle, makes a 180 degree turn and enters another mini-fascicle, pointing to the presence of repulsive guidance in the extracellular matrix.

Scale bar ABC: 50  $\mu$ m, EFG: 50  $\mu$ m.

For the “cellular component” branch, the most significantly regulated class was “extracellular matrix” (GO:0005578, 30 genes), followed by “axon” (GO:0030424, 8 genes), “guanylate cyclase complex, soluble” (GO:0008074, 3 genes), “integral to membrane” (GO:0016021, 164 genes) and “extracellular space” (GO:0005615, 29 genes). In the “molecular function” branch, the five most regulated GO classes were “neurotrophin binding” (GO:0043121, 3 genes), “calcium ion binding” (GO:0005509, 46 genes), “growth factor activity” (GO:0008083, 14 genes), “transmembrane receptor protein tyrosine kinase activity” (GO:0004714, 9 genes) and “serine-type endopeptidase activity” (GO:0004252, 13 genes). A graphic representation of the 5 classes listed above and their position within the hierarchical GO tree of each top level branch can be found in figures 3, 4 and 5 (“biological process”, “cellular component” and “molecular function”, respectively).

### *Differentially expressed gene families*

The list of differentially expressed genes was then searched for gene families of which several members were differentially expressed. Supplemental table 2 contains a list of all gene families of which at least two members were differentially regulated in neuroma tissue. Here, we will distinguish families that were predominantly upregulated, predominantly downregulated or families of which the members were both down- and upregulated.

Six gene families of which multiple genes were differentially expressed were predominantly upregulated: collagens, spondins/thrombospondins, CSPGs, SLRPs, kallikreins and the WNT family. In two gene families of which several genes were differentially

| GO.ID                     | Description  | An-notated genes | Signi-ficant genes | P-value  |
|---------------------------|--|------------------|--------------------|----------|
| <i>Biological process</i> |  |                  |                    |          |
| GO:0007155                | cell adhesion  | 798              | 51                 | 1,60E-06 |
| GO:0007411                | axon guidance  | 79               | 13                 | 8,20E-06 |
| GO:0006817                | phosphate transport  | 109              | 12                 | 7,40E-05 |
| GO:0005513                | detection of calcium ion   | 10               | 4                  | 0,00013  |
| GO:0006695                | cholesterol biosynthetic process                                 | 30               | 6                  | 0,00019  |
| GO:0006508                | proteolysis  | 748              | 39                 | 0,00028  |
| GO:0050770                | regulation of axonogenesis                                       | 33               | 6                  | 0,00033  |
| GO:0007501                | mesodermal cell fate specification                               | 2                | 2                  | 0,00084  |
| GO:0000187                | activation of MAPK activity                                      | 56               | 7                  | 0,00111  |
| GO:0046928                | regulation of neurotransmitter secretion                         | 8                | 3                  | 0,00121  |
| GO:0007263                | nitric oxide mediated signal transduction                        | 9                | 3                  | 0,00178  |
| GO:0019229                | regulation of vasoconstriction                                   | 9                | 3                  | 0,00178  |
| GO:0048169                | regulation of long-term neuronal synaptic plasticity             | 9                | 3                  | 0,00178  |
| GO:0006516                | glycoprotein catabolic process                                   | 19               | 4                  | 0,00191  |
| GO:0007610                | behavior   | 338              | 20                 | 0,00207  |
| GO:0001508                | regulation of action potential                                   | 47               | 6                  | 0,00224  |
| GO:0008038                | neuron recognition   | 20               | 4                  | 0,00233  |
| GO:0007417                | central nervous system development                               | 248              | 16                 | 0,00241  |
| GO:0001747                | eye development (sensu Mammalia)                                 | 50               | 6                  | 0,00309  |
| GO:0042063                | gliogenesis  | 35               | 5                  | 0,00316  |
| GO:0019228                | generation of action potential                                   | 4                | 2                  | 0,00483  |
| GO:0048812                | neurite morphogenesis  | 157              | 21                 | 0,00516  |
| GO:0007169                | transmembrane receptor protein tyrosine kinase signaling pathway | 222              | 14                 | 0,00536  |
| GO:0050769                | positive regulation of neurogenesis                              | 25               | 4                  | 0,00542  |
| GO:0006182                | cGMP biosynthetic process  | 13               | 3                  | 0,00556  |
| GO:0009612                | response to mechanical stimulus                                  | 13               | 3                  | 0,00556  |
| GO:0030198                | extracellular matrix organization and biogenesis                 | 57               | 6                  | 0,00595  |
| GO:0007422                | peripheral nervous system development                            | 26               | 4                  | 0,00627  |
| GO:0006690                | icosanoid metabolic process                                      | 41               | 5                  | 0,00633  |
| GO:0007399                | nervous system development                                       | 802              | 55                 | 0,00751  |
| GO:0008045                | motor axon guidance  | 5                | 2                  | 0,0079   |
| GO:0048598                | embryonic morphogenesis  | 142              | 10                 | 0,00836  |
| GO:0042490                | mechanoreceptor differentiation                                  | 15               | 3                  | 0,00848  |
| GO:0016337                | cell-cell adhesion   | 284              | 16                 | 0,00879  |
| GO:0045597                | positive regulation of cell differentiation                      | 45               | 5                  | 0,0094   |
| GO:0006928                | cell motility  | 452              | 32                 | 0,00976  |



| GO.ID                     | Description  | An-notated genes | Signi-ficant genes | P-value  |
|---------------------------|--|------------------|--------------------|----------|
| <i>Cellular component</i> |  |                  |                    |          |
| GO:0005578                | extracellular matrix (sensu Metazoa)                           | 337              | 30                 | 2,20E-06 |
| GO:0030424                | axon   | 47               | 8                  | 5,10E-05 |
| GO:0008074                | guanylate cyclase complex, soluble                             | 4                | 3                  | 9,20E-05 |
| GO:0016021                | integral to membrane   | 4503             | 164                | 0,00014  |
| GO:0005615                | extracellular space  | 540              | 29                 | 0,00092  |
| GO:0005581                | collagen   | 51               | 6                  | 0,00325  |
| GO:0043005                | neuron projection  | 87               | 13                 | 0,0051   |
| GO:0008021                | synaptic vesicle   | 61               | 6                  | 0,0079   |
| GO:0005856                | cytoskeleton   | 1060             | 44                 | 0,00846  |
| <i>Molecular function</i> |  |                  |                    |          |
| GO:0043121                | neurotrophin binding   | 4                | 3                  | 9,50E-05 |
| GO:0005509                | calcium ion binding  | 955              | 46                 | 0,00049  |
| GO:0008083                | growth factor activity   | 176              | 14                 | 0,00063  |
| GO:0004714                | transmembrane receptor protein tyrosine kinase activity        | 85               | 9                  | 0,00079  |
| GO:0004252                | serine-type endopeptidase activity                             | 160              | 13                 | 0,00079  |
| GO:0003851                | 2-hydroxyacylsphingosine 1-beta-galactosyltransferase activity | 2                | 2                  | 0,00084  |
| GO:0008489                | lactosylceramide synthase activity                             | 2                | 2                  | 0,00084  |
| GO:0030246                | carbohydrate binding   | 294              | 18                 | 0,00241  |
| GO:0004938                | alpha2-adrenergic receptor activity                            | 3                | 2                  | 0,00247  |
| GO:0004274                | dipeptidyl-peptidase IV activity                               | 10               | 3                  | 0,0025   |
| GO:0004383                | guanylate cyclase activity                                     | 10               | 3                  | 0,0025   |
| GO:0005267                | potassium channel activity                                     | 140              | 11                 | 0,00256  |
| GO:0004800                | thyroxine 5'-deiodinase activity                               | 4                | 2                  | 0,00485  |
| GO:0008260                | 3-oxoacid CoA-transferase activity                             | 4                | 2                  | 0,00485  |
| GO:0004222                | metalloendopeptidase activity                                  | 117              | 9                  | 0,00701  |
| GO:0030551                | cyclic nucleotide binding                                      | 27               | 4                  | 0,00722  |
| GO:0004067                | asparaginase activity  | 5                | 2                  | 0,00792  |
| GO:0004499                | dimethylaniline monooxygenase (N-oxide-forming) activity       | 5                | 2                  | 0,00792  |
| GO:0004181                | metallocarboxypeptidase activity                               | 29               | 4                  | 0,00934  |
| GO:0005201                | extracellular matrix structural constituent                    | 123              | 9                  | 0,00961  |

**Table 2** List of the most significantly regulated GO-classes with  $p < 0.01$  for the three top-level branches “biological process”, cellular component and “molecular function”.



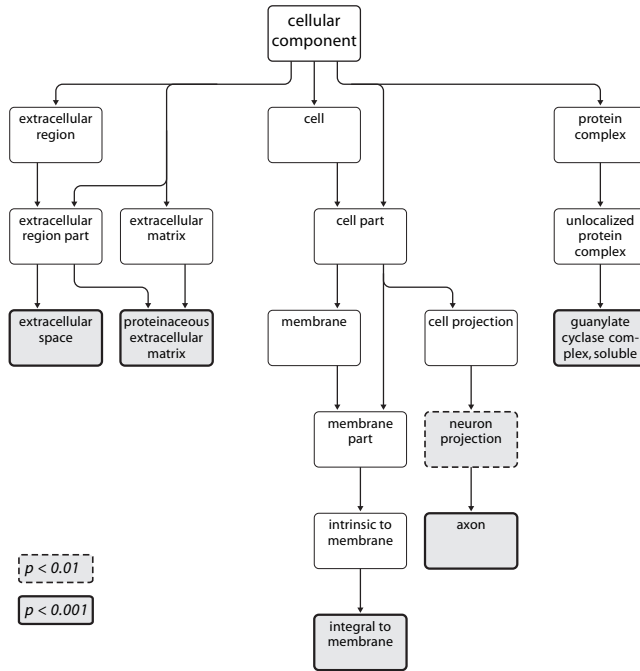


**Figure 4** Graphic representation of the 5 most significantly overrepresented GO-classes in the “cellular component” branch and their position in the GO hierarchy (see table 2 for details on the most significant classes).

regulated, the level of expression was generally lower in neuroma tissue: tetraspanins and cadherins. Finally, there were several families of which some genes were up- and others downregulated. These families include the IgG superfamily of cell adhesion molecules, contactins (which are a subgroup of the IgG superfamily), matrix metalloproteinases and the tyrosine kinase neurotrophin receptors.

*Differentially expressed genes with a role in scar formation and modulation*

As the GO classes “cell adhesion” and “extracellular matrix” were significantly overrepresented and several members of the collagen, small leucine-rich repeat protein and proteoglycan (SLRP) and chondroitin sulphate proteoglycans (CSPG) gene families were predominantly upregulated, we searched the list of 722 differentially regulated genes for individual genes that may affect extracellular matrix (ECM) formation and modulation. These genes can be broadly divided in genes encoding structural ECM components and genes encoding proteins involved in the modulation of the ECM. In general, the expression of structural ECM components appeared to be upregulated: the collagen family members COL11A1, COL12A1, COL5A2 and COL5A2 were up-

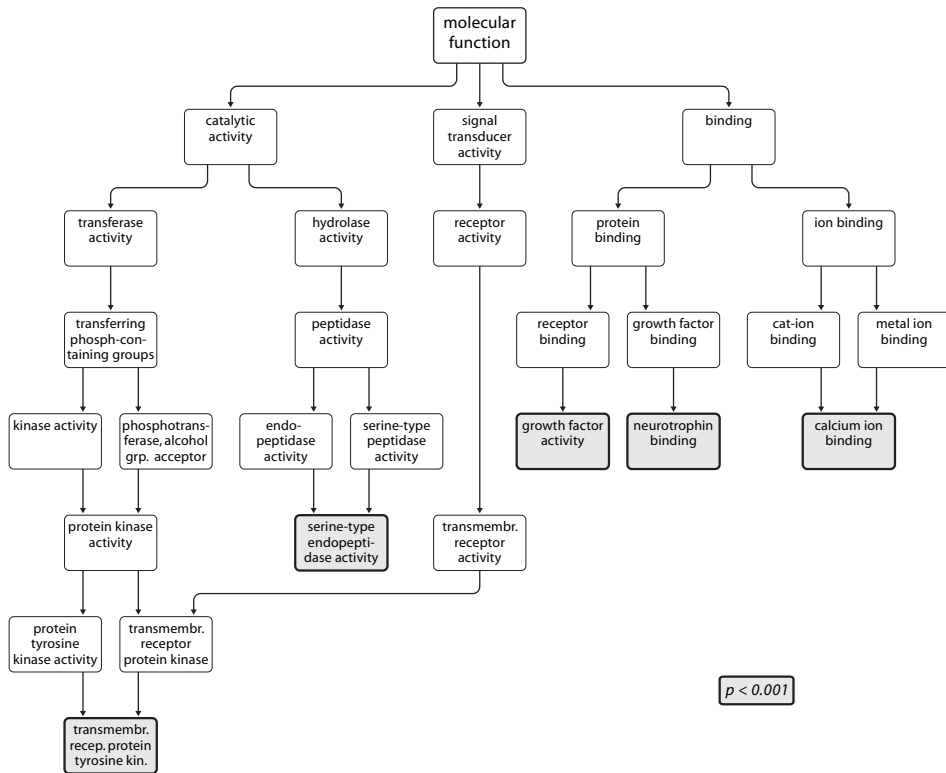


**Figure 5** Graphic representation of the 5 most significantly overrepresented GO-classes in the “molecular function” branch and their position in the GO hierarchy (see table 2 for details on the most significant classes). Transmembr. recep. protein tyrosine kin.: transmembrane receptor protein tyrosine kinase.

regulated, whereas COL8A2 was downregulated. Collagen formation, or fibrosis, has previously been shown to occur in the peripheral nerve neuroma and has been suggested to impede regeneration<sup>1,5</sup>. The expression of the structural component CSPG2 (versican) was also upregulated. CSPGs are chemorepulsive constituents of central nervous system scars<sup>58,88</sup>. Furthermore, they have also been implicated in peripheral regeneration<sup>91</sup>. SLRPs are extracellular matrix molecules involved in the regulation of the assembly of fibrillar collagens and modulation of cell adhesion<sup>92</sup>. The SLRPs BGN (biglycan), KERA (keratocan) OGN (osteo glycin) and ASPN (asporin) were all upregulated.

In addition, several individual genes encoding proteins involved in ECM modulation are differentially regulated. TGFB3 (transforming growth factor beta-3), which stimulates collagen production by fibroblasts of the peripheral nerve<sup>93</sup> was upregulated. ADAM12 (ADAM metallo peptidase domain 12), which regulates cell-extracellular

matrix interactions <sup>94</sup> and contributes to TGF-beta signaling <sup>95</sup> was also upregulated. POSTN (periostin) was strongly upregulated. POSTN is expressed in peripheral nerves <sup>96</sup> and is necessary for the cross-linking of collagen 1, thereby mediating the biomechanical properties of fibrous connective tissue <sup>97</sup>. LOXL-2 (lysyl oxidase-like 2) is required for the deposition of collagen by hepatocytes and was upregulated <sup>98</sup>. MMP16 (matrix metalloproteinase 16), a collagenolytic enzyme <sup>99</sup> that mediates cell migration <sup>98</sup> was upregulated and MMP28 (matrix metalloproteinase 28), which modulates the axonal-glial extracellular microenvironment <sup>100</sup> was downregulated.

*Differentially expressed genes with a role in axon guidance and/or regeneration*

Immunohistochemistry revealed that the neuroma contained regenerating axons and the distinct patterns of axonal outgrowth suggest that they are subject to guidance cues that are expressed in the neuroma. Furthermore, “axon guidance” was the second-most significantly overrepresented GO-class in the “biological process” branch. We therefore searched for individual differentially expressed genes with a putative effect on axonal regeneration. Not all genes in the “axon guidance” class have a well defined role in the guidance of developing or regenerating peripheral nerve axons. Conversely, a literature search revealed additional differentially expressed genes that influence axon guidance that were not part of this particular GO-class. A combination of the relevant members of the “axon guidance” GO-class and a literature search resulted in a total of 18 genes (7 of which are members of the “axon guidance” GO-class) with a putative effect on peripheral nerve regeneration or axon guidance (table 3). Of these genes, 10 have been described as genes encoding genuine chemorepulsive proteins, 3 as chemoattractive and 1 as both chemorepulsive and -attractive. Furthermore, 6 of these genes play a role in the fasciculation or defasciculation of developing axons and 1 gene influences the interaction of regenerating axons with the surrounding glia.

The expression of 8 of a total of 10 chemorepulsive proteins or receptors involved in chemorepulsive signaling was upregulated: BOC (boc homolog) <sup>101</sup>, CSPG2 (versican) <sup>88, 101</sup>, EPHB2 (EPH receptor B2, transcript variant 2) <sup>102</sup>, ROBO1 (roundabout, axon guidance receptor, homolog 1) <sup>102</sup>, SEMA5B (semaphorin 5B) <sup>103,104</sup>, TNN (tenascin-N) <sup>105</sup>, SLITRK 6 (SLIT and NTRK-like family, member 6) <sup>106</sup> and WNT5A (wingless-type MMTV integration site family, member 5A) <sup>105</sup>.

The expression of two chemorepulsive proteins was downregulated: BMP7 (bone morphogenetic protein 7) <sup>106</sup> and MT3 (metallothionein 3) <sup>107</sup>.

The expression of all three chemoattractive proteins, CDH4 (cadherin 4) <sup>107</sup>, NTF3 (neurotrophin 3) <sup>108</sup> and NRCAM (neuronal cell adhesion molecule) <sup>109</sup> was downregulated.

SPON1 (spondin 1) has been described both as chemorepulsive and as an outgrowth promoting protein. Spondin-1 is chemorepulsive to motor axons <sup>110</sup>, but promotes

regeneration of peripheral sensory neurons <sup>111</sup>. It was expressed significantly higher in the neuroma.

Of the 6 genes that have been described to affect fasciculation or defasciculation, the expression of 4 was upregulated: CSPG2 (versican) <sup>76</sup>, POSTN (periostin, osteoblast specific factor) which is structurally similar to the *Drosophila* Fasciclin <sup>96</sup>, ROBO1 <sup>102</sup>, and WNT5A <sup>105</sup>. The expression of FEZ1 (fasciculation and elongation zeta 1/ zygin I), which induces fasciculation and elongation of developing neurons in *C. elegans* <sup>112</sup> was downregulated. The expression of the defasciculation-inducing gene TLL1 (toll-like 1) <sup>113</sup>, was upregulated.

Finally, the expression of MMP-28, which is detectable along regenerating nerves before myelination during development and peripheral nerve regeneration, and is likely to modulate the axonal-glia extracellular microenvironment <sup>100</sup>, was downregulated in the neuroma.

*The extracellular matrix protein versican surrounds a number of mini-fascicles in the neuroma*

The expression of the CSPG versican was significantly higher in the neuroma. Interestingly, the enzymatic degradation of CSPGs enhances peripheral nerve regeneration across nerve gaps <sup>91</sup>. Therefore, we performed an immunohistochemical staining to determine its location. No versican staining was detected in any of the nerve samples, but in neuroma sections it was present around a relatively small subset (<5%) of mini-fascicles (figure 6). Versican is one of many CSPGs (e.g., aggrecan, neurocan, brevican, and phosphacan) <sup>114</sup> and the expression of none of these other CSPGs was significantly up- or downregulated in the neuroma. We therefore also performed a WFA staining on nerve and neuroma sections as a general marker for CSPGs. Strong WFA binding was present around virtually all axons in both nerve and neuroma sections (figure 6), indicating that CSPGs are indeed present in both nerve and neuroma tissue, but only versican is differentially expressed.

## Discussion

We performed a genome-wide gene expression analysis of the superior trunk neuroma in continuity of OBPI infants and combined these data with immunohistochemical staining of axons to perform an in-depth analysis of the molecular characteristics of these lesions. In the absence of clinical signs of functional recovery, the neuroma contained a considerable number of regenerating axons. However, the density of axons appeared reduced and axonal routing was severely disturbed. At a molecular level, we identified a unique combination of differentially expressed genes that influence scar formation and axon guidance. Finally, versican, one of the differentially expressed chemorepulsive proteins, was selectively expressed in the vicinity of regenerating axons.

The genes described in this paper may govern the disturbed axonal regeneration process in neuroma tissue and can therefore form the starting point for the development of novel therapeutic intervention strategies aimed at promoting axonal regeneration.

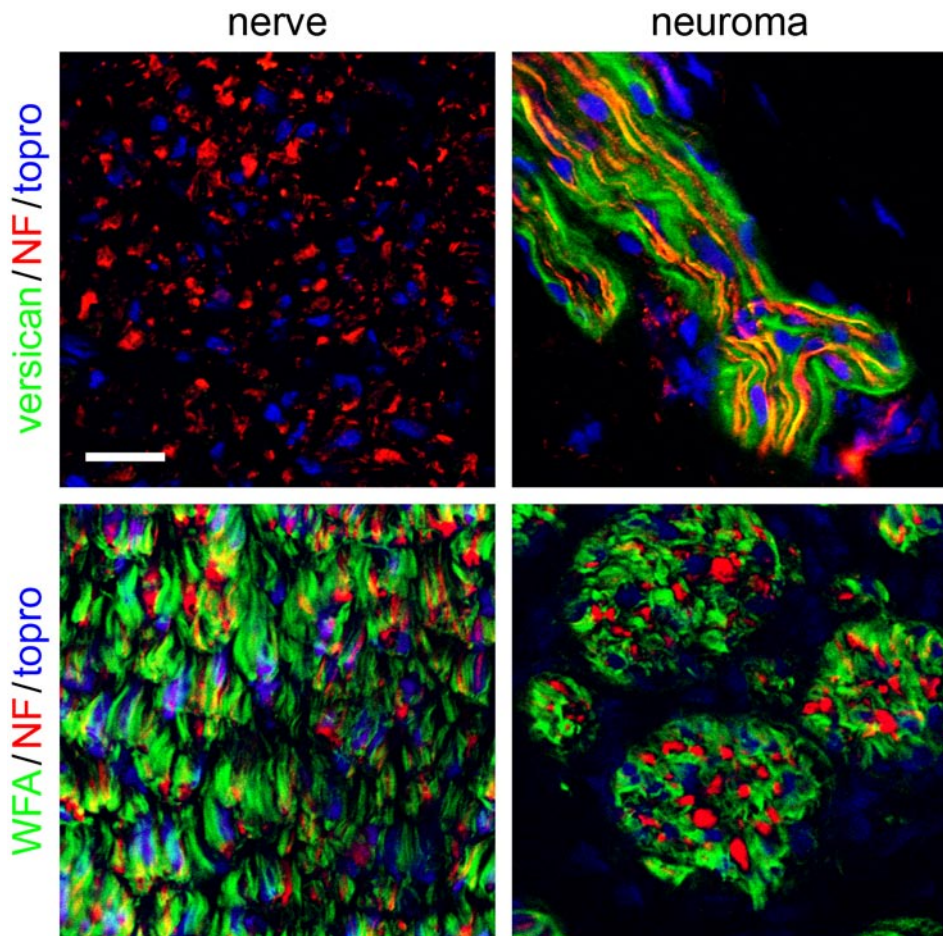


**Figure 6** Confocal laser scanning microscopy of nerve and neuroma sections stained with anti-versican (green), *Wisteria floribunda* agglutinin (WFA, green), anti-neurofilament (red) and topro (cell nuclei, blue). Versican is not detectable in the proximal nerve, but is specifically expressed in the vicinity of a small subset of mini-fascicles in the neuroma. In contrast, strong WFA binding, indicative of the presence of Chondroitin Sulphate Proteoglycans, surrounds virtually all axons in both nerve and neuroma tissue.

Scale bar: 20  $\mu$ m.



*The disorganisation of axons in the neuroma: a negative effect on functional recovery?*

The neuroma-in-continuity is generally considered to be an impediment to functional recovery<sup>1,3</sup>. The present paper shows that it contains a considerable number of axons, although the density of axons appears to be lower than in the spinal nerve proximal to the lesion. The chaotic orientation of the majority of axons implies that the guidance that is normally provided by endoneurial tubes in intact nerve fascicles<sup>8</sup> is lost. The high degree of disorganisation of regenerating axons implies that many of these are either trapped within the neuroma or are not present in their original distal endoneurial tubes, which leads to the reinnervation of inappropriate target organs. The misrouting of regenerating axons is a strong contributing factor to the lack of functional recovery in severe peripheral nerve injuries<sup>8,115,116</sup>. In conclusion, our findings imply that the misrouting of regenerating axons in the neuroma in continuity is an important factor in the lack of functional recovery.

*Formation and remodelling of the extracellular matrix in the neuroma*

The current gene expression profile provides several indications that the neuroma is a highly dynamic environment. Firstly, gene ontology analysis shows that the GO-classes “cell adhesion” and “extracellular matrix” are the most significantly overrepresented GO-classes in the “biological process” and “cellular component” branches, respectively. In general, the expression of structural ECM components (including collagen, SLRPs and versican) is upregulated. In addition, genes that promote collagen formation (TGFB3, ADAM12), are required for collagen deposition (LOXL2) or mediate collagen cross linking (POSTN) are also upregulated. Fibrosis has been shown before to be present in the peripheral nerve neuroma<sup>1,6</sup>, but the present findings are the first to demonstrate the coordinated expression of a number of genes involved in collagen formation in neuroma tissue. Apparently, the formation and consolidation of the fibrotic scar is a process that continues up to 5 months after injury. Interestingly, several genes that influence the interaction between the ECM and regenerating axons are also differentially expressed. MMP16, a collagenolytic enzyme<sup>99</sup> was upregulated and could therefore aid the regeneration of axons across fibrous tissue. MMP28 displays proteolytic activity against myelin components and its expression is negatively correlated with the myelination of regenerating neurons.<sup>100</sup> The expression of MMP28 was diminished in neuroma tissue and this may be necessary to allow remyelination of regenerating axons, but it could also result in inefficient breakdown of myelin components in the neuroma, thereby impairing regeneration.

*Axon guidance molecules are differentially regulated in the neuroma*

The observed chaotic pattern of axons in the neuroma suggests that many axons are



**Table 3** Differentially regulated genes in human neuroma tissue with a potential role on axon guidance. Expression: relative expression as a percentage of nerve control tissue (>100% indicates upregulation in the neuroma, <100% indicates downregulation). P-values for differential expression between nerve and neuroma were corrected for multiple testing using the Bonferoni correction algorithm. \*Chondroitin sulphate proteoglycans induce fasciculation, not versican specifically. \*\* Inhibition of neurite outgrowth is mediated by some splice variants of TNN.

| Gene     | Description   | Expression % | Function  | Species           |
|----------|---|--------------|---|-------------------|
| BMP7     | bone morphogenetic protein 7                          | 62           | repulsive dorsoventral guidance of commissural axons <sup>108</sup>             | mouse             |
| BOC      | boc homolog   | 316          | dorsoventral guidance of commissural axons <sup>99</sup>                        | mouse             |
| CDH4     | cadherin 4  | 66           | promotes pioneer axon outgrowth <sup>122</sup>                                  | mouse             |
| CSPG2    | versican  | 207          | scar-associated inhibitor CNS injury <sup>87</sup>                              | rat               |
|          |   |              | scar-associated inhibitor spinal cord injury <sup>100</sup>                     | rat               |
|          |   |              | induces fasciculation <sup>75*</sup>  | in vitro          |
| EPHB2    | EPH receptor B2, transcript variant 2                 | 211          | chemorepulsive, required for axon pathfinding <sup>101</sup>                    | mouse             |
| FEZ1     | fasciculation and elongation zeta 1/ zygion 1         | 70           | fasciculation and elongation of developing neurons <sup>114</sup>               | <i>C. elegans</i> |
|          |   |              | establishment of polarity in hippocampal neurons <sup>123</sup>                 | rat               |
| MMP28    | matrix metalloproteinase 28                           | 61           | modulates axonal-glia extracellular microenvironment <sup>98</sup>              | rat, mouse, frog  |
| MT3      | metallothionein 3                                     | 31           | inhibits regeneration of the peripheral nerve <sup>109</sup>                    | mouse             |
| NTF3     | neurotrophin 3  | 48           | chemoattractive proprioceptive axon guidance <sup>110</sup>                     | in vitro          |
| NRCAM    | neuronal cell adhesion molecule                       | 45           | promotes axon extension, pathfinding of RGC axons <sup>111</sup>                | in vitro          |
| POSTN    | periostin, osteoblast specific factor                 | 257          | structurally similar to <i>Drosophila</i> Fasciclin-1 <sup>93</sup>             | <i>drosophila</i> |
|          |   |              | regulates collagen I fibrillogenesis <sup>94</sup>                              | mouse             |
| ROBO1    | roundabout, axon guidance receptor, homolog 1         | 191          | chemorepulsive, restricts defasciculation of optic tract neurons <sup>102</sup> | zebrafish         |
| SEMA5B   | semaphorin 5B   | 220          | induces growth-cone collapse <sup>104</sup>                                     | in vitro          |
| SLITRK 6 | SLIT and NTRK-like family, member 6                   | 768          | inhibits neurite outgrowth <sup>106</sup>                                       | in vitro          |
| SPON1    | spondin 1   | 314          | repulsive to developing motor axons <sup>112</sup>                              | in vitro          |
|          |   |              | promotes regeneration of peripheral sensory neurons <sup>113</sup>              | rat               |
| TNN      | tenascin-N  | 305          | inhibits neurite outgrowth of hippocampal neurons <sup>105**</sup>              | in vitro          |
| TLL1     | tolloid-like 1  | 175          | controls defasciculation of developing motoneurons <sup>105</sup>               | <i>drosophila</i> |
| WNT5A    | wingless-type MMTV integration site family, member 5A | 399          | chemorepulsive axon guidance corpus callosum <sup>107</sup>                     | mouse             |
|          |   |              | induces fasciculation <sup>107</sup>  | mouse             |

misdirected and are likely to regenerate towards inappropriate target organs. However, several distinct phenomena, including fasciculation, defasciculation and turning events indicate that the regenerative path of these axons is not completely random. Instead, as they regenerate, they appear to be influenced by guidance cues in the extracellular matrix of the neuroma tissue surrounding them. Indeed, the GO-class “axon guidance” was the second most significantly overrepresented class in the “biological process” branch and we identified a total of 18 genes with a potential guiding influence on regenerating axons in the peripheral nerve.

Interestingly, the expression of the majority of outgrowth-inhibitory proteins (8 out of 10) was upregulated, whereas all three differentially expressed outgrowth-promoting proteins were downregulated. The expression of NGF, which is upregulated in painful end-neuromas<sup>86</sup> was not differentially expressed in the neuroma in continuity. The same holds true for other well-known neurotrophic factors like brain-derived neurotrophic factor and glial cell-line derived neurotrophic factor (the only differentially expressed neurotrophin, NTF3, was downregulated), indicating that a possible initial increase in expression of these factors<sup>77</sup> appears to be normalised after 5 months. It thus appears that at the time of surgery, the balance between the expression of outgrowth-promoting and outgrowth-inhibitory genes in the neuroma has shifted towards the latter, resulting in a microenvironment that is unsupportive of regeneration. Chemorepulsive guidance cues may have induced the observed turning of regenerating axons, causing some of them to become trapped in the neuroma and many others to become disorganised.

The majority of fasciculation-inducing proteins were upregulated. This finding may help to explain the presence of many mini-fascicles in the neuroma, although both the observed defasciculation of axons in neurofilament-stained sections and the upregulation of TLL1, a defasciculation-inducing gene, show that both fasciculation and defasciculation are mediated by proteins expressed by glial cells in the neuroma.

Surprisingly, semaphorin3A, which we have recently shown to be expressed in the human neuroma<sup>87</sup>, was not present in the list of significantly regulated genes in the present study, although there was indeed a trend towards higher semaphorin3A expression in the neuroma. Several factors may have contributed to this finding: first, the expression of semaphorin3A is relatively low and the qPCR method used in the previous study (which also contained more patient material) may have been more sensitive than the micro-array approach used here and a number of false-negative findings are to be expected in a micro-array approach. Second, different material was used in both studies: whereas the control tissue in the previous study was predominantly derived from proximal nerve stump C5, the control tissue in the present study was an even mix of C5 and C6 nerve tissue. Putative regional differences in semaphorin3A expression in the proximal nerve stumps may have therefore affected the measurement of the relative semaphorin3A expression in the neuroma.

The discovery of several new axon guidance proteins in this study may provide novel targets for future therapies aimed at improving regeneration after peripheral nerve injury. For instance, short interfering RNA mediated knockdown of inhibitory proteins, perhaps with the use of viral vectors<sup>90</sup>, may cause enhanced regeneration across the fibrous nerve scar. Furthermore, the ability to reduce defasciculation of regenerating axons could help to reduce the chance of misrouting of regenerating axons and thereby improve functional recovery.

#### *Versican and CSPGs surround nerve fibers*

Versican is a CSPG, and therefore a component of perineuronal nets that help stabilise neurons<sup>114</sup>. CSPGs induce fasciculation in vitro<sup>76</sup> and their presence around mini-fascicles in the neuroma may contribute to the fasciculation of regenerating axons. Although WFA staining was present around all axons in both nerve and neuroma sections, only the expression of versican was upregulated in the neuroma. This is surprising, as it was previously reported that versican is downregulated, albeit briefly, after peripheral nerve injury in the rat<sup>117</sup>. However, there is evidence that versican is a component of newly formed perineuronal nets and plays a role in their maturation<sup>114,118,119</sup>. The presence of versican around a small subset of mini-fascicles in the neuroma therefore suggests that these are recently formed “immature” mini-fascicles that are in the process of being enveloped by a new perineuronal net. As they mature, the versican-content of these nets decreases. However, the fact that they can be stained with WFA suggests that they now contain other CSPGs. As virtually all axons in both nerve and neuroma are surrounded by WFA positive ECM, it is not surprising that the expression of these other CSPGs is not differentially regulated. Furthermore, in contrast to some other CSPGs, versican is expressed by glial cells, not neurons. The upregulation of versican, the presence of CSPGs in the vicinity of mini-fascicles, the role of CSPGs in both peripheral nerve regeneration<sup>91</sup> and fasciculation<sup>76</sup> and the fact that they can be degraded enzymatically<sup>91</sup>, all make CSPGs a highly interesting target for experimental therapies aimed at the modulation and perhaps improvement of regeneration. However, there is a possibility that a degradation of CSPGs may induce defasciculation of regenerating axons, thereby increasing the chance that regenerating axons innervate inappropriate target organs.

#### **Concluding remarks**

The results described in this paper lead to the conclusion that the human neuroma in continuity contains a considerable number of highly disorganised axons, that misrouting is a major contributing factor to the lack of functional recovery and that the regenerative paths of these axons appear to be influenced by a number of axon guidance cues that are differentially expressed by the glial cells of the peripheral nerve neuroma.

The discovery of a substantial number of axons should not be misconstrued as an argument against surgical repair of the injured nerve. In fact, the high degree of disorganisation of these axons in the neuroma makes it seem unlikely that functional recovery would occur *without* some kind of intervention. However, the purpose of reconstructive surgery could be redefined: the function of implanted autologous nerve grafts is to provide longitudinally aligned scaffolds that physically guide axons (as well as providing neurotrophic support) towards the appropriate distal nerve stump. The differentially regulated axon guidance molecules described in this paper could serve as targets for therapies aimed at influencing processes like fasciculation or defasciculation of axons. However, these therapies will likely be applied in combination with, not instead of, reconstructive surgery. Viral vector mediated overexpression (or knock-down) of therapeutic proteins is technically possible in human sural nerve grafts <sup>90</sup>. Furthermore, the presence of CSPGs, specifically versican, in human neuroma tissue provides an additional argument for the therapeutic potential of enzymatic degradation of CSPGs <sup>91,120</sup> as a means to enhance peripheral nerve regeneration. These viral vector-based and enzymatic strategies may in the future provide a truly novel option to influence the functional outcome of surgery at a molecular level.

**Supplemental table 1** Complete list of all differentially regulated genes in human neuroma tissue (P<0.05). Expression: relative expression as a percentage of nerve control tissue (>100% indicates upregulation in the neuroma, <100% indicates downregulation). P-values for differential expression between nerve and neuroma were corrected for multiple testing using the Bonferroni correction algorithm.

| Gene           | Description  | Expr. (%) | P-val. |
|----------------|--|-----------|--------|
| SLITRK6        | SLIT and NTRK-like family, member 6 (SLITRK6), mRNA [NM_032229]                                      | 768       | 0.0076 |
| DCX            | doublecortin; lissencephaly, X-linked (doublecortin) (DCX), transcript variant 1, mRNA [NM_000555]   | 653       | 0.0029 |
| AL833005       | mRNA; cDNA DKFZp666D074 (from clone DKFZp666D074) [AL833005]   | 589       | 0.0283 |
| ASP            | asporin (LRR class 1) (ASP), mRNA [NM_017680]  | 553       | 0.0236 |
| THC2271582     | ALU5_HUMAN (P39192) Alu subfamily SC sequence contamination warning entry, partial (9%) [THC2271582] | 548       | 0.0334 |
| WNT5A          | wingless-type MMTV integration site family, member 5A (WNT5A), mRNA [NM_003392]                      | 399       | 0.0442 |
| LRRC38         | full-length cDNA clone CSoD1025YD24 of Placenta Cot 25-normalized of (human). [CR622769]             | 373       | 0.0042 |
| FNDC5          | fibronectin type III domain containing 5 (FNDC5), mRNA [NM_153756]                                   | 367       | 0.0061 |
| A_32_P171043   | Unknown  | 353       | 0.0257 |
| MXRA5          | matrix-remodelling associated 5 (MXRA5), mRNA [NM_015419]  | 348       | 0.0247 |
| GUCY1B3        | guanylate cyclase 1, soluble, beta 3 (GUCY1B3), mRNA [NM_000857]                                     | 346       | 0.0053 |
| AF119913       | PRO3077 mRNA, complete cds. [AF119913]   | 344       | 0.0185 |
| DKFZp434B1231  | eEF1A2 binding protein (DKFZp434B1231), mRNA [NM_178275]   | 344       | 0.0217 |
| ANGPTL1        | angiopoietin-like 1 (ANGPTL1), mRNA [NM_004673]  | 337       | 0.0419 |
| CPO            | carboxypeptidase O (CPO), mRNA [NM_173077]   | 335       | 0.0200 |
| KLK8           | kallikrein 8 (neuropsin/ovasin) (KLK8), transcript variant 2, mRNA [NM_144505]                       | 334       | 0.0148 |
| THC2277187     | Q6PKF4 (Q6PKF4) C2oorf77 protein (Fragment), partial (5%) [THC2277187]                               | 331       | 0.0300 |
| GUCY1A3        | guanylate cyclase 1, soluble, alpha 3 (GUCY1A3), mRNA [NM_000856]                                    | 331       | 0.0283 |
| THC2375612     | HXAD_HUMAN (P31271) Homeobox protein Hox-A13 (Hox-1), partial (9%) [THC2375612]                      | 330       | 0.0156 |
| THC2389705     | Unknown  | 329       | 0.0268 |
| SIX1           | sine oculis homeobox homolog 1 (Drosophila) (SIX1), mRNA [NM_005982]                                 | 328       | 0.0356 |
| C8orf57        | mRNA; cDNA DKFZp761D112 (from clone DKFZp761D112). [AL136588]  | 326       | 0.0106 |
| LECT2          | leukocyte cell-derived chemotaxin 2 (LECT2), mRNA [NM_002302]  | 321       | 0.0145 |
| CXCL13         | chemokine (C-X-C motif) ligand 13 (B-cell chemoattractant) (CXCL13), mRNA [NM_006419]                | 321       | 0.0092 |
| HSD11B1        | hydroxysteroid (11-beta) dehydrogenase 1 (HSD11B1), transcript variant 2, mRNA [NM_181755]           | 318       | 0.0257 |
| KLK11          | kallikrein 11 (KLK11), transcript variant 2, mRNA [NM_144947]  | 317       | 0.0029 |
| BOC            | Boc homolog (mouse) (BOC), mRNA [NM_033254]  | 316       | 0.0045 |
| SPON1          | spondin 1, extracellular matrix protein (SPON1), mRNA [NM_006108]                                    | 314       | 0.0333 |
| BC039414       | cDNA clone IMAGE:5302158. [BC039414]   | 313       | 0.0229 |
| FLJ40125       | hypothetical protein FLJ40125, mRNA (cDNA clone MGC:40208 IMAGE:5240955), complete cds. [BC028228]   | 311       | 0.0325 |
| THBS4          | thrombospondin 4 (THBS4), mRNA [NM_003248]   | 309       | 0.0243 |
| TNN            | tenascin N (TNN), mRNA [NM_022093]   | 305       | 0.0257 |
| KCNIP1         | Kv channel interacting protein 1 (KCNIP1), transcript variant 2, mRNA [NM_014592]                    | 303       | 0.0053 |
| BC033590       | Homo sapiens, clone IMAGE:4344826, mRNA. [BC033590]  | 301       | 0.0101 |
| LOC388002      | PREDICTED: hypothetical LOC388002 (LOC388002), mRNA [XM_373600]                                      | 300       | 0.0295 |
| LOC284112      | cDNA FLJ25640 fis, clone STM04823. [AK098506]  | 298       | 0.0036 |
| A_32_P222241   | Unknown  | 295       | 0.0133 |
| COMP           | cartilage oligomeric matrix protein (COMP), mRNA [NM_000095]   | 295       | 0.0085 |
| SPON2          | spondin 2, extracellular matrix protein (SPON2), mRNA [NM_012445]                                    | 294       | 0.0156 |
| C1orf92        | chromosome 1 open reading frame 92 (C1orf92), mRNA [NM_144702]                                       | 292       | 0.0062 |
| AY358804       | clone DNA100312 VSSW1971 (UNQ1971) mRNA, complete cds. [AY358804]                                    | 291       | 0.0050 |
| ENST0000278934 | mRNA for KIAA1867 protein, partial cds. [AB058770]   | 287       | 0.0101 |
| ENST0000380438 | mRNA; cDNA DKFZp761O1810 (from clone DKFZp761O1810). [AL713706]                                      | 283       | 0.0068 |
| ZCCHC5         | zinc finger, CCHC domain containing 5 (ZCCHC5), mRNA [NM_152694]                                     | 283       | 0.0288 |
| AK022045       | cDNA FLJ11983 fis, clone HEMBB1001337. [AK022045]  | 282       | 0.0308 |
| PTPRT          | protein tyrosine phosphatase, receptor type, T (PTPRT), transcript variant 1, mRNA [NM_133170]       | 281       | 0.0356 |
| FAP            | fibroblast activation protein, alpha (FAP), mRNA [NM_004460]   | 280       | 0.0097 |
| SFRP4          | secreted frizzled-related protein 4 (SFRP4), mRNA [NM_003014]  | 279       | 0.0462 |
| KERA           | keratocan (KERA), mRNA [NM_007035]   | 279       | 0.0054 |
| HOXC9          | homeobox C9 (HOXC9), mRNA [NM_006897]  | 277       | 0.0103 |
| ITM2A          | integral membrane protein 2A (ITM2A), mRNA [NM_004867]   | 276       | 0.0275 |

CHAPTER 3

| Gene            | Description   | Expr. (%) | P-val. |
|-----------------|---|-----------|--------|
| AK025975        | cDNA: FLJ22322 fis, clone HRC05532. [AK025975]  | 265       | 0.0164 |
| EYA1            | eyes absent homolog 1 (Drosophila) (EYA1), transcript variant 3, mRNA [NM_000503]   | 263       | 0.0292 |
| GSC             | gooseoid (GSC), mRNA [NM_173849]  | 261       | 0.0259 |
| CN479762        | CN479762 UI-H-EU0-azu-1-04-0-UI.s1 NCL_CGAP_Car1 cDNA clone UI-H-EU0-azu-1-04-0-UI 3; mRNA sequence [CN479762]  | 261       | 0.0077 |
| DIO2            | deiodinase, iodothyronine, type II (DIO2), transcript variant 1, mRNA [NM_013989]   | 260       | 0.0149 |
| AK124396        | cDNA FLJ42405 fis, clone ASTRO3000474. [AK124396]   | 260       | 0.0439 |
| ENST00000334770 | cDNA FLJ16078 fis, clone NT2NE2003252, weakly similar to Human putative serine/threonine protein kinase PRK (prk) mRNA. [AK122648]  | 259       | 0.0462 |
| POSTN           | periostin, osteoblast specific factor (POSTN), mRNA [NM_006475]   | 257       | 0.0183 |
| THC2317587      | Unknown   | 256       | 0.0417 |
| IGF1            | insulin-like growth factor 1 (somatomedin C) (IGF1), mRNA [NM_000618]   | 255       | 0.0317 |
| THC2357654      | Unknown   | 253       | 0.0062 |
| LRRC17          | leucine rich repeat containing 17 (LRRC17), transcript variant 2, mRNA [NM_005824]  | 253       | 0.0192 |
| ZMAT4           | zinc finger, matrin type 4 (ZMAT4), mRNA [NM_024645]  | 251       | 0.0189 |
| AW856073        | AW856073 RC1-CT0286-060200-015-c06 CT0286 cDNA, mRNA sequence [AW856073]  | 250       | 0.0257 |
| PPF1A2          | protein tyrosine phosphatase, receptor type, f polypeptide (PTPRF), interacting protein (liprin), alpha 2 (PPF1A2), mRNA [NM_003625]  | 249       | 0.0029 |
| SPOCK1          | sparc/osteonectin, cwcv and kazal-like domains proteoglycan (testican) 1 (SPOCK1), mRNA [NM_004598]   | 244       | 0.0384 |
| ENST00000299694 | cDNA FLJ31580 fis, clone NT2RL2002041. [AK056142]   | 244       | 0.0056 |
| THC2269852      | Q8TDP9 (Q8TDP9) 3-beta-hydroxysteroid dehydrogenase (Fragment), partial (38%) [THC2269852]  | 243       | 0.0236 |
| PCDH19          | protocadherin 19 (PCDH19), mRNA [NM_020766]   | 243       | 0.0051 |
| HAS1            | hyaluronan synthase 1 (HAS1), mRNA [NM_001523]  | 242       | 0.0283 |
| WIT1            | Wilms tumor upstream neighbor 1 (WIT1), mRNA [NM_015855]  | 242       | 0.0192 |
| FGF19           | fibroblast growth factor 19 (FGF19), mRNA [NM_005117]   | 239       | 0.0054 |
| MRC2            | mannose receptor, C type 2 (MRC2), mRNA [NM_006039]   | 239       | 0.0097 |
| BFSP1           | beaded filament structural protein 1, filensin (BFSP1), mRNA [NM_001195]  | 238       | 0.0152 |
| COL11A1         | collagen, type XI, alpha 1 (COL11A1), transcript variant B, mRNA [NM_080629]  | 238       | 0.0397 |
| TGFB3           | transforming growth factor, beta 3 (TGFB3), mRNA [NM_003239]  | 238       | 0.0203 |
| CILP            | cartilage intermediate layer protein, nucleotide pyrophosphohydrolase (CILP), mRNA [NM_003613]  | 237       | 0.0187 |
| FMO1            | flavin containing monooxygenase 1 (FMO1), mRNA [NM_002021]  | 237       | 0.0417 |
| C20orf102       | chromosome 20 open reading frame 102 (C20orf102), mRNA [NM_080607]  | 237       | 0.0144 |
| ENST00000343998 | full-length cDNA clone CS0DF020YB12 of Fetal brain of (human). [CR618658]   | 236       | 0.0185 |
| ENPEP           | glutamyl aminopeptidase (aminopeptidase A) (ENPEP), mRNA [NM_001977]  | 236       | 0.0029 |
| KIAA1217        | KIAA1217 (KIAA1217), mRNA [NM_019590]   | 236       | 0.0036 |
| T52140          | T52140 yb29h11.1r1 Stratagene fetal spleen (#937205) cDNA clone IMAGE:72645 5; mRNA sequence [T52140]   | 235       | 0.0162 |
| KLK1            | kallikrein 1, renal/pancreas/salivary (KLK1), mRNA [NM_002257]  | 234       | 0.0070 |
| DAZL            | deleted in azoospermia-like (DAZL), mRNA [NM_001351]  | 234       | 0.0257 |
| HSD3B1          | hydroxy-delta-5-steroid dehydrogenase, 3 beta- and steroid delta-isomerase 1 (HSD3B1), mRNA [NM_000862]   | 234       | 0.0291 |
| ZFPM2           | zinc finger protein, multitype 2 (ZFPM2), mRNA [NM_012082]  | 234       | 0.0145 |
| TMEM133         | transmembrane protein 133 (TMEM133), mRNA [NM_032021]   | 233       | 0.0100 |
| KIAA1904        | KIAA1904 protein (KIAA1904), mRNA [NM_052906]   | 232       | 0.0133 |
| C1QTNF2         | C1q and tumor necrosis factor related protein 2 (C1QTNF2), mRNA [NM_031908]   | 232       | 0.0421 |
| HS6ST2          | heparan sulfate 6-O-sulfotransferase 2 (HS6ST2), mRNA [NM_147175]   | 231       | 0.0200 |
| AA585242        | AA585242 LTH022 HTCDDL1 cDNA 5'/3'; mRNA sequence [AA585242]  | 230       | 0.0034 |
| JAG1            | jagged 1 (Alagille syndrome) (JAG1), mRNA [NM_000214]   | 230       | 0.0189 |
| RGS5            | regulator of G-protein signalling 5 (RGS5), mRNA [NM_003617]  | 228       | 0.0051 |
| NOV             | nephroblastoma overexpressed gene (NOV), mRNA [NM_002514]   | 228       | 0.0381 |
| CTHRC1          | collagen triple helix repeat containing 1 (CTHRC1), mRNA [NM_138455]  | 227       | 0.0338 |
| GEFT            | RAC/CDC42 exchange factor (GEFT), transcript variant 2, mRNA [NM_1333483]   | 226       | 0.0439 |
| EMILIN3         | elastin microfibril interfacer 3 (EMILIN3), mRNA [NM_052846]  | 226       | 0.0359 |
| PI16            | peptidase inhibitor 16 (PI16), mRNA [NM_153370]   | 225       | 0.0247 |
| KIAA1913        | KIAA1913 (KIAA1913), mRNA [NM_052913]   | 225       | 0.0356 |
| ENST00000261364 | PR-domain zinc finger protein 6 isoform A (PRDM6) mRNA, partial cds; alternatively spliced. [AF272898]  | 225       | 0.0156 |
| THC2339002      | Q300_MOUSE (Q02722) Protein Q300, partial (17%) [THC2339002]  | 224       | 0.0288 |
| ENST00000370548 | cDNA FLJ11317 fis, clone PLACE1010261, moderately similar to SEGREGATION DISTORTER PROTEIN. [AK002179]  | 224       | 0.0283 |
| COLEC12         | collectin sub-family member 12 (COLEC12), transcript variant II, mRNA [NM_030781]   | 223       | 0.0288 |
| PPIC            | peptidylprolyl isomerase C (cyclophilin C) (PPIC), mRNA [NM_000943]   | 222       | 0.0307 |
| HEYL            | hairly/enhancer-of-split related with YRPW motif-like (HEYL), mRNA [NM_014571]  | 222       | 0.0062 |
| SEMA5B          | sema domain, seven thrombospondin repeats (type 1 and type 1-like), transmembrane domain (TM) and short cytoplasmic domain, (semaphorin) 5B (SEMA5B), transcript variant 1, mRNA [NM_001031702] | 220       | 0.0325 |

GENE EXPRESSION IN HUMAN NEUROMA

| Gene            | Description   | Expr. (%) | P-val. |
|-----------------|---|-----------|--------|
| GHR             | growth hormone receptor (GHR), mRNA [NM_000163]   | 220       | 0.0259 |
| SLCO2A1         | solute carrier organic anion transporter family, member 2A1 (SLCO2A1), mRNA [NM_005630]                               | 219       | 0.0419 |
| THC2442939      | Unknown   | 218       | 0.0109 |
| MGC16121        | hypothetical protein MGC16121, mRNA (cDNA clone MGC:16121 IMAGE:3627113), complete cds. [BC007360]                    | 216       | 0.0215 |
| ENST00000373208 | Q7QFH7 (Q7QFH7) ENSANGP0000019298 (Fragment), partial (7%) [THC2404711]   | 216       | 0.0317 |
| BX115897        | BX115897 BX115897 Soares_multiple_sclerosis_2NbHMSP cDNA clone IMAGP99816611; IMAGE:276975, mRNA sequence [BX115897]  | 216       | 0.0156 |
| PLCL2           | phospholipase C-like 2 (PLCL2), mRNA [NM_015184]  | 216       | 0.0156 |
| BX281073        | BX281073 BX281073 NCL_CGAP_Lu24 cDNA clone IMAGP9980175628; IMAGE:2273128, mRNA sequence [BX281073]                   | 215       | 0.0075 |
| BQ897248        | AGENCOURT_8122036 Lupski_dorsal_root_ganglion cDNA clone IMAGE:6179261 5', mRNA sequence [BQ897248]                   | 215       | 0.0406 |
| BICC1           | cDNA: FLJ22476 fis, clone HRC10682. [AK026129]  | 215       | 0.0246 |
| RP11-30117.1    | proliferation-inducing protein 38 (PIG38), mRNA [NM_017993]   | 214       | 0.0308 |
| OGN             | osteo glycin (osteoinductive factor, mimecan) (OGN), transcript variant 1, mRNA [NM_033014]                           | 214       | 0.0257 |
| BX648831        | mRNA; cDNA DKFZp686j06116 (from clone DKFZp686j06116). [BX648831]   | 214       | 0.0132 |
| METTL7A         | methyltransferase like 7A (METTL7A), mRNA [NM_014033]   | 214       | 0.0496 |
| VIPR2           | vasoactive intestinal peptide receptor 2 (VIPR2), mRNA [NM_003382]  | 213       | 0.0192 |
| ENST00000380683 | PREDICTED: hypothetical protein LOC646371 (LOC646371), mRNA [XM_933567]   | 213       | 0.0350 |
| EPHB2           | EPH receptor B2 (EPHB2), transcript variant 2, mRNA [NM_004442]   | 211       | 0.0283 |
| NCALD           | neurocalcine delta (NCALD), transcript variant 8, mRNA [NM_032041]  | 211       | 0.0457 |
| NGEF            | neuronal guanine nucleotide exchange factor (NGEF), mRNA [NM_019850]  | 211       | 0.0397 |
| AK124281        | cDNA FLJ42287 fis, clone TLIVE2005866. [AK124281]   | 210       | 0.0369 |
| HMCN1           | hemichentin 1 (HMCN1), mRNA [NM_031935]   | 210       | 0.0082 |
| NMNAT2          | nicotinamide nucleotide adenyltransferase 2 (NMNAT2), transcript variant 1, mRNA [NM_015039]                          | 210       | 0.0442 |
| ENC1            | ectodermal-neural cortex (with BTB-like domain) (ENC1), mRNA [NM_003633]  | 208       | 0.0064 |
| CSPG2           | chondroitin sulfate proteoglycan 2 (versican) (CSPG2), mRNA [NM_004385]   | 207       | 0.0194 |
| CCBE1           | collagen and calcium binding EGF domains 1 (CCBE1), mRNA [NM_133459]  | 207       | 0.0304 |
| TSHZ2           | teashirt family zinc finger 2 (TSHZ2), mRNA [NM_173485]   | 207       | 0.0042 |
| THC2317900      | Q9H2Q1 (Q9H2Q1) AD031, partial (69%) [THC2317900]   | 206       | 0.0163 |
| AW015426        | UI-H-Blo-aat-h-12-0-ULs1 NCL_CGAP_Sub1 cDNA clone IMAGE:2710535 3', mRNA sequence [AW015426]                          | 206       | 0.0056 |
| GRM1            | glutamate receptor, metabotropic 1 (GRM1), mRNA [NM_000838]   | 205       | 0.0387 |
| DFNB31          | cDNA FLJ31628 fis, clone NT2RI2003344, weakly similar to PRESYNAPTIC PROTEIN SAP97. [AK056190]                        | 205       | 0.0192 |
| PTPN5           | protein tyrosine phosphatase, non-receptor type 5 (striatum-enriched) (PTPN5), transcript variant 2, mRNA [NM_032781] | 204       | 0.0054 |
| RNU12           | RNA, U12 small nuclear (RNU12) on chromosome X [NR_000041]  | 203       | 0.0288 |
| CR616003        | full-length cDNA clone CSoDM012YB14 of Fetal liver of (human). [CR616003]   | 203       | 0.0265 |
| TCF4            | transcription factor 4 (TCF4), mRNA [NM_003199]   | 203       | 0.0202 |
| C1orf54         | chromosome 1 open reading frame 54 (C1orf54), mRNA [NM_024579]  | 203       | 0.0168 |
| ENST00000256861 | Unknown   | 202       | 0.0145 |
| THC2339791      | Unknown   | 202       | 0.0495 |
| TMC4            | transmembrane channel-like 4 (TMC4), mRNA [NM_144686]   | 202       | 0.0054 |
| DAPK2           | death-associated protein kinase 2 (DAPK2), mRNA [NM_014326]   | 202       | 0.0315 |
| HTRA3           | HtrA serine peptidase 3 (HTRA3), mRNA [NM_053044]   | 201       | 0.0466 |
| WNT2B           | wingless-type MMTV integration site family, member 2B (WNT2B), transcript variant WNT-2B1, mRNA [NM_004185]           | 201       | 0.0231 |
| BE835321        | BE835321 RC5-FN0022-300600-022-G12 FN0022 cDNA, mRNA sequence [BE835321]  | 200       | 0.0401 |
| CXCR4           | chemokine (C-X-C motif) receptor 4 (CXCR4), transcript variant 1, mRNA [NM_001008540]                                 | 200       | 0.0229 |
| A_32_P160388    | Unknown   | 199       | 0.0103 |
| SUSD4           | sushi domain containing 4 (SUSD4), transcript variant 1, mRNA [NM_017982]   | 199       | 0.0257 |
| HTR2A           | 5-hydroxytryptamine (serotonin) receptor 2A (HTR2A), mRNA [NM_000621]   | 199       | 0.0076 |
| AW138903        | AW138903 UI-H-B11-aeq-e-09-0-ULs1 NCL_CGAP_Sub3 cDNA clone IMAGE:2720344 3', mRNA sequence [AW138903]                 | 198       | 0.0462 |
| A_32_P219704    | Unknown   | 198       | 0.0267 |
| TK1             | thymidine kinase 1, soluble (TK1), mRNA [NM_003258]   | 197       | 0.0229 |
| KRT12           | keratin 12 (Meesmann corneal dystrophy) (KRT12), mRNA [NM_000223]   | 197       | 0.0268 |
| OSTalpha        | organic solute transporter alpha (OSTalpha), mRNA [NM_152672]   | 196       | 0.0342 |
| AKR1C3          | aldo-keto reductase family 1, member C3 (3-alpha hydroxysteroid dehydrogenase, type II) (AKR1C3), mRNA [NM_003739]    | 195       | 0.0386 |
| STEAP1          | six transmembrane epithelial antigen of the prostate 1 (STEAP1), mRNA [NM_012449]                                     | 194       | 0.0462 |
| GLI2            | GLI-Kruppel family member GLI2 (GLI2), mRNA [NM_005270]   | 194       | 0.0318 |
| VLDLR           | very low density lipoprotein receptor (VLDLR), transcript variant 1, mRNA [NM_003383]                                 | 193       | 0.0288 |



CHAPTER 3

| Gene            | Description  | Expr. (%) | P-val. |
|-----------------|--|-----------|--------|
| SVEP1           | cDNA FLJ14964 fis, clone PLACE4000581, moderately similar to FIBROPELLIN I PRECURSOR. [AK027870]                         | 193       | 0.0149 |
| SIX2            | sine oculis homeobox homolog 2 (Drosophila) (SIX2), mRNA [NM_016932]   | 193       | 0.0409 |
| AK001062        | cDNA FLJ10200 fis, clone HEMBA1004863, highly similar to mRNA; cDNA DKFZp586M2022. [AK001062]                            | 192       | 0.0257 |
| PHACTR2         | phosphatase and actin regulator 2 (PHACTR2), mRNA [NM_014721]  | 192       | 0.0114 |
| C18orf4         | chromosome 18 open reading frame 4 (C18orf4), mRNA [NM_032160]   | 192       | 0.0147 |
| DAAM1           | dishevelled associated activator of morphogenesis 1 (DAAM1), mRNA [NM_014992]  | 192       | 0.0259 |
| CFI             | complement factor I (CFI), mRNA [NM_000204]  | 191       | 0.0097 |
| THC2304714      | Unknown  | 191       | 0.0272 |
| ROBO1           | roundabout, axon guidance receptor, homolog 1 (Drosophila) (ROBO1), transcript variant 2, mRNA [NM_133631]               | 191       | 0.0039 |
| EBF2            | early B-cell factor 2 (EBF2) mRNA, complete cds, alternatively spliced. [AY700779]                                       | 191       | 0.0101 |
| PLOD2           | procollagen-lysine, 2-oxoglutarate 5-dioxygenase 2 (PLOD2), transcript variant 1, mRNA [NM_182943]                       | 191       | 0.0201 |
| ENST00000257897 | mRNA for KIAA0167 gene, partial cds. [D79989]  | 191       | 0.0339 |
| BAPX1           | bagpipe homeobox homolog 1 (Drosophila) (BAPX1), mRNA [NM_001189]  | 191       | 0.0367 |
| KIAA0101        | KIAA0101 (KIAA0101), transcript variant 1, mRNA [NM_014736]  | 191       | 0.0205 |
| JAM2            | junctional adhesion molecule 2 (JAM2), mRNA [NM_021219]  | 190       | 0.0340 |
| CAPN6           | calpain 6 (CAPN6), mRNA [NM_014289]  | 190       | 0.0462 |
| NTRK1           | neurotrophic tyrosine kinase, receptor, type 1 (NTRK1), transcript variant 2, mRNA [NM_002529]                           | 189       | 0.0308 |
| MSC             | musculin (activated B-cell factor-1) (MSC), mRNA [NM_005098]   | 189       | 0.0330 |
| TMEM26          | transmembrane protein 26 (TMEM26), mRNA [NM_178505]  | 189       | 0.0229 |
| CRABP2          | cellular retinoic acid binding protein 2 (CRABP2), mRNA [NM_001878]  | 189       | 0.0330 |
| THC2438512      | Unknown  | 189       | 0.0142 |
| TMEM100         | transmembrane protein 100 (TMEM100), mRNA [NM_018286]  | 189       | 0.0185 |
| ANKRD29         | ankyrin repeat domain 29 (ANKRD29), mRNA [NM_173505]   | 188       | 0.0347 |
| MYO10           | cDNA clone MGC:131988 IMAGE:6164790, complete cds. [BC108736]  | 188       | 0.0141 |
| ENST00000295549 | hypothetical gene supported by BC013438, mRNA (cDNA clone IMAGE:3899073), partial cds. [BC013438]                        | 188       | 0.0276 |
| STXBP6          | syntaxin binding protein 6 (amisyn) (STXBP6), mRNA [NM_014178]   | 187       | 0.0339 |
| A_32_P9924      | Unknown  | 187       | 0.0301 |
| H19             | H19, imprinted maternally expressed untranslated mRNA (H19) on chromosome 11 [NR_002196]                                 | 186       | 0.0205 |
| BGN             | biglycan (BGN), mRNA [NM_001711]   | 185       | 0.0375 |
| KIAA2002        | cDNA FLJ34483 fis, clone HLUNG2004154. [AK091802]  | 184       | 0.0321 |
| ECM2            | extracellular matrix protein 2, female organ and adipocyte specific (ECM2), mRNA [NM_001393]                             | 183       | 0.0163 |
| DLST            | dihydrolipoamide S-succinyltransferase (E2 component of 2-oxo-glutarate complex) (DLST), mRNA [NM_001933]                | 182       | 0.0163 |
| AK125961        | cDNA FLJ43973 fis, clone TESTI4017984. [AK125961]  | 182       | 0.0283 |
| ENST00000373886 | cDNA FLJ26539 fis, clone KDNO9310. [AK130049]  | 182       | 0.0286 |
| HMMR            | hyaluronan-mediated motility receptor (RHAMM) (HMMR), transcript variant 1, mRNA [NM_012484]                             | 181       | 0.0304 |
| THC2287450      | Unknown  | 181       | 0.0265 |
| FAM83D          | family with sequence similarity 83, member D (FAM83D), mRNA [NM_030919]  | 181       | 0.0341 |
| A_32_P19616     | Unknown  | 181       | 0.0232 |
| LOXL2           | lysyl oxidase-like 2 (LOXL2), mRNA [NM_002318]   | 181       | 0.0194 |
| IRF8            | interferon regulatory factor 8 (IRF8), mRNA [NM_002163]  | 180       | 0.0257 |
| COL6A2          | collagen, type VI, alpha 2 (COL6A2), transcript variant 2C2, mRNA [NM_001849]  | 180       | 0.0292 |
| CFB             | complement factor B (CFB), mRNA [NM_001710]  | 180       | 0.0472 |
| A_24_P871726    | Unknown  | 179       | 0.0077 |
| FLJ16237        | hypothetical protein LOC392636 (FLJ16237), mRNA [NM_001004320]   | 179       | 0.0166 |
| CA421238        | CA421238 UI-H-FGo-bct-h-02-0-UI.s1 NCI_CGAP_EN1_2 cDNA clone UI-H-FGo-bct-h-02-0-UI 3', mRNA sequence [CA421238]         | 178       | 0.0317 |
| A_24_P914669    | Unknown  | 178       | 0.0325 |
| RAB31L1         | RAB3A interacting protein (rab31)-like 1 (RAB31L1), mRNA [NM_013401]   | 178       | 0.0417 |
| THC2406050      | BX324349 BX324349 T CELLS (JURKAT CELL LINE) COT 10-NORMALIZED cDNA clone CSod)008YO15 5-PRIME, mRNA sequence [BX324349] | 178       | 0.0145 |
| CTSK            | cathepsin K (pyncnodysostosis) (CTSK), mRNA [NM_000396]  | 178       | 0.0468 |
| KLK10           | kallikrein 10 (KLK10), transcript variant 1, mRNA [NM_002776]  | 178       | 0.0283 |
| ITIH5           | inter-alpha (globulin) inhibitor H5 (ITIH5), transcript variant 1, mRNA [NM_030569]                                      | 177       | 0.0305 |
| NOX4            | NADPH oxidase 4 (NOX4), mRNA [NM_016931]   | 177       | 0.0311 |
| GPR171          | G protein-coupled receptor 171 (GPR171), mRNA [NM_013308]  | 177       | 0.0089 |
| ADRA2A          | adrenergic, alpha-2A-, receptor (ADRA2A), mRNA [NM_000681]   | 177       | 0.0419 |
| FLJ31485        | cDNA FLJ31485 fis, clone NTAZE001698. [AK056047]   | 177       | 0.0085 |
| LOC651721       | hypothetical protein LOC651721, mRNA (cDNA clone IMAGE:4430430), partial cds. [BC026225]                                 | 176       | 0.0284 |
| ADAM12          | ADAM metallopeptidase domain 12 (meltrin alpha) (ADAM12), transcript variant 1, mRNA [NM_003474]                         | 176       | 0.0285 |



GENE EXPRESSION IN HUMAN NEUROMA

| Gene            | Description  | Expr. (%) | P-val. |
|-----------------|--|-----------|--------|
| ENST0000304372  | potassium channel tetramerisation domain containing 19, mRNA (cDNA clone IMAGE:5268205). [BC070103]    | 176       | 0.0325 |
| C14orf81        | cDNA FLJ32169 fis, clone PLACE6000523. [AK056731]  | 176       | 0.0370 |
| FMO3            | flavin containing monooxygenase 3 (FMO3), transcript variant 2, mRNA [NM_001002294]                    | 176       | 0.0295 |
| DLG7            | discs, large homolog 7 (Drosophila) (DLG7), mRNA [NM_014750]   | 176       | 0.0404 |
| TOP2A           | topoisomerase (DNA) II alpha 170kDa (TOP2A), mRNA [NM_0010067]   | 176       | 0.0191 |
| CLEC1A          | C-type lectin domain family 1, member A (CLEC1A), mRNA [NM_016511]                                     | 176       | 0.0102 |
| PLVAP           | plasmalemma vesicle associated protein (PLVAP), mRNA [NM_031310]                                       | 175       | 0.0359 |
| MEST            | mesoderm specific transcript homolog (mouse) (MEST), transcript variant 1, mRNA [NM_002402]            | 175       | 0.0247 |
| TLL1            | tolloid-like 1 (TLL1), mRNA [NM_012464]  | 175       | 0.0061 |
| THC2404912      | Q7XXR9 (Q7XXR9) Katanin, partial (44%) [THC2404912]  | 174       | 0.0229 |
| AK097130        | cDNA FLJ39811 fis, clone SPLEN2009581. [AK097130]  | 174       | 0.0424 |
| SOAT2           | sterol O-acyltransferase 2 (SOAT2), mRNA [NM_003578]   | 174       | 0.0066 |
| AL137560        | mRNA; cDNA DKFZp434M0320 (from clone DKFZp434M0320). [AL137560]  | 174       | 0.0417 |
| TMSL8           | thymosin-like 8 (TMSL8), mRNA [NM_021992]  | 174       | 0.0288 |
| BE716310        | CM1-HT0761-010600-238-e06 HT0761 cDNA, mRNA sequence [BE716310]  | 174       | 0.0439 |
| THC2363226      | HLMITCSEQ Hylobates lar complete mitochondrial DNA sequence, partial (3%) [THC2363226]                 | 174       | 0.0376 |
| SART2           | squamous cell carcinoma antigen recognized by T cells 2 (SART2), mRNA [NM_013352]                      | 174       | 0.0275 |
| THC2339566      | Unknown  | 173       | 0.0399 |
| PTGER4          | prostaglandin E receptor 4 (subtype EP4) (PTGER4), mRNA [NM_000958]                                    | 173       | 0.0364 |
| MAPK10          | mitogen-activated protein kinase 10 (MAPK10), transcript variant 3, mRNA [NM_138980]                   | 172       | 0.0220 |
| CYP4F8          | cytochrome P450, family 4, subfamily F, polypeptide 8 (CYP4F8), mRNA [NM_007253]                       | 172       | 0.0474 |
| PGF             | placental growth factor, vascular endothelial growth factor-related protein (PGF), mRNA [NM_002632]    | 171       | 0.0447 |
| CNTN4           | contactin 4 (CNTN4), transcript variant 1, mRNA [NM_175607]  | 171       | 0.0200 |
| PLAGL1          | pleiomorphic adenoma gene-like 1 (PLAGL1), transcript variant 2, mRNA [NM_006718]                      | 171       | 0.0317 |
| ENST00000371497 | OVC10-2 mRNA, complete cds. [AF230201]   | 171       | 0.0210 |
| TRA@            | T cell receptor alpha locus, mRNA (cDNA clone MGC:71411 IMAGE:4853814), complete cds. [BC063385]       | 170       | 0.0060 |
| THC2359080      | Unknown  | 170       | 0.0305 |
| CLEC11A         | C-type lectin domain family 11, member A (CLEC11A), mRNA [NM_002975]                                   | 170       | 0.0259 |
| FAM20A          | family with sequence similarity 20, member A (FAM20A), mRNA [NM_017565]                                | 170       | 0.0229 |
| BC015449        | Homo sapiens, clone IMAGE:4427279, mRNA. [BC015449]  | 170       | 0.0496 |
| BC006419        | cDNA clone IMAGE:3946309, complete cds. [BC006419]   | 170       | 0.0247 |
| VCAM1           | vascular cell adhesion molecule 1 (VCAM1), transcript variant 1, mRNA [NM_001078]                      | 169       | 0.0434 |
| CRTAC1          | cartilage acidic protein 1 (CRTAC1), mRNA [NM_018058]  | 169       | 0.0434 |
| U79293          | Human clone 23948 mRNA sequence. [U79293]  | 169       | 0.0229 |
| AK021606        | cDNA FLJ11544 fis, clone HEMBA1002826. [AK021606]  | 169       | 0.0451 |
| Bfsp2           | deduced filament structural protein 2, phakinin (Bfsp2), mRNA [NM_003571]                              | 169       | 0.0398 |
| A_23_P208752    | Unknown  | 169       | 0.0156 |
| COL12A1         | collagen, type XII, alpha 1 (COL12A1), transcript variant long, mRNA [NM_004370]                       | 169       | 0.0061 |
| FLJ35934        | FLJ35934 protein (FLJ35934), mRNA [NM_207453]  | 168       | 0.0381 |
| APOL6           | apolipoprotein L, 6 (APOL6), mRNA [NM_030641]  | 168       | 0.0357 |
| LPHN2           | latrophilin 2 (LPHN2), mRNA [NM_012302]  | 168       | 0.0271 |
| THC2268343      | Unknown  | 168       | 0.0356 |
| RAB23           | RAB23, member RAS oncogene family (RAB23), transcript variant 1, mRNA [NM_016277]                      | 168       | 0.0477 |
| CACNB4          | calcium channel, voltage-dependent, beta 4 subunit (CACNB4), transcript variant 1, mRNA [NM_001005747] | 168       | 0.0240 |
| BC013679        | cDNA clone IMAGE:3857956, partial cds. [BC013679]  | 168       | 0.0207 |
| TCF8            | transcription factor 8 (represses interleukin 2 expression) (TCF8), mRNA [NM_030751]                   | 167       | 0.0325 |
| PBK             | PDZ binding kinase (PBK), mRNA [NM_018492]   | 167       | 0.0325 |
| AF034187        | clone 2.2H12 Ndr Ser/Thr kinase-like protein mRNA, partial cds. [AF034187]                             | 166       | 0.0229 |
| GAB2            | GRB2-associated binding protein 2 (GAB2), transcript variant 2, mRNA [NM_012296]                       | 166       | 0.0143 |
| AK025323        | cDNA: FLJ21670 fis, clone COL09010. [AK025323]   | 166       | 0.0267 |
| AI093077        | AI093077 qa96ho2.x1 Soares_fetal_heart_NbHH19W cDNA clone IMAGE:1694643 3', mRNA sequence [AI093077]   | 166       | 0.0417 |
| PLXDC1          | plexin domain containing 1 (PLXDC1), mRNA [NM_020405]  | 165       | 0.0454 |
| ENST00000371079 | cDNA FLJ20769 fis, clone COL06674. [AK000776]  | 165       | 0.0419 |
| PLD1            | cDNA FLJ34578 fis, clone KIDNE2008404, highly similar to PHOSPHOLIPASE D1 (EC 3.1.4.4). [AK091897]     | 165       | 0.0260 |
| RNF144          | ring finger protein 144 (RNF144), mRNA [NM_014746]   | 165       | 0.0204 |
| SDSL            | serine dehydratase-like (SDSL), mRNA [NM_138432]   | 164       | 0.0232 |
| THC2380706      | Q6UXG1 (Q6UXG1) YVTM2421, partial (3%) [THC2380706]  | 164       | 0.0356 |
| ENST00000292357 | full-length cDNA clone CS0DC023YA11 of Neuroblastoma Cot 25-normalized of (human). [CR599082]          | 163       | 0.0389 |
| LOC644242       | hypothetical protein LOC644242, mRNA (cDNA clone IMAGE:4403366), partial cds. [BC015390]               | 163       | 0.0307 |

CHAPTER 3

| Gene         | Description   | Expr. (%) | P-val. |
|--------------|---|-----------|--------|
| A_23_P255111 | Unknown   | 162       | 0.0318 |
| NHS          | Nance-Horan syndrome (congenital cataracts and dental anomalies) (NHS), mRNA [NM_198270]  | 162       | 0.0496 |
| TP53l3       | tumor protein p53 inducible protein 3 (TP53l3), transcript variant 1, mRNA [NM_004881]  | 162       | 0.0133 |
| OAF          | OAF homolog (Drosophila) (OAF), mRNA [NM_178507]  | 162       | 0.0311 |
| CDC42EP2     | CDC42 effector protein (Rho GTPase binding) 2 (CDC42EP2), mRNA [NM_006779]  | 161       | 0.0333 |
| ALOX12P2     | arachidonate 12-lipoxygenase pseudogene 2 (ALOX12P2) on chromosome 17 [NR_002710]   | 161       | 0.0434 |
| BY798288     | BY798288 eye cDNA clone HE3347.seq 5', mRNA sequence [BY798288]   | 161       | 0.0482 |
| TPX2         | TPX2, microtubule-associated, homolog (Xenopus laevis) (TPX2), mRNA [NM_012112]   | 160       | 0.0496 |
| A_24_P401051 | Unknown   | 160       | 0.0462 |
| THC2442208   | Unknown   | 160       | 0.0491 |
| ANTXR1       | anthrax toxin receptor 1 (ANTXR1), transcript variant 2, mRNA [NM_053034]   | 160       | 0.0365 |
| CDC2         | cell division cycle 2, G1 to S and G2 to M (CDC2), transcript variant 1, mRNA [NM_001786]   | 159       | 0.0419 |
| THBS3        | thrombospondin 3 (THBS3), mRNA [NM_007112]  | 159       | 0.0419 |
| SLC16A12     | cDNA FLJ42911 fis, clone BRHIP3024118, weakly similar to Monocarboxylate transporter 4. [AK124901]  | 159       | 0.0485 |
| DNAJC12      | Dnaj (Hsp40) homolog, subfamily C, member 12 (DNAJC12), transcript variant 1, mRNA [NM_021800]  | 159       | 0.0215 |
| sep-06       | septin 6 (SEPT6), transcript variant V, mRNA [NM_145802]  | 159       | 0.0325 |
| SPBC25       | spindle pole body component 25 homolog (S. cerevisiae) (SPBC25), mRNA [NM_020675]   | 159       | 0.0283 |
| ITGA1        | integrin, alpha 1 (ITGA1), mRNA [NM_181501]   | 159       | 0.0356 |
| HMGCLL1      | 3-hydroxymethyl-3-methylglutaryl-Coenzyme A lyase-like 1 (HMGCLL1), transcript variant 1, mRNA [NM_019036]  | 159       | 0.0402 |
| HSF4         | heat shock transcription factor 4 (HSF4), transcript variant 1, mRNA [NM_001538]  | 159       | 0.0438 |
| CPA1         | carboxypeptidase A1 (pancreatic) (CPA1), mRNA [NM_001868]   | 158       | 0.0359 |
| PFTK1        | PFTAIRES protein kinase 1 (PFTK1), mRNA [NM_012395]   | 156       | 0.0288 |
| AK094929     | cDNA FLJ37610 fis, clone BRCOC2011398. [AK094929]   | 156       | 0.0328 |
| ROR1         | receptor tyrosine kinase-like orphan receptor 1 (ROR1), mRNA [NM_005012]  | 155       | 0.0429 |
| KLK13        | kallikrein 13 (KLK13), mRNA [NM_015596]   | 155       | 0.0192 |
| RAB6B        | RAB6B, member RAS oncogene family (RAB6B), mRNA [NM_016577]   | 154       | 0.0375 |
| CHST1        | carbohydrate (keratan sulfate Gal-6) sulfotransferase 1 (CHST1), mRNA [NM_003654]   | 154       | 0.0171 |
| LYPD1        | LY6/PLAUR domain containing 1 (LYPD1), mRNA [NM_144586]   | 154       | 0.0434 |
| MMP16        | matrix metalloproteinase 16 (membrane-inserted) (MMP16), transcript variant 2, mRNA [NM_022564]   | 154       | 0.0231 |
| MGC26647     | hypothetical protein MGC26647 (MGC26647), mRNA [NM_152706]  | 153       | 0.0381 |
| A_32_P183519 | Unknown   | 153       | 0.0454 |
| AI263220     | AI263220 qz36f10.x1 NCL_CGAP_Kid11 cDNA clone IMAGE:2029003 3' similar to TR:Q14041 Q14041 COLLAGEN VI ALPHA-1 N-TERMINAL GLOBULAR DOMAIN PRECURSOR ;, mRNA sequence [AI263220] | 153       | 0.0419 |
| CHMP4B       | chromatin modifying protein 4B (CHMP4B), mRNA [NM_176812]   | 152       | 0.0308 |
| SLC22A16     | solute carrier family 22 (organic cation transporter), member 16 (SLC22A16), mRNA [NM_033125]   | 152       | 0.0427 |
| KCNK2        | potassium channel, subfamily K, member 2 (KCNK2), transcript variant 1, mRNA [NM_001017424]   | 152       | 0.0317 |
| NXN          | nucleoredoxin (NXN), mRNA [NM_022463]   | 151       | 0.0308 |
| MLLT4        | myeloid/lymphoid or mixed-lineage leukemia (trithorax homolog, Drosophila); translocated to, 4 (MLLT4), transcript variant 3, mRNA [NM_005936]                                  | 150       | 0.0294 |
| KATNAL2      | katanin p60 subunit A-like 2 (KATNAL2), mRNA [NM_031303]  | 150       | 0.0236 |
| MCM4         | MCM4 minichromosome maintenance deficient 4 (S. cerevisiae) (MCM4), transcript variant 1, mRNA [NM_005914]  | 150       | 0.0321 |
| TCN2         | transcobalamin II; macrocytic anemia (TCN2), mRNA [NM_000355]   | 150       | 0.0328 |
| RASSF2       | Ras association (RalGDS/AF-6) domain family 2 (RASSF2), transcript variant 1, mRNA [NM_014737]  | 150       | 0.0236 |
| A_32_P190334 | Unknown   | 150       | 0.0435 |
| COL5A2       | collagen, type V, alpha 2 (COL5A2), mRNA [NM_000393]  | 150       | 0.0192 |
| SAMD3        | sterile alpha motif domain containing 3 (SAMD3), transcript variant 1, mRNA [NM_001017373]  | 149       | 0.0357 |
| ATP5D        | ATP synthase, H+ transporting, mitochondrial F1 complex, delta subunit (ATP5D), nuclear gene encoding mito-149 chondrial protein, transcript variant 2, mRNA [NM_001001975]     | 149       | 0.0430 |
| EIF4EBP1     | eukaryotic translation initiation factor 4E binding protein 1 (EIF4EBP1), mRNA [NM_004095]  | 149       | 0.0417 |
| A_24_P552131 | Unknown   | 148       | 0.0402 |
| M74720       | Human SEF2-1D protein (SEF2-1D) mRNA, partial cds. [M74720]   | 148       | 0.0188 |
| PLA2R1       | phospholipase A2 receptor 1, 180kDa (PLA2R1), transcript variant 1, mRNA [NM_007366]  | 148       | 0.0363 |
| GALNTL4      | clone 25215 mRNA sequence, partial cds. [AF131852]  | 148       | 0.0290 |
| DDR2         | discoidin domain receptor family, member 2 (DDR2), transcript variant 1, mRNA [NM_001014796]  | 147       | 0.0499 |
| THC2279352   | Q8NH31 (Q8NH31) Seven transmembrane helix receptor, partial (5%) [THC2279352]   | 147       | 0.0317 |
| A_24_P178784 | Unknown   | 147       | 0.0339 |
| ETV5         | ets variant gene 5 (ets-related molecule) (ETV5), mRNA [NM_004454]  | 146       | 0.0435 |
| CR621923     | full-length cDNA clone CSoDC01oYA19 of Neuroblastoma Cot 25-normalized of (human). [CR621923]   | 145       | 0.0381 |
| CR612178     | full-length cDNA clone CSoD1o15YM13 of Placenta Cot 25-normalized of (human). [CR612178]  | 145       | 0.0365 |
| A_24_P255509 | Unknown   | 145       | 0.0356 |

GENE EXPRESSION IN HUMAN NEUROMA

| Gene            | Description  | Expr. (%) | P-val. |
|-----------------|--|-----------|--------|
| CDKN3           | cyclin-dependent kinase inhibitor 3 (CDK2-associated dual specificity phosphatase) (CDKN3), mRNA [NM_005192]   | 144       | 0.0419 |
| HNRPLL          | heterogeneous nuclear ribonucleoprotein L-like, mRNA (cDNA clone MGC:5437 IMAGE:3449607), complete cds. [BC008217]   | 144       | 0.0283 |
| AF146694        | clone IMAGE:121412 mRNA sequence. [AF146694]   | 143       | 0.0308 |
| FOXP1           | forkhead box P1 (FOXP1), transcript variant 1, mRNA [NM_032682]  | 143       | 0.0370 |
| SULT1A2         | sulfotransferase family, cytosolic, 1A, phenol-preferring, member 2 (SULT1A2), transcript variant 2, mRNA [NM_177528]                                      | 143       | 0.0288 |
| DKFZp762E1312   | hypothetical protein DKFZp762E1312 (DKFZp762E1312), mRNA [NM_018410]   | 141       | 0.0434 |
| A_24_P118336    | Unknown  | 141       | 0.0321 |
| LOC57228        | small trans-membrane and glycosylated protein (LOC57228), transcript variant 1, mRNA [NM_001031628]  | 140       | 0.0375 |
| A_24_P913629    | Unknown  | 140       | 0.0464 |
| L3MBTL3         | l(3)mbt-like 3 (Drosophila) (L3MBTL3), transcript variant 1, mRNA [NM_032438]  | 138       | 0.0483 |
| FLJ38482        | hypothetical protein FLJ38482 (FLJ38482), mRNA [NM_152681]   | 75        | 0.0417 |
| ENST00000377411 | cDNA: FLJ23230 fis, clone CAE07143. [AK026883]   | 75        | 0.0434 |
| TIMP3           | TIMP metalloproteinase inhibitor 3 (Sorsby fundus dystrophy, pseudoinflammatory) (TIMP3), mRNA [NM_000362]   | 75        | 0.0483 |
| CTSL2           | cathepsin L2 (CTSL2), mRNA [NM_001333]   | 74        | 0.0421 |
| MGC16385        | hypothetical protein MGC16385 (MGC16385), mRNA [NM_145039]   | 74        | 0.0436 |
| LOC402573       | hypothetical LOC402573 (LOC402573), mRNA [NM_001004323]  | 74        | 0.0387 |
| FRMD1           | FERM domain containing 1 (FRMD1), mRNA [NM_024919]   | 74        | 0.0399 |
| AK096991        | cDNA FLJ39672 fis, clone SMINT2009233. [AK096991]  | 73        | 0.0492 |
| TMEM1           | transmembrane protein 1 (TMEM1), transcript variant 1, mRNA [NM_003274]  | 73        | 0.0316 |
| FDPS            | farnesyl diphosphate synthase (farnesyl pyrophosphate synthetase, dimethylallyltransferase, geranyltransferase) (FDPS), mRNA [NM_002004]                   | 73        | 0.0435 |
| UST             | uronyl-2-sulfotransferase (UST), mRNA [NM_005715]  | 73        | 0.0359 |
| AK023472        | cDNA FLJ13410 fis, clone PLACE1001720. [AK023472]  | 73        | 0.0349 |
| BQ424374        | AGENCOURT_7892842 NIH_MGC_72 cDNA clone IMAGE:6157378 5'; mRNA sequence [BQ424374]   | 73        | 0.0339 |
| LINCR           | likely ortholog of mouse lung-inducible Neutralized-related C3HC4 RING domain protein, mRNA (cDNA clone MGC:15646 IMAGE:3346442), complete cds. [BC012317] | 72        | 0.0439 |
| AGA             | aspartylglucosaminidase (AGA), mRNA [NM_000027]  | 72        | 0.0283 |
| LRP8            | low density lipoprotein receptor-related protein 8, apolipoprotein e receptor (LRP8), transcript variant 2, mRNA [NM_033300]                               | 72        | 0.0494 |
| FKBP1B          | FK506 binding protein 1B, 12.6 kDa (FKBP1B), transcript variant 2, mRNA [NM_054033]  | 72        | 0.0283 |
| BQ019626        | BQ019626 UI-H-ED0-axd-f-18-o-UI.s1 NCI_CGAP_ED0 cDNA clone IMAGE:5827217 3'; mRNA sequence [BQ019626]  | 72        | 0.0215 |
| ENST00000342275 | RST6901 Athersys RAGE Library cDNA, mRNA sequence [BG187898]   | 72        | 0.0229 |
| STON1           | stonin 1 (STON1), mRNA [NM_006873]   | 72        | 0.0485 |
| BU661610        | cl74d04.21 Hembase; Erythroid Precursor Cells (LCB:cl library) cDNA clone cl74d04 5'; mRNA sequence [BU661610]   | 72        | 0.0401 |
| KNDC1           | kinase non-catalytic C-lobe domain (KIND) containing 1 (KNDC1), transcript variant 1, mRNA [NM_152643]   | 72        | 0.0356 |
| TEKT3           | tektin 3 (TEKT3), mRNA [NM_031898]   | 71        | 0.0327 |
| OClAD2          | OClA domain containing 2 (OClAD2), transcript variant 1, mRNA [NM_001014446]   | 71        | 0.0267 |
| FTHL12          | ferritin, heavy polypeptide-like 12 (FTHL12) on chromosome 9 [NR_002205]   | 71        | 0.0419 |
| SHMT1           | serine hydroxymethyltransferase 1 (soluble) (SHMT1), transcript variant 1, mRNA [NM_004169]  | 71        | 0.0288 |
| AL049443        | mRNA; cDNA DKFZp586N2020 (from clone DKFZp586N2020). [AL049443]  | 70        | 0.0387 |
| ENST00000256367 | tetratricopeptide repeat domain 9, mRNA (cDNA clone IMAGE:5763935), partial cds. [BC047950]  | 70        | 0.0302 |
| FEZ1            | fasciculation and elongation protein zeta 1 (zygin I) (FEZ1), transcript variant 1, mRNA [NM_005103]   | 70        | 0.0451 |
| A_32_P35031     | Unknown  | 70        | 0.0259 |
| ASRGL1          | asparaginase like 1, mRNA (cDNA clone IMAGE:3952485), complete cds. [BC006267]   | 70        | 0.0325 |
| ENST00000320378 | cDNA FLJ39084 fis, clone NT2RP7018871. [AK096403]  | 70        | 0.0351 |
| LHPP            | phosphorylsine phosphohistidine inorganic pyrophosphate phosphatase (LHPP), mRNA [NM_022126]   | 70        | 0.0260 |
| AK095986        | cDNA FLJ38667 fis, clone HLUNG2006843. [AK095986]  | 70        | 0.0451 |
| LOC283481       | hypothetical protein LOC283481, mRNA (cDNA clone IMAGE:5296747). [BC033993]  | 70        | 0.0259 |
| ANKS1B          | ankyrin repeat and sterile alpha motif domain containing 1B (ANKS1B), transcript variant 2, mRNA [NM_181670]   | 70        | 0.0339 |
| GNAZ            | guanine nucleotide binding protein (G protein), alpha z polypeptide (GNAZ), mRNA [NM_002073]   | 69        | 0.0166 |
| BC030102        | cDNA clone IMAGE:4796690. [BC030102]   | 69        | 0.0156 |
| C6orf194        | chromosome 6 open reading frame 194 (C6orf194), mRNA [NM_001007531]  | 69        | 0.0434 |
| ENST00000343149 | Unknown  | 69        | 0.0419 |
| HRASL2          | HRAS-like suppressor 2 (HRASL2), mRNA [NM_017878]  | 69        | 0.0344 |
| A_32_P190864    | Unknown  | 69        | 0.0319 |
| EMP2            | epithelial membrane protein 2 (EMP2), mRNA [NM_001424]   | 69        | 0.0492 |

CHAPTER 3

| Gene            | Description  | Expr. (%) | P-val. |
|-----------------|--|-----------|--------|
| THC2281336      | Unknown  | 69        | 0.0359 |
| LOC388114       | cDNA clone IMAGE:4798730. [BC036424]   | 69        | 0.0436 |
| K-ALPHA-1       | alpha tubulin (K-ALPHA-1), mRNA [NM_006082]  | 69        | 0.0257 |
| SCD             | stearyl-CoA desaturase (delta-9-desaturase) (SCD), mRNA [NM_005063]  | 69        | 0.0467 |
| GAS7            | growth arrest-specific 7 (GAS7), transcript variant c, mRNA [NM_201433]  | 68        | 0.0305 |
| BM045853        | 603624848F1 NIH_MGC_40 cDNA clone IMAGE:5451514 5', mRNA sequence [BM045853]   | 68        | 0.0462 |
| SNTG2           | syntrophin, gamma 2 (SNTG2), mRNA [NM_018968]  | 68        | 0.0149 |
| BG943680        | BG943680 ax40g03.x1 Hembase; Erythroid Progenitor Cells (LCB:ax library) cDNA clone ax40g03 random, mRNA sequence [BG943680]                                       | 68        | 0.0308 |
| MRPS6           | mitochondrial ribosomal protein S6 (MRPS6), nuclear gene encoding mitochondrial protein, mRNA [NM_032476]  | 68        | 0.0457 |
| AK054684        | cDNA FLJ30122 fis, clone BRACE1000087. [AK054684]  | 68        | 0.0331 |
| HCA112          | hepatocellular carcinoma-associated antigen 112 (HCA112), mRNA [NM_018487]   | 68        | 0.0435 |
| C6orf1          | chromosome 6 open reading frame 1 (C6orf1), transcript variant 1, mRNA [NM_178508]   | 68        | 0.0451 |
| OXCT2           | mRNA for FLJ00030 protein, partial cds. [AK024440]   | 68        | 0.0439 |
| CXorf6          | chromosome X open reading frame 6 (CXorf6), mRNA [NM_005491]   | 68        | 0.0192 |
| ENST00000377492 | Q99Kf9 (Q99Kf9) Lrpprc protein, partial (39%) [THC2336834]   | 68        | 0.0130 |
| SCCPDH          | saccharopine dehydrogenase (putative) (SCCPDH), mRNA [NM_016002]   | 68        | 0.0359 |
| BM955917        | EST0854 HEV PCR-select cDNA clone HEV#2788 similar to olfactory receptor OR7E15P pseudogene, mRNA sequence [BM955917]  | 68        | 0.0229 |
| KIAA0232        | KIAA0232 gene product (KIAA0232), mRNA [NM_014743]   | 68        | 0.0231 |
| C9orf165        | chromosome 9 open reading frame 165 (C9orf165), mRNA [NM_198573]   | 67        | 0.0307 |
| ZSWIM3          | zinc finger, SWIM-type containing 3 (ZSWIM3), mRNA [NM_080752]   | 67        | 0.0330 |
| LGI3            | leucine-rich repeat LGI family, member 3 (LGI3), mRNA [NM_139278]  | 67        | 0.0209 |
| TNNI3K          | TNNI3 interacting kinase (TNNI3K), mRNA [NM_015978]  | 67        | 0.0406 |
| AA348270        | AA348270 EST54713 Hippocampus I cDNA 3' end similar to EST containing Alu repeat, mRNA sequence [AA348270]   | 67        | 0.0451 |
| FDFT1           | farnesyl-diphosphate farnesyltransferase 1 (FDFT1), mRNA [NM_004462]   | 67        | 0.0307 |
| MFS2D2          | major facilitator superfamily domain containing 2 (MFS2D2), mRNA [NM_032793]   | 67        | 0.0267 |
| THC2315973      | Unknown  | 67        | 0.0130 |
| ENST00000374395 | Down syndrome critical region gene 1-like 2, mRNA (cDNA clone MGC:46109 IMAGE:5770066), complete cds. [BC035854]   | 67        | 0.0229 |
| TMEM139         | transmembrane protein 139 (TMEM139), mRNA [NM_153345]  | 67        | 0.0488 |
| KIAA1026        | kazrin (KIAA1026), transcript variant B, mRNA [NM_001018000]   | 67        | 0.0243 |
| INPP5F          | inositol polyphosphate-5-phosphatase F (INPP5F), transcript variant 1, mRNA [NM_014937]  | 67        | 0.0339 |
| MLLT11          | myeloid/lymphoid or mixed-lineage leukemia (trithorax homolog, Drosophila); translocated to, 11 (MLLT11), mRNA [NM_006818]   | 67        | 0.0401 |
| THC2344033      | Unknown  | 67        | 0.0436 |
| DHCR7           | 7-dehydrocholesterol reductase (DHCR7), mRNA [NM_001360]   | 66        | 0.0356 |
| AK026697        | cDNA: FLJ23044 fis, clone LNG02454. [AK026697]   | 66        | 0.0413 |
| TMEM155         | transmembrane protein 155 (TMEM155), mRNA [NM_152399]  | 66        | 0.0316 |
| FZD8            | frizzled homolog 8 (Drosophila) (FZD8), mRNA [NM_031866]   | 66        | 0.0182 |
| A_23_P120606    | Unknown  | 66        | 0.0441 |
| LIPC            | lipase, hepatic (LIPC), mRNA [NM_000236]   | 66        | 0.0183 |
| LRRRC4C         | leucine rich repeat containing 4C (LRRRC4C), mRNA [NM_020929]  | 66        | 0.0439 |
| ANKRD43         | ankyrin repeat domain 43 (ANKRD43), mRNA [NM_175873]   | 66        | 0.0417 |
| SNX24           | sorting nexin 24 (SNX24), mRNA [NM_014035]   | 66        | 0.0259 |
| PDZD2           | PDZ domain containing 2 (PDZD2), mRNA [NM_178140]  | 66        | 0.0356 |
| ENST00000277575 | mRNA for KIAA0019 protein, partial cds. [D13644]   | 66        | 0.0257 |
| SLC20A2         | solute carrier family 20 (phosphate transporter), member 2 (SLC20A2), mRNA [NM_006749]   | 66        | 0.0297 |
| THC2302865      | FABE_HUMAN (Q01469) Fatty acid-binding protein, epidermal (E-FABP) (Psoriasis-associated fatty acid-binding protein homolog) (PA-FABP), partial (53%) [THC2302865] | 66        | 0.0434 |
| STAG3           | stromal antigen 3 (STAG3), mRNA [NM_012447]  | 65        | 0.0441 |
| RASEF           | RAS and EF-hand domain containing (RASEF), mRNA [NM_152573]  | 65        | 0.0242 |
| CDH4            | cDNA: FLJ22202 fis, clone HRC01333. [AK025855]   | 65        | 0.0381 |
| NLK             | nemo-like kinase (NLK), mRNA [NM_016231]   | 65        | 0.0338 |
| RAB37           | RAB37, member RAS oncogene family (RAB37), transcript variant 3, mRNA [NM_175738]  | 65        | 0.0205 |
| PCSK6           | proprotein convertase subtilisin/kexin type 6 (PCSK6), transcript variant 1, mRNA [NM_002570]  | 65        | 0.0201 |
| ARHGAP22        | Rho GTPase activating protein 22 (ARHGAP22), mRNA [NM_021226]  | 65        | 0.0407 |
| HSPA2           | heat shock 70kDa protein 2 (HSPA2), mRNA [NM_021979]   | 65        | 0.0182 |
| AQP11           | aquaporin 11 (AQP11), mRNA [NM_173039]   | 65        | 0.0202 |
| THC2270160      | Unknown  | 65        | 0.0491 |

GENE EXPRESSION IN HUMAN NEUROMA

| Gene         | Description   | Expr. (%) | P-val. |
|--------------|---|-----------|--------|
| FAM19A5      | family with sequence similarity 19 (chemokine (C-C motif)-like), member A5 (FAM19A5), mRNA [NM_015381]    | 65        | 0.0384 |
| CD9          | CD9 molecule (CD9), mRNA [NM_001769]  | 65        | 0.0457 |
| BG216262     | RST35951 Athersys RAGE Library cDNA, mRNA sequence [BG216262]   | 65        | 0.0258 |
| MCOLN2       | mucoilin 2 (MCOLN2), mRNA [NM_153259]   | 65        | 0.0376 |
| CMTM6        | CKLF-like MARVEL transmembrane domain containing 6 (CMTM6), mRNA [NM_017801]                              | 65        | 0.0259 |
| CMTM7        | CKLF-like MARVEL transmembrane domain containing 7 (CMTM7), transcript variant 1, mRNA [NM_138410]        | 65        | 0.0413 |
| CPXM2        | carboxypeptidase X (M14 family), member 2 (CPXM2), mRNA [NM_198148]                                       | 64        | 0.0229 |
| A_24_P255836 | Unknown   | 64        | 0.0082 |
| A_23_P113762 | Unknown   | 64        | 0.0146 |
| SORD         | sorbitol dehydrogenase (SORD), mRNA [NM_003104]   | 64        | 0.0350 |
| STMN4        | stathmin-like 4 (STMN4), mRNA [NM_030795]   | 64        | 0.0229 |
| SAMHD1       | SAM domain and HD domain 1 (SAMHD1), mRNA [NM_015474]   | 64        | 0.0275 |
| C10orf125    | chromosome 10 open reading frame 125 (C10orf125), mRNA [NM_198472]  | 64        | 0.0192 |
| CR608907     | full-length cDNA clone CS0DM002YA18 of Fetal liver of (human). [CR608907]                                 | 64        | 0.0098 |
| KLF15        | Kruppel-like factor 15 (KLF15), mRNA [NM_014079]  | 64        | 0.0164 |
| C10orf13     | chromosome 10 open reading frame 13 (C10orf13), mRNA [NM_152429]  | 64        | 0.0283 |
| TSGA2        | testis specific A2 homolog (mouse) (TSGA2), mRNA [NM_080860]  | 64        | 0.0197 |
| BZRAP1       | benzodiazepine receptor (peripheral) associated protein 1 (BZRAP1), mRNA [NM_004758]                      | 64        | 0.0499 |
| A_23_P140454 | Unknown   | 64        | 0.0121 |
| ARHGAP24     | Rho GTPase activating protein 24 (ARHGAP24), mRNA [NM_031305]   | 64        | 0.0240 |
| RAB38        | RAB38, member RAS oncogene family (RAB38), mRNA [NM_022337]   | 64        | 0.0077 |
| RDH10        | retinol dehydrogenase 10 (all-trans) (RDH10), mRNA [NM_172037]  | 64        | 0.0307 |
| FLJ25530     | hepatocyte cell adhesion molecule (FLJ25530), mRNA [NM_152722]  | 64        | 0.0101 |
| TESK2        | testis-specific kinase 2 (TESK2), mRNA [NM_007170]  | 63        | 0.0229 |
| Ells1        | hypothetical protein Ells1 (Ells1), mRNA [NM_152793]  | 63        | 0.0186 |
| HPS5         | Hermansky-Pudlak syndrome 5 (HPS5), transcript variant 1, mRNA [NM_181507]                                | 63        | 0.0260 |
| GDF1         | growth differentiation factor 1 (GDF1), mRNA [NM_001492]  | 63        | 0.0229 |
| C9orf50      | chromosome 9 open reading frame 50 (C9orf50), mRNA [NM_199350]  | 63        | 0.0171 |
| MPP6         | membrane protein, palmitoylated 6 (MAGUK p55 subfamily member 6) (MPP6), mRNA [NM_016447]                 | 63        | 0.0295 |
| C9orf58      | chromosome 9 open reading frame 58 (C9orf58), transcript variant 2, mRNA [NM_001002260]                   | 63        | 0.0259 |
| SYT1         | synaptotagmin I (SYT1), mRNA [NM_005639]  | 63        | 0.0257 |
| WFIKKN2      | WAP, follistatin/kazal, immunoglobulin, kunitz and netrin domain containing 2 (WFIKKN2), mRNA [NM_175575] | 63        | 0.0073 |
| GLDC         | glycine dehydrogenase (decarboxylating) (GLDC), mRNA [NM_000170]  | 63        | 0.0386 |
| LOC439914    | cDNA FLJ37045 fis, clone BRACE2012185. [AK094364]   | 63        | 0.0054 |
| MMD2         | monocyte to macrophage differentiation-associated 2 (MMD2), mRNA [NM_198403]                              | 63        | 0.0379 |
| ENTHD1       | ENTH domain containing 1 (ENTHD1), mRNA [NM_152512]   | 63        | 0.0292 |
| BF803942     | BF803942 CM2-CI0135-021100-477-g08 CI0135 cDNA, mRNA sequence [BF803942]                                  | 63        | 0.0180 |
| FRMD3        | FERM domain containing 3 (FRMD3), mRNA [NM_174938]  | 63        | 0.0168 |
| AK5          | adenylate kinase 5 (AK5), transcript variant 1, mRNA [NM_174858]  | 63        | 0.0152 |
| CYFIP2       | cytoplasmic FMR1 interacting protein 2 (CYFIP2), transcript variant 3, mRNA [NM_014376]                   | 63        | 0.0317 |
| THC2404004   | Q9GZC7 (Q9GZC7) RNA binding protein RGGm, partial (7%) [THC2404004]                                       | 62        | 0.0232 |
| PCDH10       | protocadherin 10 (PCDH10), transcript variant 1, mRNA [NM_032961]   | 62        | 0.0318 |
| TSPAN13      | tetraspanin 13 (TSPAN13), mRNA [NM_014399]  | 62        | 0.0361 |
| KIF13B       | kinesin family member 13B (KIF13B), mRNA [NM_015254]  | 62        | 0.0130 |
| KIAA1688     | KIAA1688 protein (KIAA1688), mRNA [NM_025251]   | 62        | 0.0215 |
| BDKRB2       | bradykinin receptor B2 (BDKRB2), mRNA [NM_000623]   | 62        | 0.0435 |
| IGSF4C       | immunoglobulin superfamily, member 4C (IGSF4C), mRNA [NM_145296]  | 62        | 0.0327 |
| PEG10        | paternally expressed 10 (PEG10), transcript variant 2, mRNA [NM_001040152]                                | 62        | 0.0334 |
| AF132203     | PRO1933 mRNA, complete cds. [AF132203]  | 62        | 0.0313 |
| FAM83F       | family with sequence similarity 83, member F (FAM83F), mRNA [NM_138435]                                   | 62        | 0.0156 |
| BMP7         | bone morphogenetic protein 7 (osteogenic protein 1) (BMP7), mRNA [NM_001719]                              | 62        | 0.0311 |
| KIAA1576     | KIAA1576 protein (KIAA1576), mRNA [NM_020927]   | 61        | 0.0256 |
| THC2438994   | Unknown   | 61        | 0.0308 |
| EYA2         | eyes absent homolog 2 (Drosophila) (EYA2), transcript variant 2, mRNA [NM_172113]                         | 61        | 0.0373 |
| TCBA1        | T-cell lymphoma breakpoint associated target 1 (TCBA1), mRNA [NM_001040214]                               | 61        | 0.0341 |
| ADARB2       | adenosine deaminase, RNA-specific, B2 (RED2 homolog rat) (ADARB2), mRNA [NM_018702]                       | 61        | 0.0185 |
| PARD6B       | par-6 partitioning defective 6 homolog beta (C. elegans) (PARD6B), mRNA [NM_032521]                       | 61        | 0.0429 |
| MMP28        | matrix metalloproteinase 28 (MMP28), transcript variant 1, mRNA [NM_024302]                               | 61        | 0.0144 |

CHAPTER 3

| Gene            | Description   | Expr. (%) | P-val. |
|-----------------|---|-----------|--------|
| RAP1GDS1        | RAP1, GTP-GDP dissociation stimulator 1 (RAP1GDS1), mRNA [NM_021159]  | 61        | 0.0196 |
| MIA             | melanoma inhibitory activity (MIA), mRNA [NM_006533]  | 61        | 0.0294 |
| OR7E24          | olfactory receptor, family 7, subfamily E, member 24 (OR7E24) on chromosome 19 [NR_002146]  | 61        | 0.0077 |
| ENST00000368025 | Unknown   | 61        | 0.0419 |
| EHBP1           | EH domain binding protein 1 (EHBP1), mRNA [NM_015252]   | 61        | 0.0334 |
| GLOXD1          | glyoxalase domain containing 1 (GLOXD1), mRNA [NM_032756]   | 61        | 0.0049 |
| MLPH            | melanophilin (MLPH), transcript variant 1, mRNA [NM_024101]   | 60        | 0.0076 |
| KHDRBS3         | KH domain containing, RNA binding, signal transduction associated 3 (KHDRBS3), mRNA [NM_006558]                                   | 60        | 0.0439 |
| BC034319        | cDNA clone IMAGE:4837650. [BC034319]  | 60        | 0.0130 |
| TMC7            | transmembrane channel-like 7 (TMC7), mRNA [NM_024847]   | 60        | 0.0090 |
| ENST00000357776 | cDNA FLJ13094 fis, clone NT2RP3002163. [AK023156]   | 60        | 0.0149 |
| METRNL          | meteorin, glial cell differentiation regulator-like (METRNL), mRNA [NM_001004431]   | 60        | 0.0485 |
| T15787          | T15787 IB1893 Infant brain, Bento Soares cDNA 3'end, mRNA sequence [T15787]   | 60        | 0.0491 |
| NEGR1           | neuronal growth regulator 1 (NEGR1), mRNA [NM_173808]   | 60        | 0.0283 |
| AP1S3           | adaptor-related protein complex 1, sigma 3 subunit (AP1S3), mRNA [NM_001039569]   | 60        | 0.0417 |
| PLLP            | transmembrane 4 superfamily member 11 (plasmolipin) (TM4SF11), mRNA [NM_015993]   | 60        | 0.0093 |
| THC2412859      | Unknown   | 60        | 0.0362 |
| FLJ30428        | cDNA FLJ30428 fis, clone BRACE2008941. [AK054990]   | 60        | 0.0088 |
| KIF5A           | mRNA for KIF5A variant protein, partial cds, clone: phoo435. [AB210045]   | 60        | 0.0179 |
| ENST00000322839 | cDNA FLJ32334 fis, clone PROST2005426. [AK056896]   | 60        | 0.0317 |
| B3GAT1          | beta-1,3-glucuronyltransferase 1 (glucuronosyltransferase P) (B3GAT1), transcript variant 1, mRNA [NM_018644]                     | 60        | 0.0259 |
| KRT16           | keratin 16 (focal non-epidermolytic palmoplantar keratoderma) (KRT16), mRNA [NM_005557]   | 60        | 0.0456 |
| ENST00000374851 | cDNA FLJ37094 fis, clone BRACE2018337. [AK094413]   | 59        | 0.0356 |
| KCNK12          | potassium channel, subfamily K, member 12 (KCNK12), mRNA [NM_022055]  | 59        | 0.0161 |
| A_24_P533142    | Unknown   | 59        | 0.0097 |
| LY75            | lymphocyte antigen 75 (LY75), mRNA [NM_002349]  | 59        | 0.0200 |
| BMP8B           | bone morphogenetic protein 8b (osteogenic protein 2) (BMP8B), mRNA [NM_001720]  | 59        | 0.0173 |
| ROM1            | retinal outer segment membrane protein 1 (ROM1), mRNA [NM_000327]   | 59        | 0.0092 |
| NRXN1           | neurexin 1 (NRXN1), transcript variant alpha, mRNA [NM_004801]  | 59        | 0.0296 |
| THC2434739      | GP27_HUMAN (Q9NS67) Probable G protein-coupled receptor 27 (Super conserved receptor expressed in brain 1), complete [THC2434739] | 59        | 0.0276 |
| SC4MOL          | sterol-C4-methyl oxidase-like (SC4MOL), transcript variant 1, mRNA [NM_006745]  | 59        | 0.0296 |
| SPTBN5          | spectrin, beta, non-erythrocytic 5 (SPTBN5), mRNA [NM_016642]   | 59        | 0.0375 |
| PRPH            | peripherin (PRPH), mRNA [NM_006262]   | 59        | 0.0359 |
| IGFBP3          | insulin-like growth factor 2 mRNA binding protein 3 (IGFBP3), mRNA [NM_006547]  | 59        | 0.0343 |
| AK090670        | cDNA FLJ33351 fis, clone BRACE2005063. [AK090670]   | 59        | 0.0077 |
| C9orf125        | chromosome 9 open reading frame 125 (C9orf125), mRNA [NM_032342]  | 59        | 0.0317 |
| A_24_P110201    | Unknown   | 59        | 0.0050 |
| BIRC7           | baculoviral IAP repeat-containing 7 (livin) (BIRC7), transcript variant 2, mRNA [NM_022161]                                       | 59        | 0.0408 |
| OR7E156P        | olfactory receptor, family 7, subfamily E, member 156 pseudogene (OR7E156P) on chromosome 13 [NR_002171]                          | 59        | 0.0050 |
| HEPN1           | associated with liver cancer (HEPN1), mRNA [NM_001037558]   | 59        | 0.0339 |
| AK125371        | cDNA FLJ43381 fis, clone OCBBF2005428. [AK125371]   | 58        | 0.0340 |
| FADS1           | fatty acid desaturase 1 (FADS1), mRNA [NM_013402]   | 58        | 0.0097 |
| DB534761        | DB534761 RIKEN full-length enriched human cDNA library, hippocampus cDNA clone Ho23029H14 3', mRNA sequence [DB534761]            | 58        | 0.0156 |
| KCTD11          | potassium channel tetramerisation domain containing 11 (KCTD11), mRNA [NM_001002914]  | 58        | 0.0230 |
| OR2W3           | olfactory receptor, family 2, subfamily W, member 3 (OR2W3), mRNA [NM_001001957]  | 58        | 0.0200 |
| BG216229        | BG216229 RST35803 Athersys RAGE Library cDNA, mRNA sequence [BG216229]  | 58        | 0.0279 |
| UGT8            | Human ceramide UDPgalactosyltransferase mRNA, complete cds. [U62899]  | 58        | 0.0192 |
| NLGN4X          | neuroligin 4, X-linked (NLGN4X), transcript variant 1, mRNA [NM_020742]   | 58        | 0.0146 |
| C20orf46        | chromosome 20 open reading frame 46 (C20orf46), mRNA [NM_018354]  | 58        | 0.0205 |
| THC2272949      | Unknown   | 58        | 0.0259 |
| BX100088        | BX100088 BX100088 Soares_testis_NHT cDNA clone IMAGp998K133560 ; IMAGE:1409412, mRNA sequence [BX100088]                          | 58        | 0.0258 |
| THC2283645      | Q71UKo (Q71UKo) Growth factor receptor (Fragment), partial (20%) [THC2283645]   | 58        | 0.0178 |
| THC2444209      | Unknown   | 58        | 0.0229 |
| ABAT            | 4-aminobutyrate aminotransferase (ABAT), nuclear gene encoding mitochondrial protein, transcript variant 1, mRNA [NM_020686]      | 58        | 0.0042 |
| AK026984        | cDNA: FLJ23331 fis, clone HEP12664. [AK026984]  | 57        | 0.0457 |
| MET             | met proto-oncogene (hepatocyte growth factor receptor) (MET), mRNA [NM_000245]  | 57        | 0.0317 |

GENE EXPRESSION IN HUMAN NEUROMA

| Gene            | Description   | Expr. (%) | P-val. |
|-----------------|---|-----------|--------|
| C20orf100       | chromosome 20 open reading frame 100 (C20orf100), mRNA [NM_032883]  | 57        | 0.0387 |
| C2orf39         | chromosome 2 open reading frame 39 (C2orf39), mRNA [NM_145038]  | 57        | 0.0156 |
| ENST00000251170 | KIAA0420 mRNA, complete cds. [AB007880]   | 57        | 0.0356 |
| COL8A2          | collagen, type VIII, alpha 2 (COL8A2), mRNA [NM_005202]   | 57        | 0.0061 |
| SNCA            | synuclein, alpha (non A4 component of amyloid precursor) (SNCA), transcript variant NACP112, mRNA [NM_007308]   | 57        | 0.0229 |
| WFDC2           | WAP four-disulfide core domain 2 (WFDC2), transcript variant 4, mRNA [NM_080734]  | 57        | 0.0166 |
| UCHL1           | ubiquitin carboxyl-terminal esterase L1 (ubiquitin thiolesterase) (UCHL1), mRNA [NM_004181]   | 57        | 0.0095 |
| ADRA2C          | adrenergic, alpha-2C-, receptor (ADRA2C), mRNA [NM_000683]  | 57        | 0.0465 |
| THC2339102      | BU616603 UI-H-FH1-bfi-p-18-0-UI.s1 NCL_CGAP_FH1 cDNA clone UI-H-FH1-bfi-p-18-0-UI 3', mRNA sequence [BU616603]  | 57        | 0.0256 |
| MFAP3L          | microfibrillar-associated protein 3-like (MFAP3L), transcript variant 2, mRNA [NM_001009554]  | 57        | 0.0356 |
| TMEM132B        | transmembrane protein 132B (TMEM132B), mRNA [NM_052907]   | 57        | 0.0304 |
| C10orf35        | chromosome 10 open reading frame 35 (C10orf35), mRNA [NM_145306]  | 57        | 0.0283 |
| THC2426594      | Unknown   | 57        | 0.0243 |
| AJ002788        | mRNA for protein kinase C beta 1, 3' UTR; fetal brain cDNA ICRFP507K04156. [AJ002788]   | 56        | 0.0404 |
| KIAA0408        | KIAA0408 (KIAA0408), mRNA [NM_014702]   | 56        | 0.0347 |
| PRX             | periaxin (PRX), transcript variant 1, mRNA [NM_020956]  | 56        | 0.0054 |
| EPPK1           | epiplakin 1 (EPPK1), mRNA [NM_031308]   | 56        | 0.0073 |
| ENST00000370599 | fibroblast growth factor homologous factor 2 isoform 1Z+1Y (FHF-2) mRNA, partial cds. [AF199613]  | 56        | 0.0267 |
| RASAL1          | RAS protein activator like 1 (GAP1 like) (RASAL1), mRNA [NM_004658]   | 56        | 0.0081 |
| BAMBI           | BMP and activin membrane-bound inhibitor homolog (Xenopus laevis) (BAMBI), mRNA [NM_012342]   | 56        | 0.0060 |
| AL564305        | AL564305 AL564305 FETAL LIVER cDNA clone CS0DM004YCo1 3-PRIME, mRNA sequence [AL564305]   | 56        | 0.0363 |
| PRKCB1          | protein kinase C, beta 1 (PRKCB1), transcript variant 2, mRNA [NM_002738]   | 56        | 0.0259 |
| SIPA1L2         | signal-induced proliferation-associated 1 like 2 (SIPA1L2), mRNA [NM_020808]  | 56        | 0.0255 |
| CDH1            | cadherin 1, type 1, E-cadherin (epithelial) (CDH1), mRNA [NM_004360]  | 56        | 0.0304 |
| AK092450        | cDNA FLJ35131 fis, clone PLACE6008824. [AK092450]   | 56        | 0.0231 |
| NRIP2           | nuclear receptor interacting protein 2 (NRIP2), mRNA [NM_031474]  | 56        | 0.0054 |
| CNTN1           | contactin 1 (CNTN1), transcript variant 1, mRNA [NM_001843]   | 56        | 0.0159 |
| ENST00000382496 | clone FBD8 Cri-du-chat critical region mRNA. [AF056434]   | 56        | 0.0054 |
| CYP51A1         | cytochrome P450, family 51, subfamily A, polypeptide 1 (CYP51A1), mRNA [NM_000786]  | 56        | 0.0283 |
| LOC645904       | PREDICTED: similar to Mitotic spindle assembly checkpoint protein MAD1 (Mitotic arrest deficient-like protein 1) (MAD1-like 1) (Mitotic checkpoint MAD1 protein-homolog) (HsMAD1) (hMAD1) (Tax-binding protein 181) (LOC645904), mRNA [XM_928876] | 55        | 0.0084 |
| RP11-35N6.1     | plasticity related gene 3 (PRG-3), transcript variant 1, mRNA [NM_207299]   | 55        | 0.0098 |
| GATM            | glycine amidinotransferase (L-arginine:glycine amidinotransferase) (GATM), mRNA [NM_001482]   | 55        | 0.0210 |
| PLAT            | plasminogen activator, tissue (PLAT), transcript variant 1, mRNA [NM_000930]  | 55        | 0.0339 |
| ENST00000309874 | cDNA FLJ33063 fis, clone TRACH2000047. [AK057625]   | 55        | 0.0210 |
| DHCR24          | 24-dehydrocholesterol reductase (DHCR24), mRNA [NM_014762]  | 55        | 0.0189 |
| ATOH8           | atonal homolog 8 (Drosophila) (ATOH8), mRNA [NM_032827]   | 55        | 0.0308 |
| S100B           | S100 calcium binding protein, beta (neural) (S100B), mRNA [NM_006272]   | 55        | 0.0405 |
| PCDH9           | protocadherin 9 (PCDH9), transcript variant 1, mRNA [NM_203487]   | 55        | 0.0325 |
| ENST00000330640 | Homo sapiens, clone IMAGE:2899977, mRNA, partial cds. [BC022980]  | 55        | 0.0283 |
| TUBB2B          | tubulin, beta 2B (TUBB2B), mRNA [NM_178012]   | 55        | 0.0362 |
| THC2318057      | Unknown   | 55        | 0.0341 |
| C10orf82        | chromosome 10 open reading frame 82 (C10orf82), mRNA [NM_144661]  | 54        | 0.0282 |
| DRP2            | dystrophin related protein 2 (DRP2), mRNA [NM_001939]   | 54        | 0.0054 |
| THC2348985      | T32824 EST54797 Human Brain cDNA 3' end similar to None., mRNA sequence [T32824]  | 54        | 0.0183 |
| TRIM58          | tripartite motif-containing 58 (TRIM58), mRNA [NM_015431]   | 54        | 0.0156 |
| FMN2            | formin 2 (FMN2), mRNA [NM_020066]   | 54        | 0.0405 |
| CHEK2           | CHK2 checkpoint homolog (S. pombe) (CHEK2), transcript variant 3, mRNA [NM_001005735]   | 54        | 0.0036 |
| AK094995        | cDNA FLJ37676 fis, clone BRHIP2012627. [AK094995]   | 54        | 0.0334 |
| NDP             | Norrie disease (pseudoglioma) (NDP), mRNA [NM_000266]   | 54        | 0.0036 |
| EDN1            | endothelin 1 (EDN1), mRNA [NM_001955]   | 54        | 0.0344 |
| ENST00000360099 | contactin 1, mRNA (cDNA clone MGC:41894 IMAGE:5273941), complete cds. [BC036569]  | 54        | 0.0256 |
| BX338933        | BX338933 BX338933 PLACENTA COT 25-NORMALIZED cDNA clone CS0DI065YH21 3-PRIME, mRNA sequence [BX338933]  | 53        | 0.0183 |
| LRRIQ1          | leucine-rich repeats and IQ motif containing 1 (LRRIQ1), mRNA [NM_032165]   | 53        | 0.0340 |
| PEX5L           | peroxisomal biogenesis factor 5-like (PEX5L), mRNA [NM_016559]  | 53        | 0.0383 |
| SOX2            | SRY (sex determining region Y)-box 2 (SOX2), mRNA [NM_003106]   | 53        | 0.0093 |
| PKP2            | plakophilin 2 (PKP2), transcript variant 2b, mRNA [NM_004572]   | 53        | 0.0201 |
| CNTN2           | contactin 2 (axonal) (CNTN2), mRNA [NM_005076]  | 53        | 0.0091 |



CHAPTER 3

| Gene            | Description  | Expr. (%) | P-val. |
|-----------------|--|-----------|--------|
| ACAT2           | acetyl-Coenzyme A acetyltransferase 2 (acetoacetyl Coenzyme A thiolase), mRNA (cDNA clone MGC:8573 IMAGE:2823036), complete cds. [BC000408]                  | 53        | 0.0257 |
| BC039411        | cDNA clone IMAGE:5301690. [BC039411]   | 53        | 0.0436 |
| CHST2           | carbohydrate (N-acetylglucosamine-6-O) sulfotransferase 2 (CHST2), mRNA [NM_004267]  | 53        | 0.0229 |
| MGC102966       | similar to Keratin, type I cytoskeletal 16 (Cytokeratin-16) (CK-16) (Keratin-16) (K16), mRNA (cDNA clone MGC:102966 IMAGE:4752428), complete cds. [BC110641] | 52        | 0.0119 |
| BF836076        | QV4-HT1018-171100-551-b09 HT1018 cDNA, mRNA sequence [BF836076]  | 52        | 0.0029 |
| PAQR6           | progesterin and adipoQ receptor family member VI (PAQR6), transcript variant 1, mRNA [NM_024897]   | 52        | 0.0259 |
| SLC13A3         | solute carrier family 13 (sodium-dependent dicarboxylate transporter), member 3 (SLC13A3), transcript variant 2, mRNA [NM_001011554]                         | 52        | 0.0235 |
| KCNMB4          | potassium large conductance calcium-activated channel, subfamily M, beta member 4 (KCNMB4), mRNA [NM_014505]   | 52        | 0.0062 |
| CNGA1           | cyclic nucleotide gated channel alpha 1 (CNGA1), mRNA [NM_000087]  | 52        | 0.0125 |
| THC2409530      | Unknown  | 52        | 0.0039 |
| TSPAN5          | cDNA FLJ31097 fis, clone IMR321000210. [AK055659]  | 52        | 0.0491 |
| HPR             | haptoglobin-related protein (HPR), mRNA [NM_020995]  | 52        | 0.0375 |
| RASL11B         | RAS-like, family 11, member B (RASL11B), mRNA [NM_023940]  | 51        | 0.0149 |
| HMGCR           | 3-hydroxy-3-methylglutaryl-Coenzyme A reductase (HMGCR), mRNA [NM_000859]  | 51        | 0.0321 |
| AL137342        | mRNA; cDNA DKFZp761G1111 (from clone DKFZp761G1111). [AL137342]  | 51        | 0.0210 |
| CHL1            | cell adhesion molecule with homology to L1CAM (close homolog of L1) (CHL1), mRNA [NM_006614]   | 51        | 0.0268 |
| BQ188373        | UI-E-EJ1-ajw-m-11-0-UI.r1 UI-E-EJ1 cDNA clone UI-E-EJ1-ajw-m-11-0-UI 5', mRNA sequence [BQ188373]  | 51        | 0.0056 |
| HRASL5          | HRAS-like suppressor 3 (HRASL5), mRNA [NM_007069]  | 51        | 0.0318 |
| AK124939        | cDNA FLJ42949 fis, clone BRSTN2006583. [AK124939]  | 51        | 0.0304 |
| CYP26B1         | cytochrome P450, family 26, subfamily B, polypeptide 1 (CYP26B1), mRNA [NM_019885]   | 51        | 0.0304 |
| BU537617        | BU537617 AGENCOURT_10224860 NIH_MGC_126 cDNA clone IMAGE:6567892 5', mRNA sequence [BU537617]  | 51        | 0.0029 |
| ARSI            | arylsulfatase family, member I, mRNA (cDNA clone IMAGE:5750037). [BC111002]  | 51        | 0.0062 |
| LOC440421       | PREDICTED: similar to keratin 17, transcript variant 1 (LOC440421), mRNA [XM_496202]   | 50        | 0.0153 |
| HCN1            | hyperpolarization activated cyclic nucleotide-gated potassium channel 1 (HCN1), mRNA [NM_021072]   | 50        | 0.0045 |
| THC2377128      | Unknown  | 50        | 0.0401 |
| THC2401542      | Unknown  | 50        | 0.0429 |
| CYB5R2          | cytochrome b5 reductase 2 (CYB5R2), mRNA [NM_016229]   | 50        | 0.0062 |
| AW268902        | AW268902 xv48h10.x1 Soares_NFL_T_GBC_S1 cDNA clone IMAGE:2816419 3', mRNA sequence [AW268902]  | 50        | 0.0127 |
| THC2343678      | Q6E5T4 (Q6E5T4) Claudin 2, partial (5%) [THC2343678]   | 50        | 0.0416 |
| UTS2            | urotensin 2 (UTS2), transcript variant 1, mRNA [NM_021995]   | 50        | 0.0247 |
| PNLIPRP2        | pancreatic lipase-related protein 2 (PNLIPRP2), mRNA [NM_005396]   | 50        | 0.0143 |
| OPCML           | opioid binding protein/cell adhesion molecule-like (OPCML), transcript variant 2, mRNA [NM_001012393]  | 50        | 0.0257 |
| THC2338229      | Unknown  | 50        | 0.0086 |
| STK32A          | serine/threonine kinase 32A (STK32A), mRNA [NM_145001]   | 50        | 0.0090 |
| A_23_P7719      | Unknown  | 50        | 0.0042 |
| IL17B           | interleukin 17B (IL17B), mRNA [NM_014443]  | 49        | 0.0054 |
| CYP2J2          | cytochrome P450, family 2, subfamily J, polypeptide 2 (CYP2J2), mRNA [NM_000775]   | 49        | 0.0171 |
| SCRN1           | secernin 1 (SCRN1), mRNA [NM_014766]   | 49        | 0.0051 |
| ENST00000311208 | MGC5.2.1.1.1.B03.F1 NIH_MGC_331 cDNA clone MGC5.2.1.1.1.B03, mRNA sequence [DR007925]  | 49        | 0.0061 |
| OR7E47P         | olfactory receptor, family 7, subfamily E, member 47 pseudogene, mRNA (cDNA clone IMAGE:5590288). [BC042060]   | 49        | 0.0029 |
| LOC63928        | hepatocellular carcinoma antigen gene 520 (LOC63928), mRNA [NM_022097]   | 49        | 0.0304 |
| NTF3            | neurotrophin 3 (NTF3), mRNA [NM_002527]  | 48        | 0.0029 |
| CR1L            | PREDICTED: complement component (3b/4b) receptor 1-like, transcript variant 3 (CR1L), mRNA [XM_931256]   | 48        | 0.0146 |
| FA2H            | fatty acid 2-hydroxylase (FA2H), mRNA [NM_024306]  | 48        | 0.0077 |
| A_32_P100830    | Unknown  | 48        | 0.0210 |
| BCAS1           | breast carcinoma amplified sequence 1 (BCAS1), mRNA [NM_003657]  | 48        | 0.0054 |
| ENST00000370306 | BX089019 Soares_testis_NHT cDNA clone IMAGP998K243513 ; IMAGE:1391375, mRNA sequence [BX089019]  | 48        | 0.0036 |
| FOLH1           | folate hydrolase (prostate-specific membrane antigen) 1 (FOLH1), transcript variant 1, mRNA [NM_004476]  | 48        | 0.0053 |
| ENST00000321925 | cDNA FLJ41687 fis, clone HCASM2006632, highly similar to UREA TRANSPORTER, ERYTHROCYTE. [AK123681]   | 48        | 0.0462 |
| C6orf142        | chromosome 6 open reading frame 142 (C6orf142), mRNA [NM_138569]   | 47        | 0.0220 |
| ALDOC           | aldolase C, fructose-bisphosphate (ALDOC), mRNA [NM_005165]  | 47        | 0.0036 |
| AL110257        | mRNA; cDNA DKFZp566P2346 (from clone DKFZp566P2346). [AL110257]  | 47        | 0.0039 |
| KRT17           | keratin 17 (KRT17), mRNA [NM_000422]   | 47        | 0.0061 |
| CR597597        | full-length cDNA clone CS0D1013YN06 of Placenta Cot 25-normalized of (human). [CR597597]   | 47        | 0.0101 |



GENE EXPRESSION IN HUMAN NEUROMA

| Gene            | Description   | Expr. (%) | P-val. |
|-----------------|---|-----------|--------|
| LOC153328       | similar to CG4995 gene product, mRNA (cDNA clone MGC:35539 IMAGE:5200129), complete cds. [BCo25747]                               | 47        | 0.0039 |
| A_24_P408449    | Unknown   | 47        | 0.0130 |
| RG59            | regulator of G-protein signalling 9 (RG59), mRNA [NM_003835]  | 47        | 0.0434 |
| THC2373072      | CB243285 UI-CF-FNo-agc-1-12-0-UI.s1 UI-CF-FNo cDNA clone UI-CF-FNo-agc-1-12-0-UI 3; mRNA sequence [CB243285]                      | 46        | 0.0029 |
| EB386378        | nbj15e01.y1 Human optic nerve. Unnormalized (nbj) cDNA clone nbj15e01 5; mRNA sequence [EB386378]                                 | 46        | 0.0180 |
| RTN1            | reticulon 1 (RTN1), transcript variant 1, mRNA [NM_021136]  | 46        | 0.0054 |
| TLL2            | tollid-like 2 (TLL2), mRNA [NM_012465]  | 46        | 0.0029 |
| FAM81A          | family with sequence similarity 81, member A (FAM81A), mRNA [NM_152450]   | 46        | 0.0045 |
| FLJ41603        | FLJ41603 protein (FLJ41603), mRNA [NM_001001669]  | 46        | 0.0106 |
| NRCAM           | neuronal cell adhesion molecule (NRCAM), transcript variant 2, mRNA [NM_005010]   | 45        | 0.0419 |
| KRT14           | keratin 14 (epidermolysis bullosa simplex, Dowling-Meara, Koebner) (KRT14), mRNA [NM_000526]                                      | 45        | 0.0045 |
| ELOVL7          | ELOVL family member 7, elongation of long chain fatty acids (yeast) (ELOVL7), mRNA [NM_024930]                                    | 45        | 0.0168 |
| THC2406238      | Q8DHD4 (Q8DHD4) Tlr2025 protein, partial (10%) [THC2406238]   | 45        | 0.0259 |
| GDPD2           | glycerophosphodiester phosphodiesterase domain containing 2 (GDPD2), mRNA [NM_017711]   | 45        | 0.0045 |
| SHRM            | shroom (SHRM), mRNA [NM_020859]   | 44        | 0.0188 |
| ENST00000382108 | mRNA; cDNA DKFZp686N20108 (from clone DKFZp686N20108). [BX648244]   | 44        | 0.0229 |
| SV2B            | synaptic vesicle glycoprotein 2B (SV2B), mRNA [NM_014848]   | 44        | 0.0205 |
| SOX2OT          | SOX2 overlapping transcript (non-coding RNA) (SOX2OT) on chromosome 3 [NR_002810]   | 44        | 0.0065 |
| DKFZp313A2432   | mRNA; cDNA DKFZp313A2432 (from clone DKFZp313A2432). [AL833119]   | 44        | 0.0215 |
| CRLF1           | cytokine receptor-like factor 1 (CRLF1), mRNA [NM_004750]   | 43        | 0.0404 |
| NTRK2           | neurotrophic tyrosine kinase, receptor, type 2 (NTRK2), transcript variant b, mRNA [NM_001007097]                                 | 43        | 0.0029 |
| MAL             | mal, T-cell differentiation protein (MAL), transcript variant a, mRNA [NM_002371]   | 43        | 0.0045 |
| BCo40293        | cDNA clone IMAGE:4820330. [BCo40293]  | 43        | 0.0192 |
| RASGEF1A        | RasGEF domain family, member 1A (RASGEF1A), mRNA [NM_145313]  | 42        | 0.0034 |
| PSMAL           | growth-inhibiting protein 26 (PSMAL), mRNA [NM_153696]  | 42        | 0.0080 |
| THC2442514      | Q9V4T7 (Q9V4T7) CG8694-PA (RE63163p), partial (4%) [THC2442514]   | 42        | 0.0029 |
| SLC17A6         | solute carrier family 17 (sodium-dependent inorganic phosphate cotransporter), member 6 (SLC17A6), mRNA [NM_020346]               | 41        | 0.0168 |
| GFAP            | glial fibrillary acidic protein (GFAP), mRNA [NM_002055]  | 41        | 0.0142 |
| THC2342207      | Unknown   | 41        | 0.0121 |
| BQ717813        | AGENCOURT_8229426 Lupski_dorsal_root_ganglion cDNA clone IMAGE:6184804 5; mRNA sequence [BQ717813]                                | 41        | 0.0050 |
| THC2442021      | Unknown   | 41        | 0.0039 |
| AW950828        | AW950828 EST362898 MAGE resequences, MAGA cDNA, mRNA sequence [AW950828]  | 39        | 0.0029 |
| C20orf39        | chromosome 20 open reading frame 39 (C20orf39), mRNA [NM_024893]  | 39        | 0.0029 |
| DKFZP586H12123  | regeneration associated muscle protease (DKFZP586H12123), transcript variant 1, mRNA [NM_015430]                                  | 38        | 0.0095 |
| PPP2R2B         | protein phosphatase 2 (formerly 2A), regulatory subunit B (PR 52), beta isoform (PPP2R2B), transcript variant 1, mRNA [NM_004576] | 38        | 0.0050 |
| ABCA13          | ATP-binding cassette, sub-family A (ABC1), member 13 (ABCA13), mRNA [NM_152701]   | 36        | 0.0092 |
| AK094523        | cDNA FLJ37204 fis, clone BRALZ2006976. [AK094523]   | 35        | 0.0029 |
| RG522           | regulator of G-protein signalling 22 (RG522), mRNA [NM_015668]  | 34        | 0.0029 |
| CP              | ceruloplasmin (ferroxidase) (CP), mRNA [NM_000096]  | 34        | 0.0077 |
| KSP37           | Ksp37 protein (KSP37), mRNA [NM_031950]   | 32        | 0.0029 |
| GAP43           | growth associated protein 43 (GAP43), mRNA [NM_002045]  | 31        | 0.0133 |
| FBXO2           | F-box protein 2 (FBXO2), mRNA [NM_012168]   | 31        | 0.0035 |
| MT3             | metallothionein 3 (growth inhibitory factor (neurotrophic)) (MT3), mRNA [NM_005954]   | 31        | 0.0029 |
| ENST0000033722  | chromosome 12 open reading frame 56, mRNA (cDNA clone IMAGE:3685952). [BCo15121]  | 31        | 0.0036 |
| GPM6A           | glycoprotein M6A (GPM6A), transcript variant 2, mRNA [NM_201591]  | 30        | 0.0033 |
| SLC27A6         | solute carrier family 27 (fatty acid transporter), member 6 (SLC27A6), transcript variant 2, mRNA [NM_001017372]                  | 30        | 0.0029 |
| NKX6-2          | NK6 transcription factor related, locus 2 (Drosophila) (NKX6-2), mRNA [NM_177400]   | 29        | 0.0036 |
| KIF5C           | mRNA for KIAA0531 protein, partial cds. [ABo11103]  | 29        | 0.0029 |
| ANGPTL7         | angiopoietin-like 7 (ANGPTL7), mRNA [NM_021146]   | 28        | 0.0035 |
| IGSF4D          | immunoglobulin superfamily, member 4D (IGSF4D), mRNA [NM_153184]  | 27        | 0.0049 |
| TSpan8          | tetraspanin 8 (TSpan8), mRNA [NM_004616]  | 27        | 0.0136 |
| SORCS3          | sortilin-related VPS10 domain containing receptor 3 (SORCS3), mRNA [NM_014978]  | 27        | 0.0029 |
| PCP4            | Purkinje cell protein 4 (PCP4), mRNA [NM_006198]  | 27        | 0.0037 |

**Supplemental table 2** List of all gene families of which multiple members are differentially regulated in human neuroma tissue ( $P < 0.05$ ). Expression: relative expression as a percentage of nerve control tissue ( $> 100\%$  indicates upregulation in the neuroma,  $< 100\%$  indicates downregulation). P-values for differential expression between nerve and neuroma were corrected for multiple testing using the Bonferroni correction algorithm.

| Go-Class             | Gene | Family   | Probe        | expr(%) | P-value |
|----------------------|------|--|--------------|---------|---------|
| cell adhesion        |      | <b>cadherins</b>   | A_23_P206359 | 56      | 0.030   |
| axon guidance        |      |  | A_23_P17593  | 65      | 0.038   |
| extracellular matrix |      |  | A_23_P170238 | 62      | 0.032   |
| axon                 |      |  | A_24_P419039 | 243     | 0.005   |
| neurotrophin binding |      |  | A_23_P420236 | 55      | 0.033   |
| calcium ion binding  |      |  |              |         |         |
|                      |      | <b>collagen</b>  | A_23_P11806  | 238     | 0.040   |
|                      |      |  | A_23_P214168 | 169     | 0.006   |
|                      |      |  | A_32_P218734 | 150     | 0.019   |
|                      |      |  | A_23_P211233 | 180     | 0.029   |
|                      |      |  | A_24_P365975 | 57      | 0.006   |
|                      |      | <b>chondroitin sulphate proteoglycans (CSPGs)</b>  |              |         |         |
|                      |      |  | A_23_P144959 | 207     | 0.019   |
|                      |      | <b>IgG superfamily</b>   | A_24_P354689 | 244     | 0.038   |
|                      |      |  | A_23_P120667 | 190     | 0.034   |
|                      |      | <b>cell adhesion molecule with homology to L1CAM (close homolog of L1), mRNA [NM_006614]</b> | A_23_P34345  | 169     | 0.043   |
|                      |      |  | A_24_P63178  | 51      | 0.027   |
|                      |      | <b>neuronal cell adhesion molecule, transcript variant 2, mRNA [NM_005010]</b>               | A_24_P252364 | 45      | 0.042   |
|                      |      |  | A_32_P447539 | 210     | 0.008   |
|                      |      | <b>Boc homolog (mouse), mRNA [NM_033254]</b>   | A_23_P257763 | 316     | 0.005   |
|                      |      |  | A_23_P5064   | 62      | 0.033   |
|                      |      | <b>immunoglobulin superfamily, member 4C, mRNA [NM_145296]</b>                               | A_32_P129200 | 27      | 0.005   |
|                      |      |  |              |         |         |
|                      |      | <b>IgG superfamily - contactins</b>  | A_23_P390700 | 56      | 0.016   |
|                      |      |  | A_24_P2901   | 53      | 0.009   |
|                      |      |  | A_23_P144020 | 171     | 0.020   |
|                      |      |  |              |         |         |





# Chapter 4

## Genetic modification of human sural nerve segments by a lentiviral vector encoding nerve growth factor

Martijn R Tannemaat, Gerard J Boer, Joost Verhaagen, Martijn J Malessy

*Neurosurgery. 2007 Dec;61(6):1286-94; discussion 1294-6*

### Abstract

**OBJECTIVE** Autologous nerve grafts are used to treat severe peripheral nerve injury, but recovery of nerve function after grafting is rarely complete. Exogenous application of neurotrophic factors may enhance regeneration, but thus far the application of neurotrophic factors has been hampered by fast degradation following local application and unwanted side effects following systemic application. These problems may be overcome with the use of lentiviral (LV) vectors which direct sustained local transgene expression in cells.

**METHODS** Human sural nerve segments were either submerged in or injected with LV vectors encoding green fluorescent protein (GFP) and cultured in vitro. Production of nerve growth factor (NGF) by nerve segments after injection of LV-NGF was quantified. The effect of NGF produced by LV-transduced fibroblasts derived from human sural nerve segments was assessed on neurite outgrowth in vitro.

**RESULTS** Injection of vector into nerve segments is a more effective way to deliver the vector than submersion of the nerve in vector-containing medium, leading to large numbers of transduced fibroblasts over a significant extent inside the nerve. The injection of LV-NGF leads to a gradual increase of NGF production, reaching a plateau after 4 days. LV-NGF-transduced human fibroblasts promote neurite outgrowth in vitro.

**CONCLUSION** We have developed a method to transduce cells in human sural nerve segments with LV vector. This approach holds promise as a powerful novel adjuvant therapy for peripheral nerve surgery and can be performed without changing the routine practice of nerve grafting.

### Objective

In patients with a complete transection of a peripheral nerve, surgical repair is necessary to allow regeneration of the nerve and the return of nerve function. When tension-free direct coaptation of the proximal and distal nerve stumps is not possible, an autologous nerve is used as a graft to bridge the gap<sup>1</sup>. The most commonly used nerve for this purpose is the sural nerve.

Two major functions of the nerve graft can be distinguished: physical guidance

and trophic support. The transplanted nerve gives physical guidance to regenerating axons by the longitudinally oriented endoneurial tubes that act as scaffolds for the regenerating axons<sup>7</sup>. The trophic support for regenerating axons comes mainly from the Schwann cells inside the nerve graft. After the graft is dissected from the donor site, activated Schwann cells start secreting a wide range of neurotrophic proteins such as nerve growth factor (NGF)<sup>9</sup>. In spite of the axon-guiding and outgrowth-supporting properties of these nerve grafts, the functional outcome of nerve grafting is often limited, especially when long nerve grafts have to be used<sup>1</sup>.

It is widely believed that surgical repair of the peripheral nerve by autologous grafts has reached optimal technical refinement and that new concepts are needed to enhance functional outcome<sup>2</sup>. Research has focused on the development of artificial nerve guides as an alternative, sometimes seeded with naïve Schwann cells<sup>122</sup>, Schwann cells genetically modified to secrete neurotrophic factors<sup>28</sup> or engineered to release neurotrophic factors<sup>121</sup>. A wide range of artificial tubes has been investigated, but so far, none has been shown unambiguously to possess better nerve outgrowth-supporting properties than the autologous nerve graft<sup>122</sup>. Theoretical advantages of artificial nerve tubes are the off-the-shelf availability and the absence of donor site morbidity. However, to ensure continuous trophic support to regenerating neurites, the addition of autologous Schwann cells seems unavoidable, but this will inherently compromise the aforementioned advantages.

We therefore believe that enhancing the outgrowth-supporting properties of the autologous nerve graft itself is another alternative which should be explored in order to improve the functional results of nerve grafting. One way to achieve this may be the application of viral vectors to induce overexpression of therapeutic proteins.

The application of first generation viral vectors such as herpes simplex viral vectors and adenoviral vectors was hampered by a vector-mediated immune response, loss of transgene expression and direct neurotoxicity of these vectors<sup>123</sup>. These problems have been overcome with the development of adeno-associated viral (AAV)<sup>126</sup> and lentiviral (LV) vectors<sup>42</sup>, which have a favourable toxicity profile, infect dividing and non-dividing cells and direct long term transgene expression in the nervous system. Currently, the vesicular stomatitis virus G glycoprotein (VSV-G) pseudotyped LV has an advantage over AAV as it infects a wide range of cells, whereas AAV serotype 2 predominantly infects neurons<sup>32</sup>. Although this may change with the ongoing development of different AAV serotypes<sup>124</sup>, for this study we applied LV vectors to transduce the non-neuronal cells in nerve segments.

The application of viral vectors has potential as an adjuvant therapy as it does not have to interfere with the clinical routine. We chose, therefore, as a first necessary step towards clinical application, to investigate whether cells in the human peripheral nerve can be transduced *ex vivo*.

## Methods

### *Lentiviral vector preparation*

The production of self-inactivating LV vectors has been described in detail previously<sup>42</sup>. The plasmids needed for the production of GFP-encoding LV vector were generously provided by Dr L Tamagnone and Dr L Naldini (Institute for Cancer Research, University of Torino, Italy). For the production of LV-NGF, cDNA coding for rat NGF was ligated into the transfer vector pRRLsinPPTh-WPRE.

Vector stocks were generated by as described previously<sup>125</sup>. All stocks were stored in 0.1 M sodium phosphate buffered saline pH 7.4 (PBS) at -80°C. For LV-GFP, the concentration of vector particles was defined by infecting HEK 293T cells and counting the number of GFP-expressing cells after 48 h. Recombinant stock titers were expressed as transducing units per ml ( $TU_{HEK293T}/ml$ ) and ranged from  $10^9$  to  $10^{10}$ .

For LV-NGF, the vector titer was determined with an HIV-p24 core profile ELISA kit (Perkin Elmer Life Sciences). HIV-p24 ELISA on an LV-GFP stock with a known concentration in  $TU_{HEK293T}/ml$  was performed simultaneously so that the titer of LV-NGF could be calculated on the same basis as LV-GFP. The concentration of the currently used LV-NGF stocks was subsequently estimated to range from  $1.7 \times 10^9$  to  $8 \times 10^9 TU_{HEK293T}/ml$ .

### *Culture and transduction of human sural nerve segments*

Residual segments of human sural nerve applied for reconstructive surgery from adult patients with a traumatic brachial plexus lesion or infants with an obstetrical brachial plexus lesion were used. These reconstructions were performed at the Department of Neurosurgery, Leiden University Medical Center. Prior to surgery, consent from patients or their guardians was obtained for the use of residual segments of sural nerve for research purposes. Sural nerve segments that would otherwise have been discarded were transferred to Isocove's modified Dulbecco culture medium, containing 10% fetal bovine serum, 100 IU/ml penicillin, 100 µg/ml streptomycin and 2 mM Glutamax (Sigma) (this will subsequently be referred to as "culture medium") at room temperature and as soon as possible, but always within 24 h, cut to a standard length of 15 mm before infection with LV vector. Two methods of transducing the cells in the nerve segments with LV vector were tested: direct injection and submersion for up to 16 h under in vitro culture conditions.

For *direct injection*, the nerve was gently stretched and attached with two metal pins to a plate containing dental wax. A glass capillary with an 80 µm tip diameter was attached to a Hamilton syringe and filled with PBS containing LV-GFP as well as 0.1% Fast Green to visualize fluid during injection. The injection volume was 2 µl (except for three trials with 5-6 µl; see table 1) with vector titers ranging from  $1.5 \times 10^9$  to  $10^{10} TU/ml$ . To be able to study the number and spread of transduced cells resulting from a single injection of vector we chose not to apply multiple injections. The vector was

**Table 1** Overview of GFP expression in LV-GFP transduced human sural nerve segments.

\* From some patients, several segments were used. Nerve segments from the same patient can be identified by corresponding numbers in the Patient # column. \*\* GFP expression is quantified as follows: - no GFP positive cells, + 0-10 GFP positive cells, ++ 10-100 GFP positive cells, +++ 100-1000 GFP positive cells, ++++ >1000 GFP positive cells on a representative section of the nerve. \*\*\* Distance between two outmost transduced cells in a section as a percentage of the length of the nerve segment (15 mm). \*\*\*\* Injection volume 5 or 6  $\mu$ l instead of 2  $\mu$ l.

injected through the epineurium in the center of the nerve, by slowly applying manual pressure to the plunger of the Hamilton syringe.

For *submersion*, nerve segments were incubated in 250  $\mu$ l culture medium, just enough to keep the segments moist, that contained LV-GFP in concentrations ranging from  $3 \times 10^6$  to  $10^8$  TU/ml. Incubation time was either 4 or 16 h under 5% CO<sub>2</sub> in a humidified incubator at 37°C.

After nerves were exposed to the viral vector, they were further cultured free floating for 3 days in 2 ml culture medium at 37°C in a humidified incubator in 5% CO<sub>2</sub> to allow for GFP to accumulate inside the cell. A total number of 21 nerve segments from 12 different patients were used for transduction with LV-GFP (Table 1).

#### *Tissue preparation and histology*

Three days after infection, the nerve segments were gently stretched and fixed with 4% paraformaldehyde in 0.1 M phosphate buffer pH 7.4 overnight, followed by 24 h incubation in 25% sucrose in phosphate buffer for cryoprotection and stored at -80°C before 4-8 series of alternative longitudinal 20  $\mu$ m thick cryostat sections were mounted on Superfrost Plus glass slides.

The efficacy of viral transduction was assessed by observing the distribution of GFP-containing cells with a fluorescence microscope on glycerol-Mowiol-embedded sections of the nerve. For each nerve, photomicrographs were made of the section containing the highest number of GFP positive cells. Scoring was performed by 2 independent observers that were blinded to the method of vector application. Nerve segments without GFP positive cells were scored 0, nerve segments with an estimated maximum of 10 GFP positive cells on a single section were scored +, 10-100 GFP positive cells ++, 100-1000 GFP positive cells +++ and nerve segments with more than 1000 GFP-positive cells on a single section were scored ++++. The maximal longitudinal distance of the area of GFP positive cells within one section was measured using ImagePro software (Media Cybernetics, Silver Spring, USA), as an indication of the spatial distribution of transduced cells. Routine thionine staining of sections was performed to visualize cell nuclei and to assess the structural integrity of the nerve segments after 4 days of culture. A special effort was made to identify the site of injection in order to assess possible damage to the endoneurial tubes.



| Method                        | Age     | Patient #* | Incubation (h) | Vector (TU/ml) | Vector (TU x106) | GFP expression** | Spread (%)***                                    | Description of GFP expression pattern                   |
|-------------------------------|---------|------------|----------------|----------------|------------------|------------------|--|---|
| <i>Injection</i><br>(2 µl)    | adult   | 1          |                | 3.5E+09        | 7                | ++               | 28   | disruption of epineurium, possibly due to injection     |
|                               |         | 2          |                | 3.5E+09        | 7                | ++               | 45   | narrow band of GFP+ cells between fascicles             |
|                               |         | 3          |                | 3.5E+09        | 7                | +++              | 45   | GFP+ cells surrounding fascicles                        |
|                               |         | 3          |                | 3.5E+09        | 7                | +                | 29   | GFP+ cells only on outer edge of nerve                  |
|                               |         | 3          |                | 3.5E+09        | 7                | +++              | 29   | GFP+ in the middle of the nerve, between fascicles      |
|                               |         | 4          |                | 3.5E+09        | 7                | -                |  |   |
|                               |         | 5          |                | 1.0E+10        | 20               | +++              | 40   | GFP+ cells near both outer edges                        |
|                               | 6       |            | 1.0E+10        | 20             | +++              | 59               | GFP+ cells surrounding fascicles (figure 1a)     |   |
|                               | 7       |            | 1.0E+10        | 60****         | +++              | 67               | GFP+ cells surrounding fascicles                 |   |
|                               | neonate | 8          |                | 3.5E+09        | 7                | ++               | 12   | longitudinal band of GFP+ cells near end of nerve       |
| 9                             |         |            | 1.5E+09        | 7.5****        | ++               | 19               | GFP+ cells between fascicles, near end of nerve  |   |
| 10                            |         |            | 1.0E+10        | 60****         | ++++             | 100              | GFP+ cells in entire nerve surrounding fascicles |   |
| <i>Submersion</i><br>(250 µl) | adult   | 1          | 4              | 7.0E+06        | 28               | +                | 17   | several GFP+ cells on one side of nerve                 |
|                               |         | 11         | 4              | 1.2E+07        | 48               | +                | 78   | GFP+ cells on one side of nerve, epineurium disrupted   |
|                               |         | 4          | 16             | 7.0E+06        | 28               | -                |  |   |
|                               |         | 5          | 16             | 2.0E+07        | 80               | -                |  |   |
|                               |         | 6          | 16             | 2.0E+07        | 80               | ++               | 73   | GFP+ cells inside nerve, epineurium disrupted           |
|                               |         | 8          | 4              | 7.0E+06        | 28               | +                | 10   | several GFP+ cells on outer edge of nerve               |
|                               | neonate | 12         | 4              | 1.0E+08        | 400              | ++               | 98   | GFP+ cells on both sides over entire length (figure 1b) |
|                               |         | 9          | 16             | 3.0E+06        | 12               | -                |  |   |
|                               |         | 9          | 16             | 3.0E+06        | 12               | -                |  |   |
|                               |         | 9          | 16             | 3.0E+06        | 12               | -                |  |   |

For immunocytochemistry, sections were washed three times in 0.1 M Tris/HCl-buffered saline pH 7.4 (TBS). To enhance antibody tissue penetration and to block unspecific antibody binding sites, sections were incubated in TBS containing 0.3% Triton X-100 and 5% fetal bovine serum for 1 h. Subsequently, sections were exposed to primary antibodies against S100 to stain Schwann cells (1:200; Dako, #Z0311, and against raldh2 (1:500; rabbit polyclonal; a gift from Dr. P. McCaffery, E. Kennedy Shriver Center, University of Massachusetts Medical School, Boston, USA)<sup>126</sup> and fibronectin (1:400; mouse monoclonal FN-3E2, Sigma) to stain fibroblasts. Primary antibody incubations were performed overnight at 4°C. The next day, sections were washed three times in TBS and incubated with fluorophore-conjugated secondary antibodies for 2 h. Depending on the desired staining, DaR-Cy3 or DaM-Cy3 were used (1:400; Jackson ImmunoReagents). Finally, the sections were washed in TBS, mounted in Moviol and coverslipped.

#### *Transduction of co-cultured Schwann cells and fibroblasts*

Co-cultures of human Schwann cells and fibroblasts were created using the serial explant method developed by Morrissey et al.<sup>127</sup>. Schwann cells from human sural nerve segments were isolated by placing small nerve segments in culture and allowing the faster migrating fibroblasts to move out. When migrated cells reached a monolayer, the explants were placed in new dishes until the monolayer showed equal densities of Schwann cells and fibroblasts. At that point, the cells were trypsinized (0.25% in PBS for 2 min), taken up in culture medium and plated out at 50% confluency on poly-L-lysine-coated glass coverslips. The next day, LV-GFP was added at a multiplicity of infection (MOI) of 1, 10 or 50 and culture continued for 48 h under 5% CO<sub>2</sub> conditions in a humidified incubator at 37°C to allow transgene expression. Subsequently cells were fixed with 4% paraformaldehyde in PBS for 30 min and stained with the fibronectin and S100 antibodies as described above.

Images were made with a confocal laser scanning microscope from random fields from 3 separate cultures per MOI. The number of GFP positive (fibronectin positive) fibroblasts and GFP positive (S100 positive) Schwann cells were counted manually per image and the relative amount of transduced cells per cell type calculated. Statistical analysis of these results was performed using a two-tailed Student's T-test assuming unequal variances.

#### *Transduction with LV-NGF and quantification of NGF production*

Three 15 mm nerve segments from one patient were transduced by injection of  $2.5 \times 10^7$  TU LV-NGF in 3  $\mu$ l PBS. An additional three segments from another patient were injected with  $10^7$  TU LV-NGF in 6  $\mu$ l PBS. For each transduced nerve segment, a 15 mm segment from the same patient served as non-transduced control. Segments from

the first patient were cultured for 7 days and segments from the second patient were cultured for 11 days. The culture medium was refreshed every 24 h, and the conditioned medium stored at  $-20^{\circ}\text{C}$  for the measurement of the NGF concentration using an NGF ELISA kit (#G7630; Promega, Madison, USA). This kit detects both human (endogenous) and rat (transgenic) NGF.

#### *Effect of overexpression of NGF on rat neurite outgrowth in vitro*

The biological activity of NGF produced by LV-NGF-transduced fibroblasts was determined with an outgrowth assay on cultured embryonic rat dorsal root ganglia (DRGs) (16). To create fibroblast cultures from small segments of human sural nerve, fibroblasts were allowed to migrate out of cultured nerve segments (which were subsequently removed) and proliferate further. To achieve optimal transduction, LV-NGF was added at an MOI of 50 when cultured fibroblasts were 50-75% confluent, using non-transduced cultures as controls. The cells were cultured in 2 ml for 72 h to allow NGF to accumulate in the medium, after which it was harvested and stored at  $-20^{\circ}\text{C}$  for bioassays.

The bioassay was performed as described previously by Niclou et al.<sup>128</sup> on DRGs isolated from E15 rat embryos that were plated as whole explants on laminin-coated glass coverslips (n=6 per condition). In short, after culturing for 48 h in either a) fresh culture medium, b) culture medium conditioned from cultured but non-transfected fibroblasts, c) culture medium conditioned from cultured fibroblasts transduced with LV-NGF, or d) culture medium to which 20 ng/ml recombinant NGF was added (#1014331, Roche, Bazel, Switzerland), the DRGs were fixed for 30 min with 4% paraformaldehyde in PBS and neurite growth visualized by neurofilament antibody staining (2H3 ascites 1:1000; Dev. Stud. Hybridoma Bank, University of Iowa, Iowa, USA) using Cy3 as chromogen in the second antibody step. Fluorescence photographs were taken with the same intensity settings for all DRGs. Neurite outgrowth was then quantified as the total area of neurofilament-stained structures outside the DRG borders using ImagePro software. Statistical evaluation was performed with two-tailed Student's T-tests assuming unequal variances.

## **Results**

### *Injection of vector is the most effective method to transduce cells in a human sural nerve graft*

Twelve nerve segments were transduced by direct injection of LV-GFP and compared to 9 nerve segments that were submerged in LV-GFP medium for either 4 (n=4) or 16 h (n=5). Thionine nuclear staining of both the injected and submerged nerve segments showed that after 4 days in culture the cytoarchitecture of the nerve segments remained intact. Occasionally a small disruption of the epineurium, likely due to the

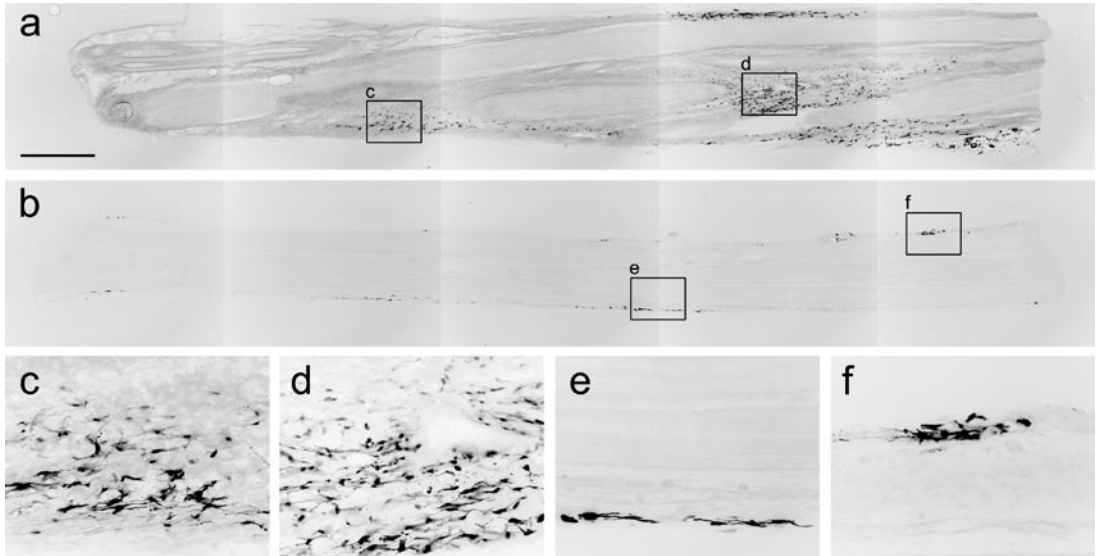


**Figure 1** In vitro transduction of human sural nerve after injection or immersion with LV-GFP. For clarity, images have been inverted so that the fluorescent signal from transduced cells appears dark on a light background.

a) Overview after injection of  $2 \times 10^7$  TU LV-GFP in  $2 \mu\text{l}$  shows numerous GFP positive cells surrounding the fascicles (subject #6 in table 1).

b) Overview after submersion in  $250 \mu\text{l}$  containing  $4 \times 10^8$  TU LV-GFP shows less transduced cells that are mainly located on the outer edges of the nerve (subject #12 in table 1).

c) and d) High magnification of boxed areas in a) revealing a dense transduction level.

e) and f) High magnification of boxed areas in b) revealing some transduced cells on the outer edges of the nerve.

Scale bar indicates 0.5 mm.

damage of the injection needle, could be observed, but generally no disruption of the nerve fascicles was visible. The majority of cells were S100 positive Schwann cells that aligned within the nerve fascicles. Staining for macrophages inside the nerve segments was negative (data not presented). In general, most cells appeared to be intact, although signs of necrosis of cells could sometimes be observed in small areas, usually at the center of the nerve segment (data not shown).

After a single *direct injection* of LV-GFP numerous GFP positive cells could be observed in 11 out of 12 nerve segments (table 1). Transduced cells were usually located in a distinct pattern in the epineurium surrounding the longitudinally oriented nerve fascicles (figure 1a). Only very rarely could a GFP positive cell be observed inside nerve fascicles. The number of transduced cells in a nerve segment was highly variable, with estimates ranging between 10 and more than a 1000 on a representative section

through the middle of the nerve (figure 1c and 1d). The average distance over which transduction could be seen was 5.5 mm, slightly more than 1/3 of the nerve, but in some nerve segments transgene expression was observed along the entire length of the nerve. After *submersion* in vector medium, low numbers of GFP positive cells were found in 5 out of 9 nerve segments (table 1), but primarily located near the ends of the nerve and outside the epineurium over the entire length (figure 1bef). The single nerve with the highest number of transduced cells was a segment that appeared to have a partially disrupted epineurium (data not shown). Submersion in higher concentrations of vector tended to increase numbers of transduced cells (table 1), but application of even larger amounts of vector is not easily feasible with the current LV vector stock concentrations. Increasing the incubation time from 4 to 16 h did not increase the number of transduced cells. No difference was observed in transduction efficiency for segments from adults or neonates with either injection or submersion.

#### *The majority of transduced cells are fibroblasts*

Immunohistochemical staining showed that more than 95% of transduced cells was *not* S100 positive. S100 positive cells were found inside the nerve fascicles, whereas most GFP positive cells were found in the epineurium surrounding the nerve fascicles (figure 2a). Although S100 staining did occasionally show a GFP positive Schwann cell, these were usually Schwann cells on the outer boundary of the nerve fascicles (figure 2b). Fibronectin (figure 2c) or raldh2 (figure 2d) immunofluorescent staining indicated that the majority of GFP-containing cells were fibroblasts, all located outside the nerve fascicles.

#### *LV-GFP transduces co-cultured fibroblasts and Schwann cells with similar efficacy*

Since the majority of transduced cells inside the human sural nerve were fibroblasts, we determined whether there is a difference in the intrinsic capability of LV to infect and transduce Schwann cells and fibroblasts. Cultured Schwann cells could easily be distinguished from fibroblasts because they showed an intense staining for S100, whereas fibroblasts stained brighter for fibronectin than Schwann cells.

*In vitro* application of increasing amounts of LV-GFP to co-cultures (n=3) led to increasing numbers of GFP positive cells. At MOI=1 only an occasionally transduced cell was found, whereas at MOI=10 and 50 respectively 12% and 21%, and 66% and 59% of fibroblasts and Schwann cells were transduced with no statistically significant differences between the cell types (figure 3). This indicates that the LV vector is capable of transducing both cell types with similar efficacy when applied in culture, i.e., in the absence of potential physical obstacles.

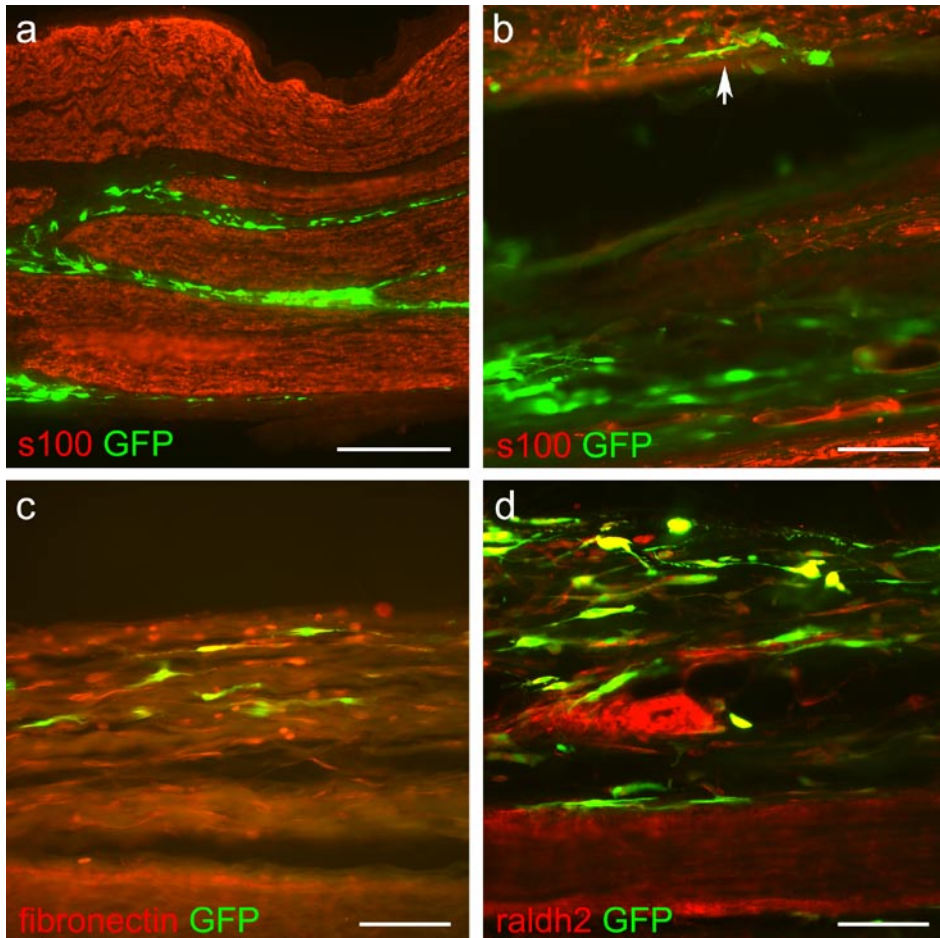


**Figure 2** Identification of the LV-GFP-transduced cells of the human sural nerve in vitro.  
 a) GFP positive cells are found outside the areas of S100 positive cells, that is not inside Schwann cell-containing nerve fascicles.  
 b) Occasionally a GFP and S100 positive cell could be seen on the edge of the nerve fascicle (arrow).  
 c) Many fibronectin-labelled fibroblasts express GFP  
 d) Raldh2-labelled fibroblasts expressing GFP.  
 Scale bar indicates 0.5 mm in a) and 0.1 mm in b), c) and d).

#### *Injection of LV-NGF leads to an increase in NGF production*

LV-NGF-transduced nerve segments secrete NGF into the culture medium at levels high enough to be detectable with ELISA. Segments either injected with  $2.5 \times 10^7$  TU LV-NGF in 3  $\mu$ l (patient 1 samples) or  $10^7$  TU in 6  $\mu$ l (patient 2 samples) strikingly produced similar amounts over time despite the 2.5x higher LV-NGF TUs applied in nerve segments from the first patient (figure 4). Culture medium harvested before, or

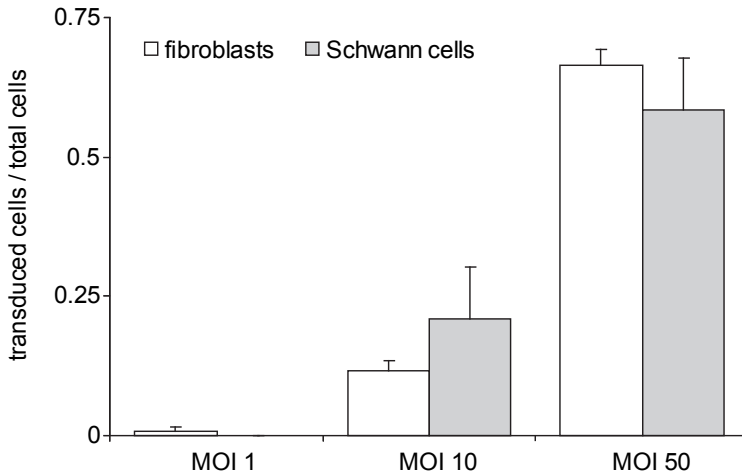


**Figure 3** Efficacy of LV-GFP transduction of human fibroblasts and Schwann cells in co-culture. Graph indicates that with increasing MOI of LV-GFP both cell types showed a comparable transduction rate. Bars indicate average  $\pm$  SEM for  $n=3$ .

1 day after LV-NGF application did not contain detectable amounts of NGF. NGF production subsequently increased and reached a plateau between 4 and 6 days ranging between 1.0 and 4.5 ng/day after which a slight decline took place up to 11 days. One nerve sample receiving a  $10^7$  TU/6  $\mu$ l injection appeared the exception and daily NGF production from this sample was roughly 2-fold higher over the entire time period. The evaluation of time points later than 11 days was not possible due to slow disintegration of the nerve segments. Non-transduced control nerve segments secreted no significant amounts of NGF (highest value 0.057 ng/day at an ELISA detection level of 0.008 ng/day), indicating that endogenous production of NGF was virtually absent. LV-NGF-transduced fibroblasts stimulate neurite outgrowth in vitro

The biological activity of NGF produced by LV-NGF-transduced and non-transduced fibroblasts was evaluated on in vitro E15 rat DRGs with negative (DRGs cultured in control medium) and positive controls (recombinant NGF).

Neurite outgrowth from DRGs, visualized by neurofilament staining, was slightly increased in conditioned medium from non-transduced fibroblasts over that of fresh medium, although this difference was not significant ( $p=0.16$ ) (figure 5). DRGs cultured in medium harvested from fibroblasts transduced with LV-NGF showed robust neurite outgrowth that was fourfold higher than that upon use of conditioned medium from non-transduced human fibroblasts ( $p=0.01$ ) and similar to the outgrowth from DRGs in 20 ng/ml recombinant NGF.

Human fibroblasts are thus capable of producing and secreting NGF that stimulates neurite outgrowth in vitro.



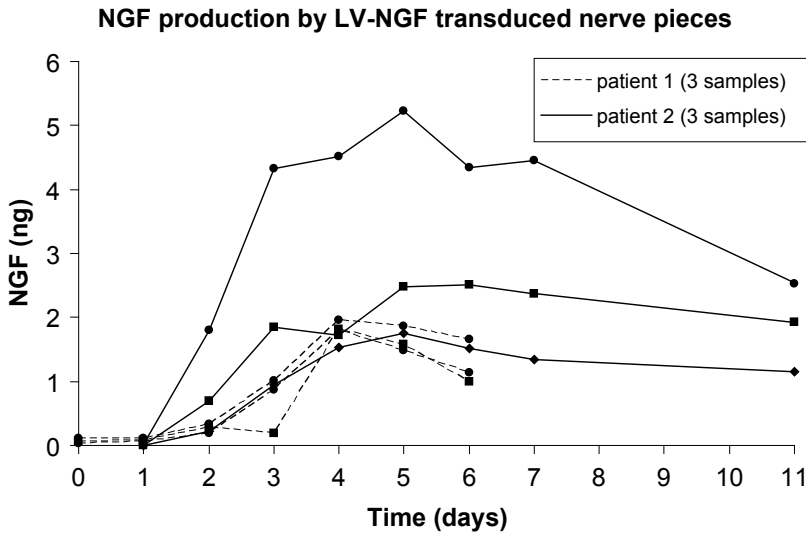


**Figure 4** NGF production by nerve segments injected with  $2.5 \times 10^7$  TU LV-NGF in  $3 \mu\text{l}$  (patient 1 samples) or  $10^7$  TU in  $6 \mu\text{l}$  (patient 2 samples).

Both the levels of NGF and the temporal pattern of production are remarkably similar in 5 of the 6 injected nerve segments, reaching a plateau in NGF production between 4 and 6 days, after which a slight decline occurs.

## Discussion

### *Injection of LV vector is the method of choice to transduce sural nerve segments*

Direct injection of the LV vector is a faster and more efficient method to deliver the transgene than submersion of the nerve in vector-containing medium. A single injection into the middle of a 15 mm nerve segment generally leads to a high number of transduced cells over a significant distance, but usually not over the entire length. The transduction of longer sural nerve grafts – for instance needed in human brachial plexus repair surgery<sup>129</sup> – will therefore require multiple injections. The observed variability in the number of transduced cells after injection may pose a potential problem for clinical application, but may decrease with multiple injections.

Transduction by submersion of the nerve segment in a vector-containing medium was limited to the boundaries of the nerve segment even at high LV vector concentrations. The greater efficacy of injection is therefore likely the result of the forced flow of vector particles through the nerve.

### *The physical properties of the nerve apparently lead to preferential transduction of fibroblasts in the epineurium*

Most GFP positive cells were localized outside the S100 positive nerve fascicles and were immuno-positive for fibronectin or raldh2. Although not all GFP positive cells



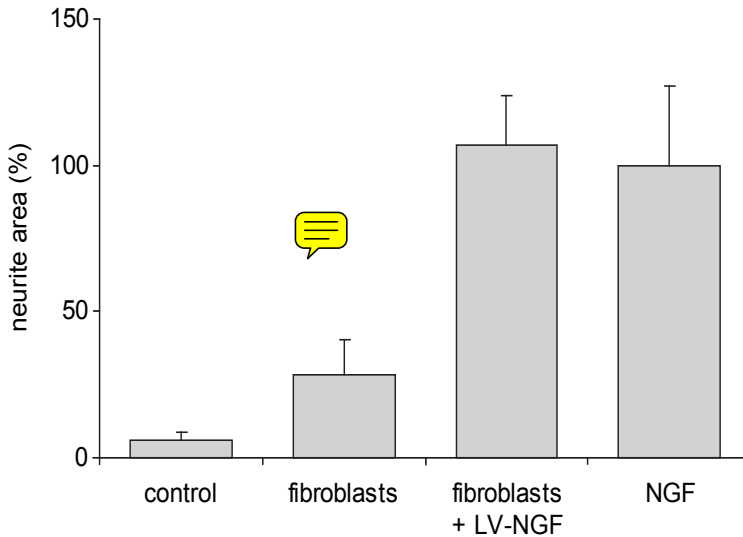


**Figure 5** Neurite outgrowth of rat E15 dorsal root ganglion (DRG) cells with conditioned medium of cultured LV-NGF-transduced human fibroblasts. A robust 4-fold higher neurite outgrowth was observed compared to the use of conditioned medium from non-transduced human fibroblasts ( $p=0.01$ ) which was comparable to the neurite outgrowth from DRGs in 20 ng/ml recombinant NGF. Neurite area of DRGs cultured in recombinant NGF is set at 100%. Bars indicate average  $\pm$  SEM for  $n=3$ .

were positive for the extracellular matrix protein fibronectin and the presence of raldh2 has so far only been described in fibroblasts of meningeal origin(4)), the absence of S100 in the transduced cells, their cell morphology and location support a conclusion that the predominant cell type that was transduced were fibroblasts.

We hypothesize that the physical properties of the human peripheral nerve lead to this result. After injection, the flow of viral vector particles will naturally follow a path of least resistance, resulting in a buildup of vector particles in the loose epineurial tissue surrounding the fascicles but not in the dense, highly myelinated fascicle itself. The spreading of viral vector along anatomical boundaries following injection in the central and peripheral nervous system has also been described following the use of adenoviral vectors<sup>130</sup>. This conclusion is further supported by the fact that LV-GFP was capable of transducing both fibroblasts and Schwann cells with similar efficiency when co-cultured on coated coverslips (i.e., in the absence of physical obstacles for vector particles).

#### *Continuous production of NGF by LV-NGF-transduced nerve segments*

One attractive feature of viral vector-mediated transduction of cells is that a single application leads to long term production of a potential therapeutic protein. LV-

NGF injected in the nerve resulted in NGF secretion for at least 11 days. LV vectors have previously been reported to give continuous transgene expression in vivo for months<sup>43,131</sup>. All present nerve segments showed a strikingly similar temporal pattern of NGF production, except for one that had a 2-fold higher production. This was one sample out of three from the same donor. This variation between segments from one patient may have been caused in part by technical difficulties involving the injection of a volume of 6  $\mu$ l in a sural nerve segment which in itself has a volume of 15-20  $\mu$ l, possibly leading to some leakage of vector containing fluid. Ideally our experiments should be repeated using tissue from the same donor with different concentrations of vector in varying volumes, but this approach requires large lengths of sural nerve that rarely become available in the clinical setting of nerve grafting.

*Transducing nerve grafts as a novel concept to enhance regeneration of the peripheral nerve*

LV vector-mediated transduction of cells inside sural nerve segments to induce continuous secretion of neurite outgrowth-promoting factors opens up an entirely novel possibility to enhance regeneration after peripheral nerve grafting. Nerve repair surgery is often performed several months after the initial trauma<sup>65</sup>, but chronic denervation of the distal nerve stump is deleterious to the results<sup>132</sup>. This may in part be due to a progressive decline<sup>22</sup> in initially enhanced levels<sup>9</sup> of neurotrophic factors in the distal nerve stump after transection. LV vector-mediated overexpression makes it possible to reconstitute neurotrophin levels. Moreover, it can be performed in minutes and can therefore be potentially included in the clinical practice of nerve grafting without major interference with the current routine.

NGF may be a good candidate for LV vector-mediated gene transfer to the nerve, as NGF applied exogenously for 4-12 weeks through diffusion from a daily filled silicon reservoir has already been shown to increase the number of sensory neurites that cross the lesion site after nerve transection<sup>133</sup>. Furthermore, the addition of NGF to fibrin sealant gave a significant improvement of functional outcome after nerve transection<sup>18</sup>. These latter approaches, however, required multiple daily injections of NGF to fill the silicon reservoir<sup>133</sup> or consisted of only one single application with limited effective exposure time<sup>18</sup>. The protocol described in this study could result in a stronger effect on regeneration, as injection of LV vector led to long term production of the desired protein inside the nerve.

A possible disadvantage of the use of NGF may be related to its possible role in the pathogenesis of pain<sup>10</sup>. However, the endogenous production of NGF distal to a peripheral nerve lesion<sup>9</sup> does not lead to pain<sup>1</sup>. A major advantage of viral vector-mediated overexpression of NGF in this respect may be that the location, production and release of NGF closely mimic the physiological situation. Furthermore, other neu-

rotrophic factors have also shown promising effects on regeneration of the peripheral nerve, including BDNF<sup>21,22</sup>, NT-3<sup>134</sup>, NT-4<sup>19</sup> and GDNF<sup>21,121</sup>. LV-mediated overexpression of CNTF in peripheral nerve transplants has positive effects on regeneration of the optic nerve<sup>137</sup>.

An important finding in this study is that cells outside the nerve fascicles, and not Schwann cells are transduced. A higher concentration of NGF may attract regenerating neurons to grow outside the fascicle, perhaps making it harder for them to be directed towards the proper end organs. On the other hand NGF produced by transduced fibroblasts in the central nervous system has been shown to diffuse 1-2 mm into the brain parenchyma<sup>135</sup>, a distance greater than the average diameter of a peripheral nerve fascicle.

To investigate whether viral vector-mediated overexpression of NGF or other neurotrophic factors will actually improve functional regeneration of the peripheral nerve, more extensive studies with transduced nerve grafts in a relevant animal model, e.g., a rat sciatic nerve lesion are needed<sup>34</sup>. If extensive functional testing of hind limb function and histological quantification of regeneration including retrograde tracing show a favorable effect of the application of LV-NGF then this would be an important step towards clinical application. The present results, the established safety and clinical applicability of LV vectors<sup>43</sup>, as well as the promising results obtained previously with NGF in other studies<sup>18,133</sup>, warrant such investigations.

## Conclusion

LV vector-mediated transduction of human sural nerve grafts is technically feasible and can potentially be performed without changing the routine clinical practice of nerve grafting in PNS repair. Large numbers of fibroblasts inside the nerve, but outside the nerve fascicles can be transduced and following the use of LV-NGF significant amounts of biologically active NGF are released. The acquired knowledge forms the basis for the further development of a novel approach to enhance regeneration after surgical peripheral nerve reconstruction.



# Chapter 5

## Neuroregenerative effects of lentiviral vector-mediated GDNF expression in reimplanted ventral roots

Ruben Eggers, William T Hendriks, Martijn R Tannemaat, Joop J van Heerikhuize, Chris W Pool, Thomas P Carlstedt, Arnaud Zaldumbide, Rob C Hoeben, Gerard J Boer, Joost Verhaagen

*Molecular and Cellular Neuroscience*. 2008 Sep;39(1):105-17

### Abstract

Traumatic avulsion of spinal nerve roots causes complete paralysis of the affected limb. Reimplantation of avulsed roots results in only limited functional recovery in humans, specifically of distal targets. Therefore, root avulsion causes serious and permanent disability. Here, we show in a rat model that lentiviral vector-mediated overexpression of glial cell line-derived neurotrophic factor (GDNF) in reimplanted nerve roots completely prevents motoneuron atrophy after ventral root avulsion and stimulates regeneration of axons into reimplanted roots. However, over the course of 16 weeks neuroma-like structures are formed in the reimplanted roots, and regenerating axons are trapped at sites with high levels of GDNF expression. A high local concentration of GDNF therefore impairs long-distance regeneration. These observations show the feasibility of combining neurosurgical repair of avulsed roots with gene-therapeutic approaches. Our data also point to the importance of developing viral vectors that allow regulated expression of neurotrophic factors.

### Introduction

Traumatic avulsion of nerve roots from the spinal cord is a devastating event that usually occurs in the brachial plexus of either young adults during motor vehicle or sports accidents or in newborn children during difficult childbirth<sup>136</sup>. Three surgical strategies to restore motor function after ventral root avulsion have been explored in human subjects: 1) reimplantation of the avulsed roots into the spinal cord<sup>137</sup>, 2) implantation of autologous nerve grafts that are connected distally to the avulsed roots<sup>137,138</sup> and 3) rerouting of healthy nonessential nerves towards the distal targets of the avulsed roots<sup>139</sup>.

Without treatment, ventral root avulsion leads to progressive atrophy of motoneurons, whereas reimplantation of a ventral root results in rescue of approximately 70% of motoneurons in experimental animals<sup>140-142</sup>. Reimplantation can result in some clinical signs of motoneuron regeneration in humans, but long distance regeneration and functional reinnervation of more distally located targets such as the hand

is extremely rare<sup>137,143-145</sup>. Hence, even with the currently available surgical options, root avulsion remains a condition that leads to serious and permanent disability. To re-establish nerve function after root reimplantation, 4 successive goals have to be achieved: 1) prevention of motoneuron atrophy after avulsion, 2) regeneration of axons through the outgrowth-inhibitory environment of the scarred spinal cord into the nerve root, 3) sustained axonal growth through the peripheral nerve to create functional connections with target organs and 4) preservation of target organs including muscles.

The survival of motoneurons following root avulsion and reimplantation in the rat can be enhanced with the application of glial cell line-derived neurotrophic factor (GDNF)<sup>146-148</sup>, a combination of riluzole and GDNF<sup>149</sup> and with viral vector-mediated overexpression of brain-derived neurotrophic factor (BDNF) or GDNF in the spinal cord<sup>24</sup>. Although motoneuron survival was achieved in the latter study, axonal outgrowth into the reimplanted nerve root was not improved and regenerating axons appeared to be trapped in the ventral spinal cord.

Here, we combined neurosurgical reimplantation of avulsed ventral spinal roots with lentiviral (LV) vector-mediated expression of BDNF or GDNF in the reimplanted roots. We hypothesized that this approach would create a neurotrophic factor gradient from the reimplanted roots to the ventral spinal cord that would attract motor axons toward the root. We examined whether enhanced expression of these neurotrophic factors by the implanted spinal roots can prevent the severe lesion-induced atrophy of motoneurons and promote the regeneration of motor axons into the roots. We also assessed the ability of motor axons to regenerate over long distances into the sciatic nerve and the functional recovery of the denervated hind limb.

## Results

### *Characterisation of LV vectors*

The titers of the LV stocks are provided in figure 1. To determine if BDNF and GDNF produced by LV vector-mediated transduced cells are biologically active, their effect on neurite outgrowth from E14 rat embryonic DRG explants was quantified following the method of Niclou et al.<sup>128</sup>. Conditioned medium from LV-BDNF- and LV-GDNF-infected 293T cells significantly increased the neurite growth of DRG explants ( $p < 0.002$  for LV-BDNF;  $p < 0.0001$  for LV-GDNF,) compared to LV-GArGFP-conditioned media (figure 2). This shows that LV-BDNF and LV-GDNF direct the expression of biologically active BDNF and GDNF protein.

### *Injection of LV vector leads to long term transgene expression in the nerve root*

In the LV-GArGFP-injected control group, GFP positive cells were observed in the avulsed and reimplanted nerve root throughout the 16 weeks post-lesion period (fig-

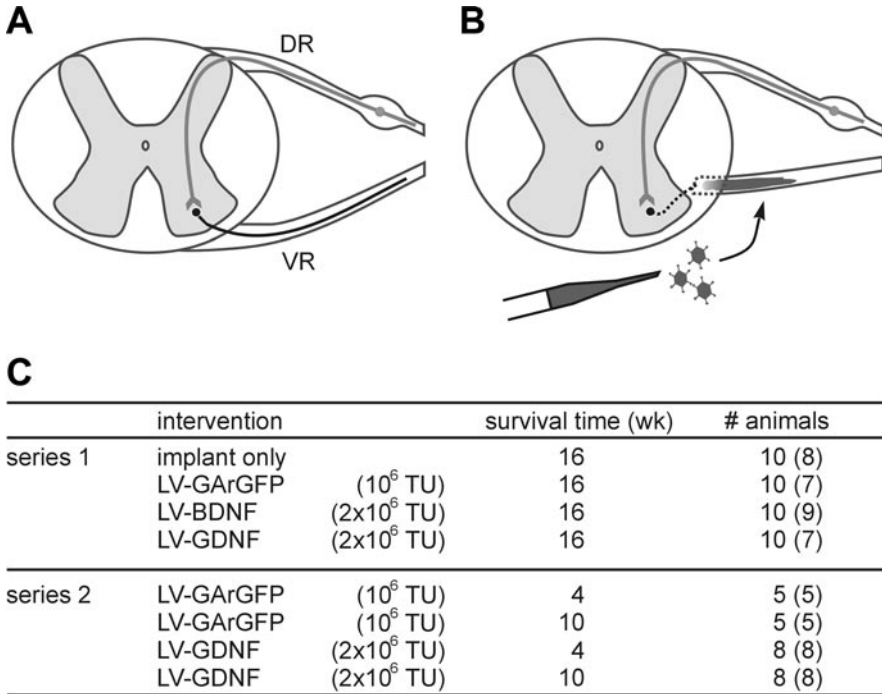


**Figure 1** Schematic representation of surgical procedures (ventral root avulsion, vector injection and root implantation) and overview of experimental groups.

A) Schematic representation of a cross section of the intact spinal cord and its dorsal (DR) and ventral root (VR) on one side.

B) After ventral root avulsion, the root is either directly reimplanted in the spinal cord just above the avulsion site or reimplanted after an injection with 1  $\mu$ l of a viral vector.

C) Overview of experimental series, treatment groups, amount of vector injected (transducing units, TU) and survival times. Some animals were lost during the experiment due to autotomy. The number in parentheses in the “# animals” column indicates the final number of animals used for all functional and histological analyses.

ure 3A). LV vector-mediated expression of BDNF and GDNF in the nerve roots was established by in situ hybridisation. In all animals numerous cells expressing high levels of BDNF (figure 3B) and GDNF mRNA (figure 3C) were present in nerve roots at 16 weeks post-lesion. Transduced cells were only found within the nerve root, close to regenerating axons, had a Schwann cell-like morphology and stained positive for S100 (figure 3A). *In vivo* transduction efficiency was further quantified on sections of LV-GArGFP injected animals at 4 weeks by measuring the distance between the two outermost transduced cells. The average longitudinal spread of transduced cells was  $2.3 \pm 0.43$  mm. In the center of the transduced area, an average of  $17 \pm 4.5\%$  of Schwann cell nuclei was positive for GArGFP. Transduced cells did not migrate into

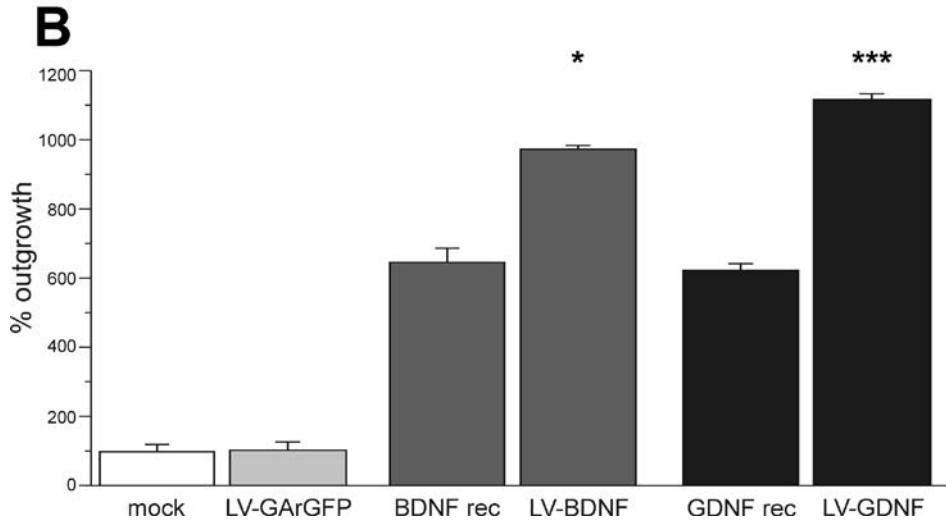
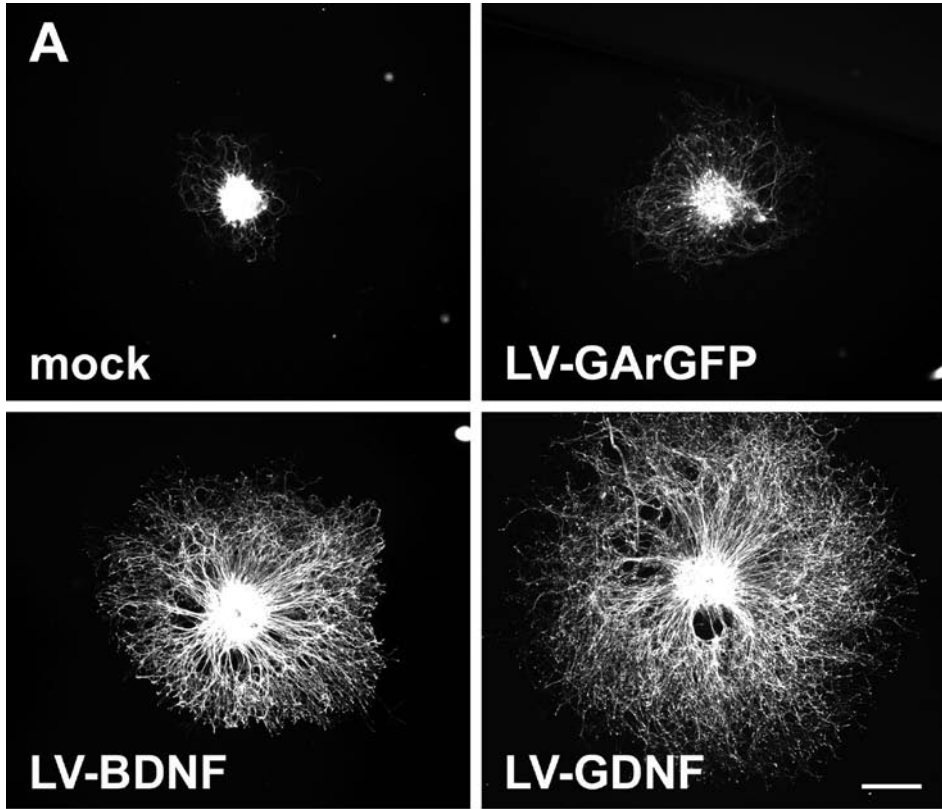




**Figure 2** Biological activity of neurotrophic factors produced by LV vector-transduced cells. A) Examples of in vitro neurite outgrowth of E14 rat embryonic dorsal root ganglia after 48 h in conditioned medium derived from LV-GArGFP, LV-BDNF or LV-GDNF transduced 293T cells. Scale bar 750  $\mu$ m.

B) Quantification of neurite outgrowth as percentage of the value of mock controls. Medium from LV-GArGFP-infected cells does not affect outgrowth, whereas medium from LV-BDNF- and LV-GDNF-infected cells increases neurite outgrowth 9- and 11-fold respectively. Under these conditions 25 ng/ml recombinant BDNF or GDNF both increase neurite outgrowth approximately 6-fold. Error bars indicate SEM for n=8 per group. \*p < 0.05; \*\*\*p < 0.001; one-way ANOVA followed by Bonferroni's post hoc testing.

the spinal cord. A single injection of 1  $\mu$ l containing  $1-2 \times 10^6$  TU LV vector thus leads to long term transgene expression, similar to what has been described previously<sup>150</sup>.

*LV vector- mediated expression of GDNF in reimplanted ventral roots completely prevents motor neuron atrophy.*

Atrophy of motoneurons was assessed on spinal cord sections 16 weeks after avulsion and implantation (figure 4). Motoneurons on the contralateral side appeared unaffected in all groups and had a normal morphology (figure 4A). Many motoneurons displayed considerable atrophy in both control groups (figure 4B), as well as in the LV-BDNF-treated group (figure 4C). In the LV-GDNF-treated animals, most motoneurons appeared to be the same size as the contralateral side (figure 4D), while some motoneurons appeared to be slightly larger with a rounder shape, possibly indicating

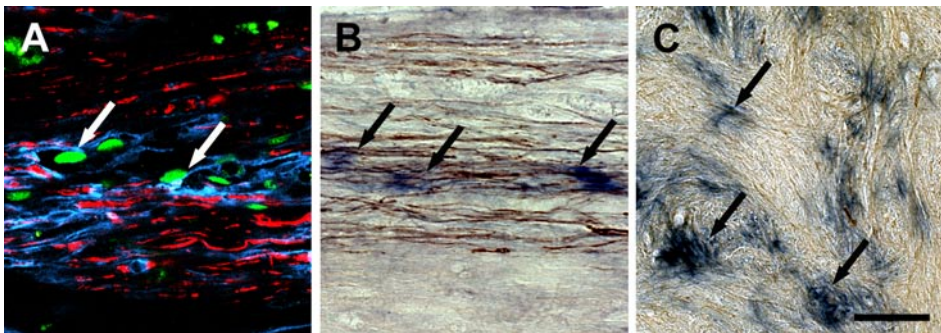
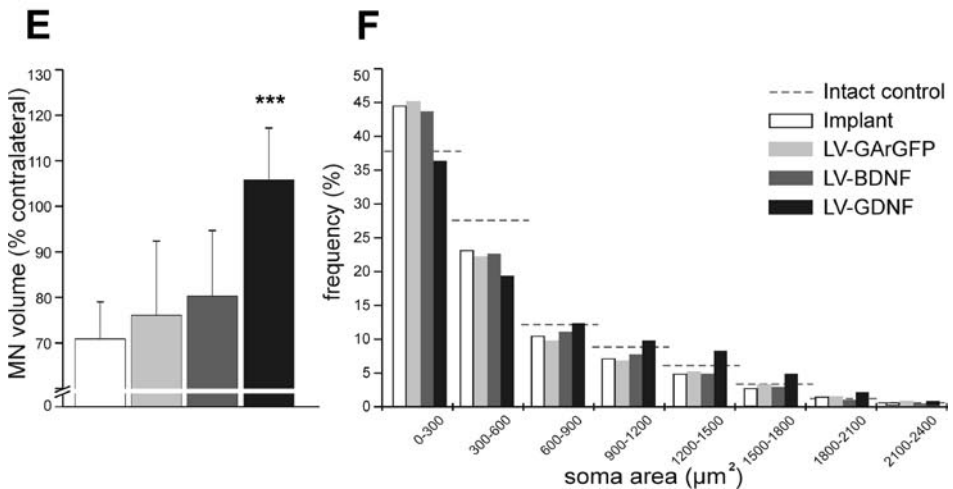
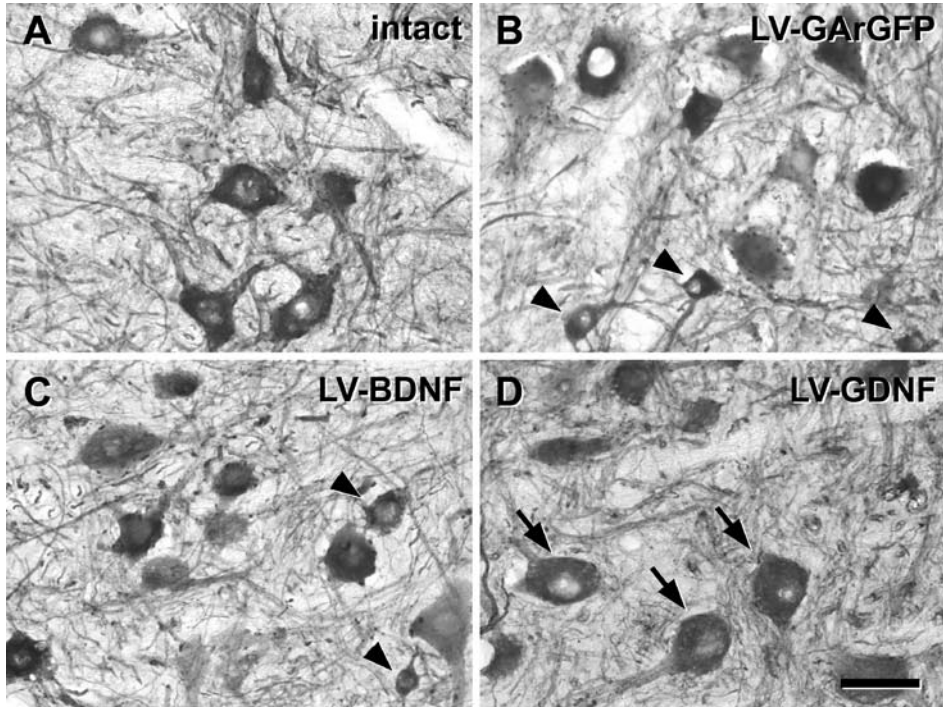


**Figure 3** Immunohistochemistry and *in situ* hybridization at 16 weeks demonstrates that injection of LV vector leads to long-term transgene expression in Schwann cells in the reimplanted ventral root.

A) GArGFP (green) is present in the nuclei of numerous S100 positive Schwann cells (blue) in close proximity to NF positive axons (red). Cells containing BDNF (B) or GDNF (C) mRNA (blue, arrows) close to ChAT positive motoneuron fibers (brown) in the ventral root.

Scale bar 50  $\mu$ m.

hypertrophy (figure 4D). Motoneuron atrophy was quantified by calculating the total volume of the motoneuron pool as a percentage of the contralateral motoneuron pool (figure 4E). In the two control groups, implant and LV-GArGFP, the total volume of ChAT positive motoneurons on the side of the avulsed roots was ~30% smaller as compared to their contralateral side ( $p < 0.001$  implant,  $p < 0.03$  LV-GArGFP). In the



LV-BDNF group the motoneuron volume had decreased by ~20%, as compared to the contralateral side, comparable to the control groups ( $p < 0.004$ ). In contrast, in LV-GDNF-treated animals, the total volume of the affected motoneurons was similar to the control side (105%,  $p=0.2$ ), and the volume of the affected side as a percentage of the contralateral side was significantly higher than all other groups ( $P < 0.0001$ ). Quantitative analysis of individual motoneuron profiles (figure 4F) revealed a significant shift towards relatively smaller profiles and a reduction of large structures when compared to the distribution of intact motoneurons (dotted lines) and to motoneurons after avulsion and reimplantation (white bars). In LV-GDNF treated animals a normalisation of soma size distribution was observed (black bars). Moreover, LV-GDNF treatment results in a small but significant proportion of hypertrophic motoneurons, as indicated by the relative increase of motor neuron profiles larger than  $900 \mu\text{m}^2$ . These findings indicate that LV vector-mediated expression of GDNF in reimplanted ventral nerve roots completely prevents the atrophy of axotomized motoneurons at 16 weeks after avulsion and reimplantation of the ventral root.

*LV vector-mediated expression of GDNF stimulates outgrowth into the reimplanted root, but also coiling of axons*

Regeneration of ChAT positive motoneurons into reimplanted roots could be observed as early as 4 weeks after avulsion and nerve root reimplantation (figure 5AB). Thin ChAT positive axons traversed the spinal cord white matter and entered the root at the site of implantation. The regenerated fibers have a clear longitudinal orientation within the root, although they are thinner and follow a more undulating path than

**Figure 4** The effect of long term LV vector-mediated overexpression of BDNF and GDNF in the avulsed/reimplanted root on motoneuron soma size in the rat spinal cord.

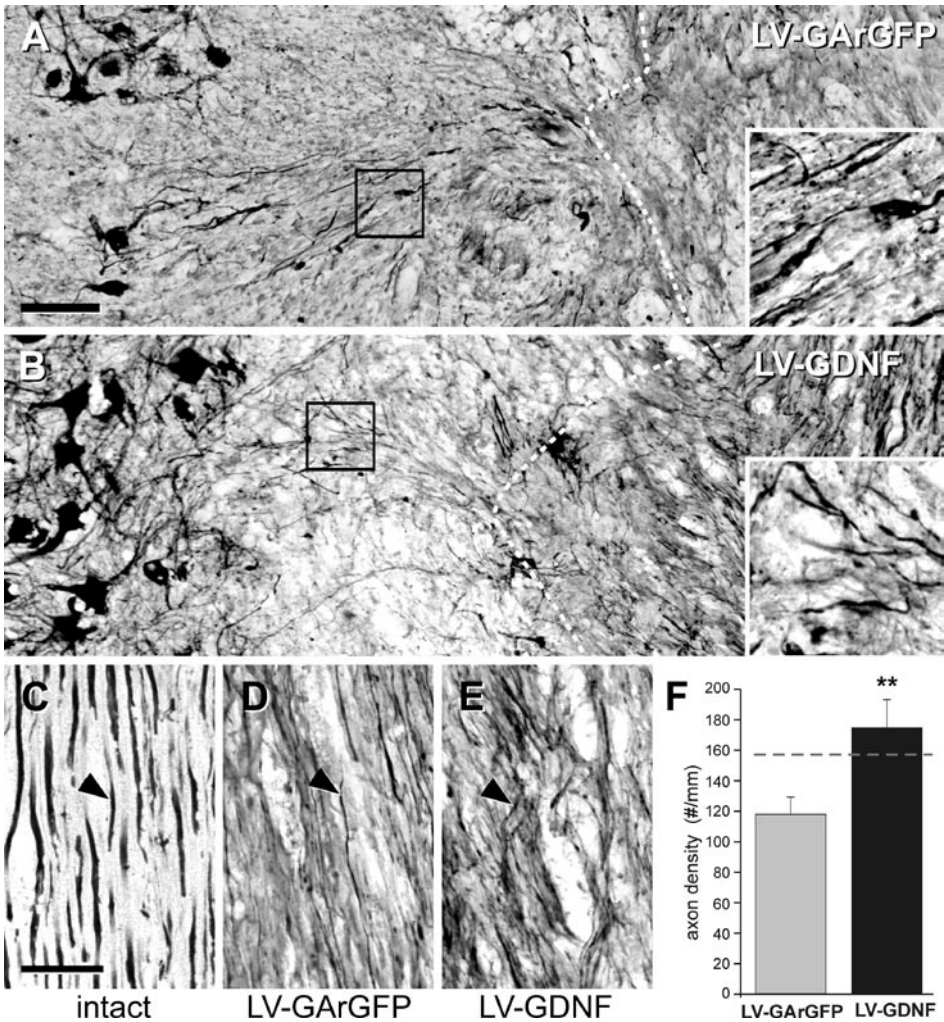
A) Representative high magnification of intact motoneurons stained for ChAT showing normal motoneuron morphology. At 16 weeks, motoneurons on the root avulsion side of the spinal cord of LV-GArGFP, (B) and LV-BDNF-treated animals, (C) display atrophied motoneurons (arrowheads). In contrast, motoneurons in the LV-GDNF group (D) display many motoneurons with a round hypertrophic morphology (arrows). Scale bar  $50 \mu\text{m}$ .

E) Quantification of total motoneuron (MN) volume displays complete rescue of motoneuron volume in LV-GDNF-treated animals and no statistically significant effects in the other groups when compared to the values of the contralateral unaffected side.

\*\*\*  $p < 0.001$ ; one-way ANOVA followed by Bonferroni's post hoc testing.

F) Frequency distribution of motoneuron size, showing that avulsion and reimplantation leads to shift in soma size distribution resulting in fewer big structures ( $>600 \mu\text{m}^2$ ) and more smaller structures ( $<300 \mu\text{m}^2$ ) in control groups (white and light grey), compared to unaffected motoneuron distribution (dotted lines). The application of LV-GDNF leads to restoration of the normal distribution, and even some hypertrophy, as indicated by the increased number of very large structures ( $900-1800 \mu\text{m}^2$ ).

axons in the intact root (figure 5CD). In the LV-BDNF group, comparable patterns of neurite outgrowth were seen as in control animals (data not shown). In contrast, LV vector-mediated expression of GDNF appeared to stimulate more axons growing into the nerve root (figure 5E). The density of axons entering the implanted root was quantified by counting the number of axons crossing a reference line perpendicular to the implanted root, just distal from its implantation site in the spinal cord at 4 weeks. The application of LV-GDNF led to a significant increase in axon density compared to LV-GArGFP ( $p=0.016$ ; figure 5F). The fiber density in LV-GDNF treated animals was comparable to that in the non-avulsed control root.





Apart from the density, both the longitudinal orientation and distribution of axons distal from the spinal cord (scored blindly at 4, 10 and 16 weeks post-lesion) in LV-GDNF-treated animals differed considerably from LV-GArGFP-injected control animals. The most striking observation was the presence of specific areas with a high density of axons with a considerably coiled appearance in ventral roots with transgenic GDNF expression. This phenomenon was present almost exclusively in the LV-GDNF-treated group and already apparent 4 weeks after the intervention (figure 6). At that stage, in the majority of animals (72%) these nerve fibers were still oriented longitudinally within the nerve root and appeared to be grouped together in thick strands (figures 5E and 6A), but in one animal (14%), small areas were seen in which axons appeared to have lost their longitudinal orientation completely. After 10 weeks, areas with coiled axons were observed in 83% of the LV-GDNF-injected animals ( $p < 0.02$  compared to LV-GArGFP, figure 6B). Moreover, these areas were larger than those observed at 4 weeks. After 16 weeks of GDNF overexpression, extreme coiling of large numbers of axons was seen in all animals ( $p < 0.001$ , figure 6CD). By then, entire nerve roots were filled with thick coils of ChAT positive axons and only a minority of axons (the fibers outside the clusters) had a longitudinal orientation (figures 6D and 7I). The increased numbers of nerve fibers were accompanied by an increase in the diameter of the injected nerve roots, occasionally to such an extent that the spinal cord was slightly displaced by the implanted nerve roots (figure 6D). Coiling of axons was not observed in any of the control LV-GArGFP-injected animals at any time point, and not seen at 16 weeks in the 'implant' group and in only one animal of the LV-BDNF group (14%).

**Figure 5** ChAT positive neurite outgrowth from the spinal cord into the implanted ventral root 4 weeks after avulsion and reimplantation.

A) Representative image at the site of implantation in a control LV-GArGFP-injected root showing a few fibers (arrowheads) traversing from motoneuron pool (left) towards the implanted root (right).

B) The implantation site in an LV-GDNF-treated animal displays a similar pattern as in A). Insets show higher magnification of boxed areas in (AB) Dotted white lines in (AB) show boundary of implanted root.

C) Typical ChAT staining of motor axons in the intact ventral root displays thick, longitudinally oriented fibers.

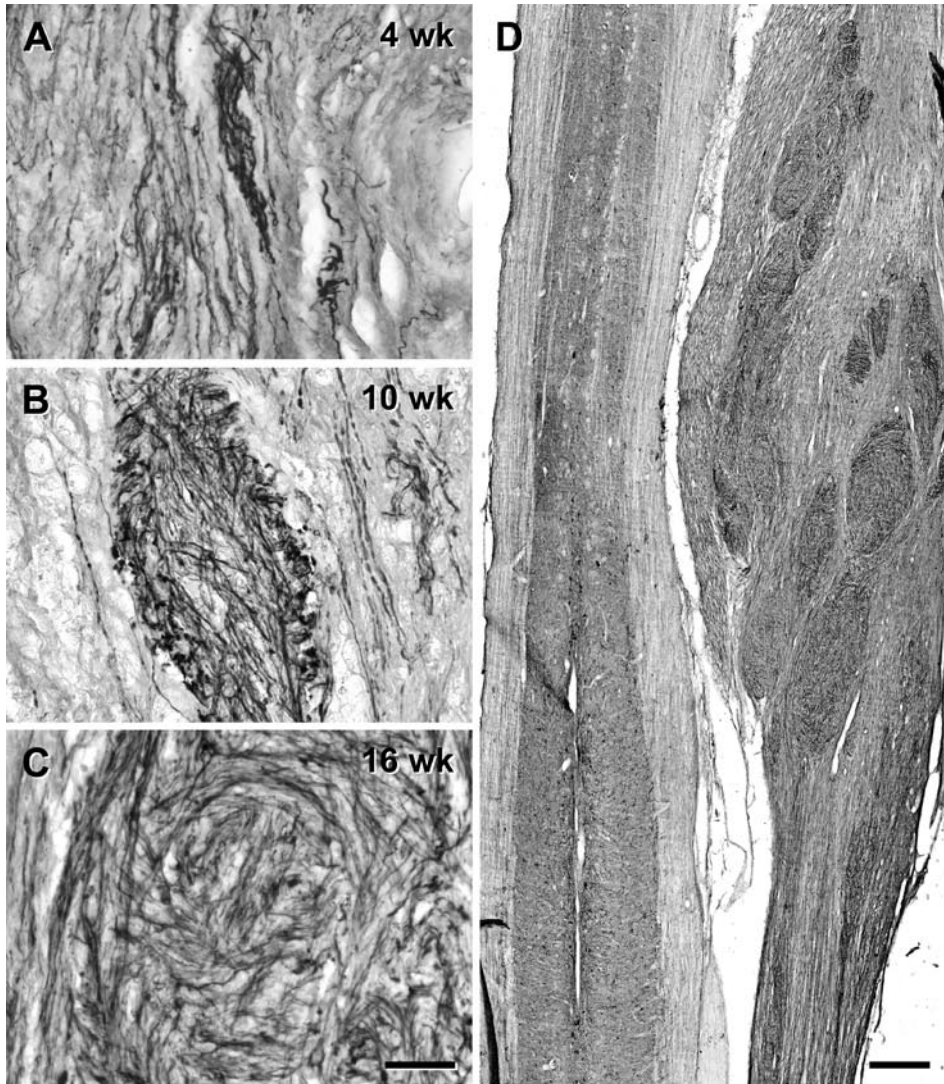
D) The ventral roots of a LV-GArGFP-treated rat distal from the implantation site shows several thin regenerating fibers.

E) A distinctly higher density of motor axons is present in the roots of LV-GDNF-treated animals.

F) Quantification of the axon density in the reimplanted root just distal from the implantation site. LV-GDNF significantly increases axon density compared to LV-GArGFP.  $**p < 0.016$ ; Kruskal-Wallis followed by Mann-Whitney U test.

Dotted gray line indicates axon density of unavulsed root.

Scale bars A-B 100  $\mu\text{m}$ ; C-E 50  $\mu\text{m}$ .



**E**

| intervention | 4 wk | 10 wk | 16 wk   |
|--------------|------|-------|---------|
| implant only | n.d. | n.d.  | 0%      |
| LV-GArGFP    | 0%   | 0%    | 0%      |
| LV-BDNF      | n.d. | n.d.  | 14%     |
| LV-GDNF      | 14%  | 83%*  | 100%*** |

Immunohistochemical staining for GDNF showed that the levels of GDNF protein were locally elevated within the LV-GDNF transduced nerve root at 4 (supplemental figure 1) and 10 weeks (figure 7). A gradient of GDNF from the spinal cord to the implanted root is thus continuously maintained after LV-mediated transduction. GDNF protein could not be detected by immunohistochemistry in non-avulsed roots (figure 7A) or in avulsed LV-GArGFP-injected and reimplanted roots (figure 7C, supplemental figure 1). Staining of adjacent sections for GDNF and ChAT in the LV-GDNF-treated group at 10 weeks showed that the increased numbers of nerve fibers co-localised with the presence of GDNF protein (figure 7). Double staining for GDNF and NF revealed a high density of NF positive fibers in GDNF positive areas, whereas ChAT staining on adjacent sections revealed that these nerve fibers were indeed axons of motoneurons (figures 7EF and 7GH). Consequently, the increased density of axons appears to be caused by the high local concentrations of GDNF after injection of LV-GDNF (figure 7I).

*LV-GDNF increases the density of Schwann cells in the implanted nerve root*

Because Schwann cells express the GDNF receptor GFR $\alpha$ -1<sup>151</sup>, we studied the effect of LV-BDNF and LV-GDNF on cell density in the implanted root. Longitudinal spinal cord sections containing unavulsed control roots or implanted roots were stained for NF (figure 8A), S100 and Hoechst and manually outlined using the NF signal. In LV-GDNF treated animals, coils were outlined and measured separately (figure 8C). S100 staining confirmed that the majority of measured cells within the nerve root were Schwann cells (data not shown). The S100 staining could, however, not be used to reliably identify and quantify individual Schwann cells since the S100-positive Schwann cells are closely packed together and the S100 signal filled the whole cell. Therefore Hoechst staining was used to quantify the cells in the nerve root. To this end

**Figure 6** ChAT staining of LV-GDNF-injected nerve roots up to 16 weeks showing the development and changing morphology of fiber coils over time.

A) At 4 weeks, numerous areas with an increased fiber density (strands) are present (72%). These areas are relatively small and fibers primarily have a longitudinal orientation. Incidentally coiled fibergrowth is observed (14%). Scale bar 50  $\mu$ m.

B) At 10 weeks, the areas with a high fiber density are larger. Many of them have a strong chaotic, coiled morphology. Scale bar 50  $\mu$ m.

C) At 16 weeks, extremely large coils of axons fill up the entire nerve root. Scale bar 50  $\mu$ m.

D) An overview of the spinal cord and nerve root at 16 weeks displays the local but large coil formation of ChAT positive fibers, resulting in an increase of root diameter and slight compression to the spinal cord. Scale bar 500  $\mu$ m.

E) Presence of coil formation was quantified at all time points and expressed as percentage of presence or absence in the number of animals. \* $p < 0.05$ ; \*\*\* $p < 0.001$ ; Pearson Chi-Square test. n.d.= not determined.



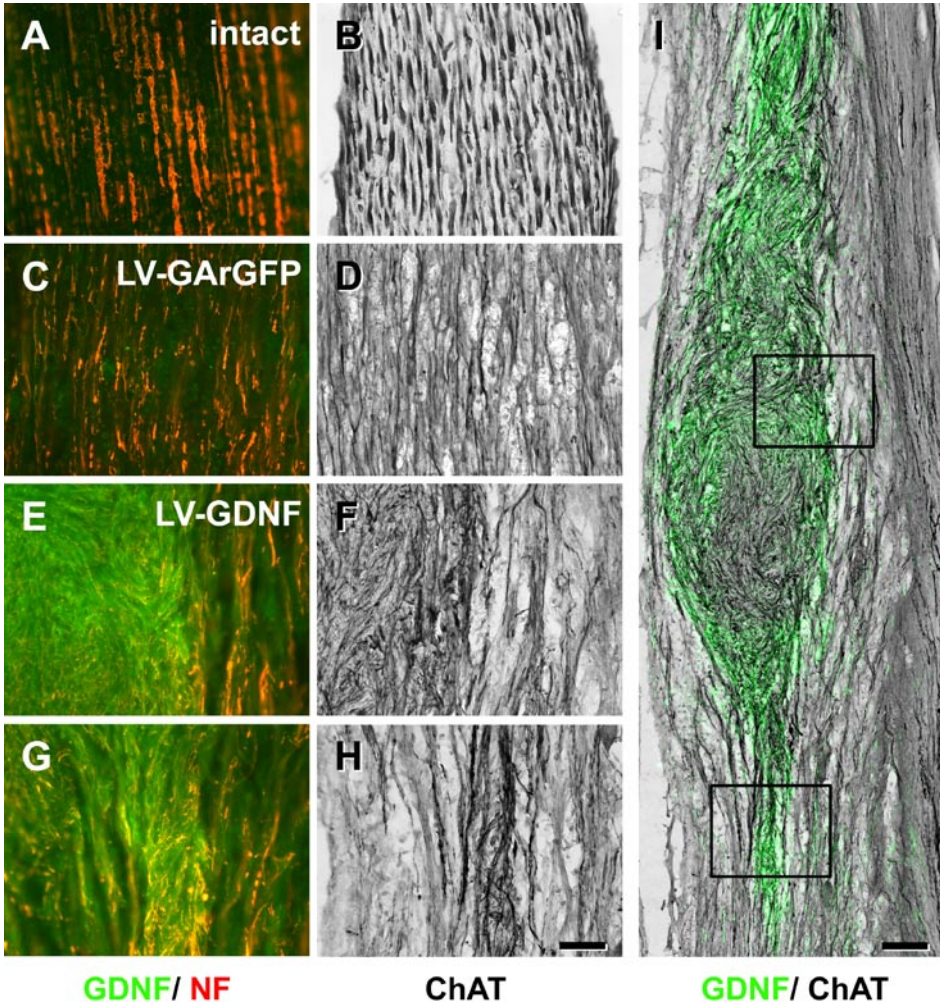


**Figure 7** Immunohistochemistry at 10 weeks shows that GDNF overexpression in the reimplanted ventral root colocalizes with dense ChAT positive motor axon fiber coils.

A-B) Immunohistochemistry on consecutive sections of a normal, non-avulsed root double-immunolabeled for GDNF and NF (A) and immunostained for ChAT (B). No GDNF staining is visible, whereas the staining pattern of NF and ChAT is similar.

C-D) Similar stainings of control LV-GArGFP-injected ventral roots display no GDNF signal, and thin regenerating fibers.

E-H) Strong GDNF staining is observed in the LV-GDNF-injected ventral roots (cf. boxes in the overview of I), in which consecutive sections show dense coils of ChAT positive fibers in the area of high GDNF expression.

I) Overlay of adjacent sections (GDNF/ChAT) displays strong colocalisation between GDNF protein and coil location which is prominently seen in the overlay picture of GDNF (green) and ChAT signal (black) from consecutive sections at lower magnification.

Scale bars A-H 50 μm; I 100 μm.



the area covered by Hoechst-labelled nuclei was calculated automatically (figure 8BD) as a proportion of the outlined area to create a measure of Schwann cell density. This quantification showed that cell density increases strongly (13-fold) after root avulsion and reimplantation alone compared to non-avulsed roots. Importantly, the application LV-GDNF led to a trend towards a higher cell density to 1.32 fold compared to “implant” ( $p < 0.09$  vs “implant”) and cell density was significantly higher within the nerve coils that contain the highest levels of GDNF ( $p < 0.003$  vs “implant”).

The measured density of nuclei could not be used to generate absolute cell counts, due to the high number of overlapping nuclei (figure 8D). However, it can be estimated that the observed densities correspond to approximately 1200, 16.000, 18.000 and 20.000 cells/mm<sup>2</sup> in non-avulsed, “implant”, LV-GDNF nerve roots and LV-GDNF coils, respectively. It should be noted that in sections with higher cell densities, this calculation likely underestimates the actual number of cells due to overlapping nuclei. S100 staining confirmed that the majority of measured cells within the nerve root were Schwann cells (data not shown).

#### *Local high levels of GDNF prevent more distal neurite outgrowth*

Long distance regeneration was quantified by counting the number of ChAT positive nerve fibers in the sciatic nerve, 7 cm distal to the site of reimplantation in the 16 week survival groups. Equal numbers of axons were present at this level in the sciatic nerve with or without the injection of LV-GArGFP (figure 9A). The application of LV-BDNF did not lead to an increase in the number of nerve fibers. Surprisingly, despite the high density of ChAT positive fibers in the ventral root, the application of LV-GDNF did not result in more, but significantly *less* regenerated axons distally, compared to ‘implant’ ( $p < 0.014$ ) and LV-BDNF ( $p < 0.005$ ) (figure 9BC). A frequency distribution of the diameters of axons in the sciatic showed that the reduction in total number of ChAT positive fibers in the distal sciatic of LV-GDNF-treated animals was predominantly the result of a significant decrease in the number of small diameter axons (figure 9D) ( $p < 0.005$  compared to ‘implant’ and LV-BDNF,  $p < 0.05$  compared to LV-GArGFP) and to a lesser extent in medium-sized fibers ( $p < 0.05$  compared to “implant”). This suggests that LV vector-mediated expression of GDNF in the reimplanted nerve roots prevents sustained long distance regeneration of motor axons into the sciatic nerve.

#### *Transduction of reimplanted nerve roots with LV-BDNF or LV-GDNF does not affect recovery of hind limb function*

Avulsion of the L4, 5 and 6 roots leads to a substantial loss of hind limb function. In the implant control group, the average modified BBB score dropped from 14 to 2.4, recovering to 5.3 at 4 weeks and remaining at this plateau up to 13 weeks. The LV-BDNF- and LV-GDNF-treated groups had an identical pattern of recovery; no differences in

the modified BBB score between groups were observed at any time point. The score per animal was generally the result of some movement in the hip, knee and ankle. No voluntary stepping, toe clearance or weight support of the affected limb was observed in any animal at any time point. No correlation was found between the number of regenerated axons in the sciatic nerve and recovery of hind limb function, either within the control groups or when analysing all animals together (data not shown). Severe muscle atrophy of the denervated hind limb was present in all animals.

## Discussion

In the present study we show that LV vector-mediated overexpression of GDNF in avulsed and reimplanted ventral nerve roots completely prevents motoneuron atrophy and leads to a significant increase in regenerating axons in the reimplanted roots. In LV-GDNF-treated animals neuroma-like structures were formed at sites of high levels of GDNF expression. The number of fibers that had regenerated to the level of the sciatic nerve was significantly lower in LV-GDNF treated animals. A local high concentration of GDNF thus appears to trap regenerating axons.

### *Transduction of reimplanted nerve roots with LV-GDNF prevents motoneuron atrophy*

A loss of neurotrophic support after root avulsion and the inability of motoneuron axons to regenerate leads to severe atrophy and virtual disappearance of 80-90% of affected motoneurons over a course of several weeks<sup>142,152</sup>. The automated quantification of the total volume of all ChAT positive structures used in the present study allowed for a comprehensive and accurate measurement of the total volume of the affected motoneuron pool. This method avoids the potential pitfall of mistaking severe motoneuron atrophy for cell death<sup>153</sup>. Furthermore, unlike retrograde tracing, it does not exclude the 20-35% of motoneurons that survive without regenerating into the implanted root<sup>154,155</sup>. Reimplantation of the avulsed root by itself partially prevents atrophy of motoneurons, but this neuroprotective effect is not sufficient for complete long term survival at longer time points<sup>142,149,156</sup>. In this paper we describe a similar, significant 30% decline of the volume of the motoneuron pool at 16 weeks after reimplantation.

Axotomized motoneurons are sensitive to a number of neurotrophic factors<sup>9</sup>. Motoneuron death after ventral root avulsion can be prevented with BDNF<sup>157,158</sup> or GDNF<sup>146</sup>. However, a single application of BDNF and/or ciliary neurotrophic factor (CNTF) does not have a notable effect<sup>159</sup>, and long term infusion of neurotrophic factors is problematic<sup>160</sup>. Viral vector-mediated overexpression is thus a very promising method for long term expression of therapeutic genes. Adeno-associated virus (AAV) vector-mediated overexpression of BDNF or GDNF in the spinal cord does indeed

promote motoneuron survival after ventral root avulsion and reimplantation <sup>24</sup>. Here, we show that expression of GDNF distal from the affected motoneuron pool, i.e., in the reimplanted nerve root, is sufficient to prevent atrophy after axotomy and causes a slight hypertrophy of motoneurons, similar to previous publications <sup>146,161,162</sup>.

*LV vector-mediated expression of BDNF in the implanted nerve root has a limited effect*

In contrast to GDNF, the continuous overexpression of BDNF has no significant effect on motoneuron survival at 16 weeks. A similar difference between these neurotrophic factors was also observed after a single application of recombinant BDNF or GDNF after root avulsion <sup>146</sup> and after AAV vector-mediated transduction of the spinal cord <sup>24</sup>, although BDNF did have a modest effect in the latter and other <sup>163</sup> studies. The GDNF and BDNF receptors are expressed differentially in injured motoneurons. The expression of the receptors for GDNF, GFR $\alpha$ -1 and c-RET, is increased up to 300% after avulsion, whereas TrkB, the high affinity receptor for BDNF is downregulated after ventral root avulsion <sup>164</sup>.

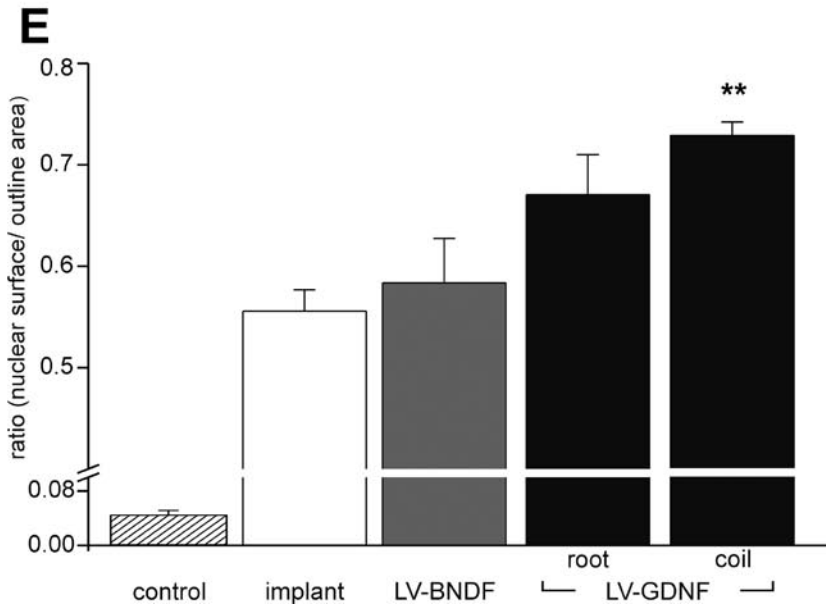
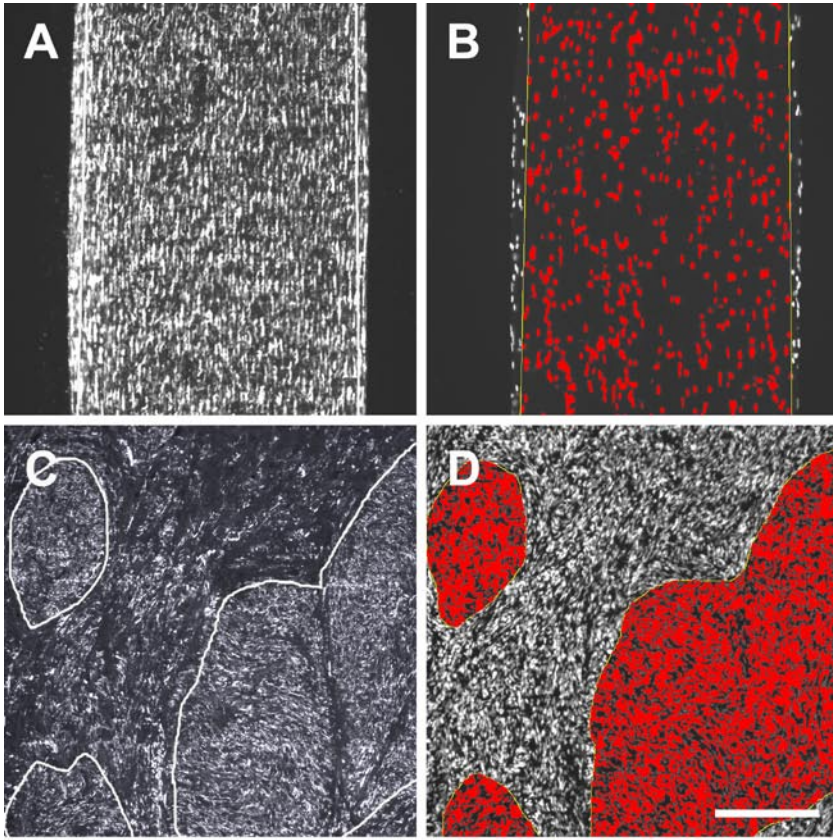
This difference, combined with the application of LV-GDNF in the nerve root may explain the lack of effect of BDNF as found in the current experiments.

*Application of LV-GDNF stimulates axonal outgrowth into the reimplanted root*

Besides preventing cell atrophy, the second goal of a treatment strategy should be to increase the number of axons entering the implanted root <sup>155</sup>. This requires axonal regeneration across the outgrowth-inhibitory environment of the spinal cord <sup>57,61</sup> and was achieved previously with a combination of GDNF and riluzole <sup>149</sup> or with the enzymatic degradation of inhibitory molecules in the spinal cord <sup>165</sup>. Our results show that LV vector-mediated overexpression of GDNF significantly increases the density of axons entering the LV-GDNF-injected nerve roots. This could be caused by an increase in the number of motoneurons that project an axon into the implanted root and/or by branching of motor axons at sites of elevated GDNF expression.

*Long term local production of GDNF negatively affects long distance regeneration*

Continuously elevated levels of GDNF results in the progressive occurrence of extreme coiling of axons within the nerve root and appear to impair long distance regeneration. After 4 weeks of transgene expression, the majority of axons still have a longitudinal alignment. The density and coiling of nerve fibers subsequently increase over the course of several weeks. After 16 weeks of transgene expression, the majority of axons are coiled in GDNF-rich areas in an extremely chaotic pattern that is reminiscent of peripheral nerve neuromas <sup>1</sup>, implying a strong *neurotropic* role for GDNF. This effect



has been described previously with motor axons failing to enter the reimplanted root after AAV-mediated overexpression in the spinal cord <sup>24</sup>. Our experiments are the first to provide a detailed temporal and spatial analysis of the growth of regenerating axons in relation to transgenic GDNF expression in reimplanted nerve roots. The formation of neuroma-like structures is probably caused by a direct effect of GDNF on axons, which express GFR $\alpha$ -1 and c-RET <sup>164</sup>. We also show that in areas of high GDNF expression the density of cells is increased and that the majority of these cells are Schwann cells. This may be the result of a direct effect on Schwann cells, which also express GFR $\alpha$ -1 <sup>151</sup> since the exogenous systemic application of GDNF causes Schwann cell proliferation and myelination of nerve fibers <sup>166</sup>. However, the observed high density of Schwann cells could also be the indirect result of the increased number of axons present in these areas. These two mechanisms can not be distinguished in this *in vivo* model where both axons and Schwann cells are affected by overexpression of GDNF. Nonetheless, Schwann cell proliferation in nerve coils is a factor that could contribute to the increased diameter of nerve roots that was observed after the application of LV-GDNF.

*Long distance regeneration is one of the prerequisites to enhance recovery of function*

The final goal of any experimental intervention to treat root avulsion injuries is to stimulate long distance regeneration and enhance recovery of function after nerve root avulsion and reimplantation. Although regenerating axons were observed the reimplanted nerve roots in all groups in the present study, only small numbers of ChAT positive fibers had regenerated to mid-thigh level of the sciatic nerve at 16 weeks and we did not observe a significant recovery of function in any treatment

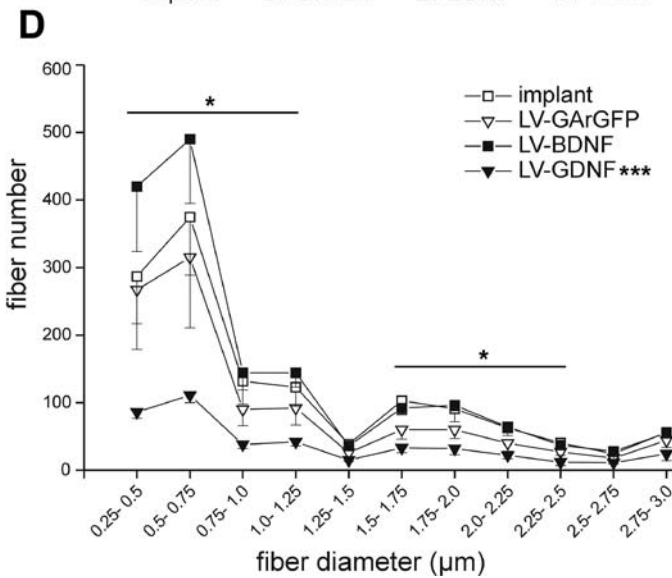
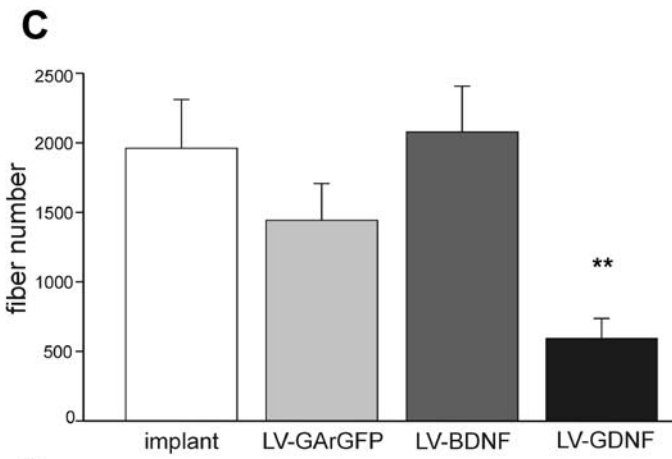
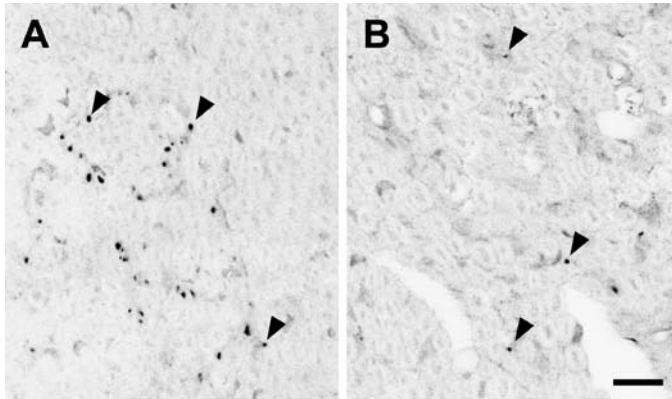
**Figure 8** Quantification of the density of cell nuclei based on Hoechst labelling and immunohistochemistry for Neurofilament (NF) shows an increased cellular density in the LV-GDNF treated roots at 16 weeks compared to controls.

AB) An outline in a non-avulsed ventral root was drawn using the NF signal (A). The surface area of Hoechst-labelled nuclei was measured with an automated filter algorithm (red) and expressed as a proportion of the outlined area (B).

CD) In LV-GDNF treated animals, dense NF positive areas (C) were used to separately outline coils and the surrounding root, resulting in specific measurement of the density of nuclei in these coils (D). Similar measurements were also made outside the coil in LV-GDNF or LV-BDNF injected roots and on implanted control roots (images not shown).

E) The area covered by cell nuclei as a proportion of the total outlined area (cell density) strongly increases after avulsion and reimplantation. Cell density is significantly increased in coils of LV-GDNF treated animals compared to “implant” \* $p < 0.003$ ; one-way ANOVA followed by Bonferroni's post hoc testing.

Scale bar 250  $\mu$ m.





group. Functional recovery has been described in root avulsion models which involve regeneration over shorter distances, i.e. towards the front paw after cervical nerve root avulsion<sup>167</sup> or towards the bladder sphincter<sup>168</sup>. In the present study, reinnervation of hind limb muscles requires regeneration over approximately twice this distance. The decline over time in the levels of neurotrophic factors produced by denervated distal Schwann cells<sup>9</sup> may contribute to the observed lack of regeneration over long distances as shown in our study. Furthermore, recovery of function depends on more factors than axonal outgrowth, including correct routing of regenerated fibers<sup>8</sup>. Enhanced hind limb function has been observed with the combined application of GDNF and riluzole after ventral root avulsion and reimplantation, but according to the authors, this was not the result of increased numbers of regenerated motoneurons in the reimplanted root<sup>149</sup>, emphasizing that the recovery of certain functional modalities can occur irrespective of long-distance axonal regeneration and may perhaps be related to enhancing plasticity at the level of the spinal cord<sup>57,120</sup>.

### *Concluding remarks*

Our results highlight that trapping of axons in areas with continuously elevated levels of neurotrophic factor poses a new challenge for the application of viral vector-mediated delivery of these factors in a ventral root reimplantation model. A possible solution for this problem lies in the application of viral vectors with regulatable expression<sup>50,51</sup>. It has been shown recently that in a spinal cord lesion model, trapping could be avoided by transient local expression of neurotrophic factors with such a vector<sup>52</sup>. Our results suggest that transient expression of GDNF for 4 weeks is sufficient to attract vast numbers of regenerating axons into the reimplanted nerve root. We predict that cessation of GDNF expression at this post-lesion time point will result in significantly more axons growing towards target organs. An alternative approach to prevent trapping of axons may consist of the transplantation of GDNF overexpressing cells

**Figure 9** LV-GDNF impairs long distance outgrowth of ChAT positive fibers in the reimplanted ventral root.

A) Representative photographs of ChAT-stained motor axons (arrowheads) in the transverse sciatic nerve, 7 cm distal from reimplantation site in a control 'implant' animal.

B) Similar to A) in an LV-GDNF-treated animal, showing a reduction in ChAT positive fibers. Scale bar 20  $\mu$ m.

C) Quantification of the total number of ChAT positive fibers in the 4 experimental groups displays a significant decrease in total fiber number in the LV-GDNF-treated group. \*\*  $p < 0.01$ ; one-way ANOVA followed by Bonferroni's post hoc testing.

D) Frequency distribution of fiber diameter shows that the LV-GDNF-treated group had a significant reduction of small diameter motor axons, usually associated with regeneration. \* $p < 0.05$ , \*\*\* $p < 0.001$ ; Kruskal-Wallis followed by Mann-Whitney U test.

<sup>169</sup> or the application of LV-transduced peripheral nerve grafts <sup>87,149</sup>. As transplanted cells are likely to migrate, expression levels of neurotrophic factors could be more homogeneously distributed within the nerve using this approach. Nonetheless, the number of axons entering the implanted root is only one aspect that influences the recovery of function in humans and future therapeutic strategies will likely need to address other problems (including chronic denervation and subsequent target organ atrophy) as well <sup>11</sup>.

## Materials and Methods

### *Lentiviral vector production*

Plasmids used for the production of the LV vectors have been described previously <sup>42</sup>. The LV-GArGFP control vector was generated by fusing the Gly-Ala repeat (GAR) domain of the Epstein-Barr nuclear antigen-1 as described by Hendriks et al. <sup>150</sup> to the N-term part of the green fluorescent protein (GFP). As described previously <sup>170</sup>, by interfering with the proteasome, the long alanine stretch of the GAR domain reduces the generation of antigen-linked MHC-I peptide and prevents a GFP-mediated cytotoxic T-lymphocyte immune response.

Lentiviral vectors encoding BDNF and GDNF were generated as follows using the pRRLsin-PPThCMV vector containing the Woodchuck posttranscriptional regulatory element <sup>171</sup>. The BamHI/XhoI BDNF cDNA excised from pc5-BDNF <sup>24</sup> was introduced into a BamHI/SalI opened LV transfer vector. The HindIII/XbaI excised GDNF cDNA (pBlue-GDNF <sup>24</sup>) was cloned into its respective site into a pAG-3 vector. Subsequently, the GDNF fragment was excised from pAG-3-GDNF with XbaI and cloned into an XbaI opened LV transfer vector. Both cDNA were under the control of the human cytomegalovirus (CMV) promoter. LV vectors were sequenced to verify the sequence and orientation of the inserts.

Lentiviral vectors were generated as described previously <sup>42</sup>. pRRLsin-PPThCMV-wpre, encoding either GArGFP, BDNF or GDNF (20 µg), the VSV-G envelope protein vector pMD.G.2 (7 µg) and the viral core-packaging construct pCMVdeltaR8.74 (13 µg) were co-transfected in 293T cells with Isocove's Modified Dulbecco's Medium (IMDM) containing 10% foetal calf serum (FCS), 100 U/ml penicillin/streptomycin (PS) and 2 mM glutamine. The next day, medium was refreshed and cells were incubated for another 24 h. Medium was harvested, spun at 176xg, the supernatant cleared through a 0.22 µm cellulose acetate filter and centrifuged at 80,000xg for 2.5 h. The pellet was resuspended in 0.1 M sodium phosphate buffer pH 7.4 in saline (PBS), aliquoted and stored at -80 °C. The titer of the LV-GArGFP vector stock was evaluated by infecting 293T cells upon serial dilution and determining the number of transducing units per ml (TU/ml), which was in the order of 10<sup>9</sup> TU/ml. In addition, viral vector stocks were titered by assay of p24 content (ng/ml) with an ELISA



(Perkin Elmer Nederland BV). The ratio between the TU/ml and p24 content of the LV-GArGFP stock was used to calculate relative TU/ml titers for the LV-BDNF and LV-GDNF stocks.

### *Biological activity of LV vector-derived neurotrophic factors*

The biological activity of BDNF and GDNF derived from LV vector-mediated transduced cells was assessed with a dorsal root ganglion (DRG) assay<sup>128</sup>. DRG neurite outgrowth of conditioned medium from LV-GArGFP-, LV-BDNF- and LV-GDNF-infected cells was expressed as percentage of control conditioned medium from mock-infected 293T cells.

### *Experimental animals and surgical procedure*

A total of 66 female Wistar rats (200-250 g; Harlan, Horst, the Netherlands) were used in this experiment. Animals were housed under standard conditions in a 12:12 h light/dark cycle with food and water ad libitum. Experimental handling and postoperative care were in accordance with the guidelines of the local committee for laboratory animal welfare and experimentation. Animals underwent a left-sided unilateral avulsion of three lumbar ventral roots (L4- L6) as described in detail previously<sup>150</sup>. Briefly, rats were anaesthetized using Hypnorm (Fentanyl/ Fluanisone; 0.08 ml/100 g body weight, i.m.; Janssen Pharmaceuticals, Beerse, Belgium) and Dormicum (Midazolam; 0.05 ml/100 g body weight s.c.; Roche, Almere, the Netherlands). Access to the ventral roots was obtained via a dorsal laminectomy (T12-L1) and opening of the dura mater. Ventral root attachment sites were used for final positive identification of L4, L5 and L6. By applying slight lateral traction with a pair of fine forceps on the root at the spinal cord exit site, avulsions were obtained directly at the surface of the spinal cord. The avulsed roots were either immediately reimplanted in the spinal cord or prior to reimplantation injected with 1  $\mu$ l of LV-GArGFP ( $10^6$  TU), LV-BDNF ( $2 \times 10^6$  TU) or LV-GDNF ( $2 \times 10^6$  TU) using a glass capillary with a 80  $\mu$ m diameter tip attached to a 10  $\mu$ l Hamilton syringe. For reimplantation a small pocket was made into the lateral spinal cord using the tip of a glass capillary approximately 1 mm above the L4, L5 and L6 avulsion sites. The three reimplanted roots were fixed in place with 2  $\mu$ l fibrin glue (TissueCol; Baxter B.V., Utrecht, the Netherlands) and covered by a piece of autologous fat tissue to prevent adhesion to the surrounding tissue. Paraspinous muscles and skin were closed in separate layers, animals were kept at 37°C until recovered and received Temgesic (buprenorphine 0.03 ml/100 g body weight s.c., Schering-Plough B.V., Maarsse, the Netherlands) for post-operative analgesia. This study was performed in two separate experimental series. The first series comprised 4 groups of 10 animals (implant, LV-GArGFP, LV-BDNF, and LV-GDNF; see figure 1C) of which functional recovery was evaluated during the 16 week survival time. At this

post-lesion time point, animals were sacrificed to study transgene expression as well as spinal motoneuron atrophy, motor axon re-innervation into the reimplanted roots and long distance regeneration to the sciatic nerve using *in situ* hybridization and immunohistochemistry. In a second series, the effect of LV-GDNF on axonal outgrowth and (motor) axon trapping was studied in more detail at 4 and 10 weeks survival times with LV-GArGFP-injected animals serving as controls (n=8 and 5 per time point for LV-GDNF and LV-GArGFP respectively).

After surgery, joints of the affected hind limb were manipulated daily to prevent contractures. Animals that displayed severe damage of the hind limb due to autotomy were promptly sacrificed; all remaining animals were included in each functional and histological analysis. Figure 1 provides a schematic overview of surgical procedures, treatment groups (including the number of animals per group) and survival times of the two experimental series.

#### *Assessment of recovery of hind limb function*

Avulsion of the lumbar ventral roots L4-6 results in a complete loss of left-sided spontaneous hind limb movement. After a two-week pre-operative training period, recovery of function was assessed at 4, 7, 9, 11 and 13 weeks post-operative with elements of the BBB open field test<sup>172</sup> that are relevant to the root avulsion model. Voluntary movement of the hip, knee and ankle joint was scored with 0, 1 or 2 for “no”, “slight” or “extensive” movement in each joint. Stepping and toe clearance were assessed and 0, 1, 2 or 3 points were scored if this occurred “never”, “occasionally”, “frequently” or “consistently”, respectively. Additional single points were given if plantar paw placement and weight support were observed, leading to a maximum cumulative score of 14 points for intact animals.

#### *Tissue processing and staining*

After 4, 10 or 16 weeks, animals were deeply anesthetized with sodium pentobarbital (Sanofi Sante, Maassluis, the Netherlands) and perfused transcardially with ice cold saline, followed by 4% PFA in PBS. The left sciatic nerve was dissected between the sciatic notch and the bifurcation into tibial and peroneal branches (7 cm distal from the implantation site). Segments of the lumbar spinal cords containing the implantation area were then dissected out under a microscope. Both nerves and spinal cords were post-fixed overnight in PFA/PBS at 4 °C. Spinal cords were then incubated overnight in 250 mM EDTA in PBS to soften possible residual bone debris. All tissue was finally cryoprotected in 25% sucrose in PBS at 4 °C for 3 days followed by embedding in OCT Compound 4583 (Tissue-Tek; Sakura, Zoeterwoude, the Netherlands), snap-freezing in 2-methylbutane and storage at -80 °C. Five series of 20 µm horizontal longitudinal spinal cord sections and transverse sciatic nerve sections were cut on a

cryostat, mounted on Superfrost Plus slides (Menzel-Gläser, Braunschweig, Germany) and stored at  $-80^{\circ}\text{C}$ .

#### *In situ hybridization*

Standard *in situ* hybridization was performed with digoxigenin(DIG)-labeled cRNA probes for BDNF or GDNF mRNA as described previously<sup>173</sup> on spinal cord tissue 16 weeks after surgery. Briefly, sections were post-fixed with 4% PFA in PBS for 20 min followed by acetylation and overnight incubation at  $60^{\circ}\text{C}$  using 200 ng/ml heat-denatured DIG-labeled cRNA probe in hybridization solution [5x standard saline citrate (SSC), 50% formamide, 5x Denhardt's, 125 mg/ml bakers yeast tRNA (Sigma, Zwijndrecht, the Netherlands)]. After stringency washes (5 min 5x SSC, 1 min 2x SSC, 30 min 0.2x SSC in 50% formamide all at  $60^{\circ}\text{C}$  and 5 min 0.2x SSC at room temperature) and blocking for 1 h in blocking reagent (Roche Nederland B.V., Almere, the Netherlands), sections were incubated with alkaline phosphatase-conjugated anti-DIG antibody (1:3000, Roche, Almere, the Netherlands) in TBS for 3 h. Enzyme activity was then visualized by overnight incubation with 300  $\mu\text{g}/\text{ml}$  nitroblue-tetrazolium and 170  $\mu\text{g}/\text{ml}$  5-bromo-4-chloro-indolyl phosphate in detection buffer (100 mM NaCl, 5 mM  $\text{MgCl}_2$ , 100 mM Tris/HCl pH 9.5), resulting in a dark purple precipitate. Sections were mounted in Aquamount solution (BDH Laboratory Supplies, Poole, England).

#### *In vivo transduction efficiency*

Transduction efficiency was determined by capturing tiled fluorescence images of longitudinal sections of LV-GArGFP injected root at 4 weeks. The distance between the most proximal and distal GArGFP transduced cells was subsequently measured using Image Pro Plus software. High magnification images were collected with a 40x objective from the center of the transduced area and the percentage of GArGFP positive nuclei was determined.

#### *GDNF, S100 and NF immunostaining*

Fluorescent double labelling to further analyze transgene protein expression was performed on nerve roots transduced with LV- GArGFP or LV-GDNF at 4, 10 and 16 weeks. Sections were washed three times in PBS and blocked in blocking buffer (PBS containing 5% FCS and 0.3% Triton X-100) for 1 h. Sections were then incubated overnight at  $4^{\circ}\text{C}$  in blocking buffer containing primary antibodies against GDNF (1:500; R&D systems, Minneapolis, MN, USA), against S100 to visualise Schwann cells (1:200; Dako, Glostrup, Denmark) or against NF(1:1000;  $\alpha$ -2H3; Developmental Studies Hybridoma bank, University of Iowa). The next day, sections were washed three times for 10 min in PBS and incubated for 2 h with biotin-conjugated or Cy3-conjugated secondary antibodies (1:400; Jackson ImmunoResearch Europe Ltd., Newmarket,

Suffolk, UK) in blocking buffer. Subsequently, sections were washed three times 10 min in PBS and incubated with Cy2-conjugated streptavidin and/or Hoechst (1 µg/ml; BioRad, Hercules CA) in blocking buffer for 30 min. After 3 washes in PBS, sections were mounted in Vectashield (Vector Laboratories, Burlingame, CA, USA). Specificity of the GDNF antibody was confirmed by absence of staining 1) on contralateral, non-injected nerve roots in a spinal cord section, 2) on LV-GArGFP injected roots, and 3) by omission of the primary antibody.

#### *ChAT motoneuron staining.*

Although choline acetyl transferase (ChAT) is temporarily downregulated, it stains motoneurons reliably when used beyond 4 weeks after root avulsion<sup>168</sup>. Therefore, ChAT immunohistochemical staining was performed to label motoneurons and their axons on spinal cords and sciatic nerve sections according to Blits et al.<sup>24</sup>. This staining protocol starts with a 10 min 0.1% Triton-X100 and 0.01mg/ml proteinase K in PBS treatment and an overnight 50% formamide treatment at 55 °C for antigen retrieval followed by standard immunohistochemistry as described above with primary anti ChAT (1:200; ChAT pAb, AB144P, Chemicon, Hampshire, UK). For spinal cord sections, the primary antibody incubation was followed by biotinylated horse anti-goat 1:300, stained with 0.035% 3, 3'-diaminobenzamidine tetrahydrochloride (DAB) in TBS containing 0.01% H<sub>2</sub>O<sub>2</sub> and 0.2 mg/ml (NH<sub>4</sub>)<sub>2</sub>.SO<sub>4</sub>.NiSO<sub>4</sub>, resulting in a dark purple precipitate. Sections were dehydrated in graded series of ethanol, cleared in xylene and embedded in Entellan for quantitative light microscopic analysis. For sciatic nerve sections, the primary antibody was followed by Cy3-conjugated donkey anti goat 1:400 (Jackson ImmunoResearch Europe Ltd.) and embedding in Aquamount solution for fluorescent quantification of axons.

#### *Quantification of total motoneuron volume and soma size distribution*

Severe atrophy of motoneurons can hamper the accurate quantification of surviving motoneurons (e.g., when nuclear condensation clouds the presence of nucleoli). Whereas some authors discard structures with a diameter <30 µm when counting motoneurons<sup>174</sup>, others show that motoneurons that have seemingly died can re-appear after a second axotomy, indicating that severe atrophy can easily be mistaken for cell death<sup>153</sup>. To avoid this issue and to quantify the atrophy of motoneurons objectively and systematically, we used automated quantification of all ChAT positive structures (≈3000 structures per animal) to calculate the total volume of the affected motoneuron pool.

To this end, high-resolution tiled digital images were captured of a series of ChAT-stained spinal cord sections at an interval of 200 µm. These images were imported in Image Pro Plus software and the entire motoneuron pools (i.e., areas containing ChAT

positive cells) of the root avulsion-affected side and contralateral (control) side were manually outlined. The motoneurons inside the motoneuron pool were then automatically segmented with a filter algorithm. The total volume of both the affected and the contralateral motoneuron pool was calculated for each animal by interpolating the total measured surface area per section to the distance between sections (200  $\mu\text{m}$ ). This volume was expressed as a percentage of the contralateral side. The soma sizes on both sides of the spinal cord were pooled for all animals in an experimental group and the frequency histogram calculated in area intervals of 300  $\mu\text{m}^2$ .

#### *Evaluation of ChAT fiber appearance and density in implanted ventral roots*

The implanted ventral roots were studied on ChAT stained sections at 4, 10 and 16 weeks by an observer blinded to treatment group. At 4 weeks, the density of axons entering the implanted root was quantified in non-avulsed, LV-GArGFP injected and LV-GDNF injected roots (n=5 per group). Three high resolution tiled images per animal were collected spanning the width of the root directly distal to the implantation site. A reference-line was drawn in Image Pro Plus software perpendicular to the implanted root. All axons crossing this line were counted manually by two investigators blinded to treatment. Furthermore, the temporal occurrence of aberrant fiber growth was studied. The presence or absence of specific areas with a high density of fibers with a longitudinal orientation (“strands”) and areas with a large number of fibers with a circular orientation (“coils”) was scored within each treatment group.

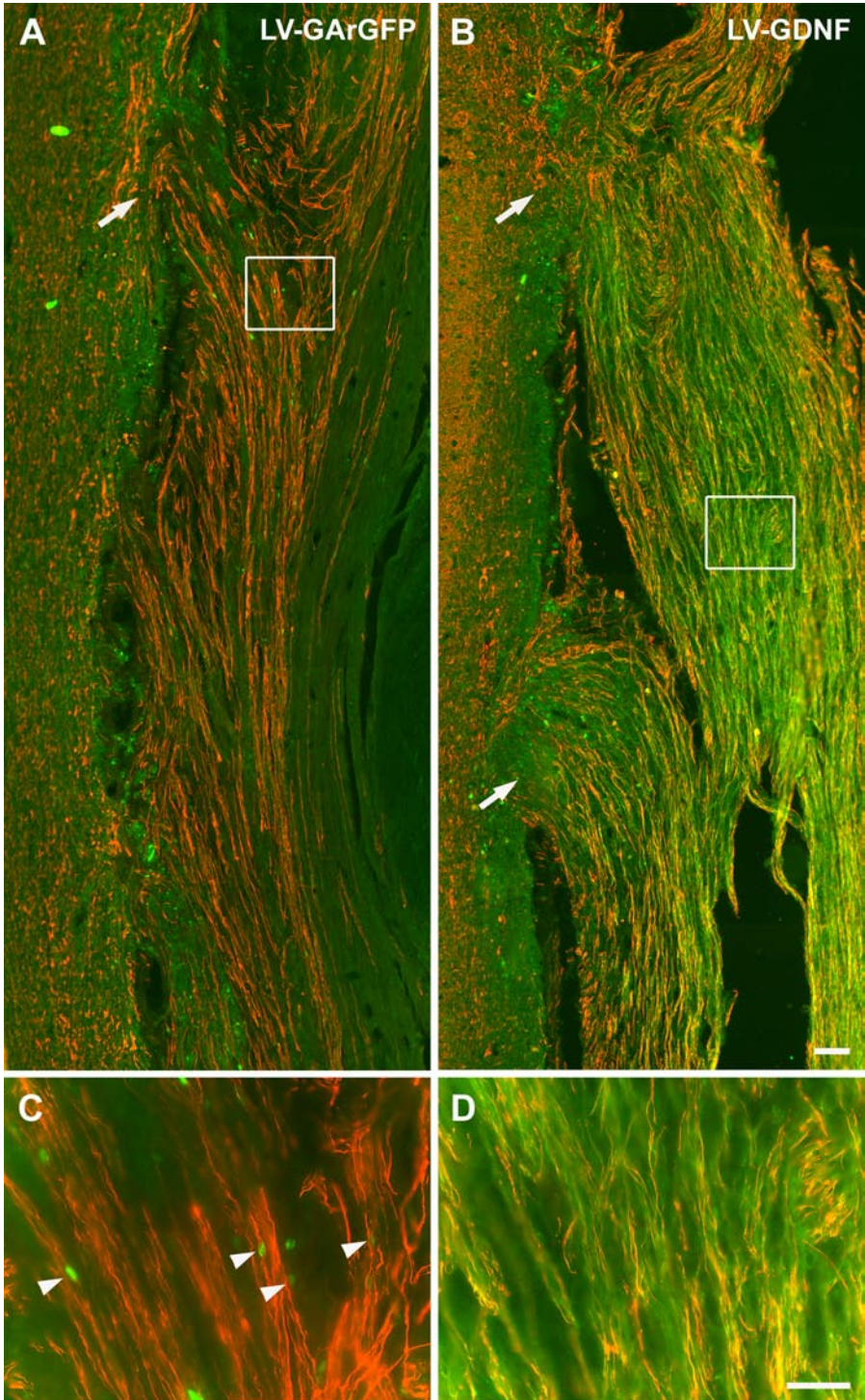
#### *Evaluation of Schwann cell density in nerve roots*

Schwann cell density was calculated in nerve roots from the “implant”, LV-BDNF and LV-GDNF groups at 16 weeks. Sections were stained for NF, S100 and Hoechst as described above. The root was outlined and if nerve coils were present (in LV-GDNF treated animals), these coils were outlined separately based on NF immunohistochemical staining. The area covered by Hoechst-labelled nuclei was calculated as a proportion of the outlined area to create a measure of cell density with an ImagePro filter algorithm based on Hoechst signal.

#### *Quantification of motor axon number and diameter in the sciatic nerve*

To quantify the number of motor axons 7 cm distal from the implantation site, images of ChAT immunofluorescence-stained transversal sciatic nerve sections were captured using an LSM410 Zeiss confocal laser scanning microscope. Equal settings for detector gain, offset and pinhole were used to acquire each image. The surface area of the sciatic nerve was calculated using a 10x objective. Subsequently, 4 random samples in this surface area were captured with a 40x objective, covering approximately 50% of the total surface area. These were used to determine the total motor axon number





and diameter with a custom-made segmentation tool on Image Pro Plus software. Finally, distribution histograms of axon diameter were made with diameter intervals of 0.25  $\mu\text{m}$ .

### *Statistical analysis*

Analysis for statistical difference between groups was performed using SPSS software (version 12.0; SPSS, Chicago, IL). One-way analysis of variance (ANOVA) followed by post-hoc Bonferroni test was performed on DRG outgrowth, motoneuron soma volume, Schwann cell density and total sciatic nerve fibers. Nonparametric analysis was performed on fiber density in implanted roots, motoneuron volume and sciatic fiber distributions using Kruskal-Wallis followed by Mann-Whitney U test. Coil formation in the ventral root was examined using a Pearson Chi-Square test. Data were considered statistically significant if  $p < 0.05$ .

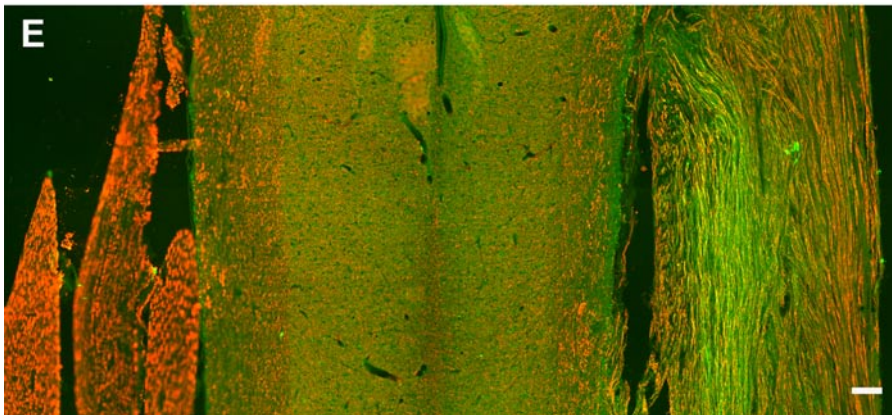
**Supplemental figure 1** GDNF is present in LV-GDNF transduced roots at 4 weeks, but not in LV-GArGFP injected or intact roots.

Immunohistochemistry for GDNF (green) and NF (red) on longitudinal spinal cord sections at the site of root reimplantation (arrows) for LV-GAr-GFP (A) and LV-GDNF (B) injected roots. No GDNF staining is visible in the LV-GAr-GFP injected root, whereas the injection of LV-GDNF leads to diffuse, strong GDNF staining in the entire root.

(C) High magnification images of boxed areas in (A) and (B). Numerous fluorescent green nuclei are present in the LV-GAr-GFP injected nerve roots (arrowheads) (C), but diffuse GDNF staining is absent. Strong, diffuse GDNF staining is present in a LV-GDNF injected root (D) and is closely associated with regenerating nerve fibers (red)

(E) Overview of the spinal cord of a LV-GDNF injected animal. GDNF staining (green) is present in the LV-GDNF injected root (right), but not in the contralateral (left) intact nerve root or within the spinal cord. NF positive axons (red) are thicker and straighter in the intact side than in the reimplanted root.

Scale bars ABE 100  $\mu\text{m}$ ; CD 50  $\mu\text{m}$ .







# Chapter 6

## Differential effects of lentiviral vector-mediated overexpression of NGF and GDNF on regenerating sensory and motor axons in the transected peripheral nerve

Martijn R Tannemaat, Ruben Eggers, William T Hendriks, Godard CW de Ruiter, Joop J van Heerikhuizen, Chris W Pool, Martijn JA Malessy, Gerard J Boer, Joost Verhaagen

*European Journal of Neuroscience (in press)*

### Abstract

Even after reconstructive surgery, major functional impairments remain in the majority of patients with peripheral nerve injuries. The application of novel emerging therapeutic strategies such as lentiviral (LV) vectors may help to stimulate peripheral nerve regeneration at a molecular level.

In the experiments described here, we examined the effect of LV vector-mediated overexpression of nerve growth factor (NGF) and glial cell-line derived neurotrophic factor (GDNF) on regeneration of the rat peripheral nerve in a transection/repair model *in vivo*.

We show that LV vectors can be used to locally elevate levels of NGF and GDNF in the injured rat peripheral nerve and this has profound and differential effects on regenerating sensory and motoneurons. For sensory neurons, increased levels of NGF and GDNF do not affect the number of regenerated neurons 1 cm distal to a lesion at 4 weeks post-lesion, but cause changes in the expression of markers for different nociceptive populations of neurons. These changes are accompanied by significant alterations in the recovery of nociceptive function. For motoneurons, overexpression of GDNF causes trapping of regenerating axons, impairing both long distance axonal outgrowth and reinnervation of target muscles, whereas NGF has no effect on these parameters.

These observations show the feasibility of combining surgical repair of the transected nerve with the application of viral vectors. Furthermore, they show a difference between the regenerative response of motor and sensory neurons to locally increased levels of NGF and GDNF.

### Introduction

Peripheral nerve injuries cause sensory and motor impairments of the affected limb. At present, the only treatment strategy for severe nerve lesions is microsurgical repair, but even then, major functional impairments remain in the majority of patients<sup>1</sup>. Future advances in the treatment of peripheral nerve injuries are likely to benefit from

the improved understanding of the effect of neurotrophic factors on regeneration. Schwann cells in the nerve distal to the injury express a range of neurotrophic factors<sup>9,77</sup> and several of these are differentially expressed in Schwann cells from sensory and motor nerves<sup>12</sup>. Two neurotrophic factors, nerve growth factor (NGF) and glial cell-line derived neurotrophic factor (GDNF) may be particularly important for peripheral nerve regeneration for several reasons.

First, nociceptive sensory neurons in the dorsal root ganglion (DRG) can be divided in two functionally distinct populations that are either sensitive to NGF or GDNF<sup>175</sup>. Peptidergic DRG neurons<sup>176</sup> express the receptor for NGF, tropomyosin receptor kinase A (trkA) and respond to NGF<sup>177,178</sup>. Non-peptidergic nociceptive neurons express a cell surface glycoconjugate that binds the *Griffonia Simplicifolia* isolectin B4 (IB4)<sup>179</sup>. These IB4-binding neurons express the receptor complex for GDNF, GFR $\alpha$  and ret<sup>180,181</sup>. In contrast to peptidergic neurons, IB4-binding neurons regenerate poorly after peripheral nerve transection<sup>182</sup>.

Second, NGF and GDNF have both been implicated in the regeneration of motoneurons<sup>9</sup>. NGF added to fibrin sealant increases the number of regenerated motoneurons in the transected rat sciatic nerve<sup>18</sup>. GDNF prevents the atrophy<sup>183</sup> and enhances the regeneration<sup>21</sup> of chronically axotomised motoneurons.

Finally, NGF is specifically upregulated in Schwann cells from sensory nerves, whereas the expression of GDNF is more pronounced in Schwann cells from motor nerves<sup>12</sup> and the application of these factors could therefore have differential effects on the regeneration of sensory and motoneurons.

The exogenous application of various neurotrophic factors has resulted in relatively small and variable effects on regeneration of the injured peripheral nerve<sup>18,20,184</sup>. The continuous and effective delivery of neurotrophic factors is difficult, as these proteins do not diffuse easily into nervous tissue and have a short half-life<sup>32</sup>. Recent work has demonstrated that lentiviral (LV) vectors can direct long-term, local transgene expression in Schwann cells *in vivo*<sup>150</sup>. In the experiments described here, we studied the effect of LV vector-mediated overexpression of NGF and GDNF on regeneration of the rat peripheral nerve *in vivo*. Specifically, we sought to compare the regenerative response of sensory and motoneurons and to examine the regeneration of distinct populations of nociceptive sensory neurons.

## Materials and Methods

### *Lentiviral vector preparation*

The production of LV vectors encoding NGF and GDNF and the biological activity of the neurotrophic factors derived from these vectors has been described previously,<sup>90,183</sup>. The control vector was LV-GArGFP, which expresses green fluorescent protein (GFP) fused to a Gly-Ala repeat (GAr) and was produced according to Hendriks et al.<sup>150</sup>. The

Gly-Ala repeat prevents a GFP-mediated cytotoxic T-lymphocyte immune response<sup>170</sup>, resulting in long term expression of this foreign protein in the peripheral nerve<sup>150</sup>.

The titers of the LV vector stocks were determined as follows. The LV-GArGFP stock titer was 1) evaluated by infecting 293T cells upon serial dilution to determine the number of transducing units per ml (TU/ml) and 2) by determining the p24 content (ng/ml) with an ELISA (Perkin Elmer, The Netherlands). The ratio between the TU/ml and p24 content of the LV-GArGFP stock was used to calculate relative TU/ml titers for the LV-NGF and LV-GDNF stocks on the basis of their p24 content. Final titers were  $2 \times 10^9$  TU/ml for LV-GArGFP and  $7 \times 10^9$  TU/ml for both LV-NGF and LV-GDNF. All experiments described in this paper were performed using the same vector stocks.

### *Experimental animals and surgical procedure*

A total of 96 female Wistar rats (200-250 g; Harlan, Horst, the Netherlands) were used. Animals were housed under standard conditions in a 12:12 h light/dark cycle with food and water ad libitum. Experimental handling and postoperative care were in accordance with the guidelines of the local committee for laboratory animal welfare and experimentation.

#### SURGERY AND VECTOR INJECTION

The left sciatic nerve was exposed through a gluteal muscle-splitting incision, transected using microsurgery scissors and immediately repaired with four epineurial 10-0 nylon sutures (Ethilon, Johnson & Johnson, Amersfoort, The Netherlands) under an operating microscope (figure 1A). A reference group received no further experimental treatment (repair only). For animals in the vector injection groups, 3  $\mu$ l containing  $6 \times 10^6$  TU (LV-GArGFP) or  $2 \times 10^7$  TU (LV-NGF and LV-GDNF) of the vector solution was then injected in the distal peroneal and tibial branches of the sciatic nerve using a glass capillary with an 80  $\mu$ m diameter tip attached to a 10  $\mu$ l Hamilton syringe. Fast green (Sigma, Zwijndrecht, the Netherlands) was added in a 0.1% concentration to the vector solution to visualize vector spread during injection (figure 1B). The skin was closed, after which the animals received Temgesic [buprenorphine 0.03 ml/100 g body weight s.c., (Schering-Plough B.V., Maarsse, the Netherlands)] for post-operative analgesia and were kept at 37°C until complete recovery from anaesthesia.

#### EXPERIMENTAL SERIES

Table 1 shows the experimental groups, survival times, animal numbers used and measurements performed. Briefly, transgene expression was quantified in series 1 of these experiments (n=18, survival 4 weeks), regeneration of sensory and motoneurons was evaluated in series 2 (n=32, retrograde tracing at 4 weeks, 5 weeks survival), and series 3 was used for additional histology at the level of the sciatic nerve (n=18, survival 4 weeks). Since no differences were found in any of the previous experiments

between the “repair only” and LV-GArGFP control groups, no “repair only” group was included in this third series. Functional recovery was finally evaluated in series 4 (n=29, survival 12 weeks)

#### *Quantification of transgene expression*

Transgene expression was evaluated 4 weeks after surgery in series 1. Fresh sciatic nerves were harvested at 4 weeks (after decapitation) and cut into four segments of 1 cm each, with 2 segments on either side of the repair site. These segments were snap-frozen on dry-ice and stored at  $-80^{\circ}\text{C}$  until further use. To quantify the amount of NGF and GDNF, the frozen nerve segments were ground with a mortar on dry-ice, suspended in 250  $\mu\text{l}$  suspension buffer containing 137 mM NaCl, 20 mM Tris/HCl pH 8.0, 10% glycerol, 0.1% Tween-20, 0.5 mM sodium orthovanadate 1% Nonidet P40 substitute (Applichem, Darmstadt, Germany) and Complete protease inhibitor (1 tablet/50 ml, Roche, Mannheim, Germany), further homogenised with an ultra-turrax (IKA-Labortechnik, Staufen, Germany) for 30 s, centrifuged and the supernatant stored in 50  $\mu\text{l}$  aliquots at  $-20^{\circ}\text{C}$ . The concentration of NGF and GDNF was measured using ELISA kits (#G7630 and #G7620; Promega, Madison, USA) according to the manufacturer’s instructions and used to calculate total content in pg/cm nerve segment. The detection limit was 31 and 62 pg/cm for NGF and GDNF respectively.

#### *Quantification of regeneration and sensory neuron size*

Retrograde tracing was performed to quantify the number of sensory and motoneurons that had extended a neurite 1 cm across the transection site (series 2). Four weeks after transection, repair and vector injection, rats underwent surgery to expose the sciatic nerve. The sciatic nerve was cut 1 cm distal from the repair site and the proximal end was placed in the cap of a small Eppendorf tube containing 3  $\mu\text{l}$  5% Fast Blue (FB) (EMS-Chemie, Gross-Umstadt, Germany) in saline. The cut nerve end was completely immersed in FB for 30 min followed by three saline washes. Animals were allowed to recover, again as described above. After allowing one week for retrograde transport of the tracer, animals were deeply anesthetized with sodium pentobarbital (Sanofi Sante, Maassluis, the Netherlands) and perfused transcardially with ice-cold saline, followed by 4% paraformaldehyde in 0.1 M sodium phosphate buffer pH 7.4 (PFA). Subsequently the L4, L5 and L6 DRGs as well as the lumbar section of the spinal cord were removed and post-fixed overnight in PFA at  $4^{\circ}\text{C}$ . All tissue was cryoprotected in 25% sucrose in 0.1 M sodium phosphate-buffered saline pH 7.4 (PBS) at  $4^{\circ}\text{C}$  for 3 days followed by embedding in OCT Compound 4583 (Tissue-Tek; Sakura, Zoeterwoude, the Netherlands), snap-freezing in 2-methylbutane and storage at  $-80^{\circ}\text{C}$  until further use. Two series of 20  $\mu\text{m}$  horizontal longitudinal spinal cord and four series of 20  $\mu\text{m}$  DRG sections were cut on a cryostat, mounted on Superfrost Plus slides (Menzel-

**Table 1** Experimental groups, survival times, animal numbers and measurements in the experiments described in this paper. (\*) Some animals were lost during the experiment due to autotomy. The number in parentheses indicates the number of animals included in functional and/or histological analysis. (\*\*) Retrograde tracing was performed 4 weeks after transection and repair. Animals were euthanized one week later to allow tracer uptake.

| Series | Intervention | Weeks   | # Animals* | Measurement  |
|--------|--------------|---------|------------|--|
| 1      | repair only  | 4       | 5 (5)      | Quantification of NGF and GDNF expression:<br><i>ELISA</i>   |
|        | LV-GArGFP    |         | 6 (5)      |  |
|        | LV-NGF       |         | 3 (3)      |  |
|        | LV-GDNF      |         | 3 (3)      |  |
| 2      | repair only  | 4 (5**) | 8 (8)      | Quantification of regeneration:<br><i>retrograde tracing 1 cm distal from repair site</i>                    |
|        | LV-GArGFP    |         | 8 (7)      |  |
|        | LV-NGF       |         | 8 (8)      |  |
|        | LV-GDNF      |         | 8 (8)      |  |
| 3      | LV-GArGFP    | 4       | 6 (6)      | Histology: <i>transgene expression, motoneuron staining, neurite outgrowth 1 cm distal from repair site</i>  |
|        | LV-NGF       |         | 6 (4)      |  |
|        | LV-GDNF      |         | 6 (5)      |  |
| 4      | repair only  | 12      | 6 (6)      | Motor reinnervation: <i>target muscle weight</i><br>Nociceptive sensory reinnervation: <i>footflick test</i> |
|        | LV-GArGFP    |         | 8 (7)      |  |
|        | LV-NGF       |         | 7 (6)      |  |
|        | LV-GDNF      |         | 8 (7)      |  |

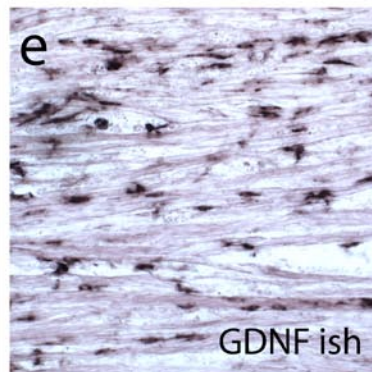
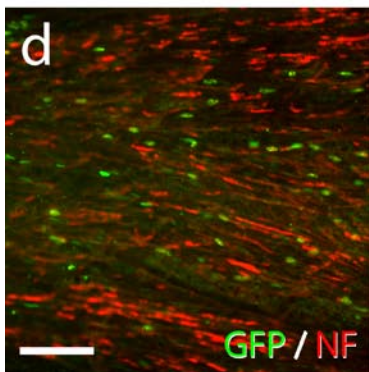
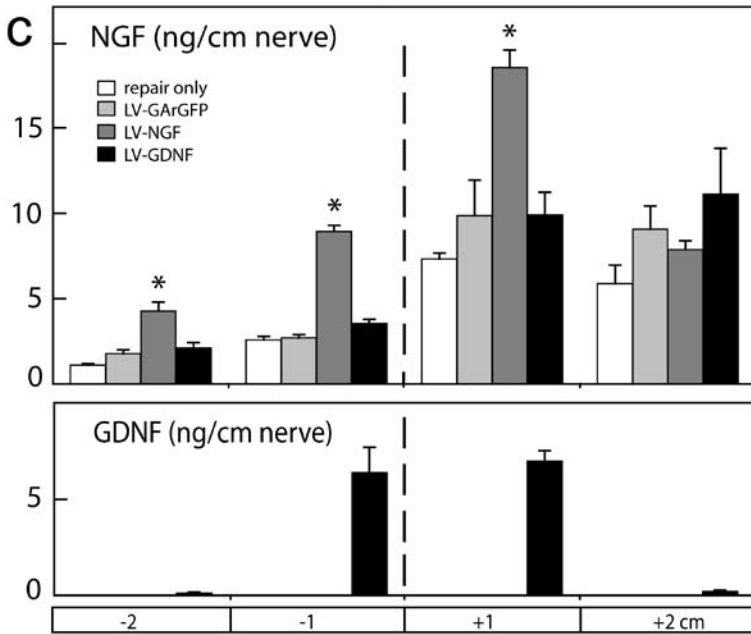
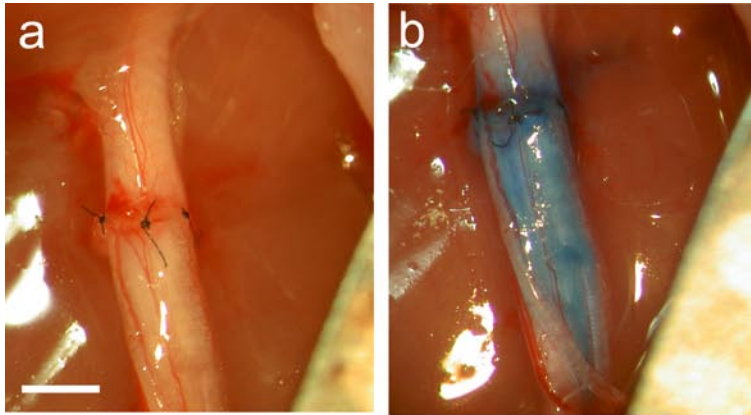
Gläser, Braunschweig, Germany) and stored at  $-80^{\circ}\text{C}$ .

#### MICROSCOPIC QUANTIFICATION OF REGENERATED NEURONS

All FB-labelled neurons containing a visible nucleus were microscopically counted on one series (out of two) of spinal cord sections and one series (out of four) of DRG sections using a Zeiss Axioplan 2 microscope. To compensate for duplicate counts of partially cut nuclei, the Abercrombie correction factor [nuclear diameter/(nuclear diameter + section thickness)] was applied to these neuron counts to calculate the number of regenerated neurons per animal<sup>185</sup>. To measure the nuclear diameter in FB-labelled cells for each animal, these visually counted sections were also photographed with an Evolution QEi digital camera (MediaCybernetics, Silverspring USA) using Image-Pro Plus software (version 6.2, MediaCybernetics, Silverspring USA).

#### AUTOMATED SEGMENTATION OF FB-LABELLED DRG NEURON PROFILES

A filter algorithm was developed with Image-Pro Plus software to identify all FB-labelled profiles and measure the diameter on all photographed DRG sections. The number of these profiles correlated strongly with the number of neurons that were counted microscopically on the same sections ( $R^2=0.94$ ). The generated profiles were plotted in a frequency distribution histogram with diameter intervals of  $4\ \mu\text{m}$  and the average profile diameter was determined in each animal.



*Regeneration of different nociceptive sensory neuron phenotypes*

The second and third set of L4, L5 and L6 DRG sections from the retrogradely traced animals of series 2 were used respectively to stain peptidergic nociceptive neurons with antibodies against calcitonin gene-related peptide (CGRP) (rabbit anti-CGRP, 1:2000; Millipore, Billerica, USA) and non-peptidergic nociceptive neurons with biotinylated IB4 (*Griffonia Simplicifolia* IB4, 1:250, Vector laboratories, Burlingame, USA). Staining procedures of glass-mounted sections were performed as described previously<sup>90</sup>. Briefly, sections were rinsed three times in 0.1 M Tris/HCl-buffered saline pH 7.4 (TBS), incubated in TBS containing 0.3% Triton X-100 and 5% fetal bovine serum (blocking buffer) for 1 h and in blocking buffer containing the primary antibody overnight at 4°C. The next day, sections were washed three times in TBS and incubated for 2 h with blocking buffer containing either Alexa594-labelled secondary antibodies or streptavidin (Invitrogen, Carlsbad, USA). Finally, the sections were washed in TBS, mounted in Aquatex (Merck, Darmstadt, Germany) and coverslipped. To minimize staining variability, DRG sections from control and vector-treated animals were stained in the same staining session. Six randomly selected sections per animal (n=3 for both the L4 and L5 DRG) were photographed as described above with identical microscope and camera settings for all sections to assess CGRP and IB4 staining intensity of the retrogradely labelled FB positive sensory neurons. With the filter algorithm mentioned above, IB4 and CGRP staining intensity was measured in all FB-labelled profiles. Because of the established strong correlation between automatically segmented profiles and manually counted neurons, these data could be used to calculate the number of double-labelled DRG neurons per animal.

**Figure 1** Surgical procedures and transgene expression.

- a) Photograph of rat sciatic nerve after complete transection and repair with four 10-0 microsutures.
  - b) Directly after repair, 3 µl fluid volume containing viral vector and 1% fast green (to visualise vector spread) was injected approximately 5 mm distal from the repair site.
  - c) Four weeks after transection, NGF protein levels are elevated in the distal stump resulting in a gradient across the repair site. The injection of LV-NGF leads to a twofold increase in NGF levels, while the NGF gradient across the repair site remains intact. The application of LV-GDNF has no effect on NGF levels. GDNF protein levels are undetectable in all except the LV-GDNF treated animals. The injection of LV-GDNF leads to an increase in GDNF levels similar to the increase in NGF found after the application of LV-NGF.
  - d) Numerous GAR GFP positive nuclei (green) are present in the nerve, 4 weeks after vector application. Transduced cells are located within the nerve fascicles, in close proximity to neurofilament-positive nerve fibers (red).
  - e) *In situ* hybridisation shows many cells containing GDNF mRNA (black) in a pattern highly similar to the GAR GFP-transduced cells in panel d.
- Scale bar: 1 mm (AB), 100 µm (DE).



*Transgene expression and neurite sprouting*

In series 3, 18 animals were operated and injected with LV vector as described above (without the “repair only” group). After 4 weeks, animals were euthanized and perfused transcardially with PFA and the sciatic nerve was removed, postfixed and stored at  $-80^{\circ}\text{C}$  as described above. Five series of  $20\ \mu\text{m}$  thick, longitudinal cryostat sections were cut, covering a segment from 5 mm proximal to 1 cm distal to the repair site. Immunohistology was performed on the first series of sections with antibodies against GFP (1:4000, Abcam, Cambridge, UK) to stain GArGFP-transduced cells and against neurofilament (1:1000; 2H3; Developmental Studies Hybridoma bank, Iowa City, USA) to stain axons using the procedures described above.

*In situ* hybridization was performed on the second series to detect GDNF mRNA using probes and procedures described previously<sup>25</sup>. Briefly, sections were post-fixed with PFA for 20 min followed by acetylation and overnight incubation at  $60^{\circ}\text{C}$  using 200 ng/ml heat-denatured DIG-labeled cRNA probe in hybridization solution [5x standard saline citrate (SSC), 50% formamide, 5x Denhardt's, 125 mg/ml bakers yeast tRNA (Sigma, Zwijndrecht, the Netherlands)]. After stringency washes (5 min 5x SSC, 1 min 2x SSC, 30 min 0.2x SSC in 50% formamide all at  $60^{\circ}\text{C}$  and 5 min 0.2x SSC at room temperature) and blocking for 1 h in blocking reagent (Roche Nederland B.V., Almere, the Netherlands), sections were incubated with alkaline phosphatase-conjugated anti-DIG antibody (1:3000, Roche, Almere, the Netherlands) in TBS for 3 h. Enzyme activity was then visualized by overnight incubation with 300  $\mu\text{g}/\text{ml}$  nitroblue-tetrazolium and 170  $\mu\text{g}/\text{ml}$  5-bromo-4-chloro-indolyl phosphate in detection buffer (100 mM NaCl, 5 mM  $\text{MgCl}_2$ , 100 mM Tris/HCl pH 9.5), resulting in a dark purple precipitate.

On the third series, axons of motoneurons were stained with antibodies against choline acetyl transferase (ChAT) (1:200; AB144P, Millipore, USA) as described previously<sup>24</sup>. Alexa 594-labeled antibodies (Invitrogen, Carlsbad, USA) were used as secondary antibodies as described above.

From the same nerve pieces,  $20\ \mu\text{m}$  thick transverse sections were cut 1 cm distal from the repair site to evaluate sprouting of regenerated neurites. These sections were stained with primary antibodies against neurofilament (2H3) using Alexa 594-labeled secondary antibodies. Three random fields were captured with an LSM410 Zeiss confocal laser scanning microscope and a filter algorithm was applied to determine by the number of neurofilament positive axons per area. This number was multiplied with the total cross-sectional area of the nerve (calculated with Image-Pro Plus software) to determine the total number of axons in the distal nerve stump 1 cm from the repair site at 4 weeks.

*Functional evaluation*

## NOCICEPTIVE SENSORY REINNERVATION

In series 4, return of nociceptive sensory function was evaluated by applying an elec-

tric stimulus to the lateral foot sole<sup>186</sup>. In healthy rats, a current of 0.1 mA elicits a prompt withdrawal response, whereas transection of the sciatic nerve results in the complete absence of any reaction. Animals were tested weekly, the minimal current (up to 0.5 mA to prevent tissue damage) needed to elicit a response was noted and expressed as percentage of pre-operative value (0% for no reaction at 0.5 mA to 100% for a withdrawal reaction at 0.1 mA). Testing was discontinued at 7 weeks, when the withdrawal response had returned to pre-operative levels in all animals.

#### TARGET MUSCLE WEIGHT

Twelve weeks after transection/repair, animals from series 4 were perfused with 4% PFA as described above, and the soleus and gastrocnemius muscles were dissected bilaterally. The weight of these muscles was regarded as a measure of return of functional reinnervation by motoneurons<sup>187</sup>. Weights were expressed as percentage of the same muscles on the contralateral side.

#### ANALYSIS OF AUTOTOMY BEHAVIOUR

Because overexpression of NGF and GDNF may affect autotomy behaviour<sup>19,184</sup>, autotomy was analyzed daily in all four experimental series. The degree of autotomy of the left hind paw was scored using a 0-5 point scale<sup>188</sup>. A score of 0 corresponds to a normal undamaged hind paw, 1 to nails nibbled, damaged or removed, 2 to one digit bitten upon or loss of up to one-third of the digit, 3 to one or two digits bitten upon or loss of one-third and one-half, 4 to one or two digits lost to more than 50% and 5 to more digits chewed upon or completely lost. Animals that reached an autotomy score of 5 were promptly euthanized (total n=8; repair only n=0, LV-GArGFP n=3, LV-NGF n=3, LV-GDNF n=2) and excluded from all functional and histological data analyses, except analysis of autotomy scores. Instead of using the average autotomy score at each time point (which may have biased the analysis due to the prompt sacrifice of animals with a score of 5), we used the maximum score achieved by each animal (n=96) to analyze differences in autotomy scores between groups.

#### *Statistical analysis*

Analysis for statistical differences between groups was performed using SPSS software (version 12.0; SPSS, Chicago, IL). Nonparametric analysis was performed on autotomy scores using Kruskal-Wallis followed by Mann-Whitney U test. Two-way analysis of variance (ANOVA) was performed on the nociceptive function test. One-way ANOVA was performed on all other data. When significant differences were found, ANOVAs were followed by post-hoc Bonferroni testing. Data were considered statistically significant if  $p < 0.05$ . In each case where the application of LV-NGF or LV-GDNF caused statistically significant differences compared to the “repair only” control, they were also significant compared to the LV-GArGFP control group.

## Results

### *Transgene expression*

In series 1, the levels of NGF and GDNF following application of LV-NGF and LV-GDNF (figure 1A) were determined and compared to endogenous levels after sciatic nerve transection and repair. The peroperative spread of viral vector was monitored with Fast Green and was typically observed from the repair site to approximately 1 cm distal (figure 1B). In control animals, endogenous NGF levels were significantly elevated in the 1 cm segments directly distal from the repair site (7-10 ng vs. ~3 ng proximally; figure 1C). The application of LV-NGF led to an increase in NGF levels from 2 cm proximal to 1 cm distal to the repair site (LV-NGF vs “repair only”,  $p=0.004$ ). The NGF levels were highest in the first 1 cm distal from the repair site, thereby increasing the NGF gradient across the lesion site as compared to the control intervention. No GDNF could be detected at the repair site of the nerve in control animals (detection threshold 62 pg/cm nerve segment), but the application of LV-GDNF led to high levels of GDNF in the range of 6-7 ng/cm directly proximal and distal from the repair site (figure 1C). In conclusion, both NGF and GDNF levels were elevated around the lesion and repair site. Importantly, the application of LV-NGF did not significantly influence GDNF levels and vice versa.

Immunohistochemistry on longitudinal sections (series 3) showed numerous cells with GAR GFP positive nuclei in close association with neurofilament positive axons in all LV-GAR GFP-injected animals (figure 1D). These cells could be found both distal and proximal from the transection and repair site, with the highest number of GAR GFP positive cells near the repair site. Similarly, *in situ* hybridization for GDNF showed numerous positive cells in all LV-GDNF-injected animals, within the nerve fascicles in a pattern similar to that of the GAR GFP positive cells (figure 1E). No GDNF mRNA was detectable in sections of control peripheral nerve (results not shown). Although the diffusion of vector particles may have contributed to the transduction of Schwann cells proximal from the transection/repair site, the elevated NGF/GDNF levels more than 1 cm proximal from the injection site suggests the migration of some transduced cells in a proximal direction as described previously<sup>189,190</sup>.

### *The effect of LV-NGF and -GDNF on peripheral nerve regeneration*

Subsequently, the effect of overexpression of NGF and GDNF in the injured peripheral nerve on regeneration was studied. To quantify the number of sensory neurons and motoneurons with a regenerated axon that reached at least 1 cm distal from the repair site at 4 weeks a retrograde tracing experiment was performed.

#### REGENERATION OF SENSORY NEURONS

The total number of FB positive, i.e., regenerated sensory neurons in the L4, L5 and L6 DRGs was not significantly different between the groups, and ranged from 6200

for the “repair only” control group to 7500 in the LV-GArGFP control group, with the averages for the LV-NGF and LV-GDNF groups ranging between these values (figure 2A). Thus, increased levels of NGF or GDNF at the repair site of the transected rat sciatic nerve do not result in a significant change in the number of regenerated sensory neurons at one month post-injury.

#### REGENERATION OF MOTONEURONS

In the “repair only”, the LV-GArGFP-injected and the LV-NGF-injected groups similar numbers of motoneurons were retrogradely labelled with FB at 4 weeks following transection and repair. The numbers of FB-labelled neurons ranged from approximately 900-1100 per animal (figure 2B). Strikingly, the application of LV-GDNF led to a strong and significant decrease in the number of regenerated motoneurons to an average of 300 per animal ( $p=0.000011$ ). Retrograde tracing thus showed that the majority of regenerating motoneurons were unable to extend an axon 1 cm distal from the repair site after local LV vector-mediated overexpression of GDNF.

To determine the fate of transected, regenerating motor axons, we performed a ChAT staining on longitudinal sections of the repaired nerve. In the LV-GArGFP (control) and LV-NGF groups, most regenerating ChAT positive motor fibers were oriented longitudinally within the section. In contrast, in all LV-GDNF-treated animals, the nerve contained high densities of chaotically oriented motor axons (figure 2). These “axon coils” were particularly evident at or near the repair area, which corresponds to the area with significantly increased GDNF mRNA and protein expression as determined in series 1 (figure 1). The decreased number of distally regenerated axons after the injection of LV-GDNF is apparently the result of trapping of motor axons in areas of the nerve that contain high levels of transgenic GDNF.

#### *LV-NGF and -GDNF cause hypertrophy of sensory neurons*

Both NGF and GDNF cause a marked hypertrophy of unlesioned sensory neurons<sup>191</sup>. To determine whether they have a similar effect on the size of regenerating sensory neurons, we developed a filter algorithm to automatically segment all FB-labelled profiles in the DRG and calculate their diameter in every fourth section (figures 3AB). When the relative proportion of cell profile diameters was plotted in a distribution histogram, a clear shift towards bigger profiles was visible in both the LV-NGF and LV-GDNF groups (figure 3C). Both LV-NGF and LV-GDNF caused a small but significant increase in the average diameter of the regenerated, retrogradely labelled cell profiles in the L4, L5 and L6 DRGs, (LV-NGF 27.4  $\mu\text{m}$  and LV-GDNF 27.3  $\mu\text{m}$  vs 25.9  $\mu\text{m}$  in “repair only” animals,  $p=0.016$  and  $0.014$  respectively; figure 3D).

#### *LV-NGF and -GDNF increase CGRP expression in regenerated neurons*

Peptidergic nociceptive neurons are sensitive to NGF<sup>177,178</sup>. The expression of CGRP

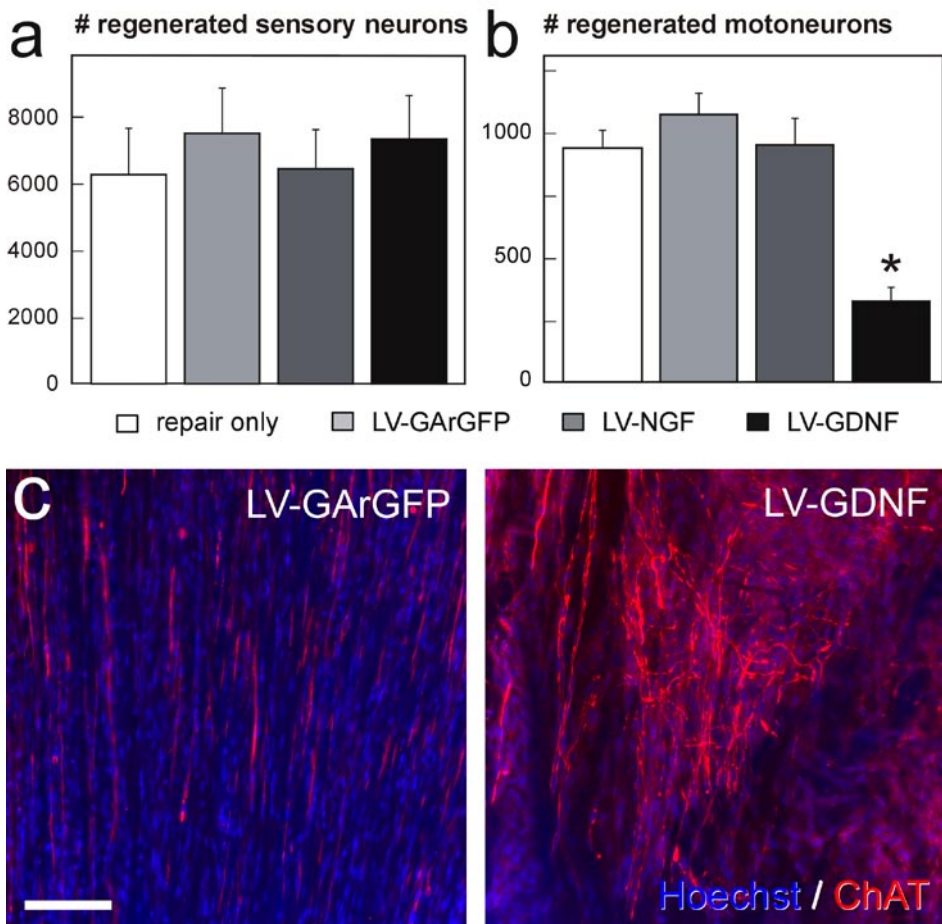


**Figure 2** Quantification of regeneration through retrograde tracing, 1 cm distal from the repair site, 4 weeks after transection/repair.

- a) The regeneration of sensory neurons is not affected by either LV-NGF or LV-GDNF, as the number of retrogradely labelled neurons is not significantly different in any group.
- b) The application of LV-GDNF severely impairs the regeneration of motoneurons, causing an approximate four-fold reduction in the number of motoneurons capable of extending an axon 1 cm from the transection/repair site ( $p=0.000011$ ).
- c) Immunohistochemistry for ChAT on longitudinal nerve sections shows that in LV-GArGFP injected control roots, the majority of motor axons are oriented longitudinally across the transection/repair site.
- d) A similar ChAT staining on a nerve section of a LV-GDNF injected animal shows that motoneurons are chaotically oriented and trapped within the nerve.

Scale bar: 50  $\mu\text{m}$ .

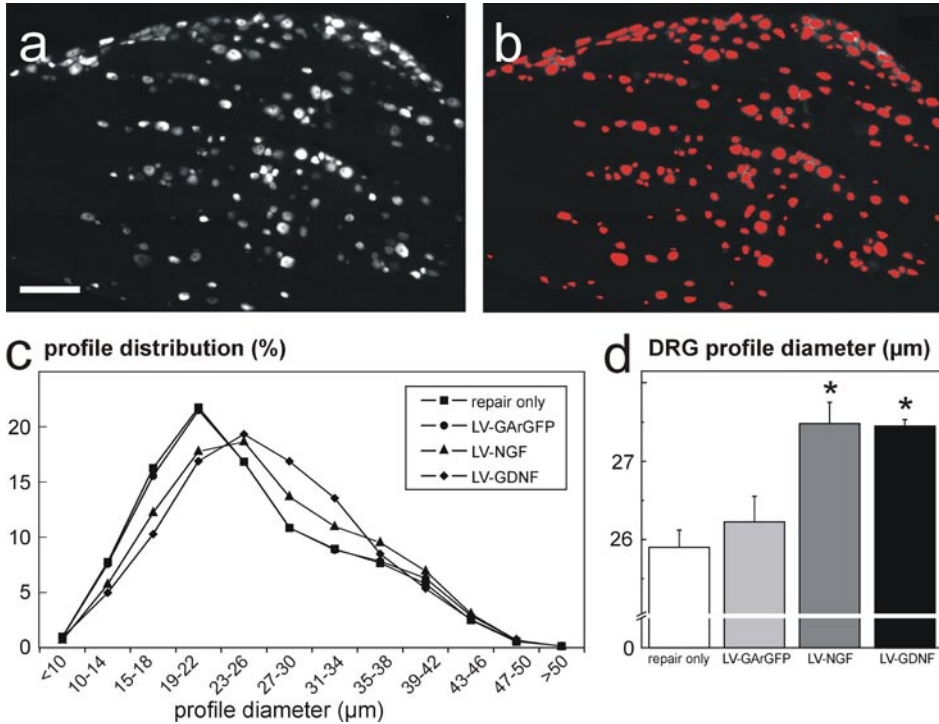


**Figure 3** LV-NGF and LV-GDNF cause hypertrophy of sensory neurons.

a) Image of a typical section of a dorsal root ganglion, with regenerated neurons containing the retrograde tracer Fast Blue (FB).

b) Using Image-Pro Plus software, a filter algorithm was developed to measure the diameter of all FB-labelled structures.

c) The average diameter of all FB-labelled profiles is slightly but significantly increased in both LV-NGF- and LV-GDNF-treated animals compared to the control animals ( $p=0.016$  and  $p=0.014$  respectively).

d) When all profiles are plotted in a frequency distribution, a clear shift towards bigger structures can be seen in both the LV-NGF and LV-GDNF groups.

Scale bar: 250 $\mu\text{m}$ .

in these neurons can be upregulated by the exogenous application of both NGF and GDNF<sup>191</sup> and by peripheral nerve transection<sup>192</sup>. We therefore stained for CGRP on DRG sections in which the regenerated neurons were retrogradely labelled with FB (series 2). In both the “repair only” and the LV-GArGFP control groups, a substantial proportion of CGRP positive cells was FB labelled (figure 4), indicating that these peptidergic neurons are capable of regeneration. As described by others<sup>187</sup>, a striking effect of both LV-mediated NGF and GDNF expression distal to the transection site was observed on the number and staining intensity of CGRP positive cells in the DRG



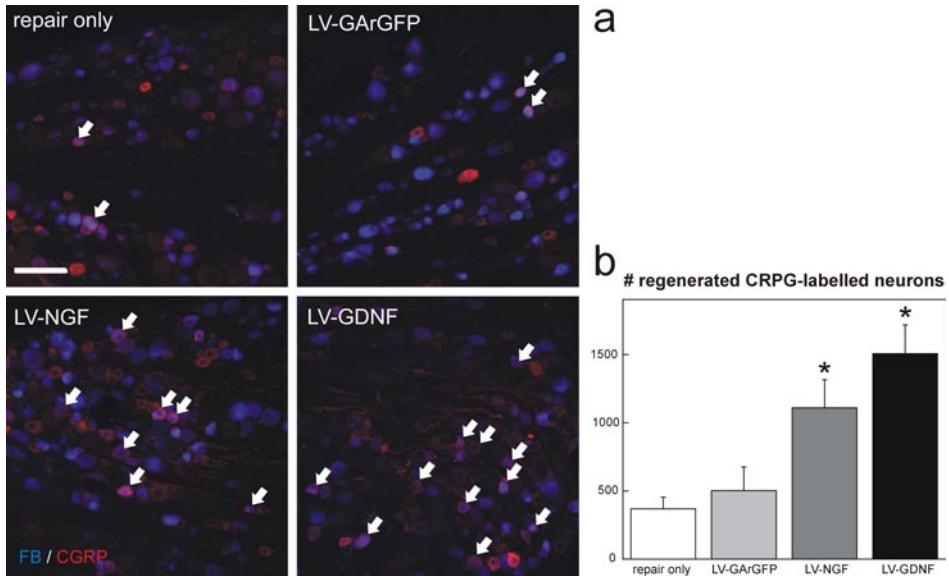


**Figure 4** The application of LV-NGF and LV-GDNF increases CGRP expression in regenerated DRG neurons 4 weeks after sciatic nerve transection and repair.

a) Immunohistochemistry for CGRP (red) on DRG sections in which all regenerated neurons are retrogradely labelled with FB (blue). In “repair only” and LV-GArGFP control groups, approximately half of all CGRP labelled neurons have regenerated. Both the application of LV-NGF and LV-GDNF increase the number of regenerated and total CGRP labelled cells. Scale bar: 250  $\mu$ m. Arrowheads point at double-labelled profiles.

b) Automated quantification of double-labelled profiles shows that the number of regenerated CGRP positive cells is significantly increased after the application of LV-NGF and LV-GDNF. \* $p=0.0039$  and  $p=0.00016$ , respectively.

compared to control groups (figure 4). In addition, the number of double-labelled (i.e., FB and CGRP positive) cells was also higher in both LV-NGF- and LV-GDNF-treated animals (1100,  $P=0.0039$  and 1500,  $P=0.00016$ , respectively, compared to 400 in the “repair only” group). However, combining the observations that a) the total number of regenerated sensory neurons was not increased (figure 2) and b) the CGRP was evidently increased in the entire DRG, we conclude that LV-NGF and LV-GDNF do not specifically enhance regeneration of CGRP-expressing neurons, but instead cause a higher number of regenerated neurons to become CGRP positive.

#### *LV-GDNF increases IB4 binding in regenerated neurons*

Non-peptidergic, IB<sub>4</sub>-binding sensory neurons are sensitive to GDNF and regenerate poorly after peripheral nerve lesions, presumably due to insufficient GDNF levels<sup>182</sup>. Furthermore, IB<sub>4</sub> binding is downregulated after a peripheral nerve lesion<sup>193</sup>. For



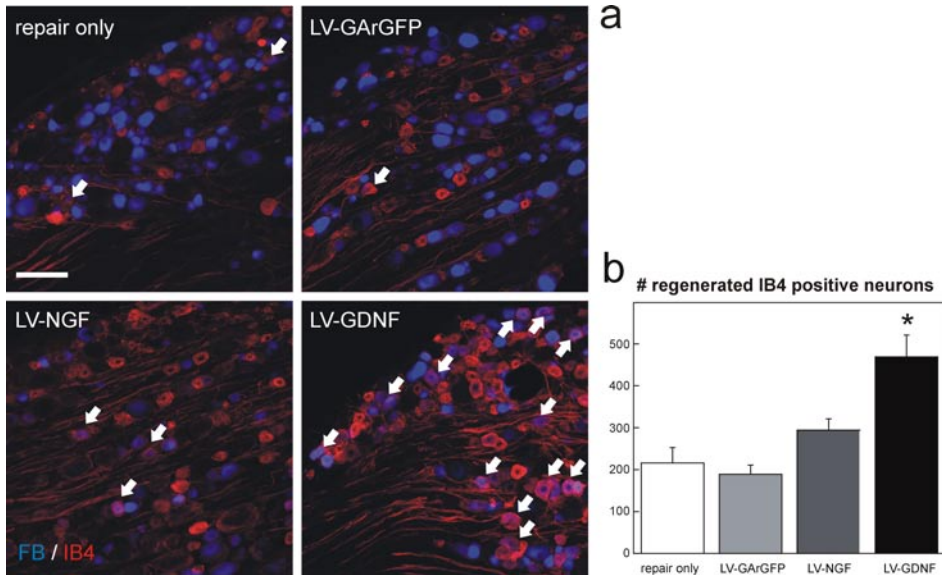


**Figure 5** The application of LV-GDNF increases IB4 binding in regenerated DRG neurons 4 weeks after sciatic nerve transection and repair.

a) Histochemistry for IB4 (red) on DRG sections in which all regenerated neurons are retrogradely labelled with FB (blue). In “repair only” and LV-GArGFP control groups, there is virtually no colocalisation of IB4 and FB, indicating that the majority of IB4 labelled neurons do not regenerate. The application of LV-GDNF increases the overall level of IB4 reactivity in the DRG and IB4 staining can be seen in numerous regenerated cells (arrows). Scale bar: 250  $\mu$ m.

b) Automated quantification of double-labelled profiles shows that the number of regenerated IB4 positive cells is significantly increased after the application of LV-GDNF ( $p=0.00021$  vs repair only).

these reasons we performed an IB4 staining to study the effect of LV-NGF and LV-GDNF. Indeed, in the “repair only”, LV-GArGFP and LV-NGF groups, there was little colocalisation with FB-labelled (regenerated) neurons and IB4 staining (figure 5A-C). Strikingly, both the number and intensity (visual observation) of IB4-labelled cells was strongly increased in LV-GDNF-treated animals and numerous double labelled cells could be observed (figure 5A). We subsequently quantified the number of double-labelled cells: in control groups, only very small numbers of FB-labelled neurons were IB4 labelled (“repair only” and LV-GArGFP had an average of approximately 200 cells per animal, figure 5B). No significant change was observed in the LV-NGF group (average 300;  $p=0.34$ ), but in the LV-GDNF group the number was significantly higher (average 500;  $p=0.00021$ ). We conclude that high levels of GDNF do not specifically enhance regeneration of IB4 positive neurons. Instead, an increase in the expression of GDNF, but not NGF, causes increased IB4 labelling intensity in regenerated sen-

sory neurons, or more precisely, reversal of the lesion-mediated loss of IB4 binding<sup>193</sup>. However, the total number of regenerated sensory neurons with an axon at 1 cm distal from the repair site at 4 weeks post-lesion is not affected.

*LV-NGF and -GDNF do not increase neurite sprouting distal from the repair site*

Retrograde tracing and immunohistochemical staining of motor axons showed that regenerating motoneurons were trapped by the local application of LV-GDNF and neither LV-NGF nor LV-GDNF influenced the regeneration of sensory neurons. However, the potential ability of these factors to induce increased sprouting of neurites distal from the transection/repair site can not be determined through retrograde tracing. To quantify this, we stained transverse sections of the sciatic nerve at 4 weeks after intervention, 1 cm distal from the repair site with an antibody against neurofilament. The average number of neurites in LV-GArGFP-injected control nerves was 11,000. This number is higher than the combined number of regenerated FB-labelled sensory and motoneurons (7,000-8,500) suggesting that a certain degree of sprouting of regenerating neurites does occur after peripheral nerve repair and accounts for this difference. The number of neurites after the application of LV-NGF and LV-GDNF was not significantly different from this control level (figure 6C), indicating that there was no effect on neurite sprouting. For LV-GDNF-treated animals, a slight decrease might have been expected as it was shown to trap regenerating motor axons (figure 2C). However, retrograde tracing showed that the majority of neurons projecting to the sciatic nerve were sensory neurons (87%; figure 2AB) and therefore an effect on motor axons is well within the measured standard error of the means of the total number of regenerated neurites.

*LV-NGF and -GDNF affect sensory and motor functional recovery*

*NOCICEPTIVE SENSORY REINNERVATION*

The return of nociceptive sensory function after peripheral nerve transection was determined by applying a noxious electric stimulus to the lateral foot sole<sup>186</sup>. After transection of the sciatic nerve, no withdrawal response was observed in any of the animals, indicating a complete loss of nociceptive function in the hind paw. In “repair only” and LV-GArGFP controls, as well as in LV-GDNF-treated animals, a withdrawal response gradually returned at 4 weeks and with time, lower currents were needed to elicit a withdrawal response until nociceptive function had completely restored at 7 weeks. The application of LV-NGF caused a significant increase in the recovery rate: more animals showed a withdrawal response at lower currents ( $p=0.037$  vs “repair only”). At 6 weeks, all LV-NGF-treated animals showed a withdrawal response at 0.1 mA and the response curves show a one week shift towards earlier recovery of nociceptive sensation in the foot sole of the hind paw (figure 7A).

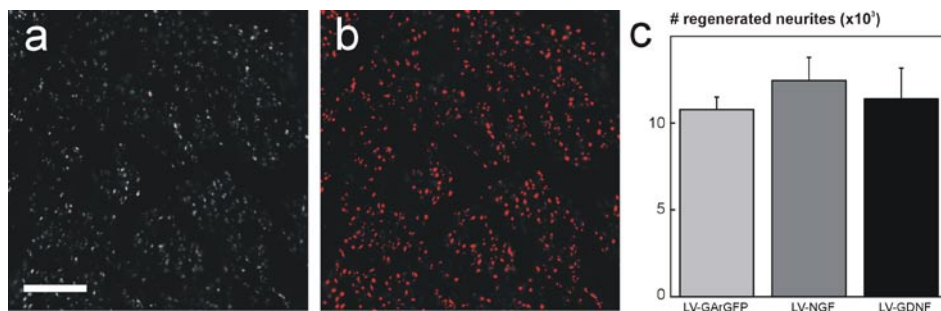


**Figure 6** Automated quantification of neurofilament positive structures 1 cm distal from the transection and repair site of the sciatic nerve at 4 weeks shows that LV-NGF and LV-GDNF treatment does not increase neurite sprouting.

a) Regenerated axons distal from the repair site stained with antibodies against neurofilament and quantified using an automated filter algorithm (b).

c) In LV-GArGFP control animals, approximately 12,000 neurites have regenerated across the repair site, this number is not affected by the application of LV-NGF or LV-GDNF.

#### MOTONEURON REINNERVATION

The ultimate measure of functional motor recovery is behavioural analysis of locomotor function of the affected hind paw. However, this type of functional recovery is strongly influenced by factors such as misrouting of regenerated axons<sup>9,117</sup> and central plasticity<sup>120</sup>. As a more simple and direct measure for the reinnervation of target muscles by regenerated motoneurons, we therefore weighed the gastrocnemius and soleus muscles 12 weeks after transection and repair, and compared them to the contralateral side<sup>187</sup>. In the “repair only”, the LV-GArGFP and the LV-NGF groups, the combined weight of these muscles was approximately 60% of the contralateral side. The application of LV-GDNF resulted in a 30% lower muscle weight ( $p=0.00018$  vs “repair only”; figure 7B). These results suggest that the impaired motor axon regeneration found by retrograde tracing and the coiling of axons at the repair site indeed impede the reinnervation of target muscles.

#### AUTOTOMY BEHAVIOUR

Both NGF<sup>194,195</sup> and GDNF<sup>18</sup> have been associated with increased autotomy behaviour in peripheral nerve lesion models. We therefore investigated if the overexpression of these factors influenced autotomy in our study (figure 7C). The development of autotomy over time appeared to correspond with the period of nociceptive function loss: it gradually increased after nerve transection, but decreased sharply as nociceptive sensation of the hind paw returned. Over this entire period, the average autotomy score was highest in the LV-GDNF group, but this difference was most pronounced at later time points, when nociceptive function was restored (cf. figures 7A and C).

The average maximum score reached by each animal was significantly higher in the LV-GDNF group ( $p=0.011$  compared to “repair only”; figure 7C). The application of LV-NGF did not appear to influence autotomy.

### Discussion

In this paper we show that LV vectors can be used *in vivo* to locally elevate levels of NGF and GDNF after transection and direct suture repair of the rat sciatic nerve. These elevated NGF and GDNF levels have profound and differential effects on regenerating sensory and motoneurons. For sensory neurons, increased levels of NGF and GDNF did not affect the total number of sensory and motoneurons from which axons had regenerated 1 cm distal to the repair site 4 weeks after repair, but changed the expression of markers for different nociceptive populations of neurons. Functionally, LV-NGF increased the rate of recovery of nociceptive function, whereas LV-GDNF increased autotomy behaviour. For motoneurons, increased expression of GDNF at the repair site was found to cause trapping of regenerating axons, with decreased numbers of motoneurons from which axons had regenerated 1 cm distal to the repair site and decreased weight of target muscles. NGF had no effect on these parameters.

#### *Lentiviral vectors mediate a long-term increase in neurotropic factor expression in the injured rat sciatic nerve*

Our quantitative analysis shows, in concordance with previously published data <sup>182</sup>, that endogenous NGF levels are much higher than GDNF levels in the peripheral nerve after a lesion. In fact, we were unable to detect any endogenous GDNF with the current protocol, although elevated GDNF mRNA and protein levels 4 weeks after peripheral nerve injury have been shown by numerous other studies <sup>12,196,197</sup>. In the present study, sciatic nerves were divided in 1 cm segments, resulting in very small amounts of homogenate that may have been insufficient to detect endogenous levels with an ELISA approach. Transduction of Schwann cell with LV vectors results in increased levels of NGF and GDNF around the transection/repair site at least up to 4 weeks. Previously, we have shown that LV-mediated transgene expression continues for at least 16 weeks in Schwann cells in reimplanted spinal nerve roots <sup>150,183</sup>. In absolute terms, transgenic NGF and GDNF tissue levels are comparable (an additional 7-10 ng in the 1 cm nerve segment directly distal from the repair site). However, because of the different endogenous levels of NGF and GDNF, LV-mediated expression of these neurotrophic factors result in an approximately two-fold increase in NGF levels, whereas the relative increase in GDNF expression was at least 100-fold.

#### *The effect of LV-NGF on regenerating sensory neurons*

Retrograde tracing shows that the two-fold increase in the expression of NGF in the

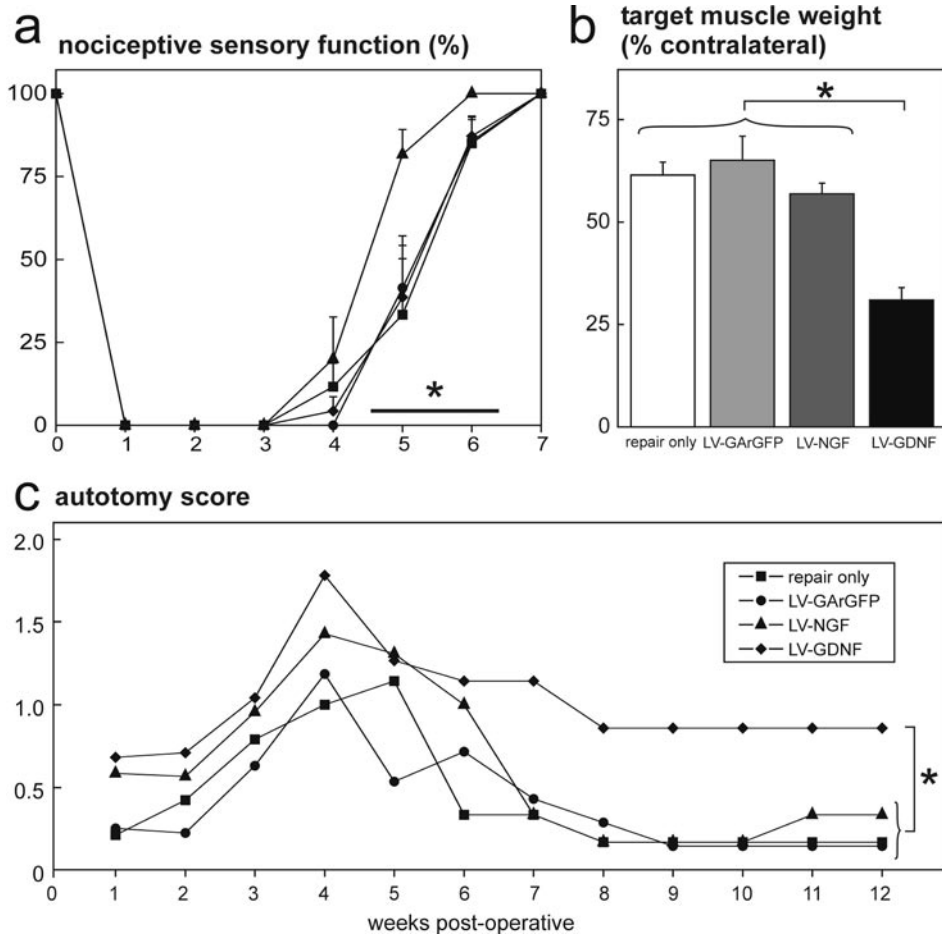


**Figure 7** Functional effects of LV-NGF and LV-GDNF following transection and repair of the rat sciatic nerve.

a) Evaluation of nociceptive function by determining the minimal electric current that has to be applied to the affected foot sole to elicit a withdrawal response. Transection of the sciatic nerve results causes the complete absence of a withdrawal response. Over the course of several weeks, gradually lower currents are needed to elicit foot withdrawal until at 7 weeks, the required stimulus returns to pre-operative levels. LV-NGF significantly accelerates the return of this response with approximately one week. \* $p=0.037$  vs “repair only”.

b) Evaluation of the weight of gastrocnemius and soleus muscles (% of contralateral) as measure for reinnervation by motoneurons at 12 weeks after transection and repair. LV-GDNF causes a significantly lower muscle weight \* $p=0.00018$  vs “repair only”.

c) After sciatic nerve transection, autotomy increases gradually, but drops sharply as nociceptive sensation of the hind paw returns (cf. panel a). The average maximum autotomy score reached by each animal is higher in LV-GDNF treated animals ( $p=0.011$  and  $0.019$  compared to the “repair only” and LV-GArGFP control groups, respectively).

genetically modified nerve does not significantly increase the number of regenerated sensory DRG neurons. Moreover, histology of the distal nerve stump reveals that distal sprouting of neurons is not significantly enhanced. However, the expression of CGRP in regenerated DRG neurons is increased and there is a significantly faster return of the withdrawal response after a noxious stimulus to the hind paw. The role of NGF in the pathogenesis of pain, specifically in the development of thermal and mechanical hyperalgesia, is well documented<sup>10,198,199</sup>. In a dorsal root avulsion model, the viral vector-mediated overexpression of NGF has been shown to cause hyperalgesia<sup>200</sup>. Furthermore, NGF causes the upregulation of CGRP in sensory neurons<sup>201</sup> and CGRP increases neuronal excitability<sup>202</sup>. The present observations show that local LV-vector-mediated expression of NGF at a peripheral nerve lesion/repair site has no effect on the number of regenerated neurons or axons at 1 cm distal at 4 weeks, but does induce the upregulation of CGRP in regenerated sensory neurons. The enhanced recovery of nociceptive function that was observed after the application of LV-NGF is therefore likely the result of the sensitization of regenerated neurons, causing increased sensitivity of the hind paw. However, a small effect of LV-NGF on the initial post-lesion temporal pattern of neurite outgrowth of nociceptive neurons may have occurred and this could have contributed to the earlier return of nociceptive function.

#### *The effect of LV-GDNF on regenerating sensory neurons*

Similar to LV-NGF, LV-GDNF did not stimulate the regeneration of sensory DRG neurons, but increased the expression of CGRP in regenerated sensory neurons. In addition to this effect, LV-GDNF also strongly increased the number of IB4-binding regenerated neurons. These histological findings correspond well with several reported effects of pharmacologically administered GDNF on sensory neurons. First, GDNF increases CGRP expression in intact sensory neurons without causing increasing thermal or mechanical pain sensitivity<sup>187</sup>. Second, GDNF prevents the axotomy-induced downregulation of IB4 binding<sup>177</sup>. Third, it prevents the loss of IB4 binding in a sciatic nerve ligation model for neuropathic pain<sup>193,203</sup>. Moreover, increased CGRP expression and IB4 binding have been observed in a model for chronic nerve compression injury, in which GDNF was also shown to accumulate<sup>204</sup>.

Furthermore, we found that LV-vector-mediated expression of GDNF in the distal stump of a transected and repaired peripheral nerve significantly affects autotomy behaviour, as reported before following the application of GDNF in fibrin sealant<sup>19</sup> in a highly similar model for nerve transection and repair. Autotomy is usually interpreted as a behavioural response to neuropathic pain<sup>188,195,205,206</sup>, but GDNF has been shown to possess strong analgesic properties<sup>193,203,207</sup>. It is interesting that in our experiments the most marked GDNF-mediated increase in autotomy was after 7 weeks when nociceptive function had been completely restored. This suggests that, instead of being the



result of neuropathic pain, autotomy behaviour in LV-GDNF treated animals may have been caused by *reduced* pain perception in the innervated hind paw: whereas autotomy is limited after re-establishment of nociceptive function in normal animals, the analgesic effect of GDNF may have prevented this feed-back, leading to continued autotomy.

Although the effect of GDNF on analgesia and on IB4 binding have been reported to occur concomitantly in a number of studies<sup>193,203,207</sup>, a precise relation between IB4 binding and pain perception remains to be elucidated. These phenomena may be linked however in the following way: the substrate for IB4 is a splice variant of the extracellular matrix proteoglycan versican<sup>208</sup>, a component of perineuronal nets that stabilise neuronal connections<sup>114</sup>. The upregulation may therefore affect cross-excitation of nociceptive DRG neurons<sup>208,209</sup> leading to decreased pain perception in the central nervous system.

In summary, LV-GDNF does not increase the number of regenerating neurons, but increases both CGRP immunoreactivity and IB4 binding in sensory neurons of the DRG. The analgesic effects of GDNF (possibly related to an increase in IB4 binding) could stimulate autotomy behaviour in LV-GDNF treated animals.

#### *Motoneurons fail to regenerate across areas of high GDNF expression*

We have previously shown that viral vector-mediated overexpression of GDNF in either the spinal cord or the ventral root in a rat ventral root avulsion and reinsertion model leads to trapping of the regenerating motor axons<sup>25,179</sup>. Motor axons continue to grow within the area of GDNF expression, leading to the development of axon-dense areas in the ventral spinal cord<sup>24</sup> or neuroma-like “nerve coils” in the reimplanted nerve roots<sup>183</sup>, a phenomenon we have previously called the “candy store effect”. Here, a highly similar effect of LV-GDNF on the regeneration of motoneurons was observed in the rat sciatic nerve which contains both motor and sensory neurons. Retrograde tracing showed that a significant number of motoneurons fail to extend axons across areas of transgenic GDNF expression and staining for (motoneuron-specific) ChAT on longitudinal sections revealed that motor axons at the repair site of the nerve have a disorganised morphology. Consequently, many regenerating motor axons in the LV-GDNF treated animals fail to re-innervate target muscles leading to a significant decrease in muscle weight. Apparently, the continuous local expression of very high levels of GDNF is detrimental to long distance regeneration, and traps regenerating motoneurons in a “candy store”.

This “candy-store effect” may have been caused by the relatively large (100-fold) increase in GDNF expression, as the trapping of regenerating axons by GDNF appears to be dose-dependent<sup>210</sup>. Therefore, it remains possible that regeneration can be enhanced by a more “physiological” elevation (e.g., two-fold) in GDNF levels. This may be achieved with viral vectors with regulatable transgene expression<sup>52</sup> or with



promoters, like the GFAP<sup>211</sup> or S-100<sup>212</sup> promoter, that would specifically direct more physiological levels of transgene expression in non-myelinating Schwann cells. This latter approach could limit the expression of GDNF to Schwann cells distal to the tip of the transected axon and this approach may thus prevent trapping.

Interestingly, regenerating sensory neurons did not appear to be trapped by high local levels of GDNF, although a dose-dependent effect of the regeneration of the central projection of DRG neurons into the spinal cord has been described by others<sup>213</sup>. This differential effect of GDNF on sensory and motor neurons could in theory be used to devise a nerve graft that preferentially allows the long distance regeneration of sensory, but not motor neurons.

### *Concluding remarks*

In recent years, the focus of peripheral nerve research has increasingly shifted towards creating a better understanding of the molecular basis of peripheral nerve regeneration<sup>211</sup>. In the present paper, we show that LV vectors are highly suitable tools to study regeneration at a molecular level, as they make it possible to investigate the regenerative effect of the highly localised overexpression of any protein of interest. Furthermore, we show that viral-vector-mediated overexpression of two well-known neurotrophic factors, NGF and GDNF influences regenerating nociceptive sensory and motor neurons in very different ways. These insights have important implications for future research. First, the specific neurotropic effect of LV-GDNF on motoneurons could theoretically be applied to direct regenerating motor axons towards the appropriate distal endoneurial tubes, although transgene expression would have to be switched off after a certain period to allow continued outgrowth. Second, the observation that motoneurons are trapped by high levels of transgenic GDNF could potentially be exploited to create nerve grafts that are specifically permissive for sensory axons (by applying LV-GDNF proximal to the nerve graft). Finally, the application of LV-GDNF to injured sensory nerves (after surgical repair) may be an attractive adjuvant therapy for the treatment of neuropathic pain.

# Chapter 7

## Summary and general discussion

### Summary of this thesis

In the research described in this thesis, we explored two related questions.

- 1) What are the molecular properties of the human peripheral nerve lesion, and in particular, why is scarring at the lesion site, or neuroma formation, detrimental to functional recovery?
- 2) Can we apply lentiviral (LV) vectors to overexpress neurotrophic factors to enhance regeneration after surgical repair?

The first two experimental chapters dealt with the first research question. We studied small segments of human neuroma tissue that were removed during reconstructive surgery and discovered that they contain the chemorepulsive protein semaphorin<sub>3A</sub>. Staining for semaphorin<sub>3A</sub> shows that the protein surrounds nerve fibers in a punctate pattern and a functional *in vitro* test shows an inhibition of the neurite outgrowth of cells from a neuronal cell line that were cultured on slices of human neuroma tissue. Encouraged by this discovery, in the next chapter we performed a genome-wide expression analysis in human neuroma tissue and found that the expression of a significant number of genes involved in scar formation and axon guidance is differentially regulated. Further investigations into the precise role of several of these factors, specifically their potential influence on phenomena such as repulsion, fasciculation and defasciculation of regenerating axons, will help to improve the understanding of the outgrowth-inhibitory nature of the neuroma. Perhaps more importantly, these investigations could yield novel targets for future therapies aimed at improving regeneration after peripheral nerve injury.

In the following chapters, LV vectors were applied to express neurotrophic factors in the injured peripheral nerve in an attempt to enhance regeneration after surgical repair. First, we developed a protocol to genetically modify cells in cultured segments of human sural nerve using LV vectors expressing the marker gene green fluorescent protein (GFP). With the application of an LV vector encoding nerve growth factor (LV-NGF) long-term production of biologically active NGF could be directed in cultured human nerve segments. This technique was subsequently used to investigate *in vivo* the effect of LV vector-mediated overexpression of brain-derived neurotrophic factor (BDNF) and glial cell line-derived neurotrophic factor (GDNF) on the regeneration of rat motoneurons after avulsion and reimplantation of the ventral nerve root. In this model, we found positive effects of LV vector-mediated overexpression of GDNF: a complete reversal of avulsion-induced motoneuron atrophy and an increased density of regenerating axons in the reimplanted roots. However, the strongest effects of LV-

GDNF were negative: high levels of transgenic GDNF expression induced a truly striking neuroma-like ‘oasis’ of coiled axons in the nerve root, and the number of regenerated fibers more distally was, in fact, lower in comparison with control treatments.

In the next chapter, the effect of LV vector-mediated overexpression of NGF and GDNF was investigated in a rat model for peripheral nerve transection and repair. The regeneration of motoneurons does not appear to be affected by the LV vector-mediated overexpression of NGF. However, similar to the root avulsion repair study, LV vector-mediated expression of GDNF in the transected nerve impaired the long-distance regeneration of motoneurons. In the affected nociceptive sensory neurons, LV vector-mediated overexpression of both NGF and GDNF causes profound phenotypic changes that are in line with the notion that these factors play an important role in the pathogenesis of pain. Although both the differential regenerative response of motor and sensory neurons upon application of these factors and the changes in nociceptive sensory neurons could form the starting point for new exciting investigations, these findings also highlight the difficulties in improving nerve regeneration and the genuine possibility of unwanted side-effects associated with LV vector-mediated overexpression of neurotrophic factors.

In this general discussion I will further evaluate the merits of the results described above, as I believe that the experiments in this thesis have yielded both clear “winners” and “losers”. I would regard the discovery of semaphorin3A, as well as several other axon guidance molecules in the human neuroma and the successful long term transgene expression in the peripheral nerve after *in vivo* application of LV vectors as “winners”, i.e. results that merit additional investigation and may form the basis of future clinical applications. As a “loser”, i.e. a strategy that did not live up to expectations, I would consider the exogenous continuous application of neurotrophic factors as a means to enhance long-distance regeneration. In the sections below, I will elaborate on these qualifications. However, the merits of new therapeutic concepts depend on their ability to advance the current clinical practice of nerve repair. Therefore, I will start by giving a concise overview of the challenges that exist in the management of peripheral nerve injuries.

### **Challenges in nerve repair – opportunities for novel therapies**

In this section I will briefly discuss the present state of the art in peripheral nerve repair. This is by no means intended as an exhaustive review of the entire body of knowledge on peripheral nerve regeneration, but instead, I will focus on those issues that are relevant to the new therapeutic strategies that have been explored in this thesis.

In contrast to the injured spinal cord, in which the regenerative process is thwarted by the abundance of growth-inhibitory factors<sup>57</sup>, the lesioned peripheral nerve is capable of regeneration<sup>81</sup>. However, regeneration, and subsequent functional recovery, depends on the degree of nerve injury<sup>1</sup>.

Clinically, the most important distinction is between axonotmetic injuries, in which axons are severed but the integrity of nerve fascicles is preserved and neurotmetic injuries, in which the physical continuity of the entire nerve (including axons and nerve fascicles) is lost. Although a regenerative response does occur in neurotmetic lesions, axons are unable to bridge the gap that forms between proximal and distal nerve stumps and surgical reconstruction is therefore usually indicated <sup>1</sup>. In contrast, axonotmetic injuries tend to regenerate completely, although this does not always result in full functional recovery. At a rate of regeneration of 1-5 mm/day <sup>1</sup>, it may take several months for regenerating axons to reinnervate their distal targets and during this time these targets may have atrophied, resulting in a poor restoration of function <sup>11</sup>. This slow rate of regeneration and associated atrophy of denervated target organs is therefore a clinical problem and a potential target for therapeutic intervention.

In cases of acute neurotmetic injuries (e.g., the complete transection of the ulnar nerve in a stab wound), the clinical strategy to treat the injured nerve is relatively straightforward and consists of immediate repair surgery, either through the direct coaptation of proximal and distal nerve stumps, or through the application of a nerve grafts that acts as a scaffold for regenerating axons.

However, the treatment strategy is not always this clear-cut, especially if a lesion is characterised by extensive intraneural fibrosis. In this so-called neuroma in continuity, both axonotmetic and neurotmetic injury types can be present, and it is therefore difficult to assess the likelihood of spontaneous recovery <sup>3</sup>. The absence of a reliable method to determine the degree of injury at an early time point means that most surgeons recommend surgical exploration when clinical examination does not show functional recovery of the associated muscle after a certain waiting period <sup>82-84</sup>. However, the regenerative potential of axotomised motoneurons diminishes over time <sup>214</sup> and therefore, this approach is in effect a trade-off between not waiting long enough (running the risk of performing surgery on injuries that would have recovered spontaneously) and waiting too long (impairing the outcome of reconstructive surgery for severe lesions) <sup>1</sup>. This is a second clinical challenge, one that could be addressed by either improving the ability to assess the degree of injury at an early time point or by enhancing the regenerative capacity of chronically axotomised neurons.

After nerve repair, both motor and sensory neurons are able to regenerate and re-establish functional connections, but there are differences in their regenerative response. Motoneurons preferentially reinnervate muscles, a phenomenon that is the result of both interaction between the motoneuron and the distal endoneurial tubes at the coaptation site <sup>215</sup> and of the “pruning” of motoneuron axons that have inaccurately entered endoneurial tubes that lead to sensory organs <sup>216</sup>. However, this increased likelihood that motoneurons reinnervate muscles, called “preferential motor reinnervation” <sup>217</sup>, does not mean that these motoneurons are capable of selectively find-

ing their original targets. Instead, the outgrowth of motor axons is a random process that frequently results in the reinnervation of inappropriate, antagonistic muscles<sup>8</sup> or even reinnervation of two muscles by branches from one motoneuron<sup>115</sup>. This leads to the cocontraction of antagonizing muscles and subsequently a failure to recover functionally. This “misrouting” phenomenon is the third challenge that provides an opportunity for future therapies.

Finally, the regeneration of motoneurons through grafts derived from purely motor nerves is better than through grafts from sensory nerves and vice versa<sup>12,218</sup>. Whereas some researchers have attributed this fact to the differential expression of several neurotrophic factors in motor and sensory nerve grafts<sup>12</sup>, others claim that physical differences play an important role. Axons of sensory neurons generally have a smaller diameter, and the endoneurial tubes in grafts derived from sensory nerves may not be ideally suited to accommodate the larger-diameter axons of motoneurons<sup>218</sup>. The most commonly used graft in human reconstructive surgery is derived from the sural nerve, because this sensory nerve can be missed without causing major deficiencies. The putative drawback of using sensory nerve grafts to support the regeneration of motoneurons is the fourth and final problem in the clinical practice of nerve repair that I would like to mention here.

In the light of the issues described above, I will now continue to discuss the merits of the work described in this thesis, starting with the “losing strategy” of applying neurotrophic factors to enhance regeneration.

### **Exogenous neurotrophic factors: useful to prevent atrophy, but probably not to promote outgrowth**

Since the discovery that NGF can promote neurite outgrowth by Rita Levi-Montalcini in 1952, neurotrophic factors have arguably been the most widely studied proteins in the field of neuroregeneration<sup>9</sup>. Interestingly, in the treatment of several *neurodegenerative* diseases (e.g., Alzheimer’s disease and Parkinson’s disease), the application of neurotrophic factors has been quite promising<sup>212</sup>. Clinical trials with neurotrophic factors for these diseases are currently underway and encouraging results have been reported<sup>131,219</sup>. In contrast, the application of neurotrophic factors to enhance *neuroregeneration* has proven to be far more difficult. One explanation for this difference must be that unlike survival, successful regeneration depends on precise time- and location-dependent expression of these factors to create an ever-shifting gradient towards which axons continue to extend, sometimes over periods of several months. The “candy-store” effect, which was first described in the spinal cord<sup>25</sup> and also observed after local application of LV-GDNF in Chapters 5 and 6 shows that in this case, more is not necessarily better. Furthermore, we have recently obtained unpublished data on the concentration of NGF, Neurotrophin-3, BDNF and GDNF in avulsed nerve

roots that clearly show the subtle temporal changes in the expression of these factors. In other words, the endogenous expression of these factors in the peripheral nerve already appears to be optimised to support continuous regeneration and it is hard to envision how their exogenous application will have any other effect than disrupting this delicate balance.

Another striking observation in this respect is that in each paradigm studied in this thesis, the peripheral nerve clearly “wants to regenerate”, probably stimulated by endogenously elevated levels of neurotrophic factors distal from the lesion site. This is exemplified by three observations: (i) the many regenerating axons in the human peripheral nerve scar (Chapter 3), (ii) the numerous motor axons crossing spinal cord white matter and entering the implanted nerve root (Chapter 5) and (iii) the high number of neurites that did grow into the nerve stump distal to a peripheral nerve lesion (Chapter 6). The robust regeneration in rat models for peripheral nerve injury (ii and iii) do not necessarily translate to the human clinical situation, where the distance to be bridged from lesion site to target organ is usually much longer<sup>11</sup>. Nonetheless, the injured human peripheral nerve is also capable of regenerating over long distances<sup>1,4</sup>, suggesting the presence of a mechanism that shifts the elevated endogenous production of neurotrophic factors ahead of regenerating axons. Exogenously and locally increasing the amount of neurotrophic factors in the nerve therefore seems neither needed nor helpful. This is disappointing, because the transduction with lentiviral vectors to overexpress a combination of motoneuron-specific neurotrophic factors<sup>12</sup> could be an interesting strategy to render sensory sural nerve grafts more supportive of the regeneration of motoneurons. As described in Chapter 6, the regenerative response to the overexpression of GDNF of sensory neurons differs from motoneurons and such findings could theoretically be exploited to create grafts that are specifically permissive for the regeneration of either sensory or motoneurons. However, unless it becomes possible to create a time- and location-dependent gradient of these factors in the nerve, this approach is not likely to enhance the long distance regeneration through nerve grafts.

In summary, the exogenous application of neurotrophic factors still faces significant challenges if the goal is to stimulate peripheral nerve *regeneration*. However, by exploiting the *survival*-enhancing properties of trophic factors, there may be several possibilities to enhance the functional outcome of nerve repair.

Firstly, as described in Chapter 5 of this thesis, the viral vector-mediated application of GDNF could be a promising approach to prevent motoneuron atrophy after nerve root avulsion, “keeping them in shape” prior to reconstructive surgery. This is of particular importance as the diminished regenerative capacity of chronically axotomised motoneurons<sup>214</sup> can be boosted by the temporary application of GDNF<sup>21</sup>. This could therefore be a way to compensate for the deleterious effect of the waiting period that is currently part of the surgical decision-making process.

Secondly, there may be a role for neurotrophic factors in the prevention of target muscle atrophy during the period of denervation. Ciliary neurotrophic factor (CNTF) has a strong myotrophic effect on denervated skeletal muscle<sup>220,221</sup>, but systemic application of CNTF causes unwanted side-effects such as severe weight loss<sup>222</sup>. Local, LV vector-mediated expression in the muscle<sup>46</sup> of CNTF may be a method to prevent muscle atrophy without causing significant side effects, thereby addressing the clinical issue of chronic denervation.

Apart from practical issues involved in applying viral vectors to, for instance, axotomised motoneurons in the spinal cord, the success of these strategies will depend on two factors: the ability to tightly regulate the amount of neurotrophic factors produced and the ability to switch off transgene expression completely when it is no longer helpful. This is theoretically possible with viral vectors with regulatable gene expression. As discussed in Chapter 1, there are still unresolved issues regarding the safety and clinical applicability of vectors that direct regulatable transgene expression. It will therefore require several years of additional research before these strategies are ready to be tested in a clinical setting.

### **Failed functional recovery: not the engine is missing, but the steering wheel**

As proposed in the previous paragraph, in most cases regeneration of the peripheral nerve does not seem to need stimulation by the exogenous application of factors like NGF and GDNF as they are already tightly and autonomously regulated to optimise continuous outgrowth. Why then, is functional recovery of the peripheral nerve after reconstructive surgery often not complete? If this is not the result of an insufficient regenerative response, there must be another reason why, for instance, patients with a brachial plexus lesion often fail to regain function of distal targets like the hand after reconstructive surgery<sup>85</sup>.

There is an increasing body of evidence suggesting that the misrouting problem is a strong contributing factor to the lack of functional recovery after nerve repair surgery<sup>115,116,223</sup>. Younger patients may be able to partially compensate for misrouted axons due to the plasticity of their still maturing central nervous system<sup>224,225</sup>, but this ability of the brain to adapt to the newly formed peripheral connections diminishes with aging. To eliminate the cocontraction of antagonising muscles, Botulinum toxin type A has been injected in the triceps muscle of patients with brachial plexus injuries<sup>116</sup>. The purpose of this approach is to facilitate motor learning by temporarily inducing the relaxation of antagonist muscles and allowing increased activity in the reinnervated biceps muscle. Other than this, there are no pharmacological options to treat misrouting and the problem is usually addressed with intensive physical therapy<sup>226</sup>.

In research, the routing problem has mainly been addressed mechanistically, for instance by applying artificial scaffolds with a three-dimensional structure to enhance



the physical guidance of regenerating axons<sup>227-230</sup>. It is true that the physical properties of the distal endoneurial tubes determine the fate of regenerating axons and thus strongly influence the degree of functional recovery<sup>7</sup>. However, surgical reconstruction of severe neurotmetic nerve injuries is inherently accompanied by a loss of continuity of nerve fascicles, impairing the ability of the nerve to physically guide regenerating axons. In addition, the sural nerve graft that is most commonly used for reconstructive surgery (see above) already contains thousands of aligned Schwann cells in longitudinally oriented endoneurial tubes, so it is difficult to imagine how this could be improved by artificial guides. Theoretically, one could envision a refinement of surgical techniques up to a level where each individual axon in the proximal stump is matched to one endoneurial tube in carefully prepared (artificial or sural) nerve grafts, but even then it is hard to imagine how the appropriate distal targets for these axons could be identified or how branching at the coaptation site could be prevented. Antibodies against neurotrophic factors have been applied in a rat model for peripheral nerve transection to reduce the branching of regenerating axons and thus improve the quality of regeneration<sup>231</sup>, but this approach carries the risk of interfering with the neurotrophic factor signalling that is needed for successful regeneration.

Another approach could be to allow regeneration to take place after repair as usual, but then enhance the ability to use the newly formed connections by increasing plasticity at the level of the spinal cord<sup>120</sup> or brain. Although this approach will not be able to compensate for synkinesias caused by the innervation of antagonising muscles by branches from the same motoneuron<sup>115</sup>, it shows the importance of including the central nervous system, perhaps in a multi-level approach, to achieve functional recovery after peripheral nerve injury.

### **Addressing the routing problem at a molecular level**

The reason why I declared the discovery of the expression of semaphorin3A and a number of other axon guidance molecules in human neuroma tissue a “winner” is that these findings show for the first time that there are molecules present within the human nerve scar itself that help determine the fate of regenerating axons. In other words, the routing of regenerating axons is not only influenced mechanically by the physical alignment of regenerating axons in endoneurial tubes, but also by lesion-induced expression of specific genes in the glial cells of the peripheral nerve. This finding may provide several new inroads to address the misrouting problem.

Firstly, the chemorepulsive protein semaphorin3A (Chapter 2, and other possible inhibitory molecules described in Chapter 3) present in the human neuroma could have contributed directly to the observed trapping and disorganisation of axons in the human nerve scar. Secondly, in Chapter 3 we describe that the expression of several axon guidance molecules is differentially regulated in human neuroma tissue.

Although this data is still preliminary, previous literature suggests that some of the newly discovered guidance molecules are likely to play a role in the branching, fasciculation (the tendency of regenerating axons to grow in the same direction) and/or defasciculation of regenerating axons. All these phenomena are highly relevant for the misrouting problem. For instance, if some of the newly discovered proteins stimulate neurite sprouting, viral vector-mediated expression of short interfering RNAs to knock down the expression of such proteins could limit the number of regenerative branches extending from one transected motoneuron. In this way an attempt can be made to diminish the likelihood of double innervation of antagonising muscles and subsequently the development of unwanted cocontractions. As described in Chapter 4, the expression of these genes in a sural nerve graft could be manipulated with the use of an LV vector.

Furthermore, some of these newly discovered axon guidance molecules may play a role in the phenomenon of “preferential motor reinnervation”, which is in part caused by an interaction of axotomised motoneurons and endoneurial tubes at the site of axotomy<sup>215</sup>. Influencing the expression of these genes could preferentially stimulate the regeneration of motoneurons, stimulate or reduce motoneuron sprouting or perhaps even stimulate the pruning of redundant axons of regenerated motoneurons, once again increasing the likelihood of accurate reinnervation of target muscles.

Perhaps an even more promising approach to address the routing problem would be to use newly discovered axon guidance cues (including semaphorin3A) to actually guide regenerating axons towards their original targets by mimicking the patterning process that takes place during development. In the developing brachial plexus of the chick embryo, axonal outgrowth indeed leads to successful target finding due to an elaborate interplay between motoneurons and the differential expression of the repulsive guidance cues semaphorin3A and semaphorin3F in the ventral and dorsal parts of the developing limb<sup>65</sup>. Provided that these motoneurons continue to express their respective receptors in the same pattern in the adult human nervous system, it may be possible to use semaphorin3A and 3F to help guide them towards their original targets after a brachial plexus injury. It is currently not known whether such patterning cues are expressed during regeneration in the same way as during development. A relatively simple first step to investigate this in humans would be to perform a comparative gene expression analysis of the parts of the brachial plexus distal to the neuroma. Small segments of the anterior and posterior divisions of the superior trunk are sometimes removed during reconstructive surgery of patients with a neuroma of the superior trunk. Analogous to the experiments performed in Chapter 3, it may be possible to identify axon guidance molecules that are differentially expressed in these respective distal trunks. Influencing the expression of such guidance cues in these trunks will perhaps provide a truly novel way to help regenerating axons find the

right target organ. Naturally, the success of this strategy relies on the assumption that the receptors to axon guidance molecules are differentially expressed by subsets of regenerating adult motoneurons (see above) which will be harder to study in human material and needs to be investigated in animal models<sup>64</sup>. A study comparing gene expression patterns during development and regeneration of the rat sciatic nerve has already shown that approximately half of the regeneration-associated genes were also significantly regulated in development, suggesting that regeneration is indeed partly a recapitulation of development<sup>55</sup>.

### **Viral vectors: highly suitable tools to study peripheral nerve regeneration**

Much has already been said on the maturity and clinical potential of viral vectors in Chapter 1 of this thesis. Indeed, the experiments described in this thesis were motivated in part by recent advances made in the field of gene transfer. Therefore, I will be brief on the advantages of the application of viral vectors, but I would like to reiterate here their tremendous suitability to study peripheral nerve regeneration. The experiments in this thesis and others from our group<sup>150</sup> show that they can be used to transduce Schwann cells of the rat peripheral nerve consistently, durably, in significant numbers in a well-defined area, without interfering with reconstructive surgery or impairing its functional outcome. The relative ease with which new, potentially interesting genes can be cloned into these vectors means that the *in vivo* effect on regeneration of many proteins can now be studied in far more efficient ways than previously possible. This is the first tangible benefit of these vectors and I expect that this will have a remarkable impact on the future direction of peripheral nerve research.

Therapies aimed at influencing peripheral nerve regeneration are, inherently, only required temporarily. Therefore, it is not unreasonable to question whether it is clinically realistic to inject vectors that will permanently insert a therapeutic gene in cells, when the need for a particular protein is only short-term. In addition, there are viral vector-related issues that need to be resolved: (i) the presently available tetracycline-controlled transactivator necessary for regulatable gene expression is of bacterial origin<sup>51</sup> and thus immunogenic<sup>221</sup>, (ii) LV vectors may cause side effects in transduced cells, and the possibility of insertional mutagenesis is repeatedly mentioned in the literature but still not reported<sup>232-234</sup>, while this may be prevented with the application of non-integrating LV vectors<sup>235</sup> and (iii) safer vectors, like adeno-associated viral (AAV) vectors, have so far been unable to transduce Schwann cells. Furthermore, the experiments described in Chapter 4 highlight another potential pitfall of translating results from animal research to the human situation. Whereas the application of LV vector results in the efficient transduction of Schwann cells in the *rat* peripheral nerve, fibroblasts are the predominantly transduced cell type in *human* nerve segments.

Therefore, at least in the near future, the most likely role for viral vectors in the peripheral nerve will remain as powerful research tools. It will take several years to definitively establish the beneficial effect of viral vector-mediated expression of a protein in animal models for peripheral nerve injury. During this time, the safety of viral vectors for human application will have been established in the clinical trials that are currently underway<sup>236</sup> and solutions will probably emerge for the issues described above. Depending on the progress that is made in the field of gene therapy, it may be possible to translate positive effects of viral vectors in animal peripheral nerve injury models directly to a gene therapy approach in humans, or alternatively the therapeutic protein could be delivered by a more conventional method such as biodegradable slow-release capsules<sup>225</sup>. Either way, viral vectors will have a great impact on the development of new therapeutic strategies to enhance the results of peripheral nerve repair, and this is why I consider the results obtained with LV vectors in this thesis to be “winners”.

### **Future perspective: the continuing miniaturization of surgical and diagnostic tools**

As described in the introduction of this thesis, the field of peripheral nerve surgery has steadily evolved since World War II<sup>1</sup>. The introduction of the operating microscope and improved microsuturing techniques has had a great impact on the outcome of surgery. Essentially, the work described in this thesis forms a logical extension of this path of continuous miniaturization by identifying new molecular targets in the human peripheral nerve scar and by developing a viral vector-based strategy to influence the expression of these targets. In this final section, I would also like to mention another form of miniaturization that will likely have a great impact on the clinical practice of nerve repair.

A significant challenge is the absence of a reliable method to determine the degree of injury (and the corresponding need to intervene surgically) in neuroma in continuity lesions. New diagnostic tools are much needed as they would enable the early repair of the most severe nerve injuries. I believe that it will not be long before novel imaging techniques like diffusion-tensor imaging and diffusion-direction-dependent imaging will make it possible to assess the integrity of individual nerve fascicles in the lesioned peripheral nerve<sup>237</sup>, and that this will greatly advance the clinical practice and timing of nerve repair. Another intriguing option stems from the recent development of radio-labelled probes that can be used to detect and quantify collagen in humans *in vivo*<sup>238</sup>. As shown in Chapter 3, the expression of several types of collagen is increased in the peripheral nerve scar at 5 months post-injury; indicating that formation of a fibrotic scar is a process that continues for at least several months. An early assessment of the degree of fibrosis in the peripheral nerve scar may constitute a highly reliable

way to predict the chances of spontaneous recovery of nerve function. The latter putative diagnostic tool may become one of the earliest novel applications based on insights obtained from the field of molecular neurobiology. However, in the future, basic science will surely have an enormous impact on the treatment of peripheral nerve injuries in many other ways as well. I hope that this thesis has provided a glimpse into the many opportunities that are provided by looking at peripheral nerve regeneration through the eyes of a molecular neurobiologist and that this work will be regarded as a small step towards the development of the field of “molecular nerve repair”.



## Nederlandse samenvatting

### Inleiding: de behandeling van zenuwletsel

Perifere zenuwen zijn verantwoordelijk voor de communicatie tussen het centrale zenuwstelsel (hersenen en ruggenmerg) en de rest van het lichaam (huid, spieren en interne organen). De perifere zenuw bestaat uit zenuwcellen (*neuronen*), die met hun cellichaam in, of vlak naast het ruggenmerg liggen en uitlopers (*axonen*) hebben naar hun doelorganen. Deze neuronen geven, door middel van elektrische geleiding over hun axonen, bewegingsopdrachten door van het ruggenmerg naar de spieren (*motoneuronen*) of gevoelsinformatie van het lichaam naar het ruggenmerg (*sensibele neuronen*). Een zenuw is een omhulsel van bindweefsel met daarin duizenden axonen die op hun beurt ieder weer omhuld worden door honderden steuncellen (*Schwanncellen*). Deze Schwanncellen zorgen onder andere voor isolatie en een snelle elektrische geleiding.

Perifere zenuwen kunnen beschadigd of geheel doorsneden worden bij ongelukken of steekwonden. Een ander type van perifeer zenuwletsel kan ontstaan tijdens de geboorte. Als er tijdens de baring aan het hoofd getrokken wordt van een kind dat met een schouder vastzit in het baringskanaal, zal overrekking van de zenuwknop van de arm (*plexus brachialis*) plaatsvinden en kan zelfs een scheuring van de zenuw optreden. Op de plaats van overrekking wordt de continuïteit van de axonen verbroken en ontstaat een litteken dat veel bindweefsel bevat. Perifere zenuwbeschadigingen leiden tot verlamming en gevoelsstoornissen in de aangedane ledematen.

Als perifere zenuwen beschadigd zijn, of doorsneden of afgescheurd, dan blijven het cellichaam en het axon aan de kant van het ruggenmerg (het *proximale* deel) meestal in leven, terwijl het axon aan de kant van het doelorgaan (het *distale* deel) afsterft en door het lichaam opgeruimd wordt. De Schwanncellen in dit distale deel van de zenuwschede beginnen vervolgens verschillende “zenuwgroeistoffen” (*neurotrofe factoren*) te maken. Het beschadigde axon wordt hierdoor tot uitgroei gestimuleerd (er treedt spontaan *regeneratie* op), en kan begeleid worden door de Schwann cellen die op een rijtje klaarliggen tot het doelorgaan. Het axon groeit met een snelheid van 1 tot 5 mm/dag vanuit proximaal naar distaal om uiteindelijk weer opnieuw verbinding te maken met het doelorgaan. In het geval van totale doorsnijding zal de chirurg er snel aan te pas komen om de uiteinden weer aan elkaar te hechten. Zo wordt de functie van de zenuw weer hersteld, hoewel het soms vele maanden kan duren voordat de axonen hun doel bereikt hebben.

Het gebeurt echter regelmatig dat er geen of weinig herstel optreedt. Dit is vooral het geval als de continuïteit van de hele zenuw (inclusief steunweefsel en Schwann cellen) verwoest is, waardoor een gat ontstaat dat niet te overbruggen is door rege-



nererende axonen, of omdat de uitgroei van axonen belemmerd wordt door ernstige littekenvorming. In die gevallen wordt er operatief ingegrepen. Soms is het nodig om eerst littekenweefsel te verwijderen, waarna of de zenuwuiteinden aan elkaar worden genaaid of - als dat niet mogelijk is - het onstane defect wordt opgevuld met een “bruggetje” van een zenuw die elders verwijderd is. Hiervoor wordt meestal de nervus suralis opgeofferd, een gevoelszenuw in de kuit die verwijderd kan worden zonder dat dit leidt tot ernstige beperkingen. Dit zenuwbruggetje bevat dus geen intacte neuronen of axonen (die worden bij het verwijderen doorgenomen en gaan verloren), maar wel Schwann cellen die netjes opgelijnd in de zenuw liggen en op die manier de regenererende axonen weer naar hun juiste doelorgaan kunnen leiden. Dit type hersteloperatie leidt meestal tot regeneratie en functieherstel. Het herstel is echter nooit volledig en patiënten met een ernstig zenuwletsel houden dus altijd levenslange functionele beperkingen in de vorm van verlammingen en/of gevoelsstoornissen.

### **Het laboratorium: bakermat voor nieuwe therapieën?**

Sinds de eerste zenuwhersteloperaties werden uitgevoerd, vanaf het begin van de vorige eeuw, zijn de microchirurgische operatietechnieken enorm verbeterd en uitontwikkeld. Toch is het herstel na een operatie is niet optimaal. Verdere verbeteringen in de prognose van patiënten met ernstige zenuwletsels zullen dus moeten voortvloeien uit de toepassing van nieuwe inzichten en recente technieken uit het laboratorium. In **Hoofdstuk 1** wordt beschreven dat de toepassing van genterapie zo'n nieuwe, veelbelovende techniek is.

Genterapie houdt in dat er genetisch materiaal wordt ingebracht in de cellen van een patiënt met als doel lokaal een therapeutisch eiwit “tot expressie te brengen” om een bepaalde aandoening te behandelen. “*Tot expressie*” wil zeggen, het ingebrachte gen wordt afgelezen en het bijbehorende eiwit wordt geproduceerd als lokaal “geneesmiddel”. Het inbrengen van dit genetische materiaal kan op vele manieren, maar een van de meest gebruikte methoden bestaat uit de toepassing van *virale vectoren*. Deze aanpak berust op het natuurlijke vermogen van virussen om cellen binnen te dringen en daar hun genetische materiaal achter te laten. Virale vectoren zijn virusdeeltjes waarbij alle ziekmakende virusgenen vervangen kunnen zijn door een therapeutisch gen naar keuze. Door het ontbreken van virusgenen kunnen deze vectordeeltjes zich niet voortplanten of ziekteverschijnselen veroorzaken. Deze vectoren dringen wel nog een cel binnen en laten daar het gen achter. Het inbouwen van een nieuw of een extra gen in een cel met behulp van virale vectoren wordt “*transductie*” genoemd en het betreffende gen een “*transgen*”.

De meest voor de hand liggende toepassing van genterapie is in de behandeling van aangeboren genetische aandoeningen, waarbij een “normaal” gen in de cel wordt gebracht om de functie over te nemen van het defecte of afwezige gen. Er zijn echter

verschillende redenen waarom genterapie ook in het beschadigde zenuwstelsel veel potentie heeft. Er zijn vele eiwitten bekend die een positief effect hebben op de uitgroei van axonen (bijvoorbeeld de hierboven genoemde neurotrofe factoren), maar deze eiwitten hebben vaak teveel bijwerkingen als ze in het hele lichaam (*systemisch*) toegediend worden, bijvoorbeeld door inspuiting in de bloedbaan. Ook kun je ze niet in pilvorm toedienen omdat ze, net als alle eiwitten al in de maag worden verteerd. Bovendien dringen deze eiwitten slecht door in zenuwweefsel als ze lokaal worden geïnjecteerd en worden ze meestal snel (binnen enkele minuten) door het lichaam afgebroken. Zeer regelmatige lokale toediening of chronische infusie is praktisch gezien niet haalbaar. Het grote voordeel van de toepassing van virale vectoren is dat je met één eenmalige vectorinjectie de cellen van het lichaam zelf kan aanzetten tot de produktie van het therapeutische eiwit, wat leidt tot een langdurige, plaatselijke afgifte. Problemen zoals bijwerkingen op andere plaatsen in het lichaam en de noodzaak van meerdere toedieningen zouden daarmee dus tot het verleden kunnen behoren en hierdoor zou het gewenste effect van de neurotrofe factoren in theorie veel krachtiger kunnen zijn.

De ontwikkeling van veilige virale vectoren heeft de laatste jaren een enorme vlucht genomen. Inmiddels zijn er over de hele wereld honderden mensen behandeld met virale vectoren voor een hele reeks aandoeningen, van rheumatoïde arthritis tot de ziekte van Alzheimer, tot dusverre nagenoeg zonder bijwerkingen. Er zijn verschillende typen virale vectoren die geschikt zijn voor toepassing in mensen. In de proeven beschreven in dit proefschrift is gewerkt met zogenoemde *lentivirale* (LV) vectoren.

### **De doelstelling van het onderzoek**

In dit proefschrift heb ik geprobeerd twee aan elkaar verwante vragen te beantwoorden: 1) Waarom remt littekenvorming ter plaatse van het zenuwletsel - zoals hierboven beschreven - het functionele herstel? Ik heb op moleculair niveau naar een verklaring gezocht voor dit fenomeen, door te kijken of er in het litteken genen tot expressie worden gebracht die een rol spelen bij zenuwuitgroei (**Hoofdstukken 2 en 3**). De expressie van deze genen zou dan in theorie met behulp van virale vectoren aan- of uitgezet kunnen worden, maar dan moet het wel mogelijk zijn om deze vectoren in zenuwweefsel toe te passen. Hieruit volgt de onderzoeksvraag: 2) Is het mogelijk om, met behulp van virale vectoren, cellen van de humane zenuw genetisch te modificeren (transduceren) om zo lokaal en langdurig de expressie van een therapeutisch eiwit te induceren (**Hoofdstuk 4**) en leidt de virale vector-gemedieerde expressie van een neurotrofe factor tot verbeterd herstel van de doorsneden en opnieuw gehechte zenuw (**Hoofdstukken 5 en 6**)?

## Het zenuwlitteken bevat verschillende eiwitten die de axonuitgroei beïnvloeden

Om de eigenschappen van het zenuwlitteken te bestuderen, hebben we onderzoek gedaan op humaan zenuwlittekenweefsel dat operatief verwijderd was. Het betrof hier materiaal van patiëntjes die tijdens de geboorte een ernstig plexus brachialisletsel hadden opgelopen, waarbij er 5 maanden na de geboorte nog geen functieherstel was opgetreden. Bij deze patiënten werd daarom een hersteloperatie uitgevoerd waarbij, na verwijdering van het littekenweefsel, zenuwen uit de kuit in het ontstane defect zijn gebracht om uitgroei van axonen naar de doelorganen van de arm te geleiden (zoals hierboven beschreven). Om te beginnen onderzochten wij of het verwijderde littekenweefsel het eiwit semaphorine 3A bevat (**Hoofdstuk 2**). Dit eiwit remt de uitgroei van axonen sterk af. Het komt ook voor in het litteken dat ontstaat bij beschadigingen van het ruggenmerg (dwarslaesies) en is een van de oorzaken van het gebrek aan herstel dat optreedt bij mensen met een dwarslaesie. Een voorbeeld: nadat de werking van semaphorine 3A was geblokkeerd bij volledig verlamde ratten met een dwarslaesie, trad er regeneratie op waardoor de verlamming gedeeltelijk verdween<sup>78</sup>. Wij ontdekten dat in het litteken van de perifere zenuw inderdaad semaphorine 3A wordt geproduceerd (net als in het beschadigde ruggenmerg), dat dit om bundels van uitgroeiende axonen heen ligt en dat het een uitgroeibelemerende functie heeft.

Aangemoedigd door deze ontdekking hebben we vervolgens een bredere aanpak gevolgd door de genexpressie van meerdere genen tegelijk te analyseren (**Hoofdstuk 3**). Met behulp van een “micro-array”, ook wel DNA-chip genoemd, kan in één experiment de expressie van 44.000 genen in het litteken worden bekeken en vergeleken met die van een normale zenuw. Uit deze analyse bleek dat er diverse genen in het litteken een verhoogde expressie laten zien die bekend waren een rol te spelen bij littekenvorming en en bij het sturen/remmen van axon-uitgroei. Deze gegevens tonen aan dat er zelfs 5 maanden na het oorspronkelijke letsel nog littekenvorming plaatsvindt en dat de regeneratie van beschadigde axonen beïnvloed wordt door een reeks verschillende eiwitten. Door de expressie van dit soort eiwitten te beïnvloeden (bijvoorbeeld door het stilleggen van de expressie van semaphorine 3A), zouden we in de toekomst kunnen proberen het herstel van de beschadigde zenuw te verbeteren.

## Virale vectoren: een nieuw instrument voor de neurochirurg?

Het tweede doel van dit proefschrift was om te kijken of virale vectoren die een gen bevatten dat codeert voor bepaalde neurotrofe factoren de regeneratie van de perifere zenuw kon bevorderen. Als eerste hebben we in **Hoofdstuk 4** onderzocht of het mogelijk is om een gen in te bouwen in de steuncellen van humane stukjes zenuw. Zoals hierboven beschreven, wordt er bij zenuwhersteloperaties vaak gebruik gemaakt van de nervus suralis, die dan dient als zenuwbruggetje. De kleine stukjes zenuw die over-

bleven hebben we gebruikt voor onderzoek. Deze stukjes kunnen gedurende enkele dagen in leven worden gehouden in een schaalpje met kweekmedium en hierdoor kon onderzocht worden of ze met behulp van een LV-vector genetisch waren te modificeren. Uiteindelijk lukte het, door injectie van de LV-vector, een transgen in de zenuw tot expressie te laten brengen. Dit kon eenvoudig waargenomen worden doordat het een gen betrof voor “green fluorescent protein”, waardoor alle cellen die het tot expressie brachten fluorescent groen werden en makkelijk zichtbaar zijn onder de microscoop. Een opvallende bevinding was, dat het niet de Schwanncellen waren die groen werden, maar vooral cellen in het omhullende bindweefsel, zogenoemde fibroblasten. Dit was onverwacht, aangezien dezelfde LV-vector in rattenzenuwen leidt tot transductie van voornamelijk Schwanncellen. Deze bevinding onderstreept hoe belangrijk het is om, naast dierproeven, ook onderzoek op humaan materiaal te doen omdat de resultaten van dierproeven niet altijd één op één te vertalen zijn naar de humane situatie.

Vervolgens hebben we onderzocht of het mogelijk was de expressie van de neurotrofe factor “nerve growth factor” (NGF) te induceren in deze humane zenuwstukjes. Dit bleek mogelijk en het zo (door fibroblasten) geproduceerde NGF was in staat de uitgroei van axonen te bevorderen in een kweekschalpje. Het is dus technisch mogelijk om met behulp van een virale vector de productie van werkzaam NGF in de humane nervus suralis flink te verhogen. Het voordeel van het hier beschreven protocol is dat het in theorie toegepast kan worden in combinatie met zenuwherstelchirurgie, zonder dat er iets hoeft te veranderen aan de dagelijkse praktijk van de operatie zoals hij momenteel wordt uitgevoerd. De chirurg neemt de nervus suralis uit, het virus wordt in de zenuw geïnjecteerd en direct daarna wordt deze geïmplantieerd als zenuwbruggetje. De vraag is natuurlijk of een zodanig lokaal verhoogde productie van NGF ook het herstel van de perifere zenuw bevordert. Dat hebben we dan ook onderzocht in de volgende hoofdstukken, gebruik makend van rattenmodellen voor zenuw schade. Als eerste hebben we onderzoek gedaan naar een zeer ernstig type zenuwletsel, de zogenoemde wortelavulsie. Bij wortelavulsies wordt de zenuw uit het ruggenmerg getrokken. De cellichamen van de motoneuronen in het ruggenmerg, waarvan het axon nu afgerukt is, zijn daarom niet in staat hun axonen te laten regenereren in die wortel, immers het contact is volledig verbroken. Ze worden in de loop van enkele weken steeds kleiner (*atrofie*) en gaan na verloop van tijd deels dood. Door het herimplanteren van de afgerukte zenuwwortel in het ruggenmerg ontstaat er wel weer de mogelijkheid tot heruitgroei en kan in principe de motoneuronatrofie gedeeltelijk voorkomen worden. Om deze redenen zijn er in de wereld enkele chirurgen die deze operatie bij mensen uitvoeren, maar dit is zeer controversieel. Over het algemeen worden de risico's van extra schade van een dergelijke operatie te groot geacht in verhouding tot het (slechts een enkele keer optredende) geringe functieherstel. In **Hoofdstuk 5** hebben we in een rattenmodel onderzocht of dat herstel te verbeteren is

met gentherapie voor neurotrofe factoren. Hiertoe hebben dezelfde “risicovolle” reïmplantatie uitgevoerd in een rattenmodel, maar voordat we de wortels reïmplanteerden hebben we ze eerst geïnjecteerd met LV-vectoren die coderen voor de eiwitten “brain-derived neurotrophic factor” (*BDNF*) of “glial cell line-derived neurotrophic factor” (*GDNF*). Hiermee hoopten we de atrofie van de motoneuronen te voorkomen en de uitgroei van de axonen de wortel in te verbeteren. De injectie van een LV-vector leidde tot de langdurige transductie van Schwanncellen in de wortel tot minstens 16 weken. Belangrijker nog was dat LV-GDNF de motoneuronatrofie volledig bleek te kunnen voorkomen en dat er meer axonen de geïmplanteerde wortel ingroeiden. Helaas werd dit bijzondere succes overschaduwed door een onverwacht bij-effect. Door de LV-vector gemedieerde expressie werd de GDNF concentratie plaatselijk zo hoog, dat de axonen die de wortel ingegroeid waren “bleven hangen” in de wortel, precies op de plek waar LV-GDNF geïnjecteerd was en de GDNF concentratie dus het hoogst was. In de loop van 16 weken ontstonden er op deze plek dikke kluwens van axonen die continue in cirkels leken te groeien. Dit fenomeen werd het “candy store effect” genoemd, omdat het doet denken aan kinderen die niet weg willen uit de snoepwinkel. Verderop in de zenuw, dichtbij de spieren waar de axonen verbinding mee moesten maken, bleek het aantal axonen dan ook *verlaagd* na toepassing van LV-GDNF, waardoor het oorspronkelijke doel, het verbeteren van de functionele herstel na een wortelavulsie, niet werd behaald.

Waar we ons in hoofdstuk 5 specifiek richtten op de uitgroei van motoneuronen, hebben we in **Hoofdstuk 6** gekeken naar een gemengde zenuw, dat wil zeggen een zenuw die axonen van zowel bewegings- (moto)neuronen als gevoels- (sensibele) neuronen bevat, de nervus ischiadicus van de rat. Deze zenuw werd doorsneden en weer aan elkaar gehecht zoals dat in de kliniek ook zou gebeuren bij patiënten met een zenuwdoorsnijding. Vervolgens injecteerden we LV-NGF of LV-GDNF distaal van de plaats van reparatie, dus in het deel van de zenuw waar de doorsneden axonen naartoe moeten groeien. Deze opzet stelde ons in staat om de regeneratieve respons van motoneuronen en sensibele neuronnen op deze factoren met elkaar te vergelijken. Er zijn verschillende soorten sensibele neuronnen die betrokken zijn bij de registratie van pijn, en die zijn onder andere te onderscheiden doordat de ene populatie gevoelig is voor NGF en de andere voor GDNF. We konden dus in deze proef ook kijken hoe de regeneratie van deze verschillende populaties was na de langdurige LV-vector gemedieerde lokale verhoging van de concentratie van deze stoffen.

Net als in hoofdstuk 5 bleek dat de Schwanncellen in de zenuw getransduceerd werden en grote hoeveelheden NGF en GDNF begonnen te produceren. Verder leidde ook hier weer het lokaal verhogen van de GDNF expressie ertoe dat de axonen van motoneuronen bleven hangen, het inmiddels bekende “candy store effect”, maar de sensibele axonen niet. LV-NGF had dit effect niet, maar gaf ook geen verbetering

van de regeneratie van motoneuronen. De verhoogde concentraties NGF en GDNF hadden geen significante effecten op het totaal aantal geregenereerde sensibele neuronen, maar er bleken wel veranderingen op te treden in de verschillende populaties (NGF- en GDNF-specifieke) pijn-registrerende neuronen. Dat leidde ook tot functionele effecten: bij LV-NGF toepassing bleek de pijnperceptie in het aangedane gebied ongeveer 10% sneller te herstellen, terwijl er literatuurwijzingen waren dat LV-GDNF juist een pijnverminderend effect zou moeten hebben. Het gevonden verschil tussen de regeneratieve respons van motoneuronen en sensibele neuronen op GDNF (wel *vs* geen “candy store effect”) en het differentiele effect van NGF en GDNF op de verschillende pijngevoelige populaties neuronen zijn beide interessante bevindingen. Echter, aangezien deze aanpak niet direct geleid heeft tot een concrete verbetering van de uitgroei van beschadigde axonen, zal er eerst nog uitgebreider onderzoek gedaan moeten worden voordat deze bevindingen vertaald kunnen worden naar klinische therapieën die het functionele herstel voor de patiënt verbeteren.

### **Toekomstperspectief: verdere miniaturisatie van de zenuwchirurgie?**

In Hoofdstuk 7, waarin ik de resultaten samenvat en het klinische probleem nogmaals kort bespreek, probeer ik een oordeel te vellen over de diverse nieuwe bevindingen van dit onderzoek voor een mogelijk toekomstige toepassing in de perifere zenuwneurochirurgie. De toepassing van neurotrofe factoren ter verbetering van de regeneratie is in de huidige opzet een minder succesvolle aanpak gebleken. De neuronen van de perifere zenuw zijn uit zichzelf goed in staat om over lange afstanden te regenereren. Ook nieuwe, nog ongepubliceerde resultaten uit ons lab suggereren dat de expressie van diverse neurotrofe factoren al is geoptimaliseerd om de continue uitgroei van axonen te waarborgen. Zoals we zagen in hoofdstukken 5 en 6 heeft het lokaal verhogen van de concentratie van deze neurotrofe factoren (of dit nu met virale vectoren of op een andere manier gebeurt) in onze proeven voornamelijk een averechts effect gehad, waarschijnlijk omdat hiermee de natuurlijke respons en de delicate balans van groeistoffen die nodig is voor de lange-afstandsregeneratie van axonen verstoord wordt. Wel zouden neurotrofe factoren toegepast kunnen worden om bijvoorbeeld de atrofie van motoneuronen te voorkomen om die cellen beter in staat te stellen tot axonregeneratie.

Wellicht wekt het verbazing dat de beschadigde axonen kennelijk ook zonder hulp van buitenaf in staat zijn om over lange afstanden opnieuw uit te groeien, terwijl er vaak nauwelijks functioneel herstel optreedt. In hoofdstuk 7 beargumenteer ik dat een belangrijke oorzakelijke factor is dat regenererende axonen wel uitgroeien, maar niet in staat zijn het juiste eindorgaan te vinden. De ontdekking van semaphorine<sub>3A</sub> (hoofdstuk 2) en andere “axon guidance” moleculen (hoofdstuk 3) is daarom zeer interessant, omdat deze misschien gebruikt kunnen worden om richting te geven

aan uitgroeiende axonen en de kans te verkleinen dat ze verbinding maken met het verkeerde doelorgaan. De gebleken mogelijkheid van toepassing van virale vectoren voor de perifere zenuw is een ander positief resultaat omdat hiermee op zeer efficiënte wijze het effect van elk willekeurig eiwit (dus niet alleen neurotrofe factoren, maar ook bijvoorbeeld “axon guidance” moleculen) op regeneratie onderzocht kan worden in verschillende proefdiermodellen. De veiligheid en toepasbaarheid van deze vectoren wordt momenteel onderzocht in grootschalige “clinical trials”, waardoor het in de toekomst wellicht mogelijk wordt om in laboratorium behaalde resultaten met vectoren direct te vertalen naar een genterapeutisch behandeling bij mensen.

Zoals beschreven heeft de chirurgie van de perifere zenuw een enorme technische verfijning doorgemaakt. In feite hebben we met dit proefschrift een logische vervolgstap gezet door het herstel van de zenuw op nog kleinere (moleculaire) schaal te bestuderen en te beïnvloeden met virale vectoren. Hoewel het duidelijk is dat er nog veel werk verricht moet worden voordat de virale vectoren als zeer verfijnd instrument opgenomen zullen worden in het arsenaal van de neurochirurg, hoop ik dat dit proefschrift een kleine bijdrage zal leveren aan het ontstaan van een nieuw vakgebied: de “moleculaire zenuwchirurgie”.



## References

1. Sunderland, S. *Nerve injuries and their repair: A Critical Appraisal*, (Churchill Livingstone, Melbourne, 1991).
2. Lundborg, G. A 25-year perspective of peripheral nerve surgery: evolving neuroscientific concepts and clinical significance. *J Hand Surg [Am]* **25**, 391-414 (2000).
3. MacKinnon, S.E. & Dellon, A.L. *Surgery of the Peripheral Nerve*, (Thieme Medical Publishers, Inc., New York, 1988).
4. Maggi, S.P., Lowe, J.B., 3rd & Mackinnon, S.E. Pathophysiology of nerve injury. *Clin Plast Surg* **30**, 109-126 (2003).
5. Badalamente, M.A., Hurst, L.C., Ellstein, J. & McDevitt, C.A. The pathobiology of human neuromas: an electron microscopic and biochemical study. *J Hand Surg [Br]* **10**, 49-53 (1985).
6. Morgenstern, D.A., *et al.* Expression and glycanation of the NG2 proteoglycan in developing, adult, and damaged peripheral nerve. *Mol Cell Neurosci* **24**, 787-802 (2003).
7. Nguyen, Q.T., Sanes, J.R. & Lichtman, J.W. Pre-existing pathways promote precise projection patterns. *Nat Neurosci* **5**, 861-867 (2002).
8. Gramsbergen, A., J, I.J.-P. & Meek, M.F. Sciatic nerve transection in the adult rat: abnormal EMG patterns during locomotion by aberrant innervation of hindleg muscles. *Exp Neurol* **161**, 183-193 (2000).
9. Boyd, J.G. & Gordon, T. Neurotrophic factors and their receptors in axonal regeneration and functional recovery after peripheral nerve injury. *Mol Neurobiol* **27**, 277-324 (2003).
10. Pezet, S. & McMahon, S.B. Neurotrophins: Mediators and Modulators of Pain. *Annu Rev Neurosci* **29**, 507-538 (2006).
11. Hoke, A. Mechanisms of Disease: what factors limit the success of peripheral nerve regeneration in humans? *Nat Clin Pract Neurol* **2**, 448-454 (2006).
12. Hoke, A., *et al.* Schwann cells express motor and sensory phenotypes that regulate axon regeneration. *J Neurosci* **26**, 9646-9655 (2006).
13. Apfel, S.C., *et al.* Efficacy and safety of recombinant human nerve growth factor in patients with diabetic polyneuropathy: A randomized controlled trial. rhNGF Clinical Investigator Group. *Jama* **284**, 2215-2221 (2000).
14. Blesch, A. & Tuszynski, M.H. Spontaneous and neurotrophin-induced axonal plasticity after spinal cord injury. *Prog Brain Res* **137**, 415-423 (2002).
15. Tria, M.A., Fusco, M., Vantini, G. & Mariot, R. Pharmacokinetics of nerve growth factor (NGF) following different routes of administration to adult rats. *Exp Neurol* **127**, 178-183 (1994).
16. Dittrich, F., *et al.* Pharmacokinetics of intrathecally applied BDNF and effects on spinal motoneurons. *Exp Neurol* **141**, 225-239 (1996).
17. Kemp, S.W., Walsh, S.K., Zochodne, D.W. & Midha, R. A novel method for establishing daily in vivo concentration gradients of soluble nerve growth factor (NGF). *J Neurosci Methods* **165**, 83-88 (2007).
18. Jubran, M. & Widenfalk, J. Repair of peripheral nerve transections with fibrin sealant containing neurotrophic factors. *Exp Neurol* **181**, 204-212 (2003).
19. Yin, Q., Kemp, G.J., Yu, L.G., Wagstaff, S.C. & Frostick, S.P. Neurotrophin-4 delivered by fibrin glue promotes peripheral nerve regeneration. *Muscle Nerve* **24**, 345-351 (2001).
20. Young, C., Miller, E., Nicklous, D.M. & Hoffman, J.R. Nerve growth factor and neurotrophin-3 affect functional recovery following peripheral nerve injury differently. *Restor Neurol Neurosci* **18**, 167-175 (2001).

## REFERENCES

21. Boyd, J.G. & Gordon, T. Glial cell line-derived neurotrophic factor and brain-derived neurotrophic factor sustain the axonal regeneration of chronically axotomized motoneurons in vivo. *Exp Neurol* **183**, 610-619 (2003).
22. Boyd, J.G. & Gordon, T. A dose-dependent facilitation and inhibition of peripheral nerve regeneration by brain-derived neurotrophic factor. *Eur J Neurosci* **15**, 613-626 (2002).
23. Barati, S., *et al.* GDNF gene delivery via the p75(NTR) receptor rescues injured motor neurons. *Exp Neurol* **202**, 179-188 (2006).
24. Blits, B., *et al.* Rescue and sprouting of motoneurons following ventral root avulsion and re-implantation combined with intraspinal adeno-associated viral vector-mediated expression of glial cell line-derived neurotrophic factor or brain-derived neurotrophic factor. *Exp Neurol* **189**, 303-316 (2004).
25. Timmer, M., Robben, S., Muller-Ostermeyer, F., Nikkhah, G. & Grothe, C. Axonal regeneration across long gaps in silicone chambers filled with Schwann cells overexpressing high molecular weight FGF-2. *Cell Transplant* **12**, 265-277 (2003).
26. Haastert, K., Lipokatic, E., Fischer, M., Timmer, M. & Grothe, C. Differentially promoted peripheral nerve regeneration by grafted Schwann cells over-expressing different FGF-2 isoforms. *Neurobiol Dis* **21**, 138-153 (2006).
27. Mann, R., Mulligan, R.C. & Baltimore, D. Construction of a retrovirus packaging mutant and its use to produce helper-free defective retrovirus. *Cell* **33**, 153-159 (1983).
28. Li, Q., Ping, P., Jiang, H. & Liu, K. Nerve conduit filled with GDNF gene-modified Schwann cells enhances regeneration of the peripheral nerve. *Microsurgery* **26**, 116-121 (2006).
29. Gravvanis, A.I., *et al.* Effect of genetically modified Schwann cells with increased motility in end-to-side nerve grafting. *Microsurgery* **25**, 423-432 (2005).
30. Geller, A.I., Keyomarsi, K., Bryan, J. & Pardee, A.B. An efficient deletion mutant packaging system for defective herpes simplex virus vectors: potential applications to human gene therapy and neuronal physiology. *Proc Natl Acad Sci U S A* **87**, 8950-8954 (1990).
31. Ho, D.Y. & Mocarski, E.S. Herpes simplex virus latent RNA (LAT) is not required for latent infection in the mouse. *Proc Natl Acad Sci U S A* **86**, 7596-7600 (1989).
32. Hendriks, W.T., Ruitenbergh, M.J., Blits, B., Boer, G.J. & Verhaagen, J. Viral vector-mediated gene transfer of neurotrophins to promote regeneration of the injured spinal cord. *Prog Brain Res* **146**, 451-476 (2004).
33. Senn, C., Fraefel, C. & Breakefield, X.O. HSV amplicon vectors for gene delivery to the nervous system. in *Gene therapy in the central Nervous system* (eds. Kaplitt, M.G. & During, M.J.) 25-38 (Academic Press, 2006).
34. Dijkhuizen, P.A., *et al.* Adenoviral vector-mediated gene delivery to injured rat peripheral nerve. *J Neurotrauma* **15**, 387-397 (1998).
35. Watanabe, T.S., *et al.* Adenoviral gene transfer in the peripheral nervous system. *J Orthop Sci* **11**, 64-69 (2006).
36. Moro, K., *et al.* Adenoviral gene transfer of BDNF and GDNF synergistically prevent motoneuron loss in the nucleus ambiguus. *Brain Res* **1076**, 1-8 (2006).
37. Araki, K., *et al.* Adenoviral GDNF gene transfer enhances neurofunctional recovery after recurrent laryngeal nerve injury. *Gene Ther* **13**, 296-303 (2006).
38. Sakamoto, T., *et al.* Adenoviral gene transfer of GDNF, BDNF and TGF beta 2, but not CNTF, cardiotrophin-1 or IGF1, protects injured adult motoneurons after facial nerve avulsion. *J Neurosci Res* **72**, 54-64 (2003).
39. Wu, Z., Asokan, A. & Samulski, R.J. Adeno-associated virus serotypes: vector toolkit for human gene therapy. *Mol Ther* **14**, 316-327 (2006).

40. Xu, Y., Gu, Y., Wu, P., Li, G.W. & Huang, L.Y. Efficiencies of transgene expression in nociceptive neurons through different routes of delivery of adeno-associated viral vectors. *Hum Gene Ther* **14**, 897-906 (2003).
41. Kaplitt, M.G., *et al.* Safety and tolerability of gene therapy with an adeno-associated virus (AAV) borne GAD gene for Parkinson's disease: an open label, phase I trial. *Lancet* **369**, 2097-2105 (2007).
42. Naldini, L., *et al.* In vivo gene delivery and stable transduction of nondividing cells by a lentiviral vector. *Science* **272**, 263-267 (1996).
43. Jakobsson, J., Ericson, C., Rosenqvist, N. & Lundberg, C. Lentiviral vectors. *Int Rev Neurobiol* **55**, 111-122 (2003).
44. Mazarakis, N.D., *et al.* Rabies virus glycoprotein pseudotyping of lentiviral vectors enables retrograde axonal transport and access to the nervous system after peripheral delivery. *Hum Mol Genet* **10**, 2109-2121 (2001).
45. Azzouz, M., *et al.* VEGF delivery with retrogradely transported lentivector prolongs survival in a mouse ALS model. *Nature* **429**, 413-417 (2004).
46. Kaspar, B.K., Llado, J., Sherkat, N., Rothstein, J.D. & Gage, F.H. Retrograde viral delivery of IGF-1 prolongs survival in a mouse ALS model. *Science* **301**, 839-842 (2003).
47. Apfel, S.C. Is the therapeutic application of neurotrophic factors dead? *Ann Neurol* **51**, 8-11 (2002).
48. Moore, K., MacSween, M. & Shoichet, M. Immobilized concentration gradients of neurotrophic factors guide neurite outgrowth of primary neurons in macroporous scaffolds. *Tissue Eng* **12**, 267-278 (2006).
49. Taylor, L., Jones, L., Tuszyński, M.H. & Blesch, A. Neurotrophin-3 gradients established by lentiviral gene delivery promote short-distance axonal bridging beyond cellular grafts in the injured spinal cord. *J Neurosci* **26**, 9713-9721 (2006).
50. Gossen, M. & Bujard, H. Tight control of gene expression in mammalian cells by tetracycline-responsive promoters. *Proc Natl Acad Sci U S A* **89**, 5547-5551 (1992).
51. Blesch, A., *et al.* Regulated lentiviral NGF gene transfer controls rescue of medial septal cholinergic neurons. *Mol Ther* **11**, 916-925 (2005).
52. Blesch, A. & Tuszyński, M.H. Transient growth factor delivery sustains regenerated axons after spinal cord injury. *J Neurosci* **27**, 10535-10545 (2007).
53. Jimenez, C.R., *et al.* Proteomics of the injured rat sciatic nerve reveals protein expression dynamics during regeneration. *Mol Cell Proteomics* **4**, 120-132 (2005).
54. Stam, F.J., *et al.* Identification of candidate transcriptional modulators involved in successful regeneration after nerve injury. *Eur J Neurosci* **25**, 3629-3637 (2007).
55. Bosse, F., Hasenpusch-Theil, K., Kury, P. & Müller, H.W. Gene expression profiling reveals that peripheral nerve regeneration is a consequence of both novel injury-dependent and reactivated developmental processes. *J Neurochem* **96**, 1441-1457 (2006).
56. Pondaag, W., Malessy, M.J., van Dijk, J.G. & Thomeer, R.T. Natural history of obstetric brachial plexus palsy: a systematic review. *Dev Med Child Neurol* **46**, 138-144 (2004).
57. Fawcett, J.W. Overcoming inhibition in the damaged spinal cord. *J Neurotrauma* **23**, 371-383 (2006).
58. Scarlato, M., Ara, J., Bannerman, P., Scherer, S. & Pleasure, D. Induction of neuropilins-1 and -2 and their ligands, Sema3A, Sema3F, and VEGF, during Wallerian degeneration in the peripheral nervous system. *Exp Neurol* **183**, 489-498 (2003).
59. Ara, J., Bannerman, P., Hahn, A., Ramirez, S. & Pleasure, D. Modulation of sciatic nerve expression of class 3 semaphorins by nerve injury. *Neurochem Res* **29**, 1153-1159 (2004).
60. Pasterkamp, R.J., Giger, R.J. & Verhaagen, J. Regulation of semaphorin III/collapsin-1 gene expression during peripheral nerve regeneration. *Exp Neurol* **153**, 313-327 (1998).

## REFERENCES

61. Lindholm, T., *et al.* Semaphorin and neuropilin expression in motoneurons after intraspinal motoneuron axotomy. *Neuroreport* **15**, 649-654 (2004).
62. Tang, X.Q., Tanelian, D.L. & Smith, G.M. Semaphorin3A inhibits nerve growth factor-induced sprouting of nociceptive afferents in adult rat spinal cord. *J Neurosci* **24**, 819-827 (2004).
63. Reza, J.N., Gavazzi, I. & Cohen, J. Neuropilin-1 is expressed on adult mammalian dorsal root ganglion neurons and mediates semaphorin3a/collapsin-1-induced growth cone collapse by small diameter sensory afferents. *Mol Cell Neurosci* **14**, 317-326 (1999).
64. Huber, A.B., *et al.* Distinct roles for secreted semaphorin signaling in spinal motor axon guidance. *Neuron* **48**, 949-964 (2005).
65. Malessy, M.J., van Duinen, S.G., Feirabend, H.K. & Thomeer, R.T. Correlation between histopathological findings in C-5 and C-6 nerve stumps and motor recovery following nerve grafting for repair of brachial plexus injury. *J Neurosurg* **91**, 636-644 (1999).
66. Hope, A.D., *et al.* Alzheimer's associated variant ubiquitin causes inhibition of the 26S proteasome and chaperone expression. *J Neurochem* **86**, 394-404 (2003).
67. Vandesompele, J., *et al.* Accurate normalization of real-time quantitative RT-PCR data by geometric averaging of multiple internal control genes. *Genome Biol* **3**, RESEARCH0034 (2002).
68. Giger, R.J., Pasterkamp, R.J., Heijnen, S., Holtmaat, A.J. & Verhaagen, J. Anatomical distribution of the chemorepellent semaphorin III/collapsin-1 in the adult rat and human brain: predominant expression in structures of the olfactory-hippocampal pathway and the motor system. *J Neurosci Res* **52**, 27-42 (1998).
69. Mason, M.R., Lieberman, A.R., Grenningloh, G. & Anderson, P.N. Transcriptional upregulation of SCG10 and CAP-23 is correlated with regeneration of the axons of peripheral and central neurons in vivo. *Mol Cell Neurosci* **20**, 595-615 (2002).
70. De Wit, J., De Winter, F., Klooster, J. & Verhaagen, J. Semaphorin 3A displays a punctate distribution on the surface of neuronal cells and interacts with proteoglycans in the extracellular matrix. *Mol Cell Neurosci* **29**, 40-55 (2005).
71. Platika, D., Boulos, M.H., Baizer, L. & Fishman, M.C. Neuronal traits of clonal cell lines derived by fusion of dorsal root ganglia neurons with neuroblastoma cells. *Proc Natl Acad Sci U S A* **82**, 3499-3503 (1985).
72. Brummelkamp, T.R., Bernards, R. & Agami, R. A system for stable expression of short interfering RNAs in mammalian cells. *Science* **296**, 550-553 (2002).
73. Pasterkamp, R.J., *et al.* Expression of the gene encoding the chemorepellent semaphorin III is induced in the fibroblast component of neural scar tissue formed following injuries of adult but not neonatal CNS. *Mol Cell Neurosci* **13**, 143-166 (1999).
74. De Winter, F., *et al.* Injury-induced class 3 semaphorin expression in the rat spinal cord. *Exp Neurol* **175**, 61-75 (2002).
75. de Wit, J., Toonen, R.F., Verhaagen, J. & Verhage, M. Vesicular trafficking of semaphorin 3A is activity-dependent and differs between axons and dendrites. *Traffic* **7**, 1060-1077 (2006).
76. Snow, D.M., Smith, J.D., Cunningham, A.T., McFarlin, J. & Goshorn, E.C. Neurite elongation on chondroitin sulfate proteoglycans is characterized by axonal fasciculation. *Exp Neurol* **182**, 310-321 (2003).
77. Frostick, S.P., Yin, Q. & Kemp, G.J. Schwann cells, neurotrophic factors, and peripheral nerve regeneration. *Microsurgery* **18**, 397-405 (1998).
78. Kaneko, S., *et al.* A selective Sema3A inhibitor enhances regenerative responses and functional recovery of the injured spinal cord. *Nat Med* **12**, 1380-1389 (2006).
79. Sinis, N., *et al.* Neuroma formation in a rat median nerve model: influence of distal stump and muscular coating. *Plast Reconstr Surg* **119**, 960-966 (2007).
80. van Tijn, P., *et al.* Dose-dependent inhibition of proteasome activity by a mutant ubiquitin associated with neurodegenerative disease. *J Cell Sci* **120**, 1615-1623 (2007).

81. Chen, Z.L., Yu, W.M. & Strickland, S. Peripheral regeneration. *Annu Rev Neurosci* **30**, 209-233 (2007).
82. Gilbert, A. & Tassin, J.L. [Surgical repair of the brachial plexus in obstetric paralysis]. *Chirurgie* **110**, 70-75 (1984).
83. Waters, P.M. Comparison of the natural history, the outcome of microsurgical repair, and the outcome of operative reconstruction in brachial plexus birth palsy. *J Bone Joint Surg Am* **81**, 649-659 (1999).
84. Clarke, H.M. & Curtis, C.G. An approach to obstetrical brachial plexus injuries. *Hand Clin* **11**, 563-580; discussion 580-561 (1995).
85. Pondaag, W. & Malessy, M.J. Recovery of hand function following nerve grafting and transfer in obstetric brachial plexus lesions. *J Neurosurg* **105**, 33-40 (2006).
86. Atherton, D.D., Taherzadeh, O., Facer, P., Elliot, D. & Anand, P. The potential role of nerve growth factor (NGF) in painful neuromas and the mechanism of pain relief by their relocation to muscle. *J Hand Surg [Br]* **31**, 652-656 (2006).
87. Tannemaat, M.R., *et al.* Human neuroma contains increased levels of semaphorin 3A, which surrounds nerve fibers and reduces neurite extension in vitro. *J Neurosci* **27**, 14260-14264 (2007).
88. Ashburner, M., *et al.* Gene ontology: tool for the unification of biology. The Gene Ontology Consortium. *Nat Genet* **25**, 25-29 (2000).
89. Alexa, A., Rahnenfuhrer, J. & Lengauer, T. Improved scoring of functional groups from gene expression data by decorrelating GO graph structure. *Bioinformatics* **22**, 1600-1607 (2006).
90. Tannemaat, M.R., Boer, G.J., Verhaagen, J. & Malessy, M.J. Genetic modification of human sural nerve segments by a lentiviral vector encoding nerve growth factor. *Neurosurgery* **61**, 1286-1294; discussion 1294-1286 (2007).
91. Hattori, T., *et al.* Chondroitinase ABC enhances axonal regeneration across nerve gaps. *J Clin Neurosci* **15**, 185-191 (2008).
92. McEwan, P.A., Scott, P.G., Bishop, P.N. & Bella, J. Structural correlations in the family of small leucine-rich repeat proteins and proteoglycans. *J Struct Biol* **155**, 294-305 (2006).
93. Nath, R.K., *et al.* Antibody to transforming growth factor beta reduces collagen production in injured peripheral nerve. *Plast Reconstr Surg* **102**, 1100-1106; discussion 1107-1108 (1998).
94. Kveiborg, M., Albrechtsen, R., Couchman, J.R. & Wewer, U.M. Cellular roles of ADAM12 in health and disease. *Int J Biochem Cell Biol* (2008).
95. Atfi, A., *et al.* The disintegrin and metalloproteinase ADAM12 contributes to TGF-beta signaling through interaction with the type II receptor. *J Cell Biol* **178**, 201-208 (2007).
96. McAllister, L., Goodman, C.S. & Zinn, K. Dynamic expression of the cell adhesion molecule fasciclin I during embryonic development in *Drosophila*. *Development* **115**, 267-276 (1992).
97. Norris, R.A., *et al.* Periostin regulates collagen fibrillogenesis and the biomechanical properties of connective tissues. *J Cell Biochem* **101**, 695-711 (2007).
98. Vadasz, Z., *et al.* Abnormal deposition of collagen around hepatocytes in Wilson's disease is associated with hepatocyte specific expression of lysyl oxidase and lysyl oxidase like protein-2. *J Hepatol* **43**, 499-507 (2005).
99. Shi, J., *et al.* Membrane-type MMPs enable extracellular matrix permissiveness and mesenchymal cell proliferation during embryogenesis. *Dev Biol* **313**, 196-209 (2008).
100. Werner, S.R., *et al.* Neural MMP-28 expression precedes myelination during development and peripheral nerve repair. *Dev Dyn* **236**, 2852-2864 (2007).
101. Okada, A., *et al.* Boc is a receptor for sonic hedgehog in the guidance of commissural axons. *Nature* **444**, 369-373 (2006).
102. Devine, C.A. & Key, B. Robo-Slit interactions regulate longitudinal axon pathfinding in the embryonic vertebrate brain. *Dev Biol* **313**, 371-383 (2008).

## REFERENCES

103. Shipp, E.L. & Hsieh-Wilson, L.C. Profiling the sulfation specificities of glycosaminoglycan interactions with growth factors and chemotactic proteins using microarrays. *Chem Biol* **14**, 195-208 (2007).
104. To, K.C., Church, J. & O'Connor, T.P. Combined activation of calpain and calcineurin during ligand-induced growth cone collapse. *Mol Cell Neurosci* **36**, 425-434 (2007).
105. Keeble, T.R., *et al.* The Wnt receptor Ryk is required for Wnt5a-mediated axon guidance on the contralateral side of the corpus callosum. *J Neurosci* **26**, 5840-5848 (2006).
106. Butler, S.J. & Dodd, J. A role for BMP heterodimers in roof plate-mediated repulsion of commissural axons. *Neuron* **38**, 389-401 (2003).
107. Ceballos, D., *et al.* Role of metallothioneins in peripheral nerve function and regeneration. *Cell Mol Life Sci* **60**, 1209-1216 (2003).
108. Genc, B., Ozdinler, P.H., Mendoza, A.E. & Erzurumlu, R.S. A chemoattractant role for NT-3 in proprioceptive axon guidance. *PLoS Biol* **2**, e403 (2004).
109. Zelina, P., Avci, H.X., Thelen, K. & Pollerberg, G.E. The cell adhesion molecule NrCAM is crucial for growth cone behaviour and pathfinding of retinal ganglion cell axons. *Development* **132**, 3609-3618 (2005).
110. Tzarfati-Majar, V., Burstyn-Cohen, T. & Klar, A. F-spondin is a contact-repellent molecule for embryonic motor neurons. *Proc Natl Acad Sci U S A* **98**, 4722-4727 (2001).
111. Burstyn-Cohen, T., Frumkin, A., Xu, Y.T., Scherer, S.S. & Klar, A. Accumulation of F-spondin in injured peripheral nerve promotes the outgrowth of sensory axons. *J Neurosci* **18**, 8875-8885 (1998).
112. Bloom, L. & Horvitz, H.R. The *Caenorhabditis elegans* gene *unc-76* and its human homologs define a new gene family involved in axonal outgrowth and fasciculation. *Proc Natl Acad Sci U S A* **94**, 3414-3419 (1997).
113. Meyer, F. & Aberle, H. At the next stop sign turn right: the metalloprotease Tolloid-related 1 controls defasciculation of motor axons in *Drosophila*. *Development* **133**, 4035-4044 (2006).
114. Carulli, D., *et al.* Composition of perineuronal nets in the adult rat cerebellum and the cellular origin of their components. *J Comp Neurol* **494**, 559-577 (2006).
115. de Ruitter, G.C., *et al.* Misdirection of regenerating motor axons after nerve injury and repair in the rat sciatic nerve model. *Exp Neurol* (2008).
116. DeMatteo, C., Bain, J.R., Galea, V. & Gjertsen, D. Botulinum toxin as an adjunct to motor learning therapy and surgery for obstetrical brachial plexus injury. *Dev Med Child Neurol* **48**, 245-252 (2006).
117. Tona, A., Perides, G., Rahemtulla, F. & Dahl, D. Extracellular matrix in regenerating rat sciatic nerve: a comparative study on the localization of laminin, hyaluronic acid, and chondroitin sulfate proteoglycans, including versican. *J Histochem Cytochem* **41**, 593-599 (1993).
118. Carulli, D., Rhodes, K.E. & Fawcett, J.W. Upregulation of aggrecan, link protein 1, and hyaluronan synthases during formation of perineuronal nets in the rat cerebellum. *J Comp Neurol* **501**, 83-94 (2007).
119. Yamagata, M. & Sanes, J.R. Versican in the developing brain: lamina-specific expression in interneuronal subsets and role in presynaptic maturation. *J Neurosci* **25**, 8457-8467 (2005).
120. Galtrey, C.M., Asher, R.A., Nothias, F. & Fawcett, J.W. Promoting plasticity in the spinal cord with chondroitinase improves functional recovery after peripheral nerve repair. *Brain* **130**, 926-939 (2007).
121. Barras, F.M., Pasche, P., Bouche, N., Aebischer, P. & Zurn, A.D. Glial cell line-derived neurotrophic factor released by synthetic guidance channels promotes facial nerve regeneration in the rat. *J Neurosci Res* **70**, 746-755 (2002).
122. Belkas, J.S., Shoichet, M.S. & Midha, R. Peripheral nerve regeneration through guidance tubes. *Neurol Res* **26**, 151-160 (2004).



123. Hermens, W.T. & Verhaagen, J. Viral vectors, tools for gene transfer in the nervous system. *Prog Neurobiol* **55**, 399-432 (1998).
124. Wang, C., Wang, C.M., Clark, K.R. & Sferra, T.J. Recombinant AAV serotype 1 transduction efficiency and tropism in the murine brain. *Gene Ther* **10**, 1528-1534 (2003).
125. Hendriks, W.T., Eggers, R., Verhaagen, J. & Boer, G.J. Gene transfer to the spinal cord neural scar with lentiviral vectors: predominant transgene expression in astrocytes but not in meningeal cells. *J Neurosci Res* (2007).
126. Berggren, K., McCaffery, P., Drager, U. & Forehand, C.J. Differential distribution of retinoic acid synthesis in the chicken embryo as determined by immunolocalization of the retinoic acid synthetic enzyme, RALDH-2. *Dev Biol* **210**, 288-304 (1999).
127. Morrissey, T.K., Kleitman, N. & Bunge, R.P. Isolation and functional characterization of Schwann cells derived from adult peripheral nerve. *J Neurosci* **11**, 2433-2442 (1991).
128. Niclou, S.P., Franssen, E.H., Ehlert, E.M., Taniguchi, M. & Verhaagen, J. Meningeal cell-derived semaphorin 3A inhibits neurite outgrowth. *Mol Cell Neurosci* **24**, 902-912 (2003).
129. Millesi, H. Brachial plexus injuries. Nerve grafting. *Clin Orthop Relat Res*, 36-42 (1988).
130. Hermens, W.T., *et al.* Transient gene transfer to neurons and glia: analysis of adenoviral vector performance in the CNS and PNS. *J Neurosci Methods* **71**, 85-98 (1997).
131. Tuszynski, M.H., *et al.* A phase 1 clinical trial of nerve growth factor gene therapy for Alzheimer disease. *Nat Med* **11**, 551-555 (2005).
132. Midha, R., *et al.* Regeneration into protected and chronically denervated peripheral nerve stumps. *Neurosurgery* **57**, 1289-1299; discussion 1289-1299 (2005).
133. Santos, X., Rodrigo, J., Hontanilla, B. & Bilbao, G. Local administration of neurotrophic growth factor in subcutaneous silicon chambers enhances the regeneration of the sensory component of the rat sciatic nerve. *Microsurgery* **19**, 275-280 (1999).
134. Sterne, G.D., Brown, R.A., Green, C.J. & Terenghi, G. Neurotrophin-3 delivered locally via fibronectin mats enhances peripheral nerve regeneration. *Eur J Neurosci* **9**, 1388-1396 (1997).
135. Tuszynski, M.H., Grill, R., Jones, L.L., McKay, H.M. & Blesch, A. Spontaneous and augmented growth of axons in the primate spinal cord: effects of local injury and nerve growth factor-secreting cell grafts. *J Comp Neurol* **449**, 88-101 (2002).
136. Terzis, J.K., Vekris, M.D. & Soucacos, P.N. Brachial plexus root avulsions. *World J Surg* **25**, 1049-1061 (2001).
137. Htut, M., Misra, V.P., Anand, P., Birch, R. & Carlstedt, T. Motor recovery and the breathing arm after brachial plexus surgical repairs, including re-implantation of avulsed spinal roots into the spinal cord. *J Hand Surg [Br]* **32**, 170-178 (2007).
138. Carlstedt, T., *et al.* Spinal nerve root repair and reimplantation of avulsed ventral roots into the spinal cord after brachial plexus injury. *J Neurosurg* **93**, 237-247 (2000).
139. Malessy, M.J. & Thomeer, R.T. Evaluation of intercostal to musculocutaneous nerve transfer in reconstructive brachial plexus surgery. *J Neurosurg* **88**, 266-271 (1998).
140. Koliatsos, V.E., Price, W.L., Pardo, C.A. & Price, D.L. Ventral root avulsion: an experimental model of death of adult motor neurons. *J Comp Neurol* **342**, 35-44 (1994).
141. Hoang, T.X. & Havton, L.A. A single re-implanted ventral root exerts neurotropic effects over multiple spinal cord segments in the adult rat. *Exp Brain Res* **169**, 208-217 (2006).
142. Gu, H.Y., *et al.* Survival, regeneration and functional recovery of motoneurons in adult rats by reimplantation of ventral root following spinal root avulsion. *Eur J Neurosci* **19**, 2123-2131 (2004).
143. Gilbert, A., Pivato, G. & Kheiralla, T. Long-term results of primary repair of brachial plexus lesions in children. *Microsurgery* **26**, 334-342 (2006).
144. Holtzer, C.A., Marani, E., Lakke, E.A. & Thomeer, R.T. Repair of ventral root avulsions of the brachial plexus: a review. *J Peripher Nerv Syst* **7**, 233-242 (2002).



## REFERENCES

145. Carlstedt, T., Anand, P., Htut, M., Misra, P. & Svensson, M. Restoration of hand function and so called "breathing arm" after intraspinal repair of C5-T1 brachial plexus avulsion injury. Case report. *Neurosurg Focus* **16**, E7 (2004).
146. Li, L., *et al.* Rescue of adult mouse motoneurons from injury-induced cell death by glial cell line-derived neurotrophic factor. *Proc Natl Acad Sci U S A* **92**, 9771-9775 (1995).
147. Henderson, C.E., *et al.* GDNF: a potent survival factor for motoneurons present in peripheral nerve and muscle. *Science* **266**, 1062-1064 (1994).
148. Airaksinen, M.S. & Saarna, M. The GDNF family: signalling, biological functions and therapeutic value. *Nat Rev Neurosci* **3**, 383-394 (2002).
149. Bergerot, A., Shortland, P.J., Anand, P., Hunt, S.P. & Carlstedt, T. Co-treatment with riluzole and GDNF is necessary for functional recovery after ventral root avulsion injury. *Exp Neurol* **187**, 359-366 (2004).
150. Hendriks, W.T., *et al.* Lentiviral vector-mediated reporter gene expression in avulsed spinal ventral root is short-term, but is prolonged using an immune "stealth" transgene. *Restor Neurol Neurosci* **25**, 585-599 (2007).
151. Hase, A., *et al.* Characterization of glial cell line-derived neurotrophic factor family receptor alpha-1 in peripheral nerve Schwann cells. *J Neurochem* **95**, 537-543 (2005).
152. Holtzer, C.A., Feirabend, H.K., Marani, E. & Thomeer, R.T. Ultrastructural and quantitative motoneuronal changes after ventral root avulsion favor early surgical repair. *Arch Physiol Biochem* **108**, 293-309 (2000).
153. McPhail, L.T., Fernandes, K.J., Chan, C.C., Vanderluit, J.L. & Tetzlaff, W. Axonal reinjury reveals the survival and re-expression of regeneration-associated genes in chronically axotomized adult mouse motoneurons. *Exp Neurol* **188**, 331-340 (2004).
154. Wu, W., *et al.* Delayed implantation of a peripheral nerve graft reduces motoneuron survival but does not affect regeneration following spinal root avulsion in adult rats. *J Neurotrauma* **21**, 1050-1058 (2004).
155. Hoang, T.X., Nieto, J.H., Dobkin, B.H., Tillakaratne, N.J. & Havton, L.A. Acute implantation of an avulsed lumbosacral ventral root into the rat conus medullaris promotes neuroprotection and graft reinnervation by autonomic and motor neurons. *Neuroscience* **138**, 1149-1160 (2006).
156. Chai, H., Wu, W., So, K.F. & Yip, H.K. Survival and regeneration of motoneurons in adult rats by reimplantation of ventral root following spinal root avulsion. *Neuroreport* **11**, 1249-1252 (2000).
157. Novikov, L., Novikova, L. & Kellerth, J.O. Brain-derived neurotrophic factor promotes axonal regeneration and long-term survival of adult rat spinal motoneurons in vivo. *Neuroscience* **79**, 765-774 (1997).
158. Novikova, L., Novikov, L. & Kellerth, J.O. Effects of neurotransplants and BDNF on the survival and regeneration of injured adult spinal motoneurons. *Eur J Neurosci* **9**, 2774-2777 (1997).
159. Lang, E.M., Schlegel, N., Sendtner, M. & Asan, E. Effects of root replantation and neurotrophic factor treatment on long-term motoneuron survival and axonal regeneration after C7 spinal root avulsion. *Exp Neurol* **194**, 341-354 (2005).
160. Jones, L.L., Oudega, M., Bunge, M.B. & Tuszynski, M.H. Neurotrophic factors, cellular bridges and gene therapy for spinal cord injury. *J Physiol* **533**, 83-89 (2001).
161. McPhail, L.T., Oschipok, L.W., Liu, J. & Tetzlaff, W. Both positive and negative factors regulate gene expression following chronic facial nerve resection. *Exp Neurol* **195**, 199-207 (2005).
162. Zhou, L.H. & Wu, W. Survival of injured spinal motoneurons in adult rat upon treatment with glial cell line-derived neurotrophic factor at 2 weeks but not at 4 weeks after root avulsion. *J Neurotrauma* **23**, 920-927 (2006).

163. Haninec, P., Dubovy, P., Samal, F., Houstava, L. & Stejskal, L. Reinnervation of the rat musculocutaneous nerve stump after its direct reconnection with the C5 spinal cord segment by the nerve graft following avulsion of the ventral spinal roots: a comparison of intrathecal administration of brain-derived neurotrophic factor and Cerebrolysin. *Exp Brain Res* **159**, 425-432 (2004).
164. Hammarberg, H., Piehl, F., Risling, M. & Cullheim, S. Differential regulation of trophic factor receptor mRNAs in spinal motoneurons after sciatic nerve transection and ventral root avulsion in the rat. *J Comp Neurol* **426**, 587-601 (2000).
165. Yang, L.J., *et al.* Sialidase enhances spinal axon outgrowth in vivo. *Proc Natl Acad Sci U S A* **103**, 11057-11062 (2006).
166. Hoke, A., *et al.* Glial cell line-derived neurotrophic factor alters axon schwann cell units and promotes myelination in unmyelinated nerve fibers. *J Neurosci* **23**, 561-567 (2003).
167. Gu, H.Y., *et al.* Survival, regeneration and functional recovery of motoneurons after delayed reimplantation of avulsed spinal root in adult rat. *Exp Neurol* **192**, 89-99 (2005).
168. Hoang, T.X., Pikov, V. & Havton, L.A. Functional reinnervation of the rat lower urinary tract after cauda equina injury and repair. *J Neurosci* **26**, 8672-8679 (2006).
169. Deshpande, D.M., *et al.* Recovery from paralysis in adult rats using embryonic stem cells. *Ann Neurol* **60**, 32-44 (2006).
170. Ossevoort, M., *et al.* Creation of immune 'stealth' genes for gene therapy through fusion with the Gly-Ala repeat of EBNA-1. *Gene Ther* **10**, 2020-2028 (2003).
171. Brun, S., Faucon-Biguët, N. & Mallet, J. Optimization of transgene expression at the posttranscriptional level in neural cells: implications for gene therapy. *Mol Ther* **7**, 782-789 (2003).
172. Basso, D.M., Beattie, M.S. & Bresnahan, J.C. A sensitive and reliable locomotor rating scale for open field testing in rats. *J Neurotrauma* **12**, 1-21 (1995).
173. Blits, B., Dijkhuizen, P.A., Boer, G.J. & Verhaagen, J. Intercostal nerve implants transduced with an adenoviral vector encoding neurotrophin-3 promote regrowth of injured rat corticospinal tract fibers and improve hindlimb function. *Exp Neurol* **164**, 25-37 (2000).
174. Nagano, I., Murakami, T., Shiote, M., Abe, K. & Itoyama, Y. Ventral root avulsion leads to downregulation of GluR2 subunit in spinal motoneurons in adult rats. *Neuroscience* **117**, 139-146 (2003).
175. Stucky, C.L. & Lewin, G.R. Isolectin B(4)-positive and -negative nociceptors are functionally distinct. *J Neurosci* **19**, 6497-6505 (1999).
176. Nagy, J.I. & Hunt, S.P. Fluoride-resistant acid phosphatase-containing neurones in dorsal root ganglia are separate from those containing substance P or somatostatin. *Neuroscience* **7**, 89-97 (1982).
177. Averill, S., McMahon, S.B., Clary, D.O., Reichardt, L.F. & Priestley, J.V. Immunocytochemical localization of trkA receptors in chemically identified subgroups of adult rat sensory neurons. *Eur J Neurosci* **7**, 1484-1494 (1995).
178. Michael, G.J., *et al.* Nerve growth factor treatment increases brain-derived neurotrophic factor selectively in TrkA-expressing dorsal root ganglion cells and in their central terminations within the spinal cord. *J Neurosci* **17**, 8476-8490 (1997).
179. Silverman, J.D. & Kruger, L. Selective neuronal glycoconjugate expression in sensory and autonomic ganglia: relation of lectin reactivity to peptide and enzyme markers. *J Neurocytol* **19**, 789-801 (1990).
180. Molliver, D.C., *et al.* IB4-binding DRG neurons switch from NGF to GDNF dependence in early postnatal life. *Neuron* **19**, 849-861 (1997).
181. Bennett, D.L., *et al.* A distinct subgroup of small DRG cells express GDNF receptor components and GDNF is protective for these neurons after nerve injury. *J Neurosci* **18**, 3059-3072 (1998).

## REFERENCES

182. Leclere, P.G., *et al.* Impaired axonal regeneration by isolectin B4-binding dorsal root ganglion neurons in vitro. *J Neurosci* **27**, 1190-1199 (2007).
183. Eggers, R., *et al.* Neuroregenerative effects of lentiviral vector-mediated GDNF expression in reimplanted ventral roots. *Mol Cell Neurosci* (2008).
184. Santos, X., Rodrigo, J., Hontanilla, B. & Bilbao, G. Regeneration of the motor component of the rat sciatic nerve with local administration of neurotrophic growth factor in silicone chambers. *J Reconstr Microsurg* **15**, 207-213 (1999).
185. Abercrombie, M. & Johnson, M.L. Quantitative histology of Wallerian degeneration: I. Nuclear population in rabbit sciatic nerve. *J Anat* **80**, 37-50 (1946).
186. De Koning, P., Brakkee, J.H. & Gispen, W.H. Methods for producing a reproducible crush in the sciatic and tibial nerve of the rat and rapid and precise testing of return of sensory function. Beneficial effects of melanocortins. *J Neurol Sci* **74**, 237-246 (1986).
187. Brenner, M.J., *et al.* Repair of motor nerve gaps with sensory nerve inhibits regeneration in rats. *Laryngoscope* **116**, 1685-1692 (2006).
188. Wall, P.D., *et al.* Autotomy following peripheral nerve lesions: experimental anaesthesia dolorosa. *Pain* **7**, 103-111 (1979).
189. Symons, N.A., Danielsen, N. & Harvey, A.R. Migration of cells into and out of peripheral nerve isografts in the peripheral and central nervous systems of the adult mouse. *Eur J Neurosci* **14**, 522-532 (2001).
190. Kimura, A., *et al.* Transmigration of donor cells involved in the sciatic nerve graft. *Transplant Proc* **37**, 205-207 (2005).
191. Ramer, M.S., Bradbury, E.J., Michael, G.J., Lever, I.J. & McMahon, S.B. Glial cell line-derived neurotrophic factor increases calcitonin gene-related peptide immunoreactivity in sensory and motoneurons in vivo. *Eur J Neurosci* **18**, 2713-2721 (2003).
192. Zheng, L.F., *et al.* Calcitonin gene-related peptide dynamics in rat dorsal root ganglia and spinal cord following different sciatic nerve injuries. *Brain Res* **1187**, 20-32 (2008).
193. Wang, R., *et al.* Glial cell line-derived neurotrophic factor normalizes neurochemical changes in injured dorsal root ganglion neurons and prevents the expression of experimental neuropathic pain. *Neuroscience* **121**, 815-824 (2003).
194. Ro, L.S., Chen, S.T., Tang, L.M. & Jacobs, J.M. Effect of NGF and anti-NGF on neuropathic pain in rats following chronic constriction injury of the sciatic nerve. *Pain* **79**, 265-274 (1999).
195. Kryger, G.S., *et al.* Nerve growth factor inhibition prevents traumatic neuroma formation in the rat. *J Hand Surg [Am]* **26**, 635-644 (2001).
196. Hoke, A., Gordon, T., Zochodne, D.W. & Sulaiman, O.A. A decline in glial cell-line-derived neurotrophic factor expression is associated with impaired regeneration after long-term Schwann cell denervation. *Exp Neurol* **173**, 77-85 (2002).
197. Hammarberg, H., *et al.* GDNF mRNA in Schwann cells and DRG satellite cells after chronic sciatic nerve injury. *Neuroreport* **7**, 857-860 (1996).
198. Shu, X.Q. & Mendell, L.M. Neurotrophins and hyperalgesia. *Proc Natl Acad Sci U S A* **96**, 7693-7696 (1999).
199. Petruska, J.C. & Mendell, L.M. The many functions of nerve growth factor: multiple actions on nociceptors. *Neurosci Lett* **361**, 168-171 (2004).
200. Romero, M.I., *et al.* Extensive sprouting of sensory afferents and hyperalgesia induced by conditional expression of nerve growth factor in the adult spinal cord. *J Neurosci* **20**, 4435-4445 (2000).
201. Ruiz, G. & Banos, J.E. The effect of endoneurial nerve growth factor on calcitonin gene-related peptide expression in primary sensory neurons. *Brain Res* **1042**, 44-52 (2005).
202. Bird, G.C., *et al.* Pain-related synaptic plasticity in spinal dorsal horn neurons: role of CGRP. *Mol Pain* **2**, 31 (2006).

203. Pezet, S., *et al.* Reversal of neurochemical changes and pain-related behavior in a model of neuropathic pain using modified lentiviral vectors expressing GDNF. *Mol Ther* **13**, 1101-1109 (2006).
204. Chao, T., Pham, K., Steward, O. & Gupta, R. Chronic nerve compression injury induces a phenotypic switch of neurons within the dorsal root ganglia. *J Comp Neurol* **506**, 180-193 (2008).
205. Li, L., Qin, H., Shi, W. & Gao, G. Local Nogo-66 administration reduces neuropathic pain after sciatic nerve transection in rat. *Neurosci Lett* **424**, 145-148 (2007).
206. Okuda, T., *et al.* The autotomy relief effect of a silicone tube covering the proximal nerve stump. *J Orthop Res* **24**, 1427-1437 (2006).
207. Boucher, T.J., *et al.* Potent analgesic effects of GDNF in neuropathic pain states. *Science* **290**, 124-127 (2000).
208. Bogen, O., Dreger, M., Gillen, C., Schroder, W. & Hucho, F. Identification of versican as an isolectin B4-binding glycoprotein from mammalian spinal cord tissue. *FEBS J* **272**, 1090-1102 (2005).
209. Amir, R. & Devor, M. Functional cross-excitation between afferent A- and C-neurons in dorsal root ganglia. *Neuroscience* **95**, 189-195 (2000).
210. Piquilloud, G., Christen, T., Pfister, L.A., Gander, B. & Papaliozios, M.Y. Variations in glial cell line-derived neurotrophic factor release from biodegradable nerve conduits modify the rate of functional motor recovery after rat primary nerve repairs. *Eur J Neurosci* **26**, 1109-1117 (2007).
211. Nolte, C., *et al.* GFAP promoter-controlled EGFP-expressing transgenic mice: a tool to visualize astrocytes and astrogliosis in living brain tissue. *Glia* **33**, 72-86 (2001).
212. Hayashi, A., *et al.* A double-transgenic mouse used to track migrating Schwann cells and regenerating axons following engraftment of injured nerves. *Exp Neurol* **207**, 128-138 (2007).
213. Mills, C.D., Allchorne, A.J., Griffin, R.S., Woolf, C.J. & Costigan, M. GDNF selectively promotes regeneration of injury-primed sensory neurons in the lesioned spinal cord. *Mol Cell Neurosci* **36**, 185-194 (2007).
214. Furey, M.J., Midha, R., Xu, Q.G., Belkas, J. & Gordon, T. Prolonged target deprivation reduces the capacity of injured motoneurons to regenerate. *Neurosurgery* **60**, 723-732; discussion 732-723 (2007).
215. Redett, R., *et al.* Peripheral pathways regulate motoneuron collateral dynamics. *J Neurosci* **25**, 9406-9412 (2005).
216. Madison, R.D., Archibald, S.J., Lacin, R. & Krarup, C. Factors contributing to preferential motor reinnervation in the primate peripheral nervous system. *J Neurosci* **19**, 11007-11016 (1999).
217. Brushart, T.M. Motor axons preferentially reinnervate motor pathways. *J Neurosci* **13**, 2730-2738 (1993).
218. Moradzadeh, A., *et al.* The impact of motor and sensory nerve architecture on nerve regeneration. *Experimental Neurology* **In Press, Corrected Proof**.
219. Elsworth, J.D., *et al.* AAV2-mediated gene transfer of GDNF to the striatum of MPTP monkeys enhances the survival and outgrowth of co-implanted fetal dopamine neurons. *Exp Neurol* **211**, 252-258 (2008).
220. Helgren, M.E., *et al.* Trophic effect of ciliary neurotrophic factor on denervated skeletal muscle. *Cell* **76**, 493-504 (1994).
221. Huang, S., Wang, F., Hong, G., Wan, S. & Kang, H. Protective effects of ciliary neurotrophic factor on denervated skeletal muscle. *J Huazhong Univ Sci Technolog Med Sci* **22**, 148-151 (2002).
222. Vergara, C. & Ramirez, B. CNTF, a pleiotropic cytokine: emphasis on its myotrophic role. *Brain Res Brain Res Rev* **47**, 161-173 (2004).

## REFERENCES

223. van Dijk, J.G., Pondaag, W. & Malessy, M.J. Botulinum toxin and the pathophysiology of obstetric brachial plexus lesions. *Dev Med Child Neurol* **49**, 318; author reply 318-319 (2007).
224. Malessy, M.J., Thomeer, R.T. & van Dijk, J.G. Changing central nervous system control following intercostal nerve transfer. *J Neurosurg* **89**, 568-574 (1998).
225. Malessy, M.J., van der Kamp, W., Thomeer, R.T. & van Dijk, J.G. Cortical excitability of the biceps muscle after intercostal-to-musculocutaneous nerve transfer. *Neurosurgery* **42**, 787-794; discussion 794-785 (1998).
226. Ramos, L.E. & Zell, J.P. Rehabilitation program for children with brachial plexus and peripheral nerve injury. *Semin Pediatr Neurol* **7**, 52-57 (2000).
227. Bozkurt, A., *et al.* In vitro assessment of axonal growth using dorsal root ganglia explants in a novel three-dimensional collagen matrix. *Tissue Eng* **13**, 2971-2979 (2007).
228. de Ruiter, G.C., *et al.* Methods for in vitro characterization of multichannel nerve tubes. *J Biomed Mater Res A* **84**, 643-651 (2008).
229. Stokols, S. & Tuszynski, M.H. The fabrication and characterization of linearly oriented nerve guidance scaffolds for spinal cord injury. *Biomaterials* **25**, 5839-5846 (2004).
230. Stokols, S., *et al.* Templated agarose scaffolds support linear axonal regeneration. *Tissue Eng* **12**, 2777-2787 (2006).
231. Streppel, M., *et al.* Focal application of neutralizing antibodies to soluble neurotrophic factors reduces collateral axonal branching after peripheral nerve lesion. *Eur J Neurosci* **15**, 1327-1342 (2002).
232. Hargrove, P.W., *et al.* Globin lentiviral vector insertions can perturb the expression of endogenous genes in beta-thalassemic hematopoietic cells. *Mol Ther* **16**, 525-533 (2008).
233. Cattoglio, C., *et al.* Hot spots of retroviral integration in human CD34+ hematopoietic cells. *Blood* **110**, 1770-1778 (2007).
234. Beard, B.C., *et al.* Comparison of HIV-derived lentiviral and MLV-based gammaretroviral vector integration sites in primate repopulating cells. *Mol Ther* **15**, 1356-1365 (2007).
235. Yanez-Munoz, R.J., *et al.* Effective gene therapy with nonintegrating lentiviral vectors. *Nat Med* **12**, 348-353 (2006).
236. Carter, B.J. Adeno-associated virus vectors in clinical trials. *Hum Gene Ther* **16**, 541-550 (2005).
237. Skorpil, M., Engstrom, M. & Nordell, A. Diffusion-direction-dependent imaging: a novel MRI approach for peripheral nerve imaging. *Magn Reson Imaging* **25**, 406-411 (2007).
238. Van den Borne, S.W., *et al.* Molecular imaging of post-infarction cardiac remodeling and effects of anti-angiotensin in therapy. *Circulation* **116**, 289-290 (2007).

## List of publications

**Tannemaat MR**, Eggers E, Hendriks WT, de Ruiter GCW, van Heerikhuizen JJ, Pool CW, Malessy MJ, Boer GJ, Verhaagen J. Differential effects of lentiviral vector-mediated overexpression of NGF and GDNF on regenerating sensory and motor axons in the transected peripheral nerve.

*Eur J Neurosci.* [in press]

**Tannemaat MR**, Verhaagen J, Malessy MJ. (2008) The application of viral vectors to enhance regeneration after peripheral nerve repair.

*Neurol Res.* [in press]

Eggers R, Hendriks WT, **Tannemaat MR**, van Heerikhuizen JJ, Pool CW, Carlstedt TP, Zaldumbide A, Hoeben RC, Boer GJ, Verhaagen J. (2008) Neuroregenerative effects of lentiviral vector-mediated GDNF expression in reimplanted ventral roots.

*Mol Cell Neurosci.* Sep;39(1):105-17.

Hendriks WT, Eggers R, Carlstedt TP, Zaldumbide A, **Tannemaat MR**, Fallaux FJ, Hoeben RC, Boer GJ, Verhaagen J. (2007) Lentiviral vector-mediated reporter gene expression in avulsed spinal ventral root is short-term, but is prolonged using an immune “stealth” transgene.

*Restor Neurol Neurosci.* 25(5-6):585-99.

**Tannemaat MR**, Boer GJ, Verhaagen J, Malessy MJ. (2007) Genetic modification of human sural nerve segments by a lentiviral vector encoding nerve growth factor.

*Neurosurgery.* Dec;61(6):1286-94; discussion 1294-6.

**Tannemaat MR**, Korecka JA, Ehlert EM, Mason MR, van Duinen SG, Boer GJ, Malessy MJ, Verhaagen J. (2007) Human neuroma contains increased levels of semaphorin 3A, which surrounds nerve fibers and reduces neurite extension in vitro.

*J Neurosci.* Dec 26;27(52):14260-4.

Miller LC, Kelly N, **Tannemaat M**, Grand RJ. (2003) Serologic prevalence of antibodies to *Helicobacter pylori* in internationally adopted children.

*Helicobacter.* Jun;8(3):173-8.

Krasinski SD, Van Wering HM, **Tannemaat MR**, Grand RJ. (2001) Differential activation of intestinal gene promoters: functional interactions between GATA-5 and HNF-1 alpha.

*Am J Physiol Gastrointest Liver Physiol.* Jul;281(1):G69-84.





## Co-author affiliations

*Gerard J Boer PhD*

Laboratory for Neuroregeneration, Netherlands Institute for Neuroscience, an Institute of the Royal Academy of Arts and Sciences, Amsterdam, the Netherlands.

*Koen Bossers MSc*

Laboratory for Neuroregeneration, Netherlands Institute for Neuroscience, an Institute of the Royal Academy of Arts and Sciences, Amsterdam, the Netherlands.

*Sjoerd G van Duinen MD PhD*

Department of Pathology/Neurology, Leiden University Medical Center, Leiden, the Netherlands

*Ruben Eggers BSc*

Laboratory for Neuroregeneration, Netherlands Institute for Neuroscience, an Institute of the Royal Academy of Arts and Sciences, Amsterdam, the Netherlands.

*Erich ME Ehlert BSc*

Laboratory for Neuroregeneration, Netherlands Institute for Neuroscience, an Institute of the Royal Academy of Arts and Sciences, Amsterdam, the Netherlands.

*Joop J van Heerikhuize BSc*

Technology and Software Development, Netherlands Institute for Neuroscience, an institute of the Netherlands Royal Academy of Arts and Sciences, Amsterdam, the Netherlands.

*William T-Hendriks PhD*

Laboratory for Neuroregeneration, Netherlands Institute for Neuroscience, an Institute of the Royal Academy of Arts and Sciences, Amsterdam, the Netherlands.

*Joanna A Korecka MSc*

Laboratory for Neuroregeneration, Netherlands Institute for Neuroscience, an Institute of the Royal Academy of Arts and Sciences, Amsterdam, the Netherlands.

*Martijn J Malessy MD PhD*

Department of Neurosurgery, Leiden University Medical Center, Leiden, the Netherlands

*Matthew RJ Mason PhD*

Laboratory for Neuroregeneration, Netherlands Institute for Neuroscience, an Institute of the Royal Academy of Arts and Sciences, Amsterdam, the Netherlands.

*Chris W. Pool PhD*

Technology and Software Development, Netherlands Institute for Neuroscience, an institute of the Netherlands Royal Academy of Arts and Sciences, Amsterdam, the Netherlands.

*Godard CW de Ruiter MD*

Department of Neurosurgery, Leiden University Medical Center, Leiden, the Netherlands

*Joost Verhaagen PhD*

Laboratory for Neuroregeneration, Netherlands Institute for Neuroscience, an Institute of the Royal Academy of Arts and Sciences, Amsterdam, the Netherlands.

## Dankwoord

*What is the feeling when you're driving away from people, and they recede on the plain till you see their specks dispersing? -it's the too huge world vaulting us, and it's good-bye. But we lean forward to the next crazy venture beneath the skies.*

Jack Kerouac, *On the Road* (1951)

De lange, soms wat kronkelige weg die ik sinds 2003 heb afgelegd heeft uiteindelijk geresulteerd in het boekje dat u nu in handen heeft. Ik heb het geluk gehad dat ik onderweg vergezeld ben door veel mensen die hebben bijgedragen aan het bereiken van de eindbestemming, of die in ieder geval de reis ernaartoe veraangenaamd hebben. Naast de incidentele voldoening van een geslaagd experiment, zijn het de nieuw opgedane vriendschappen en samenwerkingen die mijn promotie-onderzoek tot een genoegen hebben gemaakt. In het bijzonder ben ik de volgende mensen daarvoor dankbaar.

Joost, supervisor en mentor. Bijna alles wat ik weet van virale vectoren en neuroregeneratie heb ik van jou, maar belangrijker nog: jouw voorbeeld heeft me geleerd welke karaktereigenschappen er nodig zijn voor het bedrijven van wetenschap. Nieuwsgierig, gedreven, kritisch, en bovenal een warme persoonlijkheid. Ik hoop dat we nog lang blijven samenwerken en dat de H-factors daarbij tot grote hoogten gestuwd zullen worden!

Martijn Malessy, altijd betrokken en altijd oog voor de klinische relevantie van het onderzoek. Bedankt voor je niet aflatende enthousiasme, ik heb geleerd en genoten van al onze discussies over perifere zenuwregeneratie.

Gerard, je hebt je reputatie als rots in de branding weer eens waargemaakt. Bedankt voor (onder andere): je pragmatische insteek, het altijd maken van tijd, je praktische aanwijzingen bij de uitvoer van experimenten, je hulp bij het maken van figuren en de ontelbare tekstuele correcties. Jouw hand is op elke bladzijde van dit boekje zichtbaar.

Ruben, we hebben lange uren samen op de OK doorgebracht, waarbij mijn waardering voor jou, zowel professioneel als persoonlijk, steeds meer is toegenomen. Je zorgvuldigheid en je grondige voorbereiding van alles wat je doet waren onmisbaar voor het slagen van mijn experimenten. Op naar ons volgende paper!

Collega-AIO William, bij jou ging ik "in de leer" toen ik net kwam kijken in de wereld van wetenschap. Bedankt dat ik de kunst van jou mocht afkijken, het was inderdaad een fijne samenwerking!

Mijn kamergenoten, in eerste instantie Paula, Yinghui en Elske en later Koen: bedankt voor jullie onmisbare vriendschap en de dagelijks terugkerende kamer-rituelen: koffie halen, voetbalpoule checken, elkaars figuren becommentariëren, adviezen uitwisselen over hoe je omgaat met statistiek/Photoshop/Illustrator/je supervisor, etc.

Overige collega's, in het bijzonder Tam (altijd goed voor een kleine AMC-break, een goed gesprek of een feestje!), maar ook Erich, Bas, Freddy, Matthew, Harold, Kasper, Anke, Barbara, Jinte, Karianne, Nathalie, Jeroen, Jacqueline, Arja en Unga en oud-collega's Fred, Joris, Marc-Jan en Floor hebben mijn tijd op het NIN de moeite waard gemaakt.

A special thank-you to my two Polish students: Asia and Katarina. Your enthusiasm and dedication made a great difference in my PhD project. To both of you I would like to say: "Dziękuję!"

Chris en Joop, jullie hebben, soms tot diep in de nacht, ImagePro applicaties geschreven die van groot belang waren bij meerdere hoofdstukken. Henk, bedankt voor je vakkundige hulp, zowel bij het ontwerpen van verschillende figuren als bij de lay-out van dit proefschrift. Mannen van de IT: Adriaan, Maarten en Marcel, mannen van de werkplaats: Rinus, Ruud en Martin, dames van het secretariaat: Tini en Wilma en natuurlijk Jenneke van de bibliotheek: bedankt voor jullie hulp bij al mijn (soms onmogelijke) verzoeken. Jilles, bedankt voor je goeie zorg voor mijn ratjes!

Godard, oud neurochirurgie-collega én collega-onderzoeker, je hebt veel werk verzet voor hoofdstuk 6, het meeste daarvan tijdens weekends en vakanties! We hebben een mooie samenwerking opgezet en ik hoop dat er nog meer goeie resultaten uit voort zullen komen. Ik zie uit naar je boekje.

Valeria and Marleen, it was a pleasure to collaborate with you on the regenerating peripheral nerve. I enjoyed the discussions we had, ranging from regeneration to publication and from papers to pasta. Valeria, I wish you all the best in Cardiff!

Oud-collega's van de neurochirurgie: Bert, Willem, Carmen, Mark, Michiel, Chris en Jasper: met elk van jullie heb ik prettig samengewerkt, ook al heb ik uiteindelijk toch een andere weg gekozen. Nieuwe collega's van de neurologie: we kennen elkaar net, maar ik zie ernaar uit om samen met jullie aan de slag te gaan!

Zoveel vrienden hebben de afgelopen jaren mijn verhalen moeten aanhoren over de frustraties en eigenaardigheden van het wetenschappelijk onderzoek met minivirusjes, groeistofjes en rattenzenuwtjes. Jullie zijn met teveel om op te noemen, maar bedankt voor jullie geduld. ~~Nu kunnen we weer gewoon bier drinken.~~

Mijn zussen Saskia en Mariken, samen met Eric en Marinus ~~(en Frederik, Lucia en Niene natuurlijk)~~, en de familie Verjans: Omi, John & Kitty, Inge & Tim (en Lotte) en Johan: jullie oprechte belangstelling voor mijn onderzoek heeft veel betekend. Johan, mooi dat we de familiebanden nog hebben weten te gebruiken voor het starten van een nieuw onderzoeksproject!

Pap en Mam, de vanzelfsprekendheid en onvoorwaardelijkheid waarmee jullie me in al mijn beslissingen hebben gesteund heeft grote indruk op me gemaakt, net als de belangstelling waarmee jullie ieder detail van mijn onderzoek op de voet volgden. Dit proefschrift is voor jullie.

Lieve Lein, samen gaan we de toekomst in, naar dat puntje in de oneindige verte waar de weg en de horizon bij elkaar komen. Dankzij jou geniet ik van elk moment van de reis en daarvoor ben ik je dankbaarder dan woorden kunnen uitdrukken.

Martijn, Amsterdam 2008



## Curriculum vitae

Martijn Tannemaat werd op 21 mei 1976 geboren in Madrid, Spanje. In 1994 behaalde hij zijn VWO diploma (summa cum laude) aan het Christelijk Gymnasium Sorghvliet in Den Haag en begon hij de studie geneeskunde aan de Universiteit van Amsterdam. Tijdens zijn studie deed hij een onderzoeksstage in Brisbane, Australië naar de phosphorylering van het HIV-Tat eiwit (supervisie: dr. N.A. McMillan). Na het behalen van zijn doctoraal diploma in 1999, in de wachttijd voor zijn co-schappen, deed hij onderzoek in Boston, Verenigde Staten naar de prevalentie van *Helicobacter Pylori* bij geadopteerde kinderen en naar de regulatie van de expressie van het LPH gen (supervisie: prof. dr. R.J. Grand). Na het behalen van zijn artsexamen in 2002 werkte hij gedurende 4 maanden als arts-assistent op de afdeling neurochirurgie (hoofd: prof. dr. R.T. Thomeer) van het Leids Universitair Medisch Centrum (LUMC). In 2003 begon hij als promovendus te werken aan het onderzoek beschreven in dit proefschrift met de bedoeling aansluitend de opleiding tot neurochirurg te starten. Na 2 jaar lang onderzoek gecombineerd te hebben met nacht- en weekenddiensten op de afdeling neurochirurgie veranderde hij echter van gedachten en zag af van zijn ~~opleidings-~~ ~~laats~~ om zich volledig te richten op het onderzoek. In 2006 werd een presentatie over hoofdstuk 6 van dit proefschrift op het internationale “Nerve Growth Factor” congres in Lyon geselecteerd als “hot topic” en beloond met een reisbeurs. Op het jaarlijkse congres voor de “American Society for the Peripheral Nerve” in Puerto Rico in 2007 werd een presentatie over hoofdstuk 4 beloond met een prijs voor “outstanding nerve presentation”.

Sinds 1 april is hij in opleiding tot neuroloog in het LUMC (hoofd: prof. dr. R.A.C. Roos). Hij woont samen met zijn vrouw, Marjolein in Amsterdam.



